PASSENGER AND FREIGHT FLOW MANAGEMENT IN MULTI-AIRPORT SYSTEM OPERATION

YUFAN ZUO

PhD

The Hong Kong Polytechnic University

2026

The Hong Kong Polytechnic University

Department of Aeronautical and Aviation Engineering

Passenger and Freight Flow Management in Multi-Airport System Operation

Yufan ZUO

A thesis submitted in partial fulfilment of the requirements for the degree of Doctor of Philosophy

October 2025

CERTIFICATE OF ORIGINALITY

I hereby declare that this thesis is my own work and that, to the best of my knowledge and belief, it reproduces no material previously published or written, nor material that has been accepted for the award of any other degree or diploma, except where due acknowledgement has been made in the text.

_______________________(Signed)

__Yufan ZUO__ (Name of student)

Abstract

This thesis advances passenger and freight demand management in multi-airport systems to enhance efficiency and competitiveness in the Greater Bay Area. The first study analyzes passenger choices and airline strategies in a system with two major airports and a reliever airport connected by ground transfers. It models passenger equilibrium, airline pricing, and investment under cooperative and non-cooperative games, showing that cooperative payoffs and investments align with bargaining power, that cooperation between the reliever and its connected major airport is especially profitable when ground links improve, and that greater congestion relief increases profits and incentives for major-airport investment.

The second study optimizes use of passenger-flight belly capacity for air cargo under uncertain capacity and demand through a two-stage stochastic program with Sample Average Approximation, Progressive Hedging, and heuristics. Using Hong Kong and eight destinations, the approach scales well and reliably improves performance, cutting costs by roughly 7–16% typically and up to about 30%, with even larger savings when post-reservation revenues improve and residual capacity is ample, occasionally generating surpluses on some routes.

The third study examines air–high-speed rail competition under heterogeneous traveler preferences using a Hotelling framework. It finds that lower fares and greater capacity attract demand from the rival mode, that optimal prices depend on preference distributions and, when HSR also values welfare, on the welfare weight and passengers' willingness to pay. Numerical results indicate that balanced preferences are key for effective price competition, modest fare increases can benefit modes with loyal users, and gradual, balanced pricing supports sustainable competition.

The fourth study formulates cargo routing in a multi-airport transfer hub as an integer linear program with heterogeneous values of time across airports, solved via a linear programming relaxation combined with an assignment heuristic. In a Greater Bay Area case with multiple major and minor airports and inter-airport road links, the method finds high-quality integer solutions rapidly, achieving feasible solutions within two hours and within about two percent of the relaxation bound even for instances that commercial solvers cannot finish in a day. Sensitivity analyses show assignments adapt to differences in transfer-time valuations. Collectively, these studies deepen understanding of passenger and freight flow management in multi-airport systems and provide implementable frameworks for real-world decision-making.

Publications arising from the thesis

Journal paper:

Zuo, Y., Liu, T.L. & Liu, W*. (2025). On the competition and collaboration in a multi-airport system considering ground connection between airports, *Transportation Research Part A: Policy and Practice*, 192, 104387.

Zuo, Y., Li, C. & Liu, W*. (2025). Air cargo transportation by passenger flights considering cargo demand and capacity uncertainties, *Transportmetrica A: Transport Science*. (Under 2nd-round review)

Zuo, Y., Zhang, Z., Wang, K. & Liu, W*. (2025). On the competition between air transport and high-speed rail considering inherent heterogeneous travel mode preferences, *Transportation Research Part A: Policy and Practice*. (Under 1st-round review)

Conference article:

Zuo, Y., & Liu, W*. (2024, Jul 1-4). Air cargo transportation by passenger flights considering cargo demand and capacity uncertainties [Oral Presentation]. *The 27th Air Transport Research Society (ATRS) World Conference*, Lisbon

Zuo, Y., & Liu, W*. (2024, Dec 9-10). Air cargo transportation by passenger flights considering cargo demand and capacity uncertainties [Oral Presentation]. *Proceedings of the 28th International Conference of Hong Kong Society for Transportation Studies (HKSTS 2024)*, Hong Kong

Zuo, Y., & Liu, W*. (2023, Dec 11-12). On the competition and collaboration in a multi-airport system considering ground connection between airports [Oral Presentation]. *Proceedings of the 27th International Conference of Hong Kong Society for*

Transportation Studies (HKSTS 2023), Hong Kong

Acknowledgements

I am grateful to my family for always supporting me unconditionally, and to my friends for helping me whenever I needed it. I would also like to thank the mentors I have encountered along my academic journey. Each professor has provided me with substantial guidance and help at different times. My sincere thanks go to Professor Jinjun Tang of Central South University, Professor Zhiyuan Liu and Professor Xiao Fu of Nanjing Normal University, and Professor Wei Liu of The Hong Kong Polytechnic University for their professional academic guidance, which enabled me to grow from an undergraduate who knew nothing about research into someone able to complete a doctoral dissertation. I am especially grateful to my PhD supervisor, Professor Wei Liu, for his guidance throughout my doctoral studies. I am sorry that I still fall far short of his expectations for me.

I would also like to thank Professor Li-Ta Hsu of The Hong Kong Polytechnic University, Professor Yong-Hong Kuo of The Hong Kong University, and Professor Nan Zheng of Monash University for their important roles in the external review of my thesis and the oral defense. They offered many highly professional and practical suggestions that helped me improve my dissertation and enhance the quality of my academic presentation.

As I write these acknowledgements, I am struck by how wondrous a dimension time is. Standing on the timeline, I may well be a different self in a four-dimensional world. Ten years ago, I might never have imagined being able to complete a PhD, and perhaps ten years from now I will be unable to imagine that I once found myself in a phase where I had achieved nothing.

If anyone reads my dissertation and finds some inspiration for their own research, I

will feel deeply honored. If no one pays it any attention, it will still have fulfilled its most important mission: helping me earn a doctoral degree. To whoever has read this far, I want to say—never lose hope. Believe that you can overcome challenges that seem insurmountable in the moment, and always carry courage and optimism.

Contents

List of Figures

List of Tables

Chapter 1

Introduction

1.1 The concept and significance of Multi-airport System (MAS)

A MAS consists of more than one geographically proximate airports within a shared region and has been wildly considered as an increasingly essential solution to accommodate rising air cargo and passenger demands (De Neufville, 1995; Ruan et al., 2021; Adisasmita & Caroles, 2022; Li et al., 2022; Zuo et al., 2025). In air cargo transportation, MASs serve as important transfer hubs and offer unique transfer services for air cargo logistics, particularly in handling air-to-air cargo flows. The true potential of a MAS is realized through the efficient coordination and integration of operations among its constituent airports and ground handling resources (Araújo & de Paula Hocayen, 2024; Zuo et al., 2025). By strategically optimizing cargo transportation across the entire system, logistics providers and shippers can benefit from enhanced efficiency, reduced operating costs, and improved service quality. Ultimately, such optimization strengthens the competitiveness of the MAS within the air cargo market.

The aviation industry around the world has grown substantially over the past decades (before the COVID-19 pandemic). This growing trend is expected to continue after the recovery from the COVID-19 pandemic. Many airports are built to foster stronger international economic and cultural communication, especially in economically developed regions.

Multi-airport system (MAS) is a promising and "inevitable" solution for handling increasing air travel demand, which is composed of airports in geographical proximity (De Neufville, 1995; Li et al., 2022; Ruan et al., 2021; Adisasmita & Caroles, 2022). Notable implementations of MAS include those in New York City (Lall, 2018), Yangtze River Delta (YRD) region (China) (Hu et al., 2023), and Greater London (Martín & Voltes-Dorta, 2011). MAS can bring increased capacity, improved competition, better resilience, enhanced regional connectivity, service specialization, and economic benefits. It is noteworthy that the realization of the above advantages/benefits of MAS depends on the effectiveness of coordination within the MAS, and its ability to provide seamless connectivity for passengers.

1.2 Background

1.2.1 Strengthened airport cooperation in the GBA

The importance of developing an airport cluster (or MAS) to accommodate the growing aviation market in the Guangdong-Hong Kong-Macao Greater Bay Area (GBA) has been highlighted in recent years[1]. In particular, Airport Authority Hong Kong (AAHK) and Zhuhai Municipal Government reached a memorandum of understanding (MoU) for providing seamless "Fly-Via-Zhuhai-HK" services for the Chinese mainland passengers travelling on the Hong Kong-Zhuhai-Macau Bridge to reach oversea destinations through Hong Kong International Airport[2]. Such a strategy helps attract flows to the airport in Zhuhai while relieving congestion at the airport in Hong Kong. Connection/transfer services that streamline customs procedures between Hong Kong and mainland China (Zhuhai) are being implemented, which are facilitated by the Hong Kong-Zhuhai-Macau bridge[3]. Cathay Pacific (the dominant airline based in Hong Kong) has provided detailed steps on how to transfer between

[1] China Daily (2019 May) China to develop world-class airport cluster in Bay Area, available at `https://www.chinadailyhk.com/articles/157/5/62/1556675238480.html`.

[2] Airport Technology (2022 November) Hong Kong and Zhuhai airports sign agreement to boost ties, available at `https://www.airport-technology.com/news/hong-kong-zhuhai-airports/?cf-view`.

[3] Time Out (2023 December) Hong Kong and Zhuhai airports to start transfer service tomorrow, available at `https://www.timeout.com/hong-kong/news/hong-kong-and-zhuhai-airports-to-start-transfer-service-tomorrow-121123`.

Hong Kong and Zhuhai airports[4]. At the same time, it is noted that in GBA Guangzhou Baiyun International Airport is a major airport that competes with Hong Kong International Airport for passengers from China Mainland who want to travel abroad. In summary, competition and collaboration co-exist in the GBA multi-airport system. In this context, this chapter provides an economic analysis of the competition and cooperation among airlines in a MAS considering inter-airport ground transportation connections and analyzes how airlines can maximize their economic gains.

A milestone report published on 18 June 2025 also underscores the strengthened political and institutional support marked by Airport Authority Hong Kong's (AAHK) acquisition of a 35% stake in Zhuhai Airport, signaling a new era of deeper collaboration. With this high-level backing, the partnership of the two airports is ready to advance to the next stage, particularly in air cargo transportation [5]. In the multi-airport system of the Greater Bay Area (GBA), Shenzhen Bao'an International Airport and Guangzhou Baiyun International Airport are both major international cargo transit hubs, consolidating their roles as core airports in the air cargo transportation in the GBA MAS. Collaborative cargo operations are also extending to airports in Macau, Foshan, and Huizhou, reflecting a broader, networked approach to regional logistics. The ground connection realized by cargo trucks on the cross-boundary bridge (i.e., Hong Kong-Zhuhai-Macau Bridge, also called HZMB) and intercity rail are also integral to the MAS by accommodating inter-airport cargo transfer. The resource integration and operation complexity in the MAS have been providing more opportunities as well as challenges in air cargo transportation.

1.2.2 Increasing air cargo demand in the world

The globalization of trade and commerce has significantly increased the reliance on air transportation to meet the demands for just-in-time delivery of materials and goods (Huang

[4]How to travel by bus from Zhuhai to Hong Kong International Airport, available at https://www.cathaypacific.com/cx/en_HK/inspiration/hong-kong/how-to-travel-zhuhai-to-hkia.html.

[5]A report entitled "Celebrating Successful Collaboration with Hong Kong International Airport (HKIA) as Zhuhai Airport Marks 30 Years of Operation" is published on the website of the Hong Kong International Airport https://www.hongkongairport.com/en/media-centre/press-release/2025/pr_1793 on 18 June 2025.

& Chang, 2010; Lakew & Tok, 2015; Azadian et al., 2017; Bombelli et al., 2020; Rodbundith et al., 2021; Chen et al., 2024). While cargo flights are in operation, their frequency is considerably lower compared to passenger flights, as the majority of air transportation capacity is dedicated to passenger services (Sourek & Seidlova, 2018). In particular, wide-bodied passenger aircraft often have substantial unused belly space after passenger baggage is loaded (Reis & Silva, 2016). Utilizing this underutilized capacity for air cargo transportation can significantly reduce delivery times, expand air cargo services, and generate additional revenue at a marginal cost (Ma et al., 2023a). This approach not only optimizes the use of available air transportation resources but also aligns with the efficiency imperatives of modern supply chains.

According to the International Air Transport Association (IATA), the cancellation of passenger flights led to a significant reduction in belly capacity provided by passenger flights, which is an integral part of air cargo transportation. This reduction resulted in a 43.7% decline in international belly cargo capacity and a 22.7% decrease in overall industry-wide cargo capacity year-on-year for March 2020[6]. According to IATA's Air Cargo Market Analysis[7] (October 2025), global cargo demand in September 2025 rose 2.9% year over year. At the same time, jet fuel prices increased 5.4% in September despite lower crude benchmarks, exerting cost pressure on carriers. This combination, firming demand alongside rising operating costs, strengthens the case for utilizing available cargo capacity on passenger flights (bellyhold space) to expand supply efficiently, improve load factors, and mitigate unit costs without requiring additional cargo lift. Compared with dedicated cargo services and road transport, utilizing unused passenger belly space offers higher service frequency and more direct connections between airport pairs, enabling faster response to demand, shorter transit times on many airport-airport pairs, and better schedule flexibility. It can also improve load factors and reduce unit costs and emissions by leveraging capacity that would otherwise go unused.

[6] Air Cargo Market Analysis issued by IATA in March 2020 at the website: `https://www.iata.org/en/iata-repository/publications/economic-reports/air-cargo-market-analysis---march-2020/`

[7] `https://www.iata.org/en/iata-repository/publications/economic-reports/Air-Cargo-Market-Analysis-October-2025/`

These data highlights two important aspects of air cargo transportation. First, it provides clear evidence that cargo transportation relies on the belly capacity of passenger flights to some extent. If passenger flights were not used for cargo transport, their cancellations would not have led to a decline in available cargo capacity. However, the reported decrease in cargo capacity following passenger flight cancellations directly contradicts this assumption, proving that passenger flights do contribute to cargo transportation. Second, the data demonstrates that the belly capacity of passenger flights constitutes a significant portion of the total available cargo capacity in the air transport system. The fact that the cancellation of passenger flights led to an industry-wide cargo capacity reduction of 22.7% underscores the extent to which the air cargo system depends on passenger aircraft. This reinforces the importance of considering passenger flight availability when analyzing air cargo capacity and transportation efficiency.

1.2.3 The strong competitiveness of HSR against air transportation

As reported by the Liaison Office of Hong Kong[8], the recently published high-speed rail (HSR) schedule has increased the number of mainland stations with direct connections to Hong Kong to nearly one hundred. Figure 1.1 presents travel information between Hong Kong and several representative mainland cities with notable tourist attractions, illustrating the strong competitiveness of HSR in cross-border transportation due to its convenience and attractive fares.

[8] The report can be accessed at: http://www.locpg.gov.cn/20250109/3affef51db90453cba7f5021eb630130/c.html

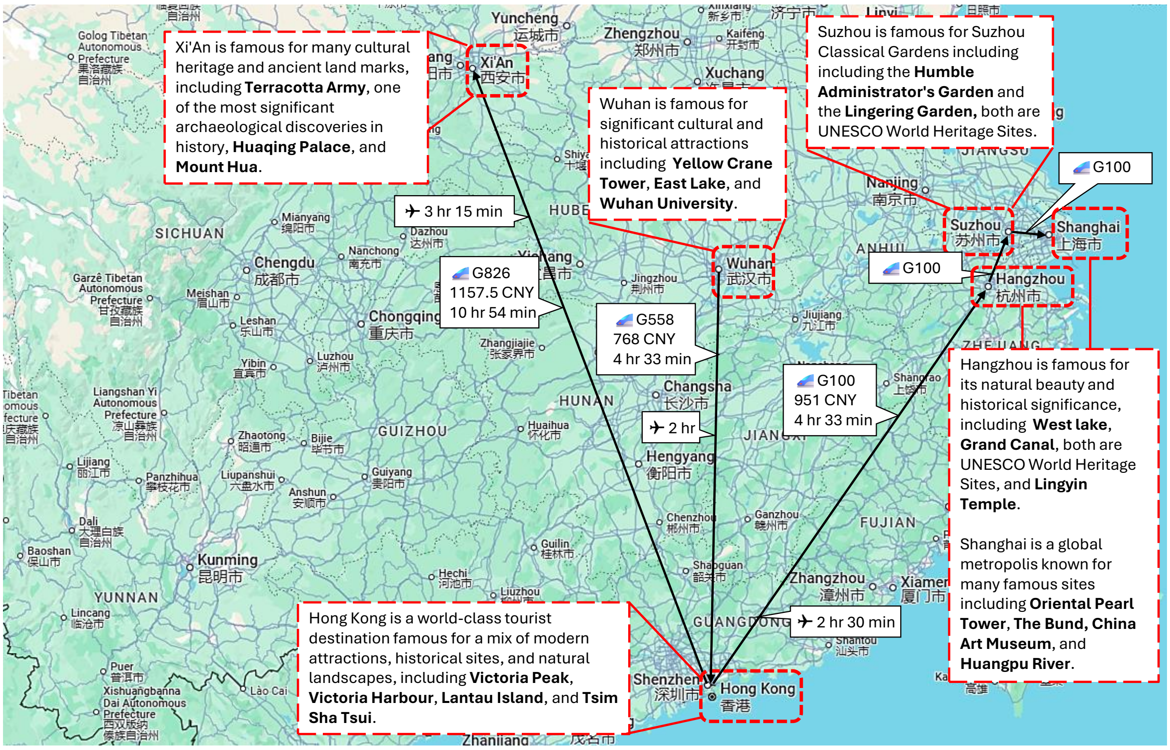

Figure 1.1: A map of High-Speed Rail and Air Transport connectivity between cities in Mainland China and Hong Kong

As the HSR network expands, more travelers are choosing between air transport (AT) and HSR, with decisions influenced by a wide range of personal preferences, including comfort, travel time, convenience, flexibility, and perceived reliability.

These personal heterogeneities mean that travelers may make different mode choices due to unobserved or idiosyncratic personal attitudes. Therefore, considering the heterogeneity of travelers' preferences is not only necessary for accurately modeling market behavior but is also crucial for designing effective and targeted pricing and service strategies. Ignoring this diversity may lead to a misunderstanding of market dynamics, and ultimately result in suboptimal decision-making by both operators and policymakers.

1.3 Contributions

This thesis delivers four complementary studies that advance the modeling, analysis, and optimization of modern aviation and intermodal transport systems. First, it develops tractable equilibrium and game-theoretic models for passenger behavior and airline strategy within a multi-airport system featuring cross-airport ground transfers. By jointly characterizing elastic passenger choices, airfare setting, and investments in ground connections under both cooperative and non-cooperative regimes, the study clarifies how fares, travel times, and capacity interact to shape path flows and generalized travel costs. It further establishes how congestion asymmetries and bargaining power determine incentives to invest in inter-airport links, demonstrating with a Greater Bay Area case that structured cooperation between airlines serving a connected major–reliever pair can increase profits for all participants—including non-cooperating competitors—while enhancing the effectiveness of congestion relief at minor airports.

Second, the thesis proposes a scalable, uncertainty-aware framework for managing unused belly capacity on passenger flights. The problem is formulated as a two-stage stochastic program that separates mid-term capacity reservations from short-term cargo-to-flight allocations, explicitly accounting for variability in cargo demand characteristics, arrival times, flight capacities, and schedules. To ensure computational tractability without sacrificing solution quality, the approach integrates sample average approximation with Progressive Hedging, Lagrangian relaxation for rigorous lower bounds, and tailored heuristics that provide tight upper bounds. Numerical experiments on medium and large instances show stable performance with modest scenario counts and deliver actionable insights into how market parameters shape robust capacity decisions under uncertainty.

Third, the thesis introduces a Hotelling-based, bi-level modeling framework to analyze competition between air transport and high-speed rail while explicitly incorporating heterogeneous traveler preferences. The framework yields closed-form comparative statics and pricing implications under both pure profit maximization and profit–welfare trade-off objectives. The analysis quantifies how each mode's prices, capacities, and congestion sensitivities influence market shares and reveals that neglecting preference heterogeneity leads to suboptimal pricing and foregone profits. The numerical results further illuminate market conditions under which aggressive fare adjustments stabilize or destabilize competition, providing guidance for balanced, welfare-enhancing pricing strategies in markets with varying degrees of traveler loyalty.

Fourth, the thesis designs and evaluates an integrated optimization framework for cargo transfer planning within a multi-airport system that operates as a coordinated minor–major hub. The study formulates an integer linear program that captures heterogeneous dwell times, air–ground–air routing, capacity coupling, and time feasibility, and introduces MAS-RnR, a branch-and-price-inspired algorithm with selective column generation, LP relaxation and greedy repair, and targeted branching. Across data-informed scenarios, the method consistently achieves smaller optimality gaps than heuristic baselines within practical time limits, demonstrating effectively efficiency gains from treating geographically proximate airports as a unified transfer hub and offering a deployable algorithmic blueprint for large-scale operations.

Taken together, these contributions provide an integrated set of models and algorithms that connect passenger demand equilibria, airline cooperation and investment, stochastic belly cargo management, intermodal price competition, and multi-airport cargo transfer design. The resulting insights and tools furnish a coherent foundation for data-driven decision making that improves profitability, resilience, and social welfare in complex, capacity-constrained, and uncertain aviation systems.

1.4 Outline

This thesis contains two application domains, air passenger and air freight, and is structured by decision scale, macro, meso, and micro levels. Figure 1.2 shows how the thesis connection passenger and freight problems across scales from strategic mode competition down to uncertainty-aware operational planning.

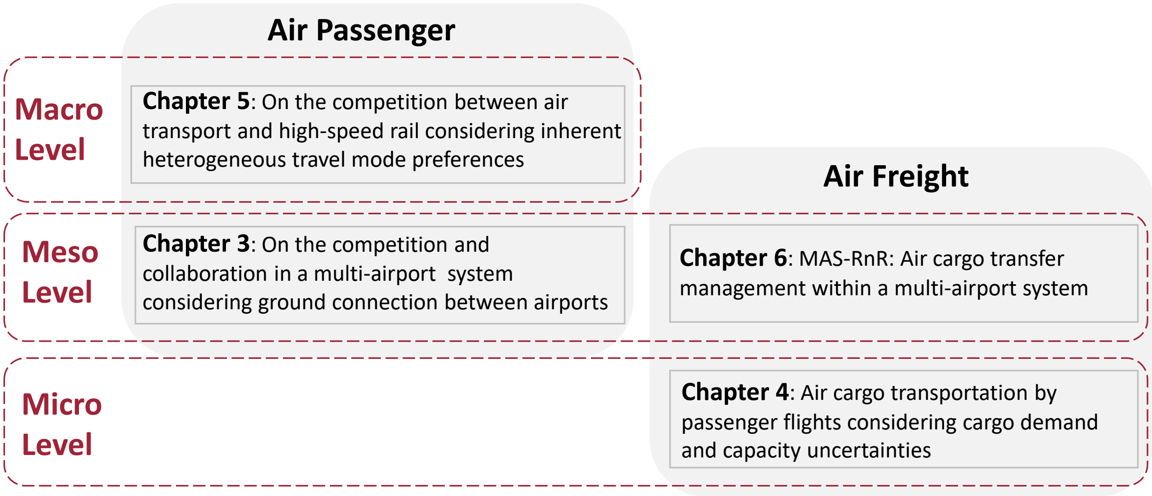

Figure 1.2: Outline

Chapter 3 examines passenger choice equilibria and airlines' strategic pricing and investment decisions in ground connections within a stylized multi-airport system that includes two major airports and a connected reliever airport. It develops tractable bi-level game-theoretic models under cooperative and non-cooperative settings, analyzes how fares, travel times, and capacities shape path flows and generalized prices, and uses a Greater Bay Area case to derive managerial recommendations on cooperation, bargaining, and congestion relief.

Chapter 4 addresses operational planning for belly cargo by proposing a two-stage stochastic programming framework that separates mid-term capacity reservations from short-term cargo-to-flight allocations under uncertainties in demand, timing, capacity, and schedules. The solution approach combines sample average approximation, Progressive Hedging, Lagrangian relaxation, and tailored heuristics to achieve scalable, high-quality solutions. Numerical experiments assess convergence, solution stability across scenario sizes, and sensitivity to market parameters, yielding implementable guidance for robust capacity management.

Chapter 5 investigates competition between air transport and high-speed rail using a Hotelling-based bi-level framework that embeds heterogeneous traveler preferences in the lower-level demand model and alternative operator objectives in the upper level. The chapter presents analytical comparative statics and numerical insights on pricing, capacity, and congestion effects, highlighting the revenue and welfare consequences of ignoring preference heterogeneity and offering strategies for stable and effective price competition across different market loyalty structures.

Chapter6 develops an integrated optimization model for cargo transfers within a coordinated minor–major airport hub, formulating an integer linear program that captures heterogeneous dwell times, air–ground–air routing, capacity coupling, and time-feasibility constraints. It introduces MAS-RnR, a branch-and-price-inspired algorithm with selective column generation, LP relaxation and repair, and targeted branching. Computational studies, informed by real-world schedules and simulated demands, demonstrate consistent improvements over heuristic baselines and provide design guidance for consolidated MAS cargo hubs.

The thesis concludes by synthesizing managerial implications across the four studies, discussing limitations related to network scope, preference and demand realism, multi-agent coordination, and information uncertainty, and outlining future research directions that integrate passenger and cargo planning, extend to richer MAS and intermodal networks, and utilize empirical data for calibration and validation.

Chapter 2

Literature review

This chapter presents a comprehensive literature review on air passenger and cargo flows in airports from macro, meso, and micro perspectives. Section 2.1 reviews methods and technologies relevant to multi-airport systems (MAS). Section 2.1.1 examines assessment and prediction approaches for resource utilization in MAS and highlights airport delay as a key factor affecting efficiency. In this context, the role of minor airports as reliever airports is emphasized for relieving congestion at major airports and improving overall MAS performance. Operational and managerial aspects of airlines and airports within MAS are also discussed in Section 2.1. A key distinction between prior work on airline competition and collaboration and the approach adopted in this thesis is the explicit treatment of physical inter-airport connectivity. We consider ground transportation links as an integral component that supports deeper, more stable airline cooperation. Section 2.2 synthesizes literature on air cargo allocation at airports. Section 2.2.1 emphasize the value of applying unused passenger capacity for cargo to enhance resource efficiency, suggesting that using residual passenger transport capacity for air cargo is a promising way. Section 2.3.2 reviews studies on travelers' mode choice behavior and analyzes determinants of mode selection, noting that inherent preferences are often underrepresented in analytical models. Section 2.3.1 examines competition between air transport (AT) and high-speed rail (HSR) in the medium-haul traveler market, arguing for greater attention to their competitive trends. Finally, Section 2.4 investigates research on hub-and-spoke networks in air cargo transfer. Section 2.4.1 highlights the importance of hub and non-hub location choices in designing these networks and their widespread application, while Section 2.4.2 discusses efficiency challenges and shows how treating an MAS as a transfer hub can improve cargo transfer efficiency by integrating resources across constituent airports. Section 2.5 summarizes the research gaps of those reviewed studies and the corresponding research has been completed in this thesis to fill those gaps.

2.1 Literature review on MAS: methods, competitive operations, and cooperative strategies

2.1.1 Methodological advances for efficient multi-airport systems: optimization, prediction, and strategic interaction

Research efforts have been made from different aspects to support efficient resource utilization in the MAS. For instance, the analytic hierarchy process (AHP) is often used to rank airports and prioritize routes in order to optimize MAS terminal manoeuvring area (TMA) operations (Zietsman & Vanderschuren, 2014; Sidiropoulos et al., 2018). To reduce the gap between the planned operations and the actual operations and thus improve the efficiency of TMA, data-driven models have been widely used to evaluate the adherence to standard routes by the actual traffic (Carmona et al., 2020). For the efficient utilization of MAS capacity, congestion delay has been a great concern (Lall, 2018). Ramanujam & Balakrishnan (2009) identified key influence factors of the capacity envelope in a MAS. Liu et al. (2017) used an optimization model to minimize the delay cost by optimally designing the flight arrival and departure schedule. Cheung et al. (2020) utilized a spatial panel model to evaluate the impact of deciding factors of airport capacity. Zhao et al. (2022) applied queuing theory to estimate the flight delay in a MAS.

Accurate prediction can provide advanced and necessary information for better resource allocation in MAS. Machine learning models are widely used for forecasting or prediction tasks. Murça & Hansman (2019) applied multi-layer clustering analysis to identify, characterize, and predict traffic flow patterns in the terminal area of MAS. Wang & Zhang (2021) proposed a data-driven deep-learning framework involving a convolutional neural network to predict real-time airport capacity in a MAS. Wang et al. (2023) combined clustering analysis, random forest and neural network model to make a prediction on medium-term estimated time of arrival for a MAS.

Some studies developed tractable models to analyze and/or optimize airports' strategies and airlines' competition and interactions within a MAS. Noruzoliaee et al. (2015) applied analytical models to scrutinize airport capacity and pricing choice of MAS under different scenarios. Hou et al. (2022) used game-theoretical models for examining the regulator's policy in airport slot allocation and airlines' airport entry decisions. Some other studies examined how high-speed rail (HSR) interact with the MAS, which might relieve airport congestion (Yang & Zhang, 2012; Xia et al., 2019; Li et al., 2022). However, limited studies have examined the competition and collaboration in a multi-airport system considering ground connection between airports, and the optimal investment for ground connection services.

2.1.2 Airline competition and coordination under the MAS context

It is noteworthy that airlines' competition and coordination have been investigated extensively, while not in the context of MAS (Martín & Román, 2003; Pels et al., 2009; Wang et al., 2016; Pilar Socorro et al., 2018). Various models are applied in investigating airlines' decisions about costs and prices, aiming at maximizing airline profits (Abdelghany et al., 2017). Many studies developed analytical models to explore airlines' cooperative/competitive strategies under different operation regimes (Wei & Hansen, 2007; Zhang et al., 2010; Vaze & Barnhart, 2012; Grauberger & Kimms, 2016; Wang et al., 2022a). Statistic models have also been used to understand airline competition (Pels et al., 2000). Lijesen & Behrens (2017) employed two-stage least-squares dummy variables regression models to estimate airlines' strategic reaction to the competitors' capacity levels. Fageda & Fernandez-Villadangos (2009) used parametric and non-parametric techniques to analyze the influence of increases in airport capacity and the entry of low-cost carriers on airline competition. Jiang & Zhang (2016) investigated the impact of HSR competition on trunk routes on the airlines' decision on network and market coverage. However, existing studies considering competition and coordination in the air sector focus on different problem contexts and cannot be applied directly to the MAS in this study considering inter-airport ground connection.

This paper fills this gap by considering cross-airport transfer enabled by the inter-airport ground connection in the MAS and how such a travel option will affect passenger choices, airline decisions, and MAS performance. Although Xia et al. (2019) previously explored a similar multimodal system composed of a road traffic system (HSR) and a MAS including two airports, our study necessitates clear differentiation. The primary distinctions lie in the research motivation, network structures, and considerations of ground connections. Firstly, Xia et al. (2019) explored revenue-sharing agreements between HSR and airlines while our study focuses on cooperation and competition among airlines. Contrary to Xia et al. (2019), who investigated air vs. air-HSR competition with direct flights, our research delves into interconnected air-air and air-land-air routes that necessitate transfers within our stylized MAS due to the absence of direct flights from domestic origins to international destinations. Additionally, we view road traffic systems as facilitative links that support seamless air travel rather than as revenue-generating entities, and we explore the financial incentive of airline operators to provide financial support for enhancing ground connection services.

2.2 Literature review on air cargo allocation operations

2.2.1 Co-modality: passenger and cargo integrated transportation

In some literature, co-modality refers to the integration of passenger and freight flows into a single transportation system by sharing transportation resources (Ma et al., 2023a; Mo et al., 2023; Yang et al., 2023, 2024).[1] We follow the definition of co-modality as "inte-

[1]This is slightly different from the "combined transport" defined by European Commission `https://en.wikipedia.org/wiki/Co-modality`, where "co-modality" is more similar to the concept of "Intermodal

grating people-and-goods transportation" (Cheng et al., 2023). Zhu et al. (2023) reported the applicability of co-modality in short-haul, low-volume deliveries that require higher time reliability. Extensive studies have explored the effects of co-modality on urban transportation systems, focusing on analytical assessments and operational optimizations such as transportation scheduling, location selection, vehicle routing, and freight delivery scheme design (Masson et al., 2017; Behiri et al., 2018; Cheng et al., 2018; Pimentel & Alvelos, 2018; Zhao et al., 2018; Ma et al., 2023a,b). These studies underscore the important role of co-modality in facilitating efficient intra-city, same-day deliveries, especially in public transportation systems. Unlike urban co-modality, utilizing unused capacity in passenger flights for cargo transportation presents unique challenges and advantages. These include greater susceptibility to scheduling uncertainties due to weather conditions, variable space availability due to fluctuating passenger baggage allowances, and the potential for significant environmental and economic benefits.

In some studies on air cargo transportation via passenger flights, the core concept of utilizing underutilized capacity operates on a larger scale, addressing intercity and international logistics. Despite its potential for cost savings and revenue enhancement, this topic has not been extensively studied. Notable works in this field include Reis & Silva (2016), which examines air cargo business models in combination airlines, highlighting the need for specific strategic adjustments rather than comprehensive business model overhauls. Other studies have identified challenges such as the potential impact on passenger service quality (Lange, 2019) and have explored pricing models to optimize profits from the combined transport of cargo and passenger baggage (Shaban et al., 2019). Furthermore, research by Ma et al. (2023a) has delved into the strategic allocation of air cargo to minimize delivery times using passenger flights' underused belly capacity. In summary, while the concept of co-modality has been applied to both public and air transportation systems, the various uncertainties associated with transporting air cargo via passenger flights remain underexplored.

Air cargo network planning and scheduling

Operations in air cargo transportation fundamentally rely on an efficient network, where

---

transportation".

air traffic resource planning and scheduling of this network are significant for providing high-quality transporting services. Central to these networks are issues such as hub location selection, flight scheduling, fleet assignment, and cargo-to-flight allocations, typically optimized to either maximize profits or minimize operational costs.

The hub-and-spoke model serves as the cornerstone of air cargo networks, where cargo is consolidated at hubs and distributed to spokes (Zheng et al., 2023). Early studies, such as Jaillet et al. (1996), highlighted the strategic importance of hub selection. Subsequent research has advanced methods for optimizing hub locations and enhancing network resilience (He et al., 2015; An et al., 2015; Kian & Kargar, 2016; Oktal & Ozger, 2013). Furthermore, the significance of non-hub airports has gained increasing recognition, influencing cargo carrier choices and being affected by forwarders (Kupfer et al., 2016; Rodrigue, 2012). Traditionally, these dynamics have been studied within regional economic contexts (Zhang, 2003; Gardiner & Ison, 2008).

Air cargo planning encompasses fleet assignment and flight scheduling, both vital for operational efficiency and similar to practices in passenger flights (Sherali et al., 2006, 2013; Lohatepanont & Barnhart, 2004; Birolini et al., 2021). Advanced models that integrate these components have been created to enhance network operations while balancing profitability and emissions considerations (Zhang et al., 2016; Kenan et al., 2018; Xu et al., 2021; Justin et al., 2022).

Air cargo routing is often optimized combined with fleet assignment and flight scheduling to improve air network performance and (Delgado et al., 2020; Delgado & Mora, 2021). Derigs et al. (2009) developed integrated models that combine the optimization of flight selection, aircraft rotation planning, and cargo routing. Additionally, Xiao et al. (2022) introduced a connection and string-based model to address aircraft tail assignment and cargo routing problems simultaneously.

Despite extensive research focused on improving air cargo system performance through the integration of hub location, fleet assignment, and routing (Aykin, 1995; Yan et al., 2006; Rodriguez-Martin et al., 2014; Zhang et al., 2017; Butun et al., 2021), operational challenges remain. The hub-and-spoke model often leads to extended cargo stay times at hubs due to consolidation processes (Zheng et al., 2023), and limited connections between certain airports can result in extended delivery times and sub-optimal responses to just-in-time cargo demands. Conversely, air passenger transportation networks, with their extensive coverage and higher connectivity, present a promising alternative for air cargo transportation, underscoring the motivation of our study.

2.2.2 Revenue management approaches in cargo transportation

Revenue management plays a crucial role in maximizing the profitability of cargo transportation, with one of its key challenges being the efficient utilization of cargo capacity. In this section, we review the literature on revenue management in cargo transportation, focusing on two main areas: overbooking and capacity management.

Overbooking is an important policy of revenue management that sells more cargo capacity than the available amount (Bodily & Pfeifer, 1992; Kasilingam, 1997; Amaruchkul & Sae-Lim, 2011). Deciding the overbooking level is complicated, especially in uncertain environments composed of booking requests, demand show-up rate, oversale costs and spoilage costs. Wang & Kao (2008) applied a fuzzy knowledge system to determine overbooking capacity by considering various uncertainties. Gui et al. (2008) proposed a two-dimensional air cargo overbooking model to maximize profit, considering both revenue and offloading costs. Wannakrairot & Phumchusri (2016) developed two-dimensional air cargo overbooking models to optimize the overbooking level for total cost minimization, assuming booking requests and show-up rate with known distributions. Overbooking is approached from the perspective of a capacity seller, which differs from the focus of our research, where we try to minimize the cost paid by the capacity user.

To maximize profits, airlines can sell cargo capacity through allotment contracts or on the spot market (Billings et al., 2003; Levin et al., 2012; Moussawi-Haidar, 2014). Allotment contracts are signed to establish long-term agreements with customers for capacity reservations, whereas deliveries in the spot market are typically more urgent and incur higher charges from airlines. Huang & Chang (2010) used a dynamic programming model to generate the control policy of air cargo space, considering the weight and volume uncertainty of air cargo shipments. Wada et al. (2017) developed a planning model to assign cargo capacity to allotment and free reservations, considering risk-neutral and risk-averse formulations. Levin et al. (2012) maximized the total expected profit by simultaneously optimizing allotment selection, bookings on the spot market and operations in the cargo loading process.

Previous studies have widely acknowledged that uncertainty in cargo transportation is more complex than in passenger transportation. Therefore, we comprehensively consider uncertainties arising from both cargo demand and flight capacities. As considering various uncertainties in air cargo transportation is a key contribution of our study, we review the relevant literature on cargo demand and flight capacity uncertainties in Section 2.2.3. Capacity selling through allotment contracts and the spot market can be seen as a combination of long-term and short-term decision-making from the capacity seller's perspective. As a capacity user, it is convincing that a two-stage framework, integrating long-term capacity reservation with short-term allocation, offers an effective strategy for air cargo transportation.

Despite these similarities, our study differs from the existing literature in several key aspects. First, while previous research approaches overbooking from the perspective of a capacity seller, our study focuses on the capacity user's viewpoint. Specifically, we aim to optimize the utilization of both owned capacity and external sources to complete cargo transportation at minimal cost. Additionally, temporal factors have not been sufficiently emphasized or comprehensively considered in prior studies. Unlike previous research, our study examines air cargo transportation via passenger flights, which operate with higher frequencies and more restricted loading time windows compared to dedicated cargo flights. Consequently, time constraints play a critical role in cargo-to-flight allocation and must be carefully accounted for in decision-making.

2.2.3 Cargo demand and flight capacity uncertainties

Many uncertainties exist in air cargo transportation, particularly including fluctuations in cargo demand and variations in flight capacity. These uncertainties can complicate the management of air cargo operations, potentially resulting in increased operational costs (Fildes & Goodwin, 2007).

Various forecasting approaches have been developed to deal with the uncertainty in air cargo demand. Suryani et al. (2012) utilized a system dynamics simulation model to improve the accuracy of demand forecasts. Similarly, Totamane et al. (2014) introduced a multiproducer-multiconsumer framework using the Potluck Problem approach to predict route-specific cargo demand for airlines. Accurate demand forecasting is essential for mitigating potential cost increases. Klindokmai et al. (2014) assessed different forecasting models by analyzing historical chargeable weight data from a company, while Magana et al. (2017) conducted a detailed case study to identify factors influencing demand forecasting, thereby enhancing the operational performance of an air cargo handler. The variability in demand, driven by external market and economic factors, makes forecasting particularly challenging (Klindokmai et al., 2014).

The belly space/capacity of passenger flights, primarily designated for passengers' baggage, also serves as a secondary freight carrier. Shaban et al. (2019) observed that last-minute purchases by passengers could reduce the available capacity for cargo transportation. To address this capacity uncertainty, Ma et al. (2023a) modelled it using an exponential distribution, examining how the reliability of capacity estimates impacts optimization outcomes. Additionally, Delgado et al. (2019) managed capacity uncertainty by employing a scenario tree with discrete capacity outcomes and associated probabilities. The uncertain cargo capacities in passenger flights are supposed to increase the difficulties of capacity management in air cargo transportation.

Time- and capacity-related uncertainties have been often considered in the optimization problem in cargo transportation systems. Shang et al. (2021) developed a credibility-based fuzzy programming model addressing the uncertainty in travel time and handling time of the cargo delivery. To deal with the time uncertainties and predict the delays with sufficient precision, Sahoo et al. (2022) proposed an improved hybrid ensemble learning model combining bagging and stacking with characteristics like time, flight schedule, and transport legs. (Amaruchkul, 2025) studied a cargo transportation problem in a two-stage decision framework, modeling demand via probability distributions (as in stochastic programming) and flight travel times via an uncertainty set (as in robust optimization). Although Amaruchkul (2025) also considers two-stage air cargo capacity management, our setting differs in key ways. First, we focus on cases where passenger flights carry air cargo; the unpredictable usage of belly space by passenger luggage introduces inherent capacity uncertainty. In contrast, Amaruchkul (2025) do not emphasize specific flights for air cargo and thus do not necessarily model flight-level capacity uncertainty. Second, they use continuous percent-allocation variables, whereas we formulate cargo-to-flight assignments as binary variables. In related work on service-time uncertainty in synchromodal freight transport, Zhang et al. (2023) proposed an online deep reinforcement learning approach considering uncertain service time, supported by an Adaptive Large Neighborhood Search heuristic that supplies state and reward information based on routing and scheduling. Lu et al. (2020) addressed a fuzzy intercontinental multimodal routing problem with uncertainties in time and train capacity, employing a defuzzification approach to solve a fuzzy mixed-integer linear program and generating instance sets to validate the model. Studying the application of unused capacity in passenger flights for transporting cargo, Ma et al. (2025) employed a new hybrid genetic algorithm to accommodate the capacity uncertainties. Büsing et al. (2019) included stochastic scenarios to simulate potential capacity updates in their proposed mixed-integer program.

In summary, while various approaches have been applied to address uncertainties in cargo demand and belly capacities, as shown in Table 2.1, our study is the first to apply a two-stage stochastic program to optimize both mid- and short-term strategies in cargo transportation by passenger flights. Our proposed two-stage capacity management approach encourages airlines to implement a medium-term capacity reservation scheme for cargo transportation in advance. This ensures sufficient loading time and allows operators to allocate any remaining capacity more effectively. The medium-term strategy is established before a planning period, such as a week or a month. Within each short-term period covered by the mid-term plan, cargo-to-flight allocations are optimized to minimize operating costs by assigning cargo to the most suitable flights. Our model accounts for multiple sources of uncertainty: the cargo's weight and its arrival time at the origin airport, as well as the realized schedules and capacities of passenger flights. We categorize these uncertainties into two groups: (i) Time-related uncertainties: affect both demand (cargo arrival times) and supply (flight departure/arrival times and schedule reliability), and (ii) Loading-related uncertainties: arise from uncertain cargo weights and variable flight capacities. Both types of uncertainty directly influence cargo-to-flight assignment and loading decisions.

Table 2.1: Selected literature considering uncertainties in air cargo capacity management

	Capacity in passenger flights	Cargo demand uncertainties		Flight uncertainties	
		Weight	Arrival time uncertainties	Flight schedule	Capacity
Han et al. (2010)	-	✓	-	-	-
Van Hui et al. (2014)	-	-	✓	✓	-
Büsing et al. (2019)	-	-	-	✓	
Delgado et al. (2019)	-	-	-	-	✓
Sahoo et al. (2022)	-	-	✓	✓	-
Ma et al. (2025)	✓	-	-	-	✓
Amaruchkul (2025)	-	-	✓	✓	-
Our study	✓	✓	✓	✓	✓

2.3 Literature review on the mode choice behavior of air passengers

2.3.1 Competition between air transport (AT) and High-speed rail (HSR)

Literature on the competition between AT and HSR includes two main types of research: analytical studies on the HSR and AT operators' strategy adjustment which subject to travelers' equilibrium choice between AT and HSR and empirical studies on the influential factors affecting mode choice between AT and HSR within the short- and mid-haul travel market.

Analytical studies on the competition between air transport (AT) and High-speed rail often applied bi-level modeling approaches to analyse travelers' mode choice between AT and HSR and planning/operation strategies/decisions made by operators of the two modes (Wang et al., 2020a; Yang & Zhang, 2012). Research frameworks in theoretical studies are often based on game theory where the airline and the HSR operator compete under various possible market structures. In the competition, operators of HSR and AT adjust their operations/decisions to maximize their profit or maximize a weighted sum of profit and social welfare (always for HSR operators) (Yang & Zhang, 2012; D'Alfonso et al., 2015; Tsunoda, 2018). In the game theoretical approaches, passengers' travel mode choices are assumed to be made under utility-maximization or cost-minimization principles (Adler et al., 2010; Jiang & Zhang, 2016). To ensure the tractability of models, heterogeneity of passengers' travel mode preference are often ignored or simplified, e.g., homogeneous characteristics of passengers are considered in the formulation. In most cases, to ensure tractability, there are only a few representative factors in the formulation of travel costs, ignoring some subjective or perceptive factors that might affect travelers' decision-making process on travel mode choices. Yang & Zhang (2012) examined the impacts of competition between AT and HSR on users, operators and social welfare. They considered business and leisure passengers with different time values. Also, they considered spatially distributed passengers with varying travel distance/time to airport and HSR station by adopting a Hotelling model. This study follows Yang & Zhang (2012) and also examines the competition between AT and HSR and their impacts. Differently, this study emphasizes the inherent heterogeneous travel mode preferences towards AT and HSR (can be either subjective or objective, such as safety preference, distance preference), where such heterogeneity is captured via the Hotelling model. Moreover, we consider a general distribution of heterogeneity, while Yang & Zhang (2012) assumed uniformly distributed passenger density (in the Hotelling modeling framework). Note that travelers' subjective travel mode preferences have rarely been considered in existing studies when examining competition between AT and HSR.

The empirical literature on travelers' mode choice between AT and HSR suggested that passengers' heterogeneous travel mode choice behaviour under the competition between AT and HSR is mainly caused by the variety existing in travel-specific attributes, exogenous factors, demographics and individual socioeconomic characteristics. Empirical studies are carried out by naming many factors and assuming the affecting mechanism between the factors and travelers' decisions on travel mode choices. In these studies, travelers' mode choices are assumed to be the dependent variables while the assumed factors are taken as the independent variables. The coefficients of the factors in the assumed model form are estimated by the collected data.

Heterogeneity in passengers' perception under the short- and mid-haul travel markets served by AT and HSR has been recognised by many studies. Raturi & Verma (2020) found that passengers' value-of-time distributions significantly affect the profitability and the market equilibrium of the game between HSR and AT. Behrens & Pels (2012) revealed that passengers with leisure travel purposes have greater fare sensitivity than business passengers. Wang et al. (2021) investigated heterogeneous risk perception of passengers and suggested that higher-health-conscious passengers have lower willingness to choose AT and HSR. Diana & Mokhtarian (2009) and Antonucci et al. (2014) found that passengers' characteristics, including gender, income, vehicle ownership, and travel frequency, affect their satisfaction with transport services. Bergantino & Madio (2020) provided evidence for the larger attractiveness of HSR services on the population with lower price elasticity and higher time sensitivity. Travelers with different demographic and trip related characteristics may have heterogeneous preferences or sensitivities, which also affect their decision-making processes. For example, individuals with high income may be relatively less sensitive to travel cost. Equally, age may impact on consumers' sensitivity to seat comfort (Zhou et al., 2020).

2.3.2 Travel mode choice behaviour

Modelling individuals' travel mode choices is crucial in transport planning and provides guidance for operators to make accommodated strategies (Pels et al., 2000; Hess et al., 2007; Chang & Sun, 2012; Can, 2013; Zou et al., 2016; Kashifi et al., 2022) and has been widely investigated in many travel behaviour studies (Dobruszkes et al., 2014). Literature suggests various determinants influence heterogeneous mode choice behaviours of respondents, including demographics and socioeconomic characteristics (such as age, gender, education, occupation, and household structure) (Bhat & Srinivasan, 2005; Ryley, 2006; De Vos et al., 2016), travel attitude (De Vos & Witlox, 2017), and trip-specific attributes (like travel time, costs, transferring, and travel purposes) (Schwanen & Mokhtarian, 2005). Through collecting plenty of data, including the revealed preference (RP) survey (Brownstone et al., 2000; Malokin et al., 2019), stated preference (SP) survey (Devarasetty et al., 2012; Zhou et al., 2019), or the joint RP-SP survey (Zou et al., 2016; Saxena et al., 2019), the influential mechanisms between considered factors and respondents' travel mode choices are quantified under assumed model structures.

Advanced statistical and econometric methods have been applied to investigate the relationship between determinants and travelers' mode choices, including various discrete choice models are widely applied such as Multinomial logit (MNL) model, Nested logit (NL) model, and Mixed logit model (McFadden & Train, 2000; Hensher & Greene, 2003; Hess et al., 2007; Can, 2013; Jung & Yoo, 2014; Xiong et al., 2018), statistical regression frameworks like Poisson regression model (Bhat & Srinivasan, 2005) and binary logistic regression model (Negm et al., 2024). Agent-based approaches with fuzzy set theory also have been applied to model the decision-making process of travelers by using assumed if-then rules (Vythoulkas & Koutsopoulos, 2003; McDonnell & Zellner, 2011; Zou et al., 2016).

Heterogeneous travel mode preferences among travelers have been investigated in travel behaviour research (Hensher & Rose, 2007; Tian et al., 2021). Susilo & Cats (2014) noted that travelers with different characteristics tend to value different determinants in assessing their travel satisfaction. Beaud et al. (2016) assessed the heterogeneous willingness of travelers to pay for reduction of travel time and elimination of travel time variability under various statistical distribution of travel time and travelers' risk attitudes. Prato et al. (2017) identified four liftstyle groups with different specific perceptions of influential factors on mode selection. Saxena et al. (2019) explored traveler's mode choice under the public transit service disruptions and found the difference values of travel time of rail users and transit users. In summary, many efforts have been paid in literature to understand heterogeneous travel mode preference which turns out to be affected by influential factors in many aspects.

2.4 Literature review on air cargo transfer operations

The complexity of air cargo operations arises not only from the geographic dispersion of origins and destinations but also from the intricate coordination required among diverse actors, infrastructure, and regulatory environments. Previous studies have devoted considerable attention to the design, management, and optimization of air cargo networks. Within this research landscape, the hub-and-spoke model has established itself as a cornerstone for consolidating flows, organizing routing, and simplifying operations. However, existing challenges such as fluctuating demand, network disruptions, and increasing service level expectations, have prompted researchers to re-examine both the strategic configuration of air cargo networks and the operational complexities associated with transfer hub management. The following review critically examines recent advances in hub location modeling, network resilience, airport choice behavior, and airport-level operational optimization, thereby providing a foundation for a focused analysis of the emerging role of multi-airport systems (MAS) as transfer hubs and their potential implications for the evolution of air cargo logistics.

2.4.1 Hub-and-spoke network in air cargo transportation

Operations in air cargo transportation fundamentally rely on the design and management of efficient networks, where planning and scheduling are critical for ensuring high-quality, reliable services. At the core of these cargo networks lies the hub-and-spoke model, which consolidates cargo from various origins at central hubs before redistributing it to final destinations (Zheng et al., 2023). The strategic selection of hub locations has long been recognized as a key determinant of network efficiency, cost-effectiveness, and service quality (Jaillet et al., 1996). Research in this area has evolved to incorporate advanced optimization methods for hub siting and to address network resilience in the face of possible disruptions (Campbell, 1994; Elhedhli & Hu, 2005). He et al. (2015) proposed an improved MIP heuristic combining branch-and-bound, Lagrangian relaxation, and linear programming relaxation for solving intermodal hub location problem. An et al. (2015) modeled a non-linear mixed integer program for solving reliable network design problems and applied Lagrangian relaxation and

Branch-and-Bound methods to get optimal solutions. Kian & Kargar (2016) provided two mixed integer nonlinear programming formulations for the single allocation p-hub location problem under congestion cost based on formulations proposed in Ernst & Krishnamoorthy (1996). The outperformance of results in Kian & Kargar (2016) was proved by comparing with the results with formulations in previous studies (Elhedhli & Wu, 2010). While the focus has often been on major hubs, the role and influence of non-hub airports are increasingly acknowledged, affecting carrier routing decisions and being shaped by cargo forwarder strategies. Gardiner & Ison (2008) identified the main influential factors considered by non-integrated cargo airlines when choosing airports. Kupfer et al. (2016) used a stated choice experiment to investigate the factors affecting the airport choice for cargo operations. In general, the effective selection of nodes within the air logistics network, and the optimal assignment of roles to each airport as a node, are both crucial for enhancing air cargo transportation efficiency.

A crucial element in hub-and-spoke networks is the cargo transferring process within the hub itself. Efficient transfer operations not only impact total transit times but also influence the network's ability to respond flexibly to demand fluctuations and service reliability requirements. Traditionally, studies have considered single airports as hubs. However, considering multiple airports in a region as a transfer hub (MAS) introduces new advantages, such as increased operational flexibility, better utilization of regional infrastructure, and enhanced connectivity for transshipment cargo. This approach helps alleviate capacity bottlenecks and response delays to cargo demand common in single-airport systems, especially in settings with high cargo volumes or constrained direct connections.

2.4.2 Challenges of hub-and-spoke model

Despite these advances, operational challenges persist. The traditional hub-and-spoke model in air cargo network with single airports serving as hubs, while efficient for consolidating demand, often results in prolonged cargo dwell times at hubs due to consolidation and transfer processes (Zheng et al., 2023). Moreover, limited direct connections between some airports may lead to extended delivery times and delayed responsiveness to just-in-time logistics requirements. In this context, considering MAS as a transfer hub introduces a promising alternative.

By harnessing the collective capabilities and connectivity of multiple airports in a region, MAS-based hub operations can reduce cargo waiting times, improve transshipment efficiency, and offer greater flexibility in routing. This approach not only enhances network performance but also addresses the limitations of single-hub systems, making it especially relevant for regions with dense airport clusters and high cargo throughput. Our study is thus motivated by the dual recognition of the pivotal role of hubs in air cargo networks and the growing need for innovation in cargo transfer operations. By focusing on MAS as a transfer hub, we seek to bridge the gap between network-level design and airport-level operational optimization, contributing new insights into the optimization and management of air cargo systems.

2.5 Summary of literature and research gaps

Despite substantial progress, the literature leaves four overarching gaps aligned with the four studies in this thesis. First, in multi-airport systems with connected major–reliever airports, existing models often simplify network structure, treat airports as largely independent, or fix ground connections exogenously. There is limited work that jointly models elastic passenger demand, path-dependent congestion, airfare setting, and endogenous investment in inter-airport ground connections under both cooperative and non-cooperative airline interactions, including bargaining with asymmetric power. To fill this research gap, Chapter 3 stylize a MAS including ground connection between a major and minor airport pair. Competition and cooperation among airlines are both analyzed under tractable model framework. Pricing strategies and investments on the ground connection services are investigated under various market structures. Empirical applications to real multi-airport regions is carried out by taking the Greater Bay Area MAS as an example.

Second, in managing unused belly capacity on passenger flights, many studies adopt deterministic or narrowly stochastic settings, with limited attention to simultaneous uncertainty in cargo arrivals, weights, flight capacities, and schedules. There is a shortage of scalable two-stage frameworks that couple mid-term capacity reservations with short-term cargo-to-flight assignments, supported by decomposition, bounding, and implementable heuristics that deliver stable, high-quality solutions at realistic sizes. Network interactions across OD pairs and joint planning with passenger baggage capacity are also underexplored. Comprehensively considering uncertainties of cargo demand and flight capacities existing in the air cargo allocation process, this thesis proposes a two-stage stochastic program to model the air cargo-to-flight allocation problem in Chapter 4. Solving framework including multiple technologies is designed and proved to be efficient in obtaining high-quality solutions.

Third, in air–high-speed rail competition, much of the literature relies on representative or segmented demand models that do not capture continuous heterogeneity in travelers' mode preferences. Transparent comparative statics linking prices, capacities, costs, and congestion across modes are limited, and operator objectives that combine profit and social welfare—relevant where HSR has public-service mandates—are not widely incorporated. Empirical calibration using revealed and stated-preference data is also limited, reducing the reliability of pricing implications. Chapter 5 applies a two-mode competition model based on the Hotelling model framework, observing the travelers' choices between AT and HSR. Travelers' inherent mode preference distributions are considered in the formulation of tractable models. Various distribution functions are assumed in the numerical studies and resulting pricing decisions, profits of AT and HSR, and the consumer surplus of the two modes are obtained to prove the importance and necessity of the consideration of travelers' inherent heterogeneous preferences on mode in affection operations of airline operators and performance of the system.

Fourth, for integrated cargo transfer within multi-airport systems, studies often abstract from heterogeneous dwell times at minor and major airports and from tight time-feasibility constraints when coupling air legs with inter-airport trucking. While column generation and branch-and-price are well established in related domains, their adaptation to joint air–ground–air cargo routing with large strategy spaces and realistic capacity coupling is underdeveloped. Assumptions of complete information and single-agent control further limit applicability to real operations that involve uncertainty, contractual frictions, and heterogeneous access rights among forwarders, airlines, and airports. To fill this gap, Chapter 6 takes a MAS as a cargo transfer hub, including minor airports, major airports, and ground connection between each minor-major pair. Cargo-to-transfer-route allocation inside the MAS is formulated as an integer linear program. Solving framework inspired by the Branch and Price method is proposed to get high-quality integer solution within short time limits. In the numerical experiments, taking the Great Bay Area MAS as a real-world example, the proposed solving framework is proved to outperforms the baseline heuristic algorithm and the commercial solver in both solution quality and computational time.

Addressing these four gaps motivates the thesis, it develops tractable models of airline pricing and investment in connected MAS, a scalable stochastic framework for belly capacity management, an intermodal competition model with heterogeneous preferences and policy-relevant objectives, and an optimization and algorithmic framework for MAS-based cargo transfers that captures operational realism and remains computationally practical.

Chapter 3

On the competition and collaboration in a multi-airport system considering ground connection between airports

This chapter examines passenger travel choices and airline decisions in a multi-airport system (MAS) with two major airports and one reliever airport. The reliever airport is connected to one major airport through ground transportation that allows cross-airport ground transfers, while the connection to the other major airport is minimal. Each airport is served by a single dominant airline. Within this stylized MAS framework, passengers have the following options: travel directly through either major airport to reach their destinations, travel to the reliever airport and then transfer to the connected major airport, or choose other alternatives, i.e., elastic demand. We model equilibrium travel choices of passengers and analyze how various system parameters affect this equilibrium. Furthermore, we investigate the airlines' optimal pricing strategy and investment strategy for the ground connection service between the reliever and major airports, considering both non-cooperative and cooperative game frameworks, while accounting for the bargaining power dynamics among cooperating airlines. Our major findings are as follows. (i) In the cooperative game, the ratio of airlines' payoffs and investments in ground connection improvements by the two cooperating airlines corresponds directly to the ratio of their bargaining power. (ii) Cooperation between the airlines serving the minor airport and the connected major airport yields substantial profits, especially under improved ground connection services. (iii) The greater the congestion relief provided by the minor airport and the ground connection to the major airport, the higher the additional profits and stronger competitiveness can be generated through cooperation, and the more willing the major airport is to invest in ground connection improvements.

3.1 Introduction

In the context of MAS with ground transportation connection services, this chapter explores the interactions between passengers' travel route choices and airlines' pricing strategies and investment decisions for the inter-airport ground connection services under cooperative games and non-cooperative games. Firstly, a stylized MAS comprising two major airports and a reliever airport is proposed. The stylized MAS considers ground connection services between one major airport and the reliever airport, which allows cross-airport transfer. The ground connection between the two airports allows passengers to arrive at the reliever airport through domestic air travel and depart from the major airport to their overseas destination. We develop an analytically tractable model to represent the stylized MAS and capture the passenger choice equilibrium (i.e., user equilibrium or UE flow pattern). Comparative statics has been carried out to investigate the effects of system parameters on passengers' travel choices. We then further examine airlines' pricing and investment strategies (in the ground connection services) to maximize profits, subject to the user equilibrium passenger flow pattern or travel path choices. In particular, airlines' pricing strategies and decisions on investments in ground connection services are explored under both cooperative and non-cooperative games, while accounting for bargaining power dynamics of cooperating airlines. The above problem setting is indeed motivated by the aforementioned real-world airport cluster example (Hong Kong - Zhuhai - Guangzhou) in the Guangdong-Hong Kong-Macao Greater Bay Area (GBA), highlighting the practical meaning of the stylized structure of our studies MAS. Numerical studies have also been conducted in the context of GBA to illustrate the analytical models and provide further understanding.

The main contributions of this chapter are summarized below. Firstly, this chapter develops tractable models and provides an economic analysis for understanding the competition and cooperation in a MAS considering the ground connection between airports. Secondly, in the context of MAS with ground connection between airports, this chapter examines how different system parameters and airlines' pricing and investment decisions will affect passenger travel choice and system performance, and analyzes the optimal pricing and investment decisions. The optimal decisions of airlines under cooperative and non-cooperative games are derived and compared, offering insights into the influence of the ground connection on airlines' operational strategies. Additionally, the bargaining powers in cooperative games are incorporated into the analysis, broadening the scope of application scenarios explored in our study. Thirdly, analytical and numerical studies provide some understanding regarding the MAS, with an emphasis on the impacts of ground connection services on airport congestion and different competition and collaboration relationships among airlines. Results demonstrate the significance of improved ground connection services, cooperation between the airports related to the ground connection, stronger airport congestion relief provided by the ground connection and the minor airport and optimized pricing strategies in attracting air travel demand, strengthening the competitiveness of cooperating airlines and attaining enhanced profitability within MAS.

In particular, we have the following major observations/results. Improved ground connection services increase profitability for airlines serving the major airport which is connected by the inter-airport ground connection. Cooperation between the two airlines based on the connected major airport and reliever airport may benefit not only the two airlines but also the non-cooperative airline based on the other airport within MAS, especially when only weaker congestion relief can be provided to the major airport connected to the minor airport by ground modes. In contrast, under the non-cooperative game between the two airlines based on the connected major airport and reliever airport, both the airline serving the reliever airport and the airline serving the other major airport (not connected to the reliever airport) will have less economic gains. This means that reliever airport-serving carriers should engage in cooperative efforts with major airport operators. Additionally, when an airline operates only one segment of a route, collaboration with the corresponding airline for the complementary segment of the air travel route is crucial. Under mild conditions, we show that lower airfares, shorter travel times, and greater airport capacities along a given (travel) path within the MAS result in increased passenger flow on that path, decreased flow on alternative paths, and a reduced minimum travel price between the origin and destination. Additionally, increased investments in ground connection services between the major airport and the reliever airport are likely to attract a larger number of passengers to the path involving cross-airport ground transfers. When stronger congestion relief can be provided by the ground connection and the minor airport, the connected major airport tends to provide more investments in improving the ground connection services.

The rest of the chapter is organized as follows. Section 3.2 provides the problem setting and the model formulation in the stylized MAS structure. Section 3.3 analyzes different operation strategies of airlines and the corresponding profits. Section 3.4 conducts numerical studies. Section 3.5 concludes this chapter and discusses possible topics for future studies.

3.2 Model Formulation

3.2.1 Problem setting

As introduced earlier, this chapter is motivated by the MAS development in the Greater Bay Area. As shown in Fig. 3.1, Hong Kong International Airport is collaborating with Zhuhai Jinwan Airport (connected via the Hong Kong-Zhuhai-Macau bridge and facilitated with simplified custom procedures), which together compete with Guangzhou Baiyun Airport. Inspired by such a real-world scenario, we consider a stylized MAS with two major airports and one reliever airport. The reliever airport is connected to one major airport through ground transportation, while its connection to the other major airport is minimal.

Given the considered MAS with two major airports and one reliever airport, we consider an (aggregate) representative origin-destination (OD) pair with a domestic origin airport and an overseas destination airport. The transportation network between the OD pair with

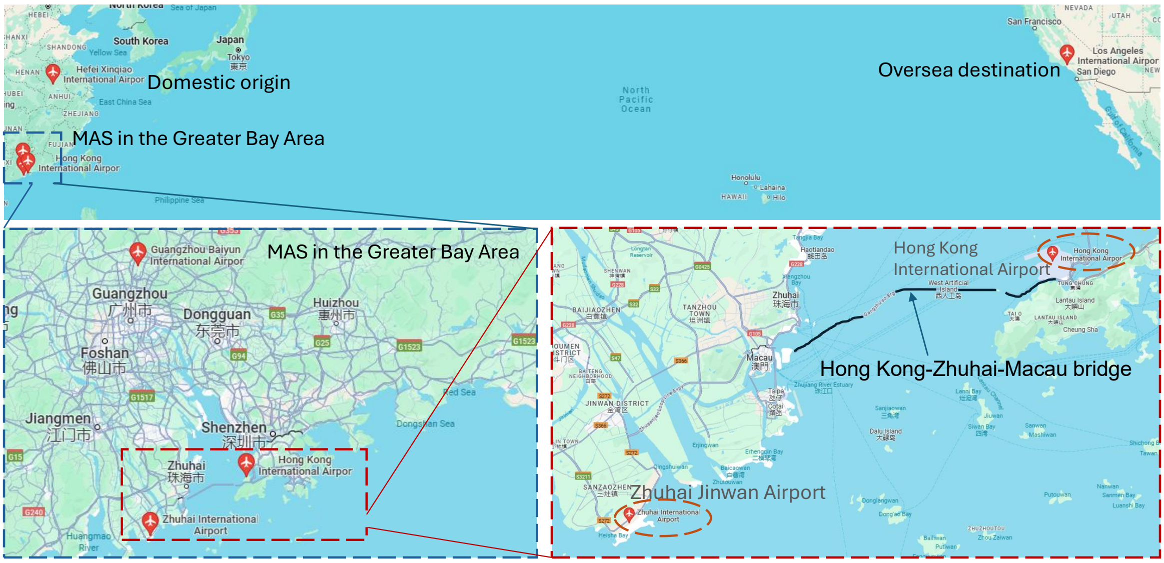

Figure 3.1: An example of a MAS in the Greater Bay Area and an OD pair served by the MAS (sourced from Google Map)

a stylized MAS is depicted in Fig. 3.2. The MAS includes three airports denoted by i, j, and k, where airports i and j are considered major international airports, offering extensive international travel services, while Airport k functions as a smaller reliever airport primarily serving domestic travel. The MAS serves an aggregate origin-destination pair, where O and D represent the origin and destination, respectively. Within this MAS framework, there are three travel routes: (i) from origin airport O to international Airport j, followed by a connection from Airport j to the overseas destination airport D (O-j-D); (ii) from origin airport O to Airport i, utilizing air services from Airport i to reach the overseas destination D (O-i-D); and (iii) from origin airport O to reliever Airport k, transferring to international Airport i, and subsequently taking a flight from Airport i to reach the overseas destination D (O-k-i-D). This stylized network structure enables the formulation of a tractable model and analytical examination of airline strategies and passenger travel choices under different market structures within the MAS.

Within the framework of the stylized network, the three airports in the multi-airport system (MAS) exhibit spatial proximity. Airport k and Airport i are connected through ground connection services, e.g., rail or rapid shuttle bus (such as the connection between the two collaborating airports: Hong Kong International Airport and Zhuhai Jinwan Airport),

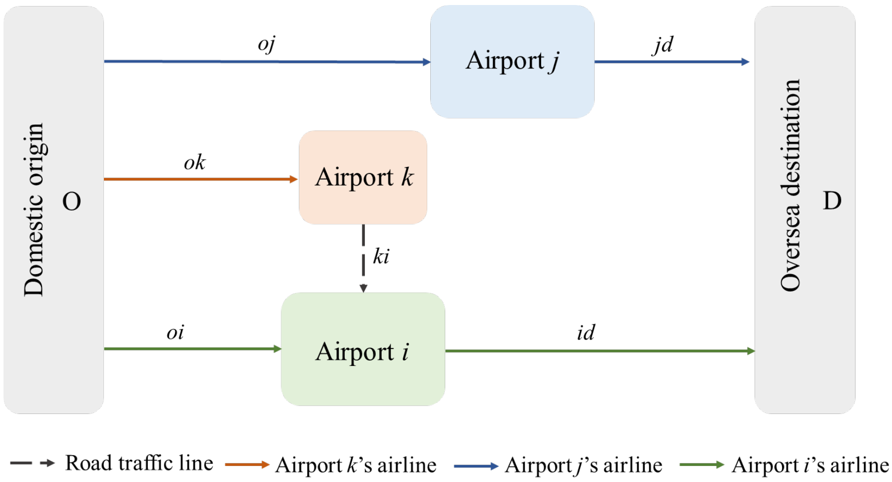

Figure 3.2: The stylized MAS structure

while Airport j and Airport k have limited connection (e.g., Zhuhai Jinwan Airport is collaborating with Hong Kong International Airport and its connection to Guangzhou Baiyun Airport is minimal/inconvenient). Note that as the two major airports are close to each other (e.g., Hong Kong and Guangzhou are close), it is considered that their service coverage is similar, i.e., they serve the same pool of passengers (who travel from domestic origins to international destinations). In line with this, as mentioned earlier, we consider an aggregate OD pair where we have a domestic origin and an overseas destination.

Before moving to the detailed model formulation, we summarize the main notations in Table 3.1.

3.2.2 Assumptions

We now outline major assumptions in this chapter and provide discussions.

Assumption 1. We consider homogeneous passengers, i.e., same OD pair (aggregate OD pair) and same user preferences.

Assumption 2. Air passengers are assumed to have complete information of the travel costs associated with each air travel route through the MAS (from information provided by airports/airlines and their past experience) and passengers are assumed to select the travel route that minimize their individual travel cost (includes both monetary cost and time-related cost).

Table 3.1: List of main notations for the MAS

Notation	Definition
A	Set of airports in the MAS, $A = \{i, j, k\}$
A_m	Set of airports on path m, $m \in M$. $A_1 = \{i\}$, $A_2 = \{j\}$, and $A_3 = \{i, k\}$
C_a	Capacity of airport a, $a \in A$
h_m	Investment in the ground connection between a major airport and the reliever airport from the airline operating along path m, $m = 1, 3$
L	Set of links, $L = \{oi, id, ok, ki, oj, jd\}$
L_m	Link set of path m, $m \in M$. $L_1 = \{oi, id\}$, $L_2 = \{oj, jd\}$, and $L_3 = \{ok, ki, id\}$
M	Set of paths, $M = \{1, 2, 3\}$, $m = 1$ means path O-i-D, $m = 2$ means path O-j-D, $m = 3$ means path O-k-i-D
T_a	Transfer cost in airport a, $a \in A$
M_a	Set of paths passing through airport a, $a \in A$. $M_i = \{1, 3\}$, $M_j = \{2\}$, and $M_k = \{3\}$
d_a	Congestion delay in airport a, $a \in A$
q_m	Passenger flow on path m, $m \in M$
q	Total demand between the origin and destination
$\mathbf{q}$	Passenger flow vector, $\mathbf{q} = (..., q_m, ...)$, $m \in M$
t_l	On-board travel time in link l, $l \in L$
V_a	Passenger volume in airport a; Passenger flows can only be accumulated once
α	Value of air-travel time of passengers
β	Value of road-travel time of passengers
δ_m	Binary variable, indicating whether passengers on path m need to take road traffic to cover the ground connection
τ_l	Transport ticket price (airfare) of link l
τ_m	Transport ticket price (airfare) of path m

Assumption 3. The airlines are profit-driven, i.e., their pricing strategies and investment decisions aim to maximize profits.

Assumption 1 simplifies the analysis by considering an aggregate (average) OD pair with homogeneous passengers. This treatment ignores user heterogeneity but focuses on an "aggregate and average" situation, which is a limitation of the current study. Future studies may further incorporate user heterogeneity while the analysis will be less tractable and more numerical-based. Assumption 2 assumes rational passengers with proper information on travel costs of different travel options. This is a widely used assumption for modeling user choice equilibrium and in this chapter it follows that a passenger choice equilibrium will exist. Note that if passengers are less rational and information is more limited, the choice pattern will deviate more from the modeled equilibrium. Further studies may consider non-equilibrium user choices (e.g., uncertainties and time-dependency). Assumption 3 states that airlines aim to maximize their profits. This reflects the current practice. Limitations associated with the above assumptions and potential future research will be more thoroughly discussed in Section 3.5.

3.2.3 Travel cost and passenger demand

As shown in Fig. 3.2, the airlines in the stylized MAS structure are directly associated with specific paths/links (Hou et al., 2022). In the subsequent illustration, the airlines operating along links on Path 1 and Path 2 are denoted as Airline O-i-D and Airline O-j-D, respectively. The airline operating on the first segment of Path 3 (i.e., link ok) is denoted as Airline O-k. The second segment of Path 3 (i.e., link id) is served by Airline O-i-D.

3.2.3.1 Travel cost or trip full price

For the three travel path options shown in Fig. 3.2 (i.e., O-j-D, O-i-D, O-k-i-D), we now formulate the travel costs or full prices. In this chapter, it is assumed that passengers possess accurate knowledge of flight schedules prior to their departures. The consideration of waiting time at the origin (O) is not explicitly modelled (implying the same average wait time at the origin for passengers). A detailed illustration of travel full prices is shown in Fig. 3.3, expressed as costs in links including monetary costs (i.e. airfares), non-monetary costs (i.e., travel time), congestion delay in arrivals, departures, and transfer costs in every transfer. As a component of the travel full price, congestion delay refers to the crowding effect, delay or inconvenience incurred due to high demand (given the limited infrastructure resources of an airport). The average congestion time per flight at Airport i, j and k are modelled as functions $d_i\left(q_1, q_3, C_i\right)$, $d_j\left(q_2, C_j\right)$ and $d_k\left(q_3, C_k\right)$, respectively. Given identical passengers' value of time as a constant, d_a also represents the cost of congestion delay. Note that in many literatures like Gong et al. (2023), q is explained as the flight volume. In our study, we assume identical flights serving the stylized MAS with an equal loading factor, therefore, our measurement of congestion delay, taking q's as passenger flows, is equivalent to those in literature (Zhang & Zhang, 2006, 2010). Moreover, our measurement facilitates modelling the transfer behaviour of passengers in the MAS. The parameter C_a represents the maximum capacity of airport a in terms of runway and terminal handling for flights (Gong et al., 2023). In the context of the air travel network with the stylized MAS structure, transfer costs T_a encompass various expenses associated with queuing or other processes such as check-in, security checks, boarding, and disembarking. With the current MAS setting, passengers need to complete two air journeys involving transfers (either intra-airport or cross-airport). Passengers taking Path 3 experience additional ground travel associated with the cross-airport transfers. Later, we will consider whether airlines might be incentivized to invest in ground connection services or not in order to improve the competitiveness of the travel option with cross-airport transfers (Path 3) (the investment is denoted by h).

It is noteworthy that there is a minimum connection time requirement when passengers transfer within the same airport or between different airports. This minimum connection time represents the time it takes for passengers to move from the arrival gate of their first flight to the departure gate of their connecting flight. The transfer cost accounts for the waiting time and other necessary procedures during the transfer process, such as queuing for security checks or boarding. Therefore, the transfer cost can be seen as a measure of discomfort caused by the queuing experience or other processes during the transfer. The minimum connection time is considered as a fixed value and is incorporated into the transfer cost formulation. The transfer cost is influenced by the passenger flow (for transfers within the same airport) and/or ground connection services (for transfers between different airports). Note that the connection time from the ground connection service is explicitly modelled (i.e., a constant cost is added to the cost formulation besides the transfer cost). In 8.1.4, we provide an analytical example where transfer cost functions explicitly include the minimum connection time.

Let p_1, p_2, and p_3 represent the travel full price of Path 1, Path 2 and Path 3, respectively. q_1, q_2, and q_3 denote passenger flows in Path 1, Path 2 and Path 3, respectively. Passengers travelling through Path 1 are served by Airline O-i-D. The air travel begins with the first leg, link oi, incurring an airfare cost of τ_{oi} and a bare travel time of t_{oi}. Upon arrival at Airport i, passengers on Path 1 encounter congestion delays at Airport i during landing and departure. The congestion delay in Airport i, d_i, is expressed as a function $d_i(q_1, q_3, C_i)$. Therefore,

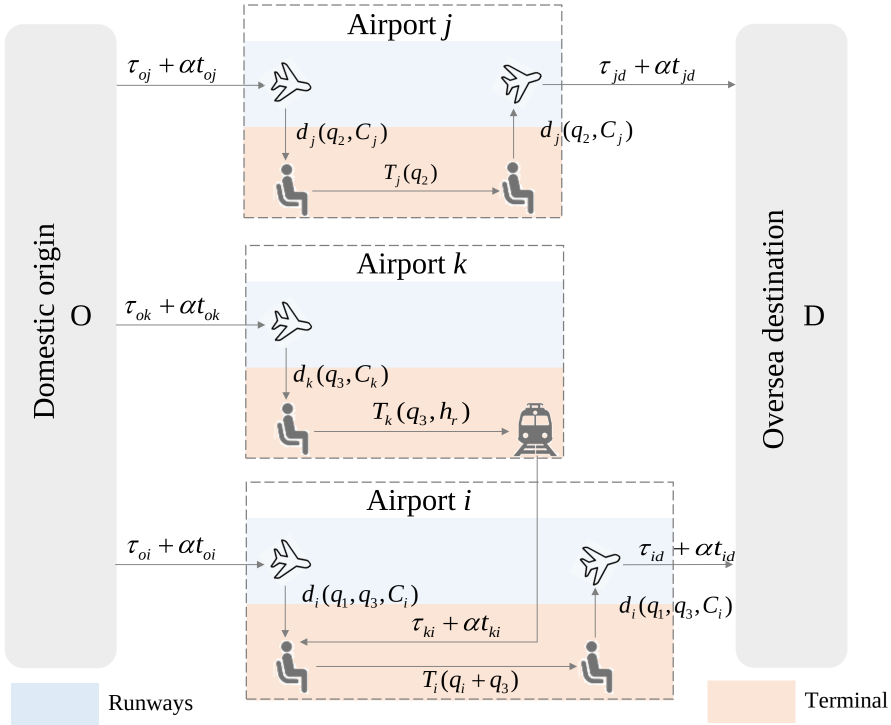

Figure 3.3: Detailed link cost in MAS structure

when calculating the travel full price of Path 1, p_1, the delay experienced in Airport i should be accounted for twice. Conversely, passengers on Path 3 only pass by Airport i during their departure. Passengers on Path 3 only experience congestion delay at Airport i during their departure. Consequently, the congestion delay in Airport i is accounted for once in the calculation of p_3. C_i is the capacity of Airport i. Notably, it is necessary to consider the different impacts of passengers on Path 1 and Path 3 on the congestion at Airport i, which will be discussed later. The concept of airport capacity encompasses a broad measure that signifies an airport's capability to accommodate travel demand. Some studies, such as Xiao et al. (2016), associate airport capacity with the infrastructure and resources available within the airport. Building upon the work of Gong et al. (2023), this chapter adopts a definition of airport capacity as the maximum capacity of runways and terminal facilities to handle flights. Given the above assumed identical loading factor of flights, the airport capacity can also be interpreted as the capacity to handle passenger flows. This definition is used here given the acknowledged impact of airport capacity on congestion delays during the air travel process. Additionally, there is a transfer cost at Airport i denoted as $T_i(V_i) = T_i(q_1 + q_3)$.

Finally, passengers incur an airfare cost of τ_{id} for the air travel on link id and a monetary value for the travel time t_{id}. The formula for p_1 can be expressed as Eq. (3.1).

$$p_1 = p_1 (q_1, q_3) = \tau_{oi} + \alpha t_{oi} + 2d_i (q_1, q_3, C_i) + T_i (q_1 + q_3) + \tau_{id} + \alpha t_{id} \tag{3.1}$$

For passengers choosing Path 2 served by Airline O-j-D, the full price of the entire journey, p_2, is the sum of the travel costs from O to j and from j to D. Passengers are required to pay the airfare τ_{oj} for link oj and the travel time t_{oj}, multiplied by the factor α, which represents the value of travel time. At Airport j, passengers on Path 2 will experience congestion delays at Airport j on both landing and departure occasions. Therefore, when calculating p_2, d_j should be accounted for twice, i.e., $2d_j \left(q_j, C_j\right)$ should be included in p_2 formulation. Besides, passengers opting for Path 2 need to pay a transfer cost defined as a function $T_j \left(V_j\right) = T_j (q_2)$, airfare τ_{jd} and the travel time t_{jd} for traversing link jd. p_2 is provided in Eq. (3.2).

$$p_2 = p_2 (q_2) = \tau_{oj} + \alpha t_{oj} + 2d_j \left(q_2, C_j\right) + T_j (q_2) + \tau_{jd} + \alpha t_{jd} \tag{3.2}$$

Passengers choosing path 3 experience twice transfers, twice air travel, and a road trip. For completing the journey passing link ok, airfare τ_{ok} and monetary form of travel time t_{ok}, αt_{ok}, should be paid. In Airport k, as passengers on Path 3 leave Airport k by ground connection, these passengers only need to face arrival congestion which cost $d_k (q_3, C_k)$ in Airport k. Passengers who choose Path 3 encounter congestion delay at Airport i during arrival and experience another congestion delay at Airport k during departure, as they depart from Airport k and arrive at Airport i via ground travel service. Therefore, congestion delay d_k and d_i are both calculated once in the formulation of p_3.

Analyzing the detailed calculation of travel prices reveals that improved ground connections have the potential to alleviate congestion at Airport i by reducing runway crowding (i.e., reducing air traffic at Airport i while passengers travel to the airport via the reliever airport and ground transportation). Furthermore, when comparing the formulation of p_1

and p_3, it becomes evident that passengers on Path 3 encounter lower congestion delays at Airport i. This reduced congestion delay may contribute to the appeal and attractiveness of Path 3 for passenger demand. Transfer cost $T_k\left(q_3, h\right)$ depends not only on path flow but also on the investment in ground connection services. Under more investment, we consider that the transfer will be more convenient, i.e., $T'_{k,h} = \frac{\partial T_k}{\partial h} < 0$. Investment in ground connection services h is considered to come from airlines on Path 1 (h_1) and Path 3 (h_3) because the ground connection is built between Airport i and Airport k, i.e., $h = h_1 + h_3$. The travel from Airport k to Airport i is completed by road transport system, the full price of this travel is represented by the summation of airfare τ_{ki} and monetary form of travel time t_{ki}, αt_{ki}. Passengers on Path 3 arrive Airport i by the ground connection, so they experience congestion delay in Airport i once (only departure congestion cost $d_i\left(q_1, q_3, C_i\right)$) and transfer cost $T_i\left(q_1 + q_3\right)$ in Airport i. Last, the travel cost from Airport i to the destination is composed of airfare τ_{id} and monetary form of travel time, αt_{id}. The cost p_3 can be calculated by Eq. (3.3).

$$\begin{aligned} p_3 = p_3\left(q_3, q_1\right) = \tau_{ok} + \alpha t_{ok} + d_k\left(q_3, C_k\right) + T_k\left(q_3, h\right) \\ + \tau_{ki} + \beta t_{ki} + d_i\left(q_1, q_3, C_i\right) + T_i\left(q_1 + q_3\right) + \tau_{id} + \alpha t_{id} \end{aligned} \tag{3.3}$$

The costs in Eqs. (3.1)-(3.3) can be rewritten as Eq. (3.4) where we let $\tau_1 = \tau_{oi} + \tau_{id}$, $\tau_2 = \tau_{oj} + \tau_{jd}$, $\tau_{3,1} = \tau_{ok}$, $\tau_{3,2} = \tau_{id}$, $t_2 = t_{oj} + t_{jd}$. Note that $\tau_{3,2}$ is the airfare for passengers on Path 3 passing link id, which is independent of τ_1.

$$p_1 = p_1\left(q_1, q_3\right) = \tau_1 + \alpha\left(t_{oi} + t_{id}\right) + 2d_i\left(q_1, q_3, C_i\right) + T_i\left(q_1 + q_3\right) \tag{3.4a}$$

$$p_2 = p_2\left(q_2\right) = \tau_2 + \alpha t_2 + 2d_j\left(q_2, C_j\right) + T_j\left(q_2\right) \tag{3.4b}$$

$$\begin{aligned} p_3 =& p_3\left(q_3, q_1\right) = \tau_{3,1} + \alpha t_{ok} + d_k\left(q_3, C_k\right) + T_k\left(q_3, h_r\right) \\ &+ \tau_{ki} + \beta t_{ki} + d_i\left(q_1, q_3, C_i\right) + T_i\left(q_1 + q_3\right) + \tau_{3,2} + \alpha t_{id} \end{aligned} \tag{3.4c}$$

3.2.3.2 User equilibrium

Understanding the distribution of passenger flow within a MAS is crucial for assessing the level of service provided by the MAS and plays a vital role in enabling decision-makers to create strategic plans for future development. A stated preference (SP) survey conducted by Loo (2008) for passengers flying from Hong Kong International Airport to various destinations highlights the importance of factors such as airfare, access time, flight frequency, and the number of airlines in influencing passengers' air travel choices within a MAS. In this chapter, as formulated earlier, we consider the above major factors in travel costs and then adopt User Equilibrium (UE) model for modeling air passengers' travel path choices, which has been used in various transport networks (Wang et al., 2022b; Liu et al., 2020; Ma et al., 2023a). The UE model relies on Assumption 2, i.e., travelers have complete information on travel costs of different options. This is plausible in the context where technological advancements and online platforms have significantly improved the availability of detailed information on flight schedules, fares, and travel times for air passengers. It is noteworthy that in practice passengers may not always follow the UE-based choices, and other discrete choice models might be considered for future research, depending on local conditions/empirical evidence.

The total demand (q) for the three paths is considered as a decreasing function of the cost. Moreover, passengers select their paths that minimize their costs. The user equilibrium (UE) passenger flow satisfies Eq. (3.5).

$$q_m \left(p_m - p^*\right) = 0, m = 1, 2, 3 \tag{3.5a}$$

$$q_m \geq 0, m = 1, 2, 3 \tag{3.5b}$$

$$p_m - p^* \geq 0, m = 1, 2, 3 \tag{3.5c}$$

$$q = \sum_m q_m \tag{3.5d}$$

$$q = q\left(p^*\right) \tag{3.5e}$$

where p^* represents the minimum travel cost from the origin to the destination through the MAS. This chapter assumes that all passengers possess precise knowledge of the full price associated with each available path. Eq. (3.5a) signifies that, under the conditions of user equilibrium (UE), all travellers experience equal and minimal travel costs, denoted as $p_m^* = p^*, \forall m \in M$. Eq. (3.5b) imposes a non-negativity constraint on the passenger flows. Furthermore, Eq. (3.5c) shows that travel prices in all feasible solutions must not be lower than the minimum price. Eq. (3.5d) serves as the flow conservation constraint. Eq. (3.5e) illustrates that the total demand between the OD pair in the MAS is defined as elastic, represented as a function of p^*.

The interior equilibrium where $q_1, q_2, q_3 > 0$ can be defined by the conditions in Eq. (3.6).

$$p_1 = p_1 (q_1, q_3) = p^* \tag{3.6a}$$

$$p_2 = p_2 (q_2) = p^* \tag{3.6b}$$

$$p_3 = p_3 (q_1, q_3) = p^* \tag{3.6c}$$

$$q_1 + q_2 + q_3 = q \tag{3.6d}$$

$$q = q (p^*) \tag{3.6e}$$

$$q_m \geq 0, m = 1, 2, 3 \tag{3.6f}$$

Eq. (3.6a), Eq. (3.6b), and Eq. (3.6c) indicate that when the MAS reaches interior equilibrium, travel full prices on Path 1, Path 2, and Path 3 are identical and equal to the minimum travel price between the aggregate OD pair. Since passengers choosing Path 1 and Path 3 are required to transfer at Airport i, both p_1 and p_3 are dependent on the passenger flows q_1 and q_3. The travel price for Path 2 is solely influenced by the passenger flow q_2 as defined in Eq. (3.6b). Passenger flow conservation condition is expressed in Eq. (3.6d). The elastic demand function, defined in Eq. (3.6e), is associated with the minimum travel price (p^*) between the origin and destination (note that as assumed, $\partial q / \partial p^* \leq 0$). The non-negative constraint on passenger flow is provided in Eq. (3.6f).

The equivalent UE minimization program to Eq. (3.5) can be written as Eq. (3.7), considering that q_1 and q_3 both affect p_1 and p_3 (in a symmetric way).

$$\begin{aligned} min \quad z(\mathbf{q}) = \frac{1}{2} \sum_{m=1,3} \left(\int_0^{q_m} p_m(\omega, q_{m'})\, d\omega + \int_0^{q_m} p_m(\omega, 0)\, d\omega \right) \\ + \int_0^{q_2} p_2(\omega)\, d\omega - \int_0^{q} F(\omega)\, d\omega \end{aligned} \tag{3.7a}$$

subject to

$$\sum_m q_m = q, m = 1, 2, 3 \tag{3.7b}$$

$$q_m \geq 0, m = 1, 2, 3 \tag{3.7c}$$

where $F(\cdot)$ represents the inverse of the demand function, which is a decreasing function of the travel price between the OD pair, and $m, m' \in \{1, 3\}$ with $m \neq m'$. It can be demonstrated that the minimization program outlined above possesses a unique optimal solution if the condition in Eq. (3.8) holds, thereby establishing the uniqueness of the UE solution. The existence and uniqueness of an interior solution to the UE condition are discussed in Section 8.1.

$$2d'_{i,q_1}\left(d'_{k,q_3} + T'_{k,V_k}\right) + T'_{i,V_i}\left(d'_{k,q_3} + T'_{k,V_k} + d'_{i,q_1} - d'_{i,q_3}\right) > 0 \tag{3.8}$$

We further define a sufficient condition which can ensure the existence and uniqueness of the UE solution as

$$d'_{k,q_3} + T'_{k,V_k} + d'_{i,q_1} - d'_{i,q_3} > 0 \tag{3.9}$$

In our stylized MAS, the resources at Airport k are expected to be underutilized and capable of alleviating congestion at Airport i when Airport i experiences high levels of congestion due to high-level air travel demand. To encourage passengers to utilize Path 3 and integrate into the MAS, the travel service on this path should be designed to ensure lower congestion delays. Consequently, Condition (3.9) is generally expected to hold.

3.2.3.3 Comparative Statics

In this subsection, we explore the impact of various system parameters on the passenger flow distribution among paths and minimum travel price between the OD pair given the interior equilibrium solution obtained by substituting travel cost equations, i.e., Eqs. (3.1)-(3.3), to Eq. (3.6). We can derive equations about the first derivative of p^*, q_1, q_2, and q_3 to variables including τ_1, τ_2, $\tau_{3,1}$, $\tau_{3,2}$, τ_{ki}, t_{oi}, t_{id}, t_{oj}, t_{jd}, t_{ok}, t_{ki}, C_i, C_j, C_k, h_1, and h_3, as displayed in 8.1.3. Given that Condition (3.9) holds, i.e., with a unique UE solution, the effects of the system parameters are summarized in Table 3.2. It should be noted that we only utilize the generalized function form of congestion delay, transfer cost, and elastic demand (no specific form for each function is adopted) to generate the results in Table 3.2, i.e., the results are "general" (note that valid under our problem setting). Section 8.1.4 provides an analytical example with specific function forms (linear functions are adopted for cost components in the full cost functions).

Table 3.2: Effect of MAS parameters on passenger's travel choices under the user equilibrium state

$\partial y/\partial x$	τ_1	τ_2	$\tau_{3,1}$	$\tau_{3,2}$	τ_{ki}	t_{oi}	t_{id}	t_{oj}	t_{jd}	t_{ok}	t_{ki}	C_i	C_j	C_k	h_1	h_3
p^*	(+)	+	+	+	+	(+)	+	+	+	+	+	-	-	-	-	-
q_1^*	-	(+)	+	+	+	-	(-)	(+)	(+)	+	+	+	(-)	-	-	-
q_2^*	(+)	-	+	+	+	(+)	+	-	-	+	+	-	+	-	-	-
q_3^*	+	+	-	-	-	+	-	+	+	-	-	-	-	+	+	+

Note: "(+)" and "(−)" means that "+" and "−" hold when and only when Condition (3.10) holds

$$d'_{k,q_3} + T'_{k,V_k} + d'_{i,q_3} - d'_{i,q_1} > 0 \tag{3.10}$$

The condition depicted in Eq. (3.10) indicates that the marginal increase in the combined congestion delay cost and transfer cost at Airport k, resulting from the inclusion of additional passengers on Path 3, exceeds the marginal increase in arrival/departure congestion delay cost at Airport i caused by the presence of additional passengers on Path 3. By incorporating equivalent terms on both sides of the inequality in Eq. (3.10), the following result can be readily derived as Eq. (3.11).

$$\frac{\partial p_3}{\partial q_3} = d'_{k,q_3} + T'_{k,V_k} + d'_{i,q_3} + T'_{i,V_i} > d'_{i,q_1} + T'_{i,V_i} = \frac{\partial p_3}{\partial q_1} \tag{3.11}$$

By referring to Eq. (3.11), Eq. (3.10) can be explained as follows: given the current distribution of passenger flows, adding an extra passenger to Path 1 causes a greater marginal increase in the total travel cost of Path 3 than the increase in the travel cost of Path 3 caused by adding an extra passenger directly to Path 3. In practice, it is hard for the travel path, including the inter-airport transfer, to attract passengers, not to say help relieve the congestion in the major airport if the travel price of the path grows rapidly with the increase of passengers in the interacted path. Therefore, this condition is expected to be satisfied under our studied context.

Based on the condition expressed in Eq. (3.10) and the information presented in Table 3.2, we have the following observations. (i) Higher airfares (specifically τ_1, τ_2, $\tau_{3,1}$, and $\tau_{3,2}$) and longer travel times (namely t_{oi}, t_{id}, t_{oj}, t_{jd}, t_{ok}, and t_{ki}) result in increased minimum travel cost between the OD pair. Conversely, higher airport capacities (C_i, C_j, and C_k) and greater investment in the ground connection services (h_1 and h_3) lead to reduced minimum travel costs between the OD pair by reducing time-related expenses associated with congestion delays and transfers. (ii) Passengers exhibit a preference for a particular path when the airfares and travel times associated with that path decrease, or when the airfares or travel times of alternative paths increase. (iii) Higher capacities at airports i, j, and k respectively attract a larger passenger flow to select Path 1, Path 2, and Path 3, resulting in decreased passenger flow on other paths. (iv) Increased investment in the ground connection services (specifically larger values of h_1 and h_3) makes Path 3 more favorable compared to Path 2 and Path 1.

3.2.4 Airline Profit

An airline's profit is considered as the ticket revenue from passengers minus the airport charges and the operating costs associated with the passenger flow and the corresponding congestion delay. Consistent with the airfare expression in the formula of passenger's travel full price, The three airlines' profits can be formulated as Eq. (3.12).

$$\begin{aligned}\pi_1\left(\tau_1,\tau_{3,2}\right) &= \tau_1 q_1 + \tau_{3,2} q_3 - \rho_{i,1} q_1 - \rho_{i,3} q_3 - \left(w_{oi,1} + w_{id,1}\right) q_1 - w_{id,3} q_3 \\ &\quad - \mu_{i,1} d_i\left(q_1, q_3, C_i\right) q_1 - \mu_{i,3} d_i\left(q_1, q_3, C_i\right) q_3\end{aligned} \tag{3.12a}$$

$$\pi_2(\tau_2) = \tau_2 q_2 - \rho_{j,2} q_2 - \left(w_{oj,2} + w_{jd,2}\right) q_2 - \mu_{j,2} d_j\left(q_2, C_j\right) q_2 \tag{3.12b}$$

$$\pi_3(\tau_{3,1}) = \tau_{3,1} q_3 - \rho_{k,3} q_3 - w_{ok,3} q_3 - \mu_{k,3} d_k\left(q_3, C_k\right) q_3 \tag{3.12c}$$

where π_1, π_2, π_3, are profits of the Airline O-i-D, Airline O-j-D, Airline O-k, which are operating on Path 1, Path 2, and the first segment of Path 3, respectively. Airline O-i-D also provides air travel services on the second segment of Path 3 (i.e., link id). In Eq. (3.12a), τ_1 represents the total airfare of Path 1. $\tau_{3,2}$ mean the airfare of the second segment of Path 3. $\rho_{i,1}$ and $\rho_{i,3}$ are airport charge at Airport i per passenger on Path 1 and per passenger on Path 3, respectively. $w_{oi,1}$ and $w_{id,1}$ are the fixed costs for transporting passengers through link oi and link id on Path 1, respectively. $w_{id,3}$ is the fixed transporting cost in link id on Path 3. $\mu_{i,1} d_i$ represents the average congestion delay cost per passenger on Path 1 at Airport i. Similarly, $\mu_{i,3} d_i$ denotes the average congestion delay cost per passenger on Path 3 at Airport i. In Eq. (3.12b), τ_2 indicates the total airfares of Path 2. $\rho_{j,2}$ is airport charge at Airport j per passenger on Path 2. $w_{oj,2}$ and $w_{jd,2}$ represent the fixed costs of Airline O-j-D operating on link oj and link jd, i.e., two segments of Path 2. $\mu_{j,2} d_j$ means the average congestion delay cost at Airport j of each passenger on Path 2. In Eq. (3.12c), $\tau_{3,1}$ means the airfare of the first leg of Path 3. $\rho_{k,3}$ is airport charge at Airport k of each passenger on Path 3. $w_{ok,3}$ is the fixed transporting cost in link ok on Path 3. $\mu_{k,3} d_k$ is the extra cost per passenger on Path 3 brought by air traffic congestion in Airport k. Passengers are supposed to pay the total airfare for the chosen routes instead of paying for every leg separately. Passengers on Path 1 or Path 2 pay for the two legs of their chosen routes simultaneously to the same carrier while the passengers choosing Path 3 pay for the two segments of Path 3 to different carriers but in a single order.

3.3 Different operation regimes of airlines

This section examines four cases with regard to different competitive/collaborative relationships among airlines and decisions regarding pricing strategies and investments in inter-airport ground connection services. Follow related literature (Pels et al., 2000; Zhang & Zhang, 2010; Li et al., 2022; Gong et al., 2023), profit-maximization-oriented airlines are considered in this chapter. Specifically, the four cases considered are summarized in Table 3.3. Case 1 and Case 2 consider airlines' decisions on airfares under the given inter-airport ground connection while Case 3 and Case 4 take both airfares and investments (from Airline O-i-D and Airline O-k) in the ground connection services as decision variables. In Case 1 and Case 3, the three airlines operate under the Nash game where each operator optimizes their individual profit by choosing optimal decision variables. Consequently, Case 1 and Case 3 are referred to as non-cooperative games in this chapter. Case 2 and Case 4 explore cooperative games where cooperation exists between Airline O-i-D and Airline O-k, i.e., Nash bargaining game to maximize their joint payoff. Airline O-j-D aims to maximize its own profit subject to the cooperation of the other two airlines.

Table 3.3: Four cases examined in this chapter

		Nash game	Nash bargaining game	Investment in the ground connection
Case 1	Airline O-i-D	✓		
	Airline O-j-D	✓		
	Airline O-k	✓		
Case 2	Airline O-i-D		✓	
	Airline O-j-D	✓		
	Airline O-k		✓	
Case 3	Airline O-i-D	✓		✓
	Airline O-j-D	✓		
	Airline O-k	✓		✓
Case 4	Airline O-i-D		✓	✓
	Airline O-j-D	✓		
	Airline O-k		✓	✓

3.3.1 Airline operations under given inter-airport ground connection

In this subsection, we consider the cooperative game and the non-cooperative game under the given ground connection services between Airport i and Airport k. The optimal airfares are derived and analyzed.

3.3.1.1 Non-cooperative game

This subsection considers the Nash equilibrium among the three airlines, where the airline operators maximize their individual profits simultaneously by choosing the optimal airfares. It should be noted that the investments in the inter-airport ground connection from Airline O-i-D and Airline O-k operators are not considered, i.e., the ground connection service between Airport i and Airport k refers to given ground transport services. Airline operators under Nash game with given ground connection services solve:

$$max \quad \pi_1 = \pi_1\left(\tau_1, \tau_{3,2}\right) \tag{3.13a}$$

$$max \quad \pi_2 = \pi_2\left(\tau_2\right) \tag{3.13b}$$

$$max \quad \pi_3 = \pi_3\left(\tau_{3,1}\right) \tag{3.13c}$$

Considering interior solutions to the airline operator's profit maximization problem, we can derive the first-order optimality conditions, as expressed in Eq. (3.14).

$$\begin{aligned} & q_1 + \tau_1\frac{\partial q_1}{\partial \tau_1} - \rho_{i,1}\frac{\partial q_1}{\partial \tau_1} - \left(w_{oi,1} + w_{id,1}\right)\frac{\partial q_1}{\partial \tau_1} - \mu_{i,1}d_i\frac{\partial q_1}{\partial \tau_1} - \mu_{i,1}q_1 d_{i,q_1}^{'}\frac{\partial q_1}{\partial \tau_1} - \mu_{i,3}q_3 d_{i,q_1}^{'}\frac{\partial q_1}{\partial \tau_1} \\ & + \tau_{3,2}\frac{\partial q_3}{\partial \tau_1} - \rho_{i,3}\frac{\partial q_3}{\partial \tau_1} - w_{id,3}\frac{\partial q_3}{\partial \tau_1} - \mu_{i,1}q_1 d_{i,q_3}^{'}\frac{\partial q_3}{\partial \tau_1} - \mu_{i,3}d_i\frac{\partial q_3}{\partial \tau_1} - \mu_{i,3}q_3 d_{i,q_3}^{'}\frac{\partial q_3}{\partial \tau_1} = 0 \end{aligned} \tag{3.14a}$$

$$\begin{aligned} & \tau_1\frac{\partial q_1}{\partial \tau_{3,2}} + \tau_{3,2}\frac{\partial q_3}{\partial \tau_{3,2}} - \rho_{i,1}\frac{\partial q_1}{\partial \tau_{3,2}} - \rho_{i,3}\frac{\partial q_3}{\partial \tau_{3,2}} - \left(w_{oi,1} + w_{id,1}\right)\frac{\partial q_1}{\partial \tau_{3,2}} - w_{id,3}\frac{\partial q_3}{\partial \tau_{3,2}} \\ & - \mu_{i,1}d_i\frac{\partial q_1}{\partial \tau_{3,2}} - \mu_{i,1}q_1 d_{i,q_1}^{'}\frac{\partial q_1}{\partial \tau_{3,2}} - \mu_{i,1}q_1 d_{i,q_3}^{'}\frac{\partial q_3}{\partial \tau_{3,2}} - \mu_{i,3}q_3 d_{i,q_3}^{'}\frac{\partial q_3}{\partial \tau_{3,2}} - \mu_{i,3}d_i\frac{\partial q_3}{\partial \tau_{3,2}} = 0 \end{aligned} \tag{3.14b}$$

$$q_2 + \tau_2\frac{\partial q_2}{\partial \tau_2} - \rho_{j,2}\frac{\partial q_2}{\partial \tau_2} - \left(w_{oj,2} + w_{jd,2}\right)\frac{\partial q_2}{\partial \tau_2} - 4\mu_{j,2}q_2 d_{j,Q_j}^{'}\frac{\partial q_2}{\partial \tau_2} - 2\mu_{j,2}d_j\frac{\partial q_2}{\partial \tau_2} = 0 \tag{3.14c}$$

$$q_3 + \tau_{3,1}\frac{\partial q_3}{\partial \tau_{3,1}} - \rho_{k,3}\frac{\partial q_3}{\partial \tau_{3,1}} - w_{ok,3}\frac{\partial q_3}{\partial \tau_{3,1}} - \mu_{k,3}d_k\frac{\partial q_3}{\partial \tau_{3,1}} - \mu_{k,3}q_3 d_{k,Q_k}^{'}\frac{\partial q_3}{\partial \tau_{3,1}} = 0 \tag{3.14d}$$

In Eq. (3.14a), given a marginal increase in airfare of link oi, the first term on the left-hand side, q_1, is the additional fare collected from the q_1 passengers due to the airfare increase; the second term, $\tau_1\frac{\partial q_1}{\partial \tau_1}$, is the marginal revenue loss due to a decreased air travel demand on Path 1 caused by the airfare of Path 1 increase; the third term, $-\rho_{i,1}\frac{\partial q_1}{\partial \tau_1}$, is the marginal saving on Airport i's charge under a decreased demand on Path 1; the fourth term, $-(w_{oi,1} + w_{id,1})\frac{\partial q_1}{\partial \tau_1}$, is the marginal saving on operating cost induced by decreased demand on Path 1 due to increased airfare on Path 1; the fifth term, $-\mu_{i,1} d_i \frac{\partial q_1}{\partial \tau_1}$, is the marginal saving on the total congestion delay (including the arrival and departure congestion delay) cost induced by the decreased demand on Path 1 caused by increased airfare on Path 1; the sixth term, $-\mu_{i,1} q_1 d^{'}_{i,q_1} \frac{\partial q_1}{\partial \tau_1} - \mu_{i,3} q_1 d^{'}_{i,q_3} \frac{\partial q_3}{\partial \tau_1}$, is the marginal saving on congestion delay cost due to released congestion in Airport i because of the decreased demand on Path 1 caused by airfare increase; the seventh term, $\tau_{3,2}\frac{\partial q_3}{\partial \tau_1}$, is the additional revenue of link id caused by the increased demand on Path 3 (thus in link id); the eighth term, $-\rho_{i,3}\frac{\partial q_3}{\partial \tau_1}$, is the Airport i's additional charge for increased demand on Path 3; the ninth term, $-w_{id,3}\frac{\partial q_3}{\partial \tau_1}$, is the additional operating cost increased by increased demand on Path 3 due to increased airfare on Path 1; the tenth term, $-\mu_{i,1} q_1 d^{'}_{i,q_3} \frac{\partial q_3}{\partial \tau_1}$, is the marginal increase of the total congestion delay cost related to passengers on Path 1 caused by increased passengers on Path 3 due to the increased airfare τ_1; the eleventh term, $-\mu_{i,3} d_i \frac{\partial q_3}{\partial \tau_1}$, is the marginal increase of congestion delay cost due to a increased demand on Path 3 caused by airfare of Path 1 increase; the last term, $-\mu_{i,3} q_3 d^{'}_{i,q_3} \frac{\partial q_3}{\partial \tau_1}$, is the marginal increase of congestion delay cost due to released congestion in Airport i because of a decreased demand on Path 3 caused by airfare of Path 1 increase. The fifth term and sixth term, and the tenth term and the eleventh term both show the two-way impact of airfare on the congestion delay: (i) change the passenger flow on the path; (ii) change the level of congestion in the airports.

In Eq. (3.14c), given a marginal increase in airfare of Path 2, the first term on the left-hand side, q_2, is the additional fare collected from the q_2 passengers due to the path airfare of Path 2 increase; the second term, $\tau_2\frac{\partial q_2}{\partial \tau_2}$, is the marginal revenue loss due to a decreased air travel demand on Path 2 caused by the path airfare increase; the third term, $-\rho_{j,2}\frac{\partial q_2}{\partial \tau_2}$, is the marginal saving on Airport j's charge under a decreased demand on Path 2; the fourth term, $-\left(w_{oj,2} + w_{jd,2}\right)\frac{\partial q_2}{\partial \tau_{oj}}$, is the marginal saving on operating cost induced by decreased demand on Path 2 due to increased path airfare; the fifth term, $-\mu_{j,2} d^{'}_{j,q_2} \frac{\partial q_2}{\partial \tau_2}$, is the marginal saving on the total congestion delay cost due to released congestion in Airport j because of a decreased demand on Path 2 caused by airfare increase; the sixth term, $-\mu_{j,2} d_j \frac{\partial q_2}{\partial \tau_{oj}}$, is the marginal saving on congestion delay cost induced by the decreased demand on Path 2 caused by increased airfare of Path 2.

In Eq. (3.14d), the first term in the left-hand side, q_3, is the additional revenue collected from the q_3 passengers due to the airfare of the first part of Path 3 increase; the second term, $\tau_{3,1}\frac{\partial q_3}{\partial \tau_{3,1}}$, is the marginal revenue loss due to a decreased air travel demand on Path 3 caused by the airfare increase; the third term, $-\rho_{k,3}\frac{\partial q_3}{\partial \tau_{3,1}}$, is the marginal saving on Airport k's charge under a decreased demand on Path 3; the fourth term, $-w_{ok,3}\frac{\partial q_3}{\partial \tau_{3,1}}$, is the marginal saving on operating cost in link ok induced by decreased demand on Path 3 due to increased airfare of link ok; the fifth term, $-\mu_{k,3}d_k\frac{\partial q_3}{\partial \tau_{3,1}}$, is the marginal saving on the arrival congestion delay cost in Airport k induced by the decreased demand on Path 3 caused by airfare $\tau_{3,1}$ increase; the sixth term, $-\mu_{k,3}q_3d^{'}_{k,q_3}\frac{\partial q_3}{\partial \tau_{3,1}}$, is the marginal saving on congestion delay cost due to released congestion in Airport k because of a decreased demand on Path 3 caused by airfare increase.

To facilitate the presentation and analysis, we define the total operating costs of airlines in Eq. (3.15).

$$W_{\pi_1}(q_1,q_3) = \left[\rho_{i,1} + \left(w_{oi,1} + w_{id,1}\right) + \mu_{i,1}d_i\left(q_1,q_3,C_i\right)\right]q_1 + \left[\rho_{i,3} + w_{id,3} + \mu_{i,3}d_i\left(q_1,q_3,C_i\right)\right]q_3 \tag{3.15a}$$

$$W_{\pi_2}(q_2) = \left[\rho_{j,2} + w_{oj,2} + w_{jd,2} + \mu_{j,2}d_j\left(q_j,C_j\right)\right]q_2 \tag{3.15b}$$

$$W_{\pi_3}(q_3) = \left[\rho_{k,3} + w_{ok,3} + \mu_{k,3}d_k\left(q_3,C_k\right)\right]q_3 \tag{3.15c}$$

and we can derive the first derivatives of the above-defined operating cost functions, as shown in Eq. (3.16).

$$W^{'}_{\pi_1,q_1} = \frac{\partial W_{\pi_1}}{\partial q_1} = \rho_{i,1} + w_{oi,1} + w_{id,1} + \mu_{i,1}d_i + \mu_{i,1}q_1d^{'}_{i,q_1} \tag{3.16a}$$

$$W^{'}_{\pi_1,q_3} = \frac{\partial W_{\pi_1}}{\partial q_3} = \rho_{i,3} + w_{id,3} + \mu_{i,1}q_1d^{'}_{i,q_3} + \mu_{i,3}d_i + \mu_{i,3}q_3d^{'}_{i,q_3} \tag{3.16b}$$

$$W^{'}_{\pi_2,q_2} = \frac{\mathbf{d}W_{\pi_2}}{\partial q_2} = \rho_{j,2} + w_{oj,2} + w_{jd,2} + \mu_{j,2}d_j + \mu_{j,2}q_2d^{'}_{j,q_2} \tag{3.16c}$$

$$W^{'}_{\pi_3,q_3} = \frac{\mathbf{d}W_{\pi_3}}{\partial q_3} = \rho_{k,3} + w_{ok,3} + \mu_{k,3}d_k + \mu_{k,3}q_3d^{'}_{k,q_3} \tag{3.16d}$$

By applying the point elasticity and the marginal total operating cost functions in Eq. (3.16), we can write Eq. (3.14) as Eq. (3.17).

$$\left(q_1 + q_1\sigma_{\tau_1}^{q_1}\right)\tau_1 + q_3\sigma_{\tau_1}^{q_3}\tau_{3,2} - W'_{\pi_1,q_3}q_3\sigma_{\tau_1}^{q_3} - W'_{\pi_1,q_1}q_1\sigma_{\tau_1}^{q_1} = 0 \tag{3.17a}$$

$$q_1\sigma_{\tau_{3,2}}^{q_1}\tau_1 + \left(q_3 + q_3\sigma_{\tau_{3,2}}^{q_3}\right)\tau_{3,2} - W'_{\pi_1,q_1}q_1\sigma_{\tau_{3,2}}^{q_1} - W'_{\pi_1,q_3}q_3\sigma_{\tau_{3,2}}^{q_3} = 0 \tag{3.17b}$$

$$\left(q_2 + q_2\sigma_{\tau_2}^{q_2}\right)\tau_2 - W'_{\pi_2,q_2}q_2\sigma_{\tau_2}^{q_2} = 0 \tag{3.17c}$$

$$\left(q_3 + q_3\sigma_{\tau_{3,1}}^{q_3}\right)\tau_{3,1} - W'_{\pi_3,q_3}q_3\sigma_{\tau_{3,1}}^{q_3} = 0 \tag{3.17d}$$

where $\sigma_x^y = \frac{\partial y}{\partial x}\frac{x}{y}$, indicating the point elasticity of y with respect to x. By solving Eq. (3.17), we have

$$\tau_1^{NE} = \frac{\sigma_{\tau_1}^{q_3}}{\left(1+\sigma_{\tau_1}^{q_1}\right)\left(1+\sigma_{\tau_{3,2}}^{q_3}\right) - \sigma_{\tau_1}^{q_3}\sigma_{\tau_{3,2}}^{q_1}}\frac{q_3}{q_1}W'_{\pi_1,q_3} + \frac{\left(1+\sigma_{\tau_{3,2}}^{q_3}\right)\sigma_{\tau_1}^{q_1} - \sigma_{\tau_1}^{q_3}\sigma_{\tau_{3,2}}^{q_1}}{\left(1+\sigma_{\tau_1}^{q_1}\right)\left(1+\sigma_{\tau_{3,2}}^{q_3}\right) - \sigma_{\tau_1}^{q_3}\sigma_{\tau_{3,2}}^{q_1}}W'_{\pi_1,q_1} \tag{3.18a}$$

$$\tau_2^{NE} = \frac{\sigma_{\tau_2}^{q_2}W'_{\pi_2,q_2}}{1+\sigma_{\tau_2}^{q_2}} = W'_{\pi_2,q_2} + \left(-\frac{1}{1+\sigma_{\tau_2}^{q_2}}\right)W'_{\pi_2,q_2} \tag{3.18b}$$

$$\tau_{3,1}^{NE} = \frac{\sigma_{\tau_{3,1}}^{q_3}W'_{\pi_3,q_3}}{1+\sigma_{\tau_{3,1}}^{q_3}} = W'_{\pi_3,q_3} + \left(-\frac{1}{1+\sigma_{\tau_{3,1}}^{q_3}}\right)W'_{\pi_3,q_3} \tag{3.18c}$$

$$\tau_{3,2}^{NE} = \frac{\left(1+\sigma_{\tau_1}^{q_1}\right)\sigma_{\tau_{3,2}}^{q_3} - \sigma_{\tau_1}^{q_3}\sigma_{\tau_{3,2}}^{q_1}}{\left(1+\sigma_{\tau_1}^{q_1}\right)\left(1+\sigma_{\tau_{3,2}}^{q_3}\right) - \sigma_{\tau_1}^{q_3}\sigma_{\tau_{3,2}}^{q_1}}W'_{\pi_1,q_3} + \frac{\sigma_{\tau_{3,2}}^{q_1}}{\left(1+\sigma_{\tau_1}^{q_1}\right)\left(1+\sigma_{\tau_{3,2}}^{q_3}\right) - \sigma_{\tau_1}^{q_3}\sigma_{\tau_{3,2}}^{q_1}}\frac{q_1}{q_3}W'_{\pi_1,q_1} \tag{3.18d}$$

It can be seen that the optimal airfare of Airline O-i-D and optimal airfare of the second part of Airline O-k (i.e., link id) under Nash Equilibrium are similar, where both consist of marginal impact of passenger demand of Path 1 and Path 3 on total operating cost of Airline O-i-D. Eq. (3.18b) and Eq. (3.18c) indicates that the optimal airfares increase more than marginal total operation cost given marginal increase of demand.

According to results in the comparative statics, we have $\sigma_{\tau_2}^{q_2} < 0$ and $\sigma_{\tau_{3,1}}^{q_3} < 0$. It can be further inferred that $\sigma_{\tau_2}^{q_2} < -1$ and $\sigma_{\tau_{3,1}}^{q_3} < -1$ given that the airfares are expected to be positive. This indicates that the operators of Airline O-j-D and Airline O-k operate on the elastic portion of the demand curve for the air travel services provided by the two airlines.

This means that a reduction of airfare for Path 2 (i.e., τ_2) increases total revenue for Airline O-j-D and a reduction of airfare for the first leg of Path 3 (i.e., $\tau_{3,1}$) increases total revenue for Airline O-k.

It can be readily shown that $\sigma_{\tau_1}^{q_1}\sigma_{\tau_{3,2}}^{q_3} = \sigma_{\tau_{3,2}}^{q_1}\sigma_{\tau_1}^{q_3}$, and Eq. (3.18a) and Eq. (3.18d) can be further simplified as follows:

$$\tau_1^{NE} = \frac{\sigma_{\tau_1}^{q_3}}{1+\sigma_{\tau_1}^{q_1}+\sigma_{\tau_{3,2}}^{q_3}}\frac{q_3}{q_1}W'_{\pi_1,q_3} + \frac{\sigma_{\tau_1}^{q_1}}{1+\sigma_{\tau_1}^{q_1}+\sigma_{\tau_{3,2}}^{q_3}}W'_{\pi_1,q_1} \tag{3.19a}$$

$$\tau_{3,2}^{NE} = \frac{\sigma_{\tau_{3,2}}^{q_3}}{1+\sigma_{\tau_1}^{q_1}+\sigma_{\tau_{3,2}}^{q_3}}W'_{\pi_1,q_3} + \frac{\sigma_{\tau_{3,2}}^{q_1}}{1+\sigma_{\tau_1}^{q_1}+\sigma_{\tau_{3,2}}^{q_3}}\frac{q_1}{q_3}W'_{\pi_1,q_1} \tag{3.19b}$$

We discuss two cases with different conditions about the denominator in Eq. (3.19). Firstly, we consider that $1+\sigma_{\tau_1}^{q_1}+\sigma_{\tau_{3,2}}^{q_3} > 0$, given $\sigma_{\tau_1}^{q_1} < 0$ and $\sigma_{\tau_{3,2}}^{q_3} < 0$, we then can derive that $-1 < \sigma_{\tau_1}^{q_1} < 0$ and $-1 < \sigma_{\tau_{3,2}}^{q_3} < 0$. This means that the operator of Airline O-i-D operates on the relatively flattened portion of the demand curve for the air travel services on Path 1 and the second leg of Path 3. Different from the results for airfares of Path 2 and the first leg of Path 3, an increase of airfare of Path 1 or airfare of the second leg of Path 3 is likely to increase total revenue for Airline O-i-D. Then we can get:

$$\sigma_{\tau_1}^{q_3} q_3 W'_{\pi_1,q_3} > -\sigma_{\tau_1}^{q_1} q_1 W'_{\pi_1,q_1} \tag{3.20a}$$

$$\sigma_{\tau_{3,2}}^{q_1} q_1 W'_{\pi_1,q_1} > -\sigma_{\tau_{3,2}}^{q_3} q_3 W'_{\pi_1,q_3} \tag{3.20b}$$

The product in the left-hand side of Eq. (3.20a) represents the impact of airfares for Path 1 (τ_1) on the passenger flow on Path 3 (the interacted path with Path 1) and then affects the total operating cost of Airline O-i-D. The right-hand side of Eq. (3.20a) indicates the impact of airfares for Path 1 (τ_1) on the passenger flow on Path 1 and then affects the total operating cost of Airline O-i-D. Similarly, the product in the left-hand side of Eq. (3.20b) represents the impact of airfares for the second leg of Path 3 ($\tau_{3,2}$) on the passenger flow on

Path 1 (the interacted path with Path 3) and then affects the total operating cost of Airline O-i-D. The right-hand side of Eq. (3.20b) indicates the impact of airfares for the second leg of Path 3 ($\tau_{3,2}$) on the passenger flow on Path 3 and then affects the total operating cost of Airline O-i-D. Therefore, it is expected that if Airline O-i-D operates on the relatively flattened portion of the demand curve for travel services provided on Path 1 and the second leg of Path 3 (link id), the increase in total operating cost of Airline O-i-D will primarily be caused by the influence of $\tau_{3,2}$ on q_1 and τ_1 on q_3, rather than the impact of $\tau_{3,2}$ on q_3 and τ_1 on q_1.

Conversely, if we consider that $1 + \sigma_{\tau_1}^{q_1} + \sigma_{\tau_{3,2}}^{q_3} < 0$, i.e., $\sigma_{\tau_1}^{q_1} + \sigma_{\tau_{3,2}}^{q_3} < -1$, which means that the operators of Airline O-i-D operate on the relatively elastic portion of the demand curve for the air travel services provided for Path 1 and the second leg of Path 3. then we can have

$$\sigma_{\tau_1}^{q_3} q_3 W'_{\pi_1,q_3} < -\sigma_{\tau_1}^{q_1} q_1 W'_{\pi_1,q_1} \tag{3.21a}$$

$$\sigma_{\tau_{3,2}}^{q_1} q_1 W'_{\pi_1,q_1} < -\sigma_{\tau_{3,2}}^{q_3} q_3 W'_{\pi_1,q_3} \tag{3.21b}$$

Eq. (3.21a) means that the marginal increased total operating cost of Airline O-i-D caused by the increased passenger flow in Path 3 induced by the increased τ_1 is larger than the marginal saving total operating cost of Airline O-i-D caused by the decreased passenger flow in Path 1 induced by the increased τ_1. Eq. (3.21b) means that the marginal increased total operating cost of Airline O-i-D caused by the increased passenger flow in Path 1 induced by the increased $\tau_{3,2}$ is larger than that the marginal saving total operating cost of Airline O-i-D caused by the increased passenger flow in Path 3 induced by the increased $\tau_{3,2}$.

By substituting Eqs. (3.18b)-(3.18c) and Eq. (3.19) into Eq. (3.12), we can derive the airline profits as follows:

$$\begin{aligned}\pi_1^{NE} = &\left(\frac{\sigma_{\tau_1}^{q_3} + \sigma_{\tau_{3,2}}^{q_3}}{1 + \sigma_{\tau_1}^{q_1} + \sigma_{\tau_{3,2}}^{q_3}} - 1\right) W'_{\pi_1,q_3} q_3 + \left(\mu_{i,1} q_1 d'_{i,q_1} + \mu_{i,3} q_3 d'_{i,q_3}\right) q_3 \\ &+ \left(\frac{\sigma_{\tau_{3,2}}^{q_1} + \sigma_{\tau_1}^{q_1}}{1 + \sigma_{\tau_1}^{q_1} + \sigma_{\tau_{3,2}}^{q_3}} - 1\right) W'_{\pi_1,q_1} q_1 + \mu_{i,1} q_1 d'_{i,q_1} q_1\end{aligned} \tag{3.22a}$$

$$\pi_2^{NE} = \left(\mu_{j,2} q_2 d'_{j,q_2} - \frac{1}{1+\sigma_{\tau_2}^{q_2}} W'_{\pi_2,q_2}\right) q_2 \tag{3.22b}$$

$$\pi_3^{NE} = \left(\mu_{k,3} q_3 d'_{k,q_3} - \frac{1}{1+\sigma_{\tau_{3,1}}^{q_3}} W'_{\pi_3,q_3}\right) q_3 \tag{3.22c}$$

In general, more passengers on Path 2 and Path 3 will bring more profits for Airline O-j-D and Airline O-k, respectively. The higher profits of the two airlines can be obtained by reducing airfares for the corresponding paths. Considering the two parameters in Eq. (3.15a) related to q_1 and q_3, we let:

$$R_{\pi_1,q_1} = \rho_{i,1} + w_{oi,1} + w_{id,1} + \mu_{i,1} d_i\left(q_1, q_3, C_i\right) \tag{3.23a}$$

$$R_{\pi_1,q_3} = \rho_{i,3} + w_{id,3} + \mu_{i,3} d_i\left(q_1, q_3, C_i\right) \tag{3.23b}$$

where R_{π_1,q_1} and R_{π_1,q_3} can be explained as the average total operating cost in Airline O-i-D per passenger on Path 1 and per passenger flow on Path 3, respectively. Then Eq. (3.22a) can be rewritten as:

$$\pi_1^{NE} = \left(\frac{\sigma_{\tau_1}^{q_3} + \sigma_{\tau_{3,2}}^{q_3}}{1+\sigma_{\tau_1}^{q_1} + \sigma_{\tau_{3,2}}^{q_3}} W'_{\pi_1,q_3} - R_{\pi_1,q_3}\right) q_3 + \left(\frac{\sigma_{\tau_{3,2}}^{q_1} + \sigma_{\tau_1}^{q_1}}{1+\sigma_{\tau_1}^{q_1} + \sigma_{\tau_{3,2}}^{q_3}} W'_{\pi_1,q_1} - R_{\pi_1,q_1}\right) q_1 \tag{3.24}$$

So it can be inferred that when the condition expressed in Eq. (3.25) holds, more passengers on Path 3 will bring more profits for Airline O-i-D, and when the condition indicated by Eq. (3.26) holds, attracting more passengers choosing Path 1 will benefit Airline O-i-D. This shows that when the marginal increased total operating cost caused by the additional passenger flow on a path reaches a certain proportion of the current average total operating cost per passenger in the path, then the airline should change pricing strategies to attract demand on the path.

$$\frac{\sigma_{\tau_1}^{q_3} + \sigma_{\tau_{3,2}}^{q_3}}{1+\sigma_{\tau_1}^{q_1} + \sigma_{\tau_{3,2}}^{q_3}} W'_{\pi_1,q_3} > R_{\pi_1,q_3} \tag{3.25}$$

$$\frac{\sigma_{\tau_{3,2}}^{q_1} + \sigma_{\tau_1}^{q_1}}{1+\sigma_{\tau_1}^{q_1} + \sigma_{\tau_{3,2}}^{q_3}} W'_{\pi_1,q_1} > R_{\pi_1,q_1} \tag{3.26}$$

3.3.1.2 Cooperative game

Given the MAS structure, it is evident that the passenger flow on Path 3 has implications for the profit of Airline O-i-D and also generates revenue for Airline O-k. Therefore, cooperation between Airline O-i-D and Airline O-k can be potentially beneficial. In this subsection, we examine the Nash bargaining game between Airline O-i-D and Airline O-k, where they jointly optimize their decision variables (τ_1, $\tau_{3,1}$, $\tau_{3,2}$) to maximize their joint payoff against a disagreement point, such as profits under Nash equilibrium (NE). The analysis of optimal airfares of Airline O-i-D and Airline O-k under Nash bargaining game is based on a disagreement point (π_1^{NE}, π_3^{NE}) under the Nash game, assuming the absence of collaboration between Airline O-i-D and Airline O-k. Following the idea applied in Huang et al. (2024), we consider the bargaining power difference between airlines serving Airport i and airlines serving Airport k. Then the optimization problem of the Nash Bargaining Game is given by:

$$\max U\left(\tau_1, \tau_{3,1}, \tau_{3,2}, h_1, h_3\right) = \left(\pi_1 - \pi_1^{NE}\right)^{\chi}\left(\pi_3 - \pi_3^{NE}\right)^{1-\chi}, \tag{3.27}$$

subject to (i) $\pi_3 \geq \pi_3^{NE}$, $\pi_1 \geq \pi_1^{NE}$; (ii) the user equilibrium defined in Eq. (3.5) and Eqs. (3.1)-(3.3); and (iii) all airfares are non-negative. The above mathematical model also complies with the equilibrium condition defined in Eq. (3.5). χ and $1-\chi$ represent the bargaining power of airlines serving Airport i and airlines serving Airport k, respectively. The solution to the optimization problem defined by Eq. (3.27) is referred to as the Nash bargaining solution (NBS). Considering the collective behavior of the two airline operators, we explore the Nash game involving Airline O-j-D and the combination of Airline O-i-D and Airline O-k where the operator of Airline O-j-D optimizes its decision variables (τ_2) to maximize its profit, as follows:

$$max \quad \pi_2 = \pi_2(\tau_2). \tag{3.28}$$

The solutions to program defined in Eq. (3.28) is similar with that in the non-cooperative game discussed in Section 3.3.1, thus the detailed description is omitted. Considering interior solutions, the optimality conditions of problem (3.27) can be expressed as Eq. (3.29).

$$
\begin{aligned}
\frac{\partial U}{\partial \tau_1} = \frac{\pi_3 - \pi_3^{NE}}{\pi_1 - \pi_1^{NE}} \times \left(\tau_1 \frac{\partial q_1}{\partial \tau_1} - W'_{\pi_1,q_1} \frac{\partial q_1}{\partial \tau_1} + \tau_{3,2} \frac{\partial q_3}{\partial \tau_1} - W'_{\pi_1,q_3} \frac{\partial q_3}{\partial \tau_1} + q_1\right) \\
+ \frac{1-\chi}{\chi} \times \left(\tau_{3,1} \frac{\partial q_3}{\partial \tau_1} - W'_{\pi_3,q_3} \frac{\partial q_3}{\partial \tau_1}\right) = 0
\end{aligned}
\tag{3.29a}
$$

$$
\begin{aligned}
\frac{\partial U}{\partial \tau_{3,1}} = \frac{\pi_3 - \pi_3^{NE}}{\pi_1 - \pi_1^{NE}} \times \left(\tau_1 \frac{\partial q_1}{\partial \tau_{3,1}} - W'_{\pi_1,q_1} \frac{\partial q_1}{\partial \tau_{3,1}} + \tau_{3,2} \frac{\partial q_3}{\partial \tau_{3,1}} - W'_{\pi_1,q_3} \frac{\partial q_3}{\partial \tau_{3,1}}\right) \\
+ \frac{1-\chi}{\chi} \times \left(\tau_{3,1} \frac{\partial q_3}{\partial \tau_{3,1}} - W'_{\pi_3,q_3} \frac{\partial q_3}{\partial \tau_{3,1}} + q_3\right) = 0
\end{aligned}
\tag{3.29b}
$$

$$
\begin{aligned}
\frac{\partial U}{\partial \tau_{3,2}} = \frac{\pi_3 - \pi_3^{NE}}{\pi_1 - \pi_1^{NE}} \times \left(\tau_1 \frac{\partial q_1}{\partial \tau_{3,2}} - W'_{\pi_1,q_1} \frac{\partial q_1}{\partial \tau_{3,2}} + \tau_{3,2} \frac{\partial q_3}{\partial \tau_{3,2}} - W'_{\pi_1,q_3} \frac{\partial q_3}{\partial \tau_{3,2}} + q_3\right) \\
+ \frac{1-\chi}{\chi} \times \left(\tau_{3,1} \frac{\partial q_3}{\partial \tau_{3,2}} - W'_{\pi_3,q_3} \frac{\partial q_3}{\partial \tau_{3,2}}\right) = 0
\end{aligned}
\tag{3.29c}
$$

Based on Eqs. (3.29b)-(3.29c), it can be inferred that

$$
\frac{\pi_1 - \pi_1^{NE}}{\pi_3 - \pi_3^{NE}} = \frac{\chi}{1-\chi}, \tag{3.30}
$$

which shows the equality between the ratio of airlines' market power and the ratio of extra profits they can obtain from the cooperation. By substituting Eq. (3.30) to Eq. (3.29), and substituting Eq. (3.12) to Eq. (3.30), we can derive the formulation of optimal airfares under the cooperation between Airline O-k and Airline O-i-D as follows:

$$
\tau_1 = W'_{\pi_1,q_1} + \Pi_1 q_1 + \Pi_2 q_3, \tag{3.31a}
$$

$$
\begin{aligned}
\tau_{3,1} = (1-\chi) \left[\left(W'_{\pi_1,q_1} + \Pi_1 q_1 + \Pi_2 q_3\right) \frac{q_1}{q_3} + W'_{\pi_1,q_3} + W'_{\pi_3,q_3}\right] \\
- (1-\chi) \left[q_3 + (\Pi_1 q_1 + \Pi_2 q_3) \frac{\frac{\partial q_1}{\partial \tau_{3,1}}}{\frac{\partial q_3}{\partial \tau_{3,1}}} + \frac{W_{\pi_1} + \pi_1^{NE}}{q_3}\right] + \chi \frac{W_{\pi_3} + \pi_3^{NE}}{q_3},
\end{aligned}
\tag{3.31b}
$$

and

$$\tau_{3,2} = \chi\left[W'_{\pi_1,q_3} + W'_{\pi_3,q_3} - q_3 - (\Pi_1 q_1 + \Pi_2 q_3)\frac{\frac{\partial q_1}{\partial \tau_{3,1}}}{\frac{\partial q_3}{\partial \tau_{3,1}}} - \frac{W_{\pi_3} + \pi_3^{NE}}{q_3}\right] + (1-\chi)\left[\frac{W_{\pi_1} + \pi_1^{NE}}{q_3} - \frac{q_1}{q_3}\left(W'_{\pi_1,q_1} + \Pi_1 q_1 + \Pi_2 q_3\right)\right], \tag{3.31c}$$

where

$$\Pi_1 = -\frac{\frac{\partial q_3}{\partial \tau_{3,1}}}{\frac{\partial q_1}{\partial \tau_1}\frac{\partial q_3}{\partial \tau_{3,1}} - \frac{\partial q_1}{\partial \tau_{3,1}}\frac{\partial q_3}{\partial \tau_1}}, \tag{3.32a}$$

$$\Pi_2 = \frac{\frac{\partial q_3}{\partial \tau_1}}{\frac{\partial q_1}{\partial \tau_1}\frac{\partial q_3}{\partial \tau_{3,1}} - \frac{\partial q_1}{\partial \tau_{3,1}}\frac{\partial q_3}{\partial \tau_1}}. \tag{3.32b}$$

We can deduce that $\Pi_1 > 0$ and $\Pi_2 > 0$ when $\frac{\partial q_1}{\partial \tau_1}\frac{\partial q_3}{\partial \tau_{3,1}} > \frac{\partial q_1}{\partial \tau_{3,1}}\frac{\partial q_3}{\partial \tau_1}$. This implies that the direct influence of airfares on passenger flow along the same route (represented by $\frac{\partial q_1}{\partial \tau_1}$ and $\frac{\partial q_3}{\partial \tau_{3,1}}$) is stronger than its influence on passenger flow along a different route (represented by $\frac{\partial q_1}{\partial \tau_{3,1}}$ and $\frac{\partial q_3}{\partial \tau_1}$). Conversely, $\Pi_1 < 0$ and $\Pi_2 < 0$ when $\frac{\partial q_1}{\partial \tau_1}\frac{\partial q_3}{\partial \tau_{3,1}} < \frac{\partial q_1}{\partial \tau_{3,1}}\frac{\partial q_3}{\partial \tau_1}$, indicating that the indirect effects of airfares on passenger flows on the same path are more significant than the direct effects of airfares on passenger flows on other paths. Then we substitute above airfares into airlines' profit formulation Eq. (3.12a) and Eq. (3.12c) to get profits of Airline O-k and Airline O-i-D under cooperative game, which are denoted as π_1^{NBS} and π_3^{NBS}.

$$\pi_1^{NBS} = \chi\left[\left(W'_{\pi_1,q_1} + \Pi_1 q_1 + \Pi_2 q_3\right)q_1 + \left(W'_{\pi_1,q_3} + W'_{\pi_3,q_3} - q_3 - \frac{\frac{\partial q_1}{\partial \tau_{3,1}}}{\frac{\partial q_3}{\partial \tau_{3,1}}}(\Pi_1 q_1 + \Pi_2 q_3)\right)q_3\right] - \chi\left[\left(W_{\pi_3} + \pi_3^{NE}\right) + W_{\pi_1}\right] + (1-\chi)\,\pi_1^{NE} \tag{3.33a}$$

$$\pi_3^{NBS} = (1-\chi)\left[\left(W'_{\pi_1,q_1} + \Pi_1 q_1 + \Pi_2 q_3\right)q_1 + \left(W'_{\pi_1,q_3} + W'_{\pi_3,q_3} - q_3 - \frac{\frac{\partial q_1}{\partial \tau_{3,1}}}{\frac{\partial q_3}{\partial \tau_{3,1}}}(\Pi_1 q_1 + \Pi_2 q_3)\right)q_3\right] - (1-\chi)\left(W_{\pi_1} + \pi_1^{NE} + W_{\pi_3}\right) + \chi\pi_3^{NE} \tag{3.33b}$$

From Eq. (3.33), it is clear that airlines with greater bargaining power experience less impact on their profits under a cooperative game from those obtained in a non-cooperative game. Additionally, the profits of both airlines will simultaneously increase or decrease; however, the rate of change will vary and depends on their respective bargaining powers. Profits derived from the cooperative game are positively correlated with those under the non-cooperative game: higher profits in the former typically lead to higher profits in the latter. The total payoff get from the cooperation between Airline O-i-D and Airline O-k, i.e., $TP = \left(\pi_1^{NBS} - \pi_1^{NE}\right) + \left(\pi_3^{NBS} - \pi_3^{NE}\right)$, can be formulated as:

$$
\begin{aligned}
TP = \; & \underbrace{\left(W'_{\pi_1,q_1} + \Pi_1 q_1 + \Pi_2 q_3\right) q_1}_{\text{revenue from passengers on path O-i-D}} + \underbrace{\left(W'_{\pi_1,q_3} + W'_{\pi_3,q_3} - q_3 - (\Pi_1 q_1 + \Pi_2 q_3) \frac{\frac{\partial q_1}{\partial \tau_{3,1}}}{\frac{\partial q_3}{\partial \tau_{3,1}}}\right) q_3}_{\text{revenue from passengers on path O-k-i-D}} \\
& - \underbrace{\left(W_{\pi_1} + W_{\pi_3}\right)}_{\text{total operating cost}} - \underbrace{\left(\pi_1^{NE} + \pi_3^{NE}\right)}_{\substack{\text{total profit from the} \\ \text{non-cooperation game}}} .
\end{aligned}
\tag{3.34}
$$

By substituting the formulation of marginal operating costs (i.e., W'_{π_1,q_3}, W'_{π_1,q_3}, and W'_{π_3,q_3}) and the operating costs (i.e., W_{π_1} and W_{π_3}), TP can be rewritten as:

$$
\begin{aligned}
TP = & \left(\mu_{i,1} d'_{i,q_1} + \Pi_1\right) q_1 q_1 + \Pi_2 q_1 q_3 + \left(\mu_{i,3} d'_{i,q_3} + \mu_{k,3} d'_{k,q_3} - 1 - \Pi_2 \frac{\frac{\partial q_1}{\partial \tau_{3,1}}}{\frac{\partial q_3}{\partial \tau_{3,1}}}\right) q_3 q_3 \\
& - \Pi_1 \frac{\frac{\partial q_1}{\partial \tau_{3,1}}}{\frac{\partial q_3}{\partial \tau_{3,1}}} q_1 q_3 - \left(\pi_1^{NE} + \pi_3^{NE}\right).
\end{aligned}
\tag{3.35}
$$

Assuming the first-order derivatives of congestion delay (i.e., d'_{i,Q_i}, d'_{k,Q_k}) and the derivatives of passenger flows with respect to airfares (i.e., $\frac{\partial q1}{\partial \tau_1}$, $\frac{\partial q_1}{\partial \tau_{3,1}}$, $\frac{\partial q_3}{\partial \tau_1}$, and $\frac{\partial q_3}{\partial \tau_{3,1}}$) are constant rather than functions of passenger flows, it follows that Π_1 and Π_2 are also constants. Under the conditions where $\Pi_1 > 0$ and $\Pi_2 > 0$, an increase in passenger flow on the path O-i-D (q_1) will lead to higher profits for the cooperative airlines. Similarly, when the condition specified in Eq.(3.36) is met, an increase in passenger flow on the path O-k-i-D (q_3) will also enhance the profits of these airlines. Conversely, when the condition in Eq.(3.36) does not hold, if q_3 meets the condition outlined in Eq.(3.37)—implying that the passenger flow on path O-k-i-D is below a certain threshold relative to the flow on path O-i-D—then an increase in q_3 will additionally yield profits for the cooperation between the two airlines.

$$\left(\mu_{i,3}d'_{i,q_3} + \mu_{k,3}d'_{k,q_3} - 1 - \Pi_2\frac{\frac{\partial q_1}{\partial \tau_{3,1}}}{\frac{\partial q_3}{\partial \tau_{3,1}}}\right) \geq 0 \tag{3.36}$$

$$q_3 < -\frac{\left(\Pi_2 - \Pi_1\frac{\frac{\partial q_1}{\partial \tau_{3,1}}}{\frac{\partial q_3}{\partial \tau_{3,1}}}\right)q_1}{\left(\mu_{i,3}d'_{i,q_3} + \mu_{k,3}d'_{k,q_3} - 1 - \Pi_2\frac{\frac{\partial q_1}{\partial \tau_{3,1}}}{\frac{\partial q_3}{\partial \tau_{3,1}}}\right)} \tag{3.37}$$

In a scenario where both $\Pi_1 < 0$ and $\Pi_2 < 0$, if the inequality $\mu_{i,1}d'_{i,q_1} + \Pi_1 \geq 0$ holds, then an increase in passenger flow on the path O-i-D (q_1) will lead to higher profits for the cooperative airlines. Conversely, if $\mu_{i,1}d'_{i,q_1} + \Pi_1 < 0$, then q_1 must meet the condition specified in Eq. (3.38) to ensure that a larger q_1 results in increased total profits (TP).

$$q_1 < -\frac{\Pi_2 - \Pi_1\frac{\frac{\partial q_1}{\partial \tau_{3,1}}}{\frac{\partial q_3}{\partial \tau_{3,1}}}}{\mu_{i,1}d'_{i,q_1} + \Pi_1}q_3 \tag{3.38}$$

When $\mu_{i,3}d'_{i,Q_i} + \mu_{k,3}d'_{k,q_3} - 1 - \Pi_2\frac{\frac{\partial q_1}{\partial \tau_{3,1}}}{\frac{\partial q_3}{\partial \tau_{3,1}}} \leq 0$, an increase in demand on Path 3 will invariably result in decreased total profits (TP). Conversely, if $\mu_{i,3}d'_{i,q_3} + \mu_{k,3}d'_{k,q_3} - 1 - \Pi_2\frac{\frac{\partial q_1}{\partial \tau_{3,1}}}{\frac{\partial q_3}{\partial \tau_{3,1}}} > 0$, then q_3 must satisfy the condition specified in Eq. (3.39) to ensure that its increase contributes to greater profits for the cooperative airlines.

$$q_3 > -\frac{\left(\Pi_2 - \Pi_1\frac{\frac{\partial q_1}{\partial \tau_{3,1}}}{\frac{\partial q_3}{\partial \tau_{3,1}}}\right)}{\mu_{i,3}d'_{i,q_3} + \mu_{k,3}d'_{k,q_3} - 1 - \Pi_2\frac{\frac{\partial q_1}{\partial \tau_{3,1}}}{\frac{\partial q_3}{\partial \tau_{3,1}}}}q_1 \tag{3.39}$$

3.3.2 Consideration of investments in ground connection services

It can be beneficial for airlines to make investments that improve service equality for passengers (Gayle & Yimga, 2018) and enhance their competitive advantages within the aviation industry (Shen et al., 2022). In this subsection, it is considered that the ground connection services between Airport i and Airport k can be improved if the Airline O-i-D and Airline O-k provide investment in it (the investment might be realized via the airport/local authority). When operating under the cooperative/non-cooperative games, operators of Airline O-i-D and Airline O-k take both airfares and the investments in the ground connection services as decision variables.

We consider that each route is serviced exclusively by a single airline. As a result, airlines might be incentivized to invest in enhanced ground connection services, which can lead to increased passenger satisfaction of their chosen air travel route and, consequently, more demand. Although current ground connection services, such as the shuttle buses of the Hong Kong-Zhuhai-Macao Bridge and the buses of the Shenzhen Bay Port, are available, they operate on fixed departure intervals and may not be directly coordinated with associated air services. In such cases, airlines can optimize/increase the shuttle bus timetable/frequency to ensure seamless connections between connecting flights, particularly when both flights are sold as part of a single order. By doing so, airlines can reduce turnaround times, lower operating costs, and ultimately improve profitability. In current practice, for contemporary ticketing platforms like Qunar, a range of advantageous offerings, such as airport pick-up and drop-off services, are commonly available to provide efficient connection in passengers' journeys, thereby augmenting the overall quality of travel services. Furthermore, airlines frequently furnish passengers with connecting tickets, accompanied by dedicated resting facilities, with the aim of enhancing the overall passenger experience. Consequently, we conjecture that when ground transportation is required for connecting two flights along a given route, airlines operating such a route might be financially incentivized to invest in the enhancement of connection services.

3.3.2.1 Non-cooperative game

We now consider that operators of Airline O-i-D and Airline O-k choose the investments on ground connection services to maximize their respective profits. However, as Airline O-j-D does not directly benefit from the ground connection, it is considered that Airline O-j-D does not invest in the ground connection services. Note that investing in enhanced ground connections does not imply that airlines directly operate and manage the ground transportation system. Instead, we explore the incentive of airlines to provide financial support to existing ground transportation operators for higher connection services including increased frequency of service, more dynamic trips that are tightly synchronized with flight schedules and so on. This subsection investigates the analytical formulation of the optimal decisions and the corresponding airline profits considering both airfares and investments as decision variables under the non-cooperative game (i.e., Nash game). Considering the investments provided by Airline O-i-D and Airline O-k (denoted as h_1 and h_3, respectively), the airline profit of Airline O-i-D and Airline O-k are rewritten as:

$$\begin{aligned}\pi_1(\tau_1, \tau_{3,2}, h_1) = \tau_1 q_1 + \tau_{3,2} q_3 - \rho_{i,1} q_1 - \rho_{i,3} q_3 - (w_{oi,1} + w_{id,1}) q_1 - w_{id,3} q_3 \\ - \mu_{i,1} d_i(q_1, q_3, C_i) q_1 - \mu_{i,3} d_i(q_3, C_i) q_3 - h_1\end{aligned} \tag{3.40a}$$

$$\pi_2(\tau_2) = \tau_2 q_2 - \rho_{j,2} q_2 - (w_{oj,2} + w_{jd,2}) q_2 - \mu_{j,2} d_j(q_2, C_j) q_2 \tag{3.40b}$$

$$\pi_3(\tau_{3,1}, h_3) = \tau_{3,1} q_3 - \rho_{k,3} q_3 - w_{ok,3} q_3 - \mu_{k,3} d_k(q_3, C_k) q_3 - h_3 \tag{3.40c}$$

It is assumed that the price of the ground connection services between Airport k and Airport i is negligible (or included in the airfare for Path 3), i.e., τ_{ki} is set as zero. Considering the investments from airline operators in the ground connection services are treated as independent variables, the first-order conditions (FOCs) with respect to airfares under Nash game and Nash bargaining game will be similar to those in Eq. (3.14) and Eq. (3.29), respectively. Therefore, the equations of the optimal airfares are similar to Eq. (3.18) under Nash game and Eq. (3.31) under the Nash bargaining game. However, it is noteworthy that passenger flow patterns under the cooperative game and the non-cooperative game are very likely different since the chosen optimal investments are likely to be different. Therefore, similar FOC formulations can result in different numerical solutions. The FOCs with respect to investments from Airline O-i-D and Airline O-k in ground connection services are as:

$$\tau_1 \frac{\partial q_1}{\partial h_1} + \tau_{3,2} \frac{\partial q_3}{\partial h_1} - \rho_{i,1} \frac{\partial q_1}{\partial h_1} - \rho_{i,3} \frac{\partial q_3}{\partial h_1} - \left(w_{oi,1} + w_{id,1}\right) \frac{\partial q_1}{\partial h_1} - w_{id,3} \frac{\partial q_3}{\partial h_1} - 2\mu_{i,1} d_i \frac{\partial q_1}{\partial h_1}$$
$$- \mu_{i,1} d'_{i,q_1} q_1 \frac{\partial q_1}{\partial h_1} - \mu_{i,1} d'_{i,q_3} q_1 \frac{\partial q_3}{\partial h_1} - \mu_{i,3} d_i \frac{\partial q_3}{\partial h_1} - \mu_{i,3} d'_{i,q_3} q_3 \frac{\partial q_3}{\partial h_1} - 1 = 0 \tag{3.41a}$$

and

$$\tau_{3,1} \frac{\partial q_3}{\partial h_3} - \rho_{k,3} \frac{\partial q_3}{\partial h_3} - w_{ok,3} \frac{\partial q_3}{\partial h_3} - \mu_{k,3} d_k \frac{\partial q_3}{\partial h_3} - \mu_{k,3} d'_{k,Q_k} q_3 \frac{\partial q_3}{\partial h_3} - 1 = 0. \tag{3.41b}$$

In Eq. (3.41a), the first term in the left-hand side, $\tau_1 \frac{\partial q_1}{\partial h_1}$, is the marginal decreased revenue gained from the decreased passenger in Airline O-i-D, q_1, which caused by the marginal increased investment in road transport; the second term, $\tau_{3,2} \frac{\partial q_3}{\partial h_1}$, is the marginal increased revenue gained from the increased passenger in Airline O-k, q_3, which caused by the marginal increased investment in the road transport system from Airline O-i-D; the third term, $-\rho_{i,1} \frac{\partial q_1}{\partial h_1}$, is the marginal saving airport charge because of the decreased passenger flow on Airline O-i-D; the forth term, $-\rho_{i,3} \frac{\partial q_3}{\partial h_1}$, is the additional airport charge paid for the increased passenger flow on Airline O-k caused by increased h_1; the fifth term, $-(w_{oi,1} + w_{id}) \frac{\partial q_1}{\partial h_1}$, is the marginal saving operating cost in Airline O-i-D in link oi and id for transporting decreased passengers caused by marginal increase of investment in road transport from Airline O-i-D; the sixth term, $-w_{id,3} \frac{\partial q_3}{\partial h_1}$, is the increased operating cost in link id for transporting increased passengers in Airline O-k caused by marginal increase of investment in road transport from Airline O-i-D; the seventh term, $-\mu_{i,1} d_i \frac{\partial q_1}{\partial h_1}$, is the marginal saving of congestion delay cost caused by decreased passenger flow on Path 1 because of the increase of investment in the road transport; the eighth term, $-\mu_{i,1} d'_{i,q_1} q_1 \frac{\partial q_1}{\partial h_1} - \mu_{i,1} d'_{i,q_3} q_1 \frac{\partial q_3}{\partial h_1}$, is the marginal saving of congestion delay cost caused by released congestion in Airport i because of the decreased passenger flow on Path 1 caused by the increased investment from Airline O-i-D on road transport; the ninth term, $-\mu_{i,3} d_i \frac{\partial q_3}{\partial h_1}$, is the marginal increase of congestion delay cost in Airport i caused by increased passenger flow on Path 3 because of the increase of the investment from Airline O-i-D in road transport; the tenth term, $-\mu_{i,3} d'_{i,q_3} q_3 \frac{\partial q_3}{\partial h_1}$, is the marginal increase of congestion delay cost caused by severer congestion because of the increased passenger flow on Path 3 caused by the increased investment in road transport; the last term, -1, is the marginal decreased profit of Airline O-i-D because of marginal increased investment in road transport from the operator of Airline O-i-D.

In Eq. (3.41b), the first term of the left-hand side, $\tau_{3,1}\frac{\partial q_3}{\partial h_3}$, is the marginal increased revenue of Airline O-k caused by the marginally increased passenger flow on Path 3 because of the increased investment from Airline O-k; the second term, $-\rho_{i,3}\frac{\partial q_3}{\partial h_3}$ is the additional airport charge in Airport k because of the increase of passenger demand in Airline O-k; the third term, $-w_{ok,3}\frac{\partial q_3}{\partial h_3}$, is the marginally increased operating cost of Airline O-k in link ok for transporting increased passengers caused by marginal increase of investment in road transport from Airline O-k; the forth term, $-\mu_{k,3}d_k\frac{\partial q_3}{\partial h_3}$, is the marginal increase of congestion delay cost in Airport k caused by increased passenger flow on Path 3 because of the increase of the investment from Airline O-k in road transport; the fifth term, $-\mu_{k,3}d^{'}_{k,q_3}q_3\frac{\partial q_3}{\partial h_3}$, is the marginal saving of congestion delay cost caused by released congestion in Airport k because of the decreased passenger flow on Path 3 caused by the increased investment from Airline O-k on road transport; the last term, -1, is the marginal decreased profit of Airline O-k because of marginal increased investment in road transport from the operator of Airline O-k.

By solving Eq. (3.41), we can get the optimal investments of Airline O-i-D and Airline O-k under Nash equilibrium as:

$$h_1^{NE} = \left(\tau_1^{NE} - W^{'}_{\pi_1,q_1}\right) q_1\sigma_{h_1}^{q_1} + \left(\tau_{3,2}^{NE} - W^{'}_{\pi_1,q_3}\right) q_3\sigma_{h_1}^{q_3} \tag{3.42a}$$

and

$$h_3^{NE} = \left(\tau_{3,1}^{NE} - W^{'}_{\pi_3,q_3}\right) q_3\sigma_{h_3}^{q_3}. \tag{3.42b}$$

Eq. (3.42a) shows that the operator of Airline O-i-D can increase airfares of Path 1 and the second leg of Path 3, i.e., τ_1 and $\tau_{3,2}$ through providing more investments in the ground connection. From Eq. (3.42b), it can be investigated that only when $\tau_{3,1}^{NE} > W^{'}_{\pi_3,q_3}$, i.e., the optimal airfare of the first leg of Path 3 decided by Airline O-k is higher than the marginal increased total operating cost caused by an additional unit of demand on Path 3, the operator of Airline O-k need to provide investment under Nash game.

By substituting Eq. (3.18a), Eq. (3.18c) and Eq. (3.18d) to the above equations, we can further get the investment expression as follows:

$$h_1^{NE} = -\frac{\sigma_{\tau_{3,2}}^{q_3}}{1+\sigma_{\tau_{3,2}}^{q_3}+\sigma_{\tau_1}^{q_1}} W'_{\pi_1,q_3} q_3 \sigma_{h_1}^{q_3} - \frac{\sigma_{\tau_1}^{q_1}}{1+\sigma_{\tau_{3,2}}^{q_3}+\sigma_{\tau_1}^{q_1}} W'_{\pi_1,q_1} q_1 \sigma_{h_1}^{q_1} \tag{3.43a}$$

$$h_3^{NE} = -\frac{1}{1+\sigma_{\tau_{3,1}}^{q_3}} W'_{\pi_3,q_3} q_3 \sigma_{h_3}^{q_3} \tag{3.43b}$$

It can be seen that the more passenger flow on Path 3 is related to higher investments both from Airline O-i-D and Airline O-k while lower passenger flow on Path 1 is often caused by higher investment in the ground connection by Airline O-i-D. It is expected that to maximize profit, the operator of Airline O-i-D should adjust the investments to manage passenger flows on both Path 1 and Path 3. Since the marginal profit brought by investment (for the ground connection) can vary, airlines should stop investing when the marginal profit falls below the cost of the investment.

3.3.2.2 Cooperative Game

Under the Nash Bargaining game where Airline O-i-D and Airline O-k operators take the investments as decision variables, the optimization problem can be modelled as follows:

$$max \quad U(\tau_1, \tau_{3,1}, \tau_{3,2}, h_1, h_3) = \left(\pi_1 - \pi_1^{NE}\right)^{\chi} \left(\pi_3 - \pi_3^{NE}\right)^{(1-\chi)} \tag{3.44}$$

The above model is similar as the optimization problem defined in Eq. (3.28), but now includes the investments on ground connection services as decision variables. The first order optimality conditions include those with respect to airfares defined in Eq. (3.29), which are not repeated here, and those related to airlines' investments, which are presented as

$$\begin{aligned}\frac{\partial U}{\partial h_1} &= \frac{\pi_3 - \pi_3^{NE}}{\pi_1 - \pi_1^{NE}} \times \left(\tau_1 \frac{\partial q_1}{\partial h_1} - W'_{\pi_1,q_1} \frac{\partial q_1}{\partial h_1} + \tau_{3,2} \frac{\partial q_3}{\partial h_1} - W'_{\pi_1,q_3} \frac{\partial q_3}{\partial \tau_1} - 1\right) \\ &+ \frac{1-\chi}{\chi} \times \left(\tau_{3,1} \frac{\partial q_3}{\partial h_1} - W'_{\pi_3,q_3} \frac{\partial q_3}{\partial h_1}\right) = 0\end{aligned} \tag{3.45a}$$

and

$$\begin{aligned}\frac{\partial U}{\partial h_3} &= \frac{\pi_3 - \pi_3^{NE}}{\pi_1 - \pi_1^{NE}} \times \left(\tau_1 \frac{\partial q_1}{\partial h_3} - W'_{\pi_1,q_1} \frac{\partial q_1}{\partial h_3} + \tau_{3,2} \frac{\partial q_3}{\partial h_3} - W'_{\pi_1,q_3} \frac{\partial q_3}{\partial h_3}\right) \\ &+ \frac{1-\chi}{\chi} \times \left(\tau_{3,1} \frac{\partial q_3}{\partial h_3} - W'_{\pi_3,q_3} \frac{\partial q_3}{\partial h_3} - 1\right) = 0.\end{aligned} \tag{3.45b}$$

It should be noted that π_1 and π_3 in Eq. (3.45) refer to the airline profits defined in Eq. (3.40). The optimal investments of Airline O-i-D and Airline O-k under Nash bargaining game can be solved as

$$\begin{aligned}h_1^{NBS} &= \frac{\chi}{(1-\chi)} \left[\left(W'_{\pi_1,q_1} - \tau_1\right) \sigma_{h_3}^{q_1} q_1 + \left(W'_{\pi_1,q_3} + W'_{\pi_3,q_3} - \tau_{3,2} - \tau_{3,1}\right) \sigma_{h_3}^{q_3} q_3\right] \\ &+ \frac{\chi}{(1-\chi)} \left(W_{\pi_3} + \pi_3^{NE} - \tau_{3,1} q_3\right) + q_1 \tau_1 + q_3 \tau_{3,2} - W_{\pi_1} - \pi_1^{NE}\end{aligned} \tag{3.46a}$$

and

$$h_3^{NBS} = \left(W'_{\pi_1,q_1} - \tau_1\right) \sigma_{h_3}^{q_1} q_1 + \left(W'_{\pi_1,q_3} + W'_{\pi_3,q_3} - \tau_{3,2} - \tau_{3,1}\right) \sigma_{h_3}^{q_3} q_3. \tag{3.46b}$$

By substituting the optimal airfares under the cooperative game in Eq. (3.31), we can further simplify the formulation of investments from Airline O-i-D and Airline O-k as

$$h_1^{NBS} = \frac{\chi}{(1-\chi)} \left[- \left(\Pi_1 q_1 + \Pi_2 q_3\right) \sigma_{h_3}^{q_1} q_1 + \left(q_3 - \left(\Pi_1 q_1 + \Pi_2 q_3\right) \frac{\frac{\partial q_1}{\partial \tau_{3,1}}}{\frac{\partial q_3}{\partial \tau_{3,1}}}\right) \sigma_{h_3}^{q_3} q_3\right] \tag{3.47a}$$

and

$$h_3^{NBS} = - \left(\Pi_1 q_1 + \Pi_2 q_3\right) \sigma_{h_3}^{q_1} q_1 + \left(q_3 - \left(\Pi_1 q_1 + \Pi_2 q_3\right) \frac{\frac{\partial q_1}{\partial \tau_{3,1}}}{\frac{\partial q_3}{\partial \tau_{3,1}}}\right) \sigma_{h_3}^{q_3} q_3. \tag{3.47b}$$

It can be easily found that

$$\frac{h_1^{NBS}}{h_3^{NBS}} = \frac{\chi}{(1-\chi)} \tag{3.48}$$

and

$$h_1^{NBS} + h_3^{NBS} = \frac{1}{(1-\chi)} \left[-(\Pi_1 q_1 + \Pi_2 q_3)\, \sigma_{h_3}^{q_1} q_1 + \left(q_3 - (\Pi_1 q_1 + \Pi_2 q_3) \frac{\frac{\partial q_1}{\partial \tau_{3,1}}}{\frac{\partial q_3}{\partial \tau_{3,1}}} \right) \sigma_{h_3}^{q_3} q_3 \right]. \tag{3.49}$$

Eq. (3.48) indicates that the airline with larger market power simultaneously gain more payoff from the cooperation and provide more investment for stronger ground connection between airports. Eq. (3.49) shows that more investment should be provided to develop the ground connection between Airport i and Airport k given stronger bargaining power of Airline O-k. It is clear that with conditions that $\Pi_1 > 0$ and $\Pi_2 > 0$, more investments should be provided from both airlines given higher demand on both paths. Conversely, when $\Pi_1 < 0$ and $\Pi_2 < 0$, less investments should be provided given increase of passenger flow q_1. When $1 - \frac{\frac{\partial q_1}{\partial \tau_{3,1}}}{\frac{\partial q_3}{\partial \tau_{3,1}}} \Pi_2 \geq 0$, then an increase of passenger flow q_3 will cause less investments for the connection services. If $1 - \frac{\frac{\partial q_1}{\partial \tau_{3,1}}}{\frac{\partial q_3}{\partial \tau_{3,1}}} \Pi_2 < 0$, then when the condition in Eq. (3.50) holds, more investments should be provided given more demand on Path 3.

$$q_3 > -\frac{\left(\sigma_{h_3}^{q_1} \Pi_2 + \frac{\frac{\partial q_1}{\partial \tau_{3,1}}}{\frac{\partial q_3}{\partial \tau_{3,1}}} \sigma_{h_3}^{q_3} \Pi_1 \right)}{\sigma_{h_3}^{q_3} \left(1 - \frac{\frac{\partial q_1}{\partial \tau_{3,1}}}{\frac{\partial q_3}{\partial \tau_{3,1}}} \Pi_2 \right)} q_1 \tag{3.50}$$

3.4 Numerical Studies

We now carry out numerical studies in the context of Guangdong-Hong Kong-Macao Greater Bay Area (GBA) serving an specific OD pair, which consists of Hong Kong International Airport (Airport i), Guangzhou Baiyun International Airport (Airport j) and Zhuhai Jinwan International Airport (Airport k). This section investigates four distinct scenarios within the context of the Multi-Airport System (MAS) in the Greater Bay Area. Each scenario explores the strategic behavior of airlines and the impact of ground connection investments on pricing strategies, passenger flow distribution, and airline profits. The four scenarios are as follows. i) Non-cooperative game without investment for the ground connection (denoted as NG-O): In this scenario, the three airlines independently formulate their pricing strategies (Nash game), without making any investments in the ground connection. ii) Cooperative game without investment for the ground connection (denoted as CG-O): The airline serving Hong Kong International Airport and the airline serving Zhuhai Jinwan Airport engage in cooperative behavior (Nash bargaining game), and together they compete with the airline serving Guangzhou Baiyun Airport (Nash game). No investments are made in the ground connection in this scenario. iii) Non-cooperative game with investments for the ground connection (denoted as NG-I): This scenario maintains the same market structure as scenario i), but considers that the airlines serving Hong Kong International Airport (HKIA) and Jinwan Airport can choose to invest in ground connection services between the two airports. iv) Cooperative game with investment for the ground connection (denoted as CG-I): This scenario maintains the same market structure as scenario ii), but considers that the airlines serving Hong Kong International Airport and Jinwan Airport can choose to invest in ground connection services between the two airports. In particular, for scenario CG-I, we analyze three distinct pairs of bargaining power for the two cooperative airlines, specifically $\chi/(1-\chi) = 1$, $\chi/(1-\chi) = 2$, and $\chi/(1-\chi) = 3$. Furthermore, although passengers on Path 1 and Path 3 in order to investigate the impact of passengers

3.4.1 Numerical setting

We take the Great Bay Area (GBA) as the region served by a MAS consisting of Hong Kong International Airport (HKG) as Airport i, Guangzhou Baiyun International Airport (CAN) as Airport j and Zhuhai Jinwan International Airport (ZUH) as Airport k. As mentioned earlier, we focus on an aggregate origin and destination pair composed of a domestic airport and an overseas airport. According to AAHK Sustainability Report 2017/18, over 100 airlines operate at Hong Kong International Airport (HKIA), connecting Hong Kong to over 220 destinations worldwide[1]. Therefore, for residents of cities with limited international

[1]The report has been published in the website: https://www.hongkongairport.com/iwov-resources/html/sustainability_report/eng/SR1718/our-future-airport/economic-contribution/

flight options, transferring through HKIA presents an excellent solution for reaching global destinations.

Hefei Airport provides non-stop flights to 62 destinations in 6 countries, such as Zhuhai, Guangzhou and Hong Kong. However, it does not offer direct flights to many international locations like Los Angeles Airport[2]. Consequently, Hefei residents planning to travel abroad may need to first travel to an airport in the GBA MAS to find a connecting flight to their overseas destination. In this case, we have selected Xinqiao Airport in Hefei, Anhui Province in China as the origin (O), and Los Angeles International Airport (LAX) as the destination (D). This choice is based on the fact that there are very few airlines offering direct flights from Xinqiao Airport to Los Angeles International Airport. Consequently, travelers in the vicinity of Xinqiao Airport must connect through another airport to reach international destinations. Note that our choice of HFE-LAX as the real-world OD does not imply that our proposed framework is limited to the specific pair. Rather, our framework can be applied to any domestic origin and international destination pair, provided they are connected through the stylized MAS in the GBA.

According to the airline timetable information available on Qunar as of January 26th, passengers have the option to first travel to Guangzhou Baiyun Airport (via China Southern Airlines flight CZ38784) and then proceed to Los Angeles International Airport (via China Southern Airlines flight CZ327). Therefore, we assume that passengers from Hefei are more likely to choose to arrive in the MAS within the Greater Bay Area and then transfer to Los Angeles. Zhuhai Jinwan Airport serves Chinese domestic flights but no international flights. Passengers can have international air travel services after cross-airport transfer from Zhuhai Jinwan Airport to Hong Kong International Airport by shuttle buses operating on the Hong Kong-Zhuhai-Macao Bridge. Thus, we consider Jinwan Airport as the reliever airport (i.e., the minor airport) within the MAS.

As outlined in Section 3.2.1, we consider a stylized MAS where each air travel path is exclusively served by a single airline. In this subsection, we make specific assumptions

[2] The direct destinations from Hefei Airport haven been visualized in the website: `https://www.flightconnections.com/flights-from-hefei-hfe`

regarding the airlines operating on different paths. For instance, we assume that Path 1 (from O to D with a transfer at Airport i) is serviced by Cathay Pacific, covering the route from Xinqiao Airport (HFE) to Los Angeles Airport (LAX), with a transfer at Hong Kong International Airport (HKG). Furthermore, we assume that Cathay Pacific also operates the flight from Hong Kong International Airport to Los Angeles Airport. Moving on to Path 2 (from O to D with a transfer at Airport j), we consider China Southern Airlines as the provider for the journey from Xinqiao Airport to Los Angeles Airport, with a transfer at Guangzhou Baiyun Airport (CAN). Lastly, we assume that China Eastern Airlines operates the air travel between Xinqiao Airport and Jinwan Airport. While our assumption associates each airline with the respective carrier in charge, it is crucial to acknowledge that in reality, there may be no connecting services for certain airlines. Although our analysis assumes that specific airlines operate distinct air travel routes, this does not guarantee that these routes will actually be managed by the assumed airlines. The information provided about airlines and airfares serves merely as a foundation for understanding the current situation. By adopting the above airfares, we can solve the UE passenger flows on Path 1, Path 2, and Path 3 and profits of the corresponding airlines.

According to the information provided on the Qunar website, the estimated travel time from Xinqiao Airport to an airport within the MAS is approximately 3 hours. Therefore, we set t_{oi}, t_{ok}, and t_{oj} to be 3 hours each. The travel time from an airport within the MAS to Los Angeles Airport is approximately 15 hours, taking into account the waiting time at the transfer airport. Hence, we set t_{id} and t_{jd} as 15 hours. Based on the transfer procedure outlined by Cathay Pacific on their website [3], which details the journey from Zhuhai Jinwan Airport to Hong Kong International Airport via the Hong Kong-Zhuhai-Macau Bridge, the estimated travel time by shuttle buses is approximately 1 hour. Taking into account additional time requirements such as waiting and boarding, we set t_{ki} to be 1.5 hours in the numerical study.

The airport capacity setting takes the passenger volume of airports in 2019 as a refer-

[3] Cathay Pacific reported the step-by-step recap of the journey from Zhuhai Jinwan Airport to Hong Kong International Airport on its website: `https://www.cathaypacific.com/cx/en_HK/inspiration/hong-kong/how-to-travel-zhuhai-to-hkia.html`

ence. In 2019, the annual passenger volume of Zhuhai Jinwan Airport, Guangzhou Baiyun International Airport and Hong Kong International Airport was 12.3 million, 73 million, 71.5 million, respectively[4]. The turnaround time of long-haul travel is 90-120 minutes [5], so we focus on the capacity of an airport within 2 hours. Airport capacities are set as those in Table 3.4. The current rate of the Air Passenger Departure Tax is 120 HKD per passenger departing by air from Hong Kong through Hong Kong International Airport[6]. The operating cost is set to be 120 HKD/seat [7]. In this chapter, we consider that the airport charge varies based on the type of flight, distinguishing between short-haul and long-haul flights. As such, we assign an airport charge of 120 HKD for passengers on long-haul flights and 30 HKD for passengers on short-haul flights. Specifically, we denote the airport charge at Airport i and Airport j on long-haul flights as $\rho_{i,1} = \rho_{i,3} = \rho_{i,2} = 120$ HKD and the charge at Airport k on short-haul flights as $\rho_{k,3} = 30$ HKD.

Different functional forms for elastic demand have been used in the literature, including linear (Gong et al., 2023), logarithmic, exponential (Ma et al., 2023b), or polynomial functions. In this chapter, we adopt an exponential function as the elastic demand function. It is defined as the product of the potential aggregate demand and an exponential function that decreases as the minimum travel cost between origin and destination (OD) increases. As discussed earlier, we assume that the ticket fare for ground transportation is already included in the airfares, denoted as $\tau_{ki} = 0$. The congestion delay is assumed to be larger under higher passenger flows or reduced airport capacity, and it is calculated as a parameter multiplied by the passenger traffic divided by the airport capacity. The transfer cost is influenced by queuing behaviors and is defined as a linear function related to passenger flows (for passengers on

[4]For year 2019, the number of passengers traveling via Zhuhai Jinwan Airport is available at: `https://en.wikipedia.org/wiki/Zhuhai_Jinwan_Airport`; The number of passengers traveling via Guangzhou Baiyun Airport is available at: `https://www.baiyunairport.com/byairport-web/menu/index?urlKey=airport-basic-facts`; The number of passengers traveling via Hong Kong International Airport is available at: `https://www.hongkongairport.com/sc/the-airport/hkia-at-a-glance/fact-figures.page`.

[5]Aircraft turnaround process is shown on the following website: `https://simpleflying.com/aircraft-turnaround-process/`

[6]Air passenger departure tax is introduced on the website: `https://www.cad.gov.hk/english/departure_tax.html`

[7]Passenger Airlines Operating Costs in the United States at year 2019 are published by "The Geography of Transport Systems": `https://transportgeography.org/contents/chapter5/air-transport/airline-operating-costs/`

a path without cross-airport transfer, i.e., $\delta_m = 0$). However, for passengers on Path 3, which includes a cross-airport transfer ($\delta_m = 1$), the transfer cost is determined by both passenger flow and the investment made by airlines for ground connection services. It is defined as a combination of a linear function related to passenger flow and the passenger flow divided by the investment for the ground connection services.

We assume that the utilized aircraft are widebody aircraft with 300 seats. According to statistics from the Federal Aviation Administration[8], which analyzes the operating expenses of airlines, we can derive average costs per block hour for widebody aircraft over 300 seats (\$10,351) and widebody aircraft under 300 seats (\$8,285). Using these figures, we can estimate that the average hourly operating cost per passenger is approximately 242 HKD. Based on these calculations, we can allocate operating costs for different types of air travel in this chapter. For short-haul flights arriving at major international airports (e.g., link oi and link oj), the operating cost is set as 400 HKD/passenger, while for long-haul flights (e.g., link id and link jd), the operating cost is 3000 HKD/passenger. For short-haul air travel connecting the origin airport and the minor airport (i.e., link ok), the operating cost is set to be 200 HKD/passenger. Specifically, we denote the operating costs for different links as $w_{oi,1} = w_{oj,2} = 400$ HKD , $w_{ok,3} = 200$ HKD, and $w_{id,1} = w_{jd,2} = w_{id,3} = 3000$ HKD.

In our stylized MAS, passengers travelling along Path 3 depart exclusively from Airport i, whereas passengers on Path 1 both arrive at and depart from Airport i. Consequently, the differing runway usage patterns of the two airlines serving path O-i-D and path O-k-i-D can result in passengers on the two paths exerting distinct impacts on the congestion at Airport i. In the GBA MAS, Zhuhai Jinwan Airport can be taken as a reliever airport for alleviating congestion by handling part of international air passengers from domestic areas. We investigate operators' pricing strategies and investment decisions given different congestion delay functions to reflect the varying impacts of passenger flows on paths HFE-HKG-LAX and HFE-ZUH-HKG-LAX on congestion at HKIA. This investigation not only underscores the significance of ZUH in GBA MAS in alleviating congestion in HKIA but also

[8]Airlines' most significant operating expenses are discussed here: https://simpleflying.com/the-cost-of-flying/

emphasizes the importance of ground connection inside a MAS in promoting cooperation between a minor airport and a major airport and achieving high profitability for the MAS. Specifically, We test three cases with different impact coefficients of passengers in the functions of congestion delay cost: i) $d_i = 0.06(2q_1 + q_3)^2/C_i$, $d_j = 0.06(2q_2)^2/C_j$, and $d_k = 0.06q_3^2/C_k$; ii) $d_i = 0.06(1.5q_1+q_3)^2/C_i$, $d_j = 0.06(1.5q_2)^2/C_j$, and $d_k = 0.06q_3^2/C_k$; and iii) $d_i = 0.06(q_1+q_3)^2/C_i$, $d_j = 0.06q_2^2/C_j$, and $d_k = 0.06q_3^2/C_k$. The congestion delay functions defined in case i) and case ii) illustrate the more significant impact of passengers both arriving at and departing from an airport on congestion, compared to the impact of passengers only arriving or only departing, while case iii) assumes an equal impact from both types of passengers. Other parameters are assumed given limited access to data, which are shown in Table 3.4.

We also conducted an analysis of passenger flow distribution and airline profits given the current airfare information of the assumed OD pair (from Xinqiao Airport to Los Angeles International Airport). There is one connecting option available for the route from Xinqiao Airport to Los Angeles International Airport via Baiyun Airport, operated by China Southern Airlines on 1st April (CZ3814 and CZ327). The price of this option is 7897 HKD. However, there is currently no airline offering a direct route from Xinqiao Airport to Los Angeles International Airport via Hong Kong International Airport. Therefore, passengers traveling from Xinqiao Airport to Los Angeles International Airport would need to purchase separate tickets and rely on ground transportation to reach Hong Kong International Airport. In this case, we simply take the sum of two ticket fares as the total fare for that particular route.

The economy class fares for the flights mentioned are as follows: Cathay Pacific offers a flight (CX882) from Hong Kong International Airport to Los Angeles International Airport at a price of 7868 HKD. China Eastern Airlines provides a flight (MU2067) from Xinqiao Airport to Hong Kong International Airport, priced at 1092 HKD. Hainan Airlines offers a flight (HU7643) from Xinqiao Airport to Jinwan Airport, with a fare of 657 HKD. It is important to note that these fares pertain specifically to economy class reservations for the respective flights.

Table 3.4: Summary of numerical settings

Parameters and Functions	Specifications
Value of air travel time (HKD/hour)	α=100
Value of road travel time (HKD/hour)	β=120
Airport capacity (passenger/2 hours)	$C_i = 20000$; $C_j = 20000$; $C_k = 3000$
Cost of ground connection services (HKD)	$\tau_{ki} = 0$
Air travel time (hour)	$t_{oi} = 3$; $t_{id} = 15$; $t_{oj} = 3$;$t_{jd} = 15$; $t_{ok} = 3$
Road travel time (hour)	$t_{ki} = 1.5$
Congestion delay cost of passengers	$d_i = 0.06(N_i q_1 + q_3)^2/C_i$, $d_j = 0.06(N_j q_2)^2/C_j$, and $d_k = 0.06q_3^2/C_k$. N_i and N_j can be interpreted as impact coefficients which can be 1, 1.5 and 2.
Transfer cost (HKD)	$T_a = 0.04V_a + [0.08V_a/(h_1 + h_3 + 1)] \times \sigma_a$, $\sigma_i = 0$, $\sigma_j = 0$, $\sigma_k = 1$
Elastic demand function	$q = q_0 \times exp(-\theta p)$, $q_0 = 40000$, $\theta = -0.8 \times 10^{-4}$
Operating cost (HKD)	$w_{oi,1} = 400$; $w_{oj,2} = 400$; $w_{ok,3} = 200$; $w_{id,1} = 3000$; $w_{jd,2} = 3000$; $w_{id,3} = 3000$
Delay cost parameter of airlines	$\mu_{i,1} = 0.6$; $\mu_{j,2} = 0.6$; $\mu_{i,3} = 0.2$; $\mu_{k,3} = 0.2$
Airport charge (HKD/passenger)	$\rho_{i,1} = 120$, $\rho_{i,3} = 120$, $\rho_{j,2} = 120$, $\rho_{k,3} = 30$

3.4.2 Comparison of different games and the current state of the MAS

In this subsection, we investigate the equilibrium passenger flow distribution and corresponding airline profits under cooperative games and non-cooperative games with or without airlines' investments in ground connection services. Under the numerical settings assumed in Table 3.4, the optimal airfares and investments (if considered), passenger flows at UE, consumer surplus, and airline profits are shown in Table 3.5, Table 3.6 and Table 3.7 given congestion delay functions defined as cases i), ii) and iii) aforementioned in Section 3.4.1, respectively. Note that the pricing strategies and investment decisions made by airlines are based on the assumption that the airlines within the MAS striving to maximize their profits. Moreover, the analysis of passenger flow distribution presented in this section focuses exclusively on the travel demand between the representative OD pair (from Xinqiao Airport to Los Angeles International Airport). Other demands, such as those traveling between different OD pairs through the MAS have not been considered. Therefore, variations in passenger flows on these paths should not be interpreted as indicative of corresponding changes in travel demand at the related airports. In this subsection, we consider route HFE-HKG-LAX, route HFE-CAN-LAX, and route HFE-ZUH-HKG-LAX as the real-world examples of route O-i-D, route O-j-D, and route O-k-i-D, respectively. Besides, Airline HFE-HKG-LAX, Airline HFE-CAN-LAX, and Airline HFE-ZUH indicate the airlines operating inside our stylized MAS serving air travel demand between the chosen OD pair.

Table 3.5: Results from different cases given impact coefficients in congestion delay functions being 2

	Status quo	NG-O	CG-O	NG-I	CG-I $\chi/(1-\chi)=1$	CG-I $\chi/(1-\chi)=2$	CG-I $\chi/(1-\chi)=3$
$h_1(10^4$ HKD)	0	0	0	3.2	8.0	8.0	7.0
$h_3(10^4$ HKD)	0	0	0	8.0	8.0	4.0	2.3
τ_1 (HKD)	8960	8500	9820	9000	9290	9320	9370
τ_2 (HKD)	7897	8400	9200	9280	9120	9190	9220
τ_3 (HKD)	8525	8530	9520	9040	8970	8920	8920
$\tau_{3,1}$ (HKD)	657	1030	1720	1180	1260	1080	990
$\tau_{3,2}$ (HKD)	7868	7500	7800	7860	7710	7840	7930
q_1	4030	5982	4397	5405	3983	3805	3660
q_2	8746	7697	7816	6679	7060	6934	6916
q_3	3610	2665	3157	3656	4695	4976	5094
q	16386	16344	15370	15740	15738	15715	15670
Consumer surplus (10^6)	211.06	209.02	194.00	199.02	199.34	199.03	198.67
$\pi_1(10^5$ HKD)	361.09	368.77	395.42	397.85	391.43	401.53	406.73
$\pi_2(10^5$ HKD)	334.64	342.78	409.57	341.81	370.02	369.15	346.58
$\pi_3(10^5$ HKD)	13.53	20.56	45.78	31.98	43.42	36.97	33.19

Table 3.6: Results from different cases given impact coefficients in congestion delay functions being 1.5

	Status quo	NG-O	CG-O	NG-I	CG-I $\chi/(1-\chi)=1$	CG-I $\chi/(1-\chi)=2$	CG-I $\chi/(1-\chi)=3$
$h_1(10^4$ HKD)	0	0	0	1.2	5.5	5.0	5.0
$h_3(10^4$ HKD)	0	0	0	2.5	5.5	2.5	1.67
τ_1 (HKD)	8960	8040	8240	8400	8640	8680	8790
τ_2 (HKD)	7897	8150	8160	8140	8650	8660	8720
τ_3 (HKD)	8525	8090	8260	8500	8500	8650	8900
$\tau_{3,1}$ (HKD)	657	650	700	680	1050	990	940
$\tau_{3,2}$ (HKD)	7868	7440	7560	7820	7450	7660	7830
q_1	3893	7305	6249	6637	5473	5938	5945
q_2	10133	8230	8421	8876	7880	8002	8075
q_3	2889	1866	2601	1755	3399	2759	2563
q	16916	17401	17271	17268	16752	16699	16592
Consumer surplus (10^6)	214.02	271.61	216.00	215.61	209.28	208.55	207.16
$\pi_1(10^5$ HKD)	334.81	376.90	379.39	382.00	395.35	401.59	406.40
$\pi_2(10^5$ HKD)	401.38	358.47	366.55	381.75	384.43	390.55	398.58
$\pi_3(10^5$ HKD)	11.37	7.58	11.52	7.68	25.85	19.88	17.39

We first analyze the comparison between Scenario NG-O and the status quo to investigate the impact of airlines serving routes HFE-ZUH-HKG-LAX and HFE-HKG-LAX entering

Table 3.7: Results from different cases given impact coefficients in congestion delay functions being 1

	Status quo	NG-O	CG-O	NG-I	CG-I $\chi/(1-\chi)=1$	CG-I $\chi/(1-\chi)=2$	CG-I $\chi/(1-\chi)=3$
$h_1 (10^4$ HKD)	0	0	0	0	5.0	4.0	4.0
$h_3 (10^4$ HKD)	0	0	0	4.0	5.0	2.0	1.33
τ_1 (HKD)	8960	7000	7400	8400	8580	8860	8920
τ_2 (HKD)	7897	6960	7120	7800	8420	8720	8820
τ_3 (HKD)	8525	7100	7400	8350	8480	8590	8690
$\tau_{3,1}$ (HKD)	657	400	500	650	1460	1360	1250
$\tau_{3,2}$ (HKD)	7868	6700	6900	7700	6820	7230	7440
q_1	2841	9373	8065	6265	5001	5156	5459
q_2	12391	9885	10448	11002	9275	9028	8839
q_3	2201	257	571	673	3168	2881	2677
q	17433	19515	19084	17940	17444	17074	16975
Consumer surplus (10^6)	217.22	240.07	235.12	220.89	214.18	209.32	207.90
$\pi_1 (10^5$ HKD)	255.55	318.78	321.98	329.83	355.30	380.34	397.34
$\pi_2 (10^5$ HKD)	508.11	322.66	355.60	446.91	440.11	456.21	456.04
$\pi_3 (10^5$ HKD)	8.97	0.44	1.53	2.41	37.19	31.40	26.70

the market. The differences in passenger distribution and revenue among the three routes under Scenario NG-O and the status quo, as shown in Tables 3.5-3.7, reveal that the route HFE-HKG-LAX has been overlooked by airline operators, leading to suboptimal fare-setting strategies. Regardless of the impact coefficient values, optimizing the pricing strategies for Airline HFE-HKG-LAX results in improved profitability. When the impact coefficients are set to 1 or 1.5, the profits of Airline HFE-ZUH and Airline HFE-CAN-LAX decrease after Airline HFE-HKG-LAX enters the market. However, lower airfares introduced by operators attract more passengers to the multi-airport system (MAS), resulting in higher consumer surplus. These results suggest that a ground connection between a minor airport and a major airport can significantly enhance MAS profitability, especially if it can significantly help alleviate congestion at the major airport. Furthermore, the comparison highlights the importance of refining pricing strategies to benefit airlines, particularly when ground connections can improve the competitiveness of routes served by these airlines and related to the ground connection. Comparing the results of airline profits under Scenario NG-O and Scenario NG-I, as shown in the three tables, it can be concluded that even without cooperation, Airline HFE-ZUH and Airline HFE-HKG-LAX achieve higher profits with improved ground connection services. Meanwhile, Airline HFE-CAN-LAX benefits from these improved services only when the congestion relief provided by the ground connections and Zhuhai Airport is less significant, specifically, when the impact coefficient in the congestion delay function is 1 or 1.5. However, when the cooperation of Zhuhai Airport and HKIA has stronger competitiveness due to the connectivity advantages brought by the Hong Kong-Zhuhai-Macau Bridge (i.e., the impact coefficient is 2), Baiyun Airport experiences a profit loss as the connections between the other two airports become stronger.

A comparison of Scenarios NG-O and CG-O under different impact coefficients reveals that cooperation between Airline HFE-HKG-LAX and Airline HFE-ZUH effectively converts consumer surplus into airline profits within the MAS. In this cooperative framework, even without additional investment in ground connections, all participating airlines benefit from the cooperation between airlines serving routes HFE-HKG-LAX and HFE-ZUH due to the higher airfares of all airlines in the MAS. However, the profit growth rate for Airline HFE-HKG-LAX is relatively modest compared to Airline HFE-ZUH. To maximize joint profitability, it is crucial for Airline HFE-ZUH to see a revenue boost. To achieve this, Airline HFE-HKG-LAX moderates fare increases on the HKG-LAX segment. This strategy ensures that the route HFE-ZUH-HKG-LAX remains attractive to passengers despite the higher fares introduced by Airline HFE-ZUH to increase its profits. This balanced approach maintains the competitiveness of the route while enhancing overall joint profitability.

By comparing the investment decisions of Airline HFE-HKG-LAX under Scenario NG-I and Scenario CG-I with varying marketing power (as shown in Tables 3.5-3.7), we can conclude that Airline HFE-HKG-LAX is more likely to invest in improved ground connection services when passengers on the route HFE-ZUH-HKG-LAX have a lower impact on congestion at HKIA compared to passengers on the route HFE-HKG-LAX. Additionally, Airline HFE-ZUH achieves higher profits when the impact coefficient is 1, compared to scenarios where the coefficient is 1.5. This is due to reduced congestion at major airports because of the weaker impact of passenger flows on airport congestion (i.e., smaller impact coefficients), which helps attract more passengers. However, the total profit of Airline HFE-ZUH and Airline HFE-HKG-LAX is lower when the impact coefficient is 1 than when it is 1.5, indicating reduced competitive advantages in the cooperation between these two airlines.

An analysis of passenger flows on routes HFE-HKG-LAX and HFE-ZUH-HKG-LAX under scenario CG-I with varying impact coefficients reveals important pricing strategy dynamics. When the impact coefficient is 2, operators of Airline HFE-HKG-LAX achieve higher profits by leveraging greater bargaining power to adjust pricing strategies. This involves reducing passenger numbers on the direct route HFE-HKG-LAX and increasing passenger flow on route HFE-ZUH-HKG-LAX including the ground connection. In contrast, when the impact coefficients are 1 or 1.5, operators with higher bargaining power tend to adjust pricing strategies to attract more passengers to the direct route HFE-HKG-LAX instead of the connecting route HFE-ZUH-HKG-LAX to increase profitability. These findings suggest that the greater the congestion relief provided by the minor airport, the more investment the airline serving the major airport is likely to allocate to improving ground connections. This, in turn, attracts more passengers and enhances overall profitability.

Based on the above analysis, we have the following recommendations. First, HKIA should enter the market by optimising the airfares of airlines serving international air travel and prioritize enhancing its connections with Zhuhai Airport by establishing high-quality ground connections to maximize operational benefits and alleviate congestion. Airlines serving HKIA need to develop a clear cooperation mechanism for collaborations with routes serving Zhuhai Airport to facilitate revenue growth through joint efforts. Moreover, airlines serving Zhuhai Airport (i.e., Airline HFE-ZUH) should actively seek partnerships with HKIA to boost their competitiveness within the network and make efforts to provide improved congestion relief for the connected major airport. Zhuhai Airport is advised to invest in robust ground transportation links and manage the increased passenger flows effectively to capitalize on these collaborations. Lastly, airlines serving Baiyun International Airport (i.e., HFE-CAN-LAX) should dynamically adjust their airfares based on the cooperative and pricing strategies of other airlines in the MAS as well as the impact of passenger flows on airport congestion. Furthermore, the airline serving a relatively independent major airport in a MAS should explore collaborative opportunities with other carriers to enhance profitability and market appeal.

3.5 Conclusions

In this chapter, we consider a MAS consisting of two major airports and a reliever airport connected to one of the major airports, involving possible cross-airport ground transfers. In this context, this chapter develops tractable models to explore the passengers' travel choices and airlines' pricing strategies and investments in the ground connection services under both cooperative and non-cooperative games.

In the context of MAS, passengers have several options: travel directly through either major airport to reach their destinations, travel to the reliever airport and then transfer to the connected major airport, or choose other alternatives (i.e., elastic demand). We model the passenger choice equilibrium under elastic demand and analyze how different system parameters may impact this equilibrium. Considering that an additional passenger affects travel costs more on paths with cross-airport transfers than those through the major airport connected to the reliever airport, we found that lower airfares, shorter travel times, and larger airport capacities along a path increase passenger flow on that path, decrease flow on alternative paths, and reduce the minimum travel price between the origin and destination. Additionally, increased investments in ground connection services between the major airport and the reliever airport will attract more passengers to the path involving cross-airport transfers.

We have developed tractable bi-level models to derive optimal airfares and investments in the ground connection services. Firstly, we consider the Nash game among the three airlines without investments in ground connection services. It is found that operators of the airline serving the major airport without any connection to other airports and the airline serving the reliever airport operate on the elastic portion of the demand curve for the air travel services provided by the two airlines. Then we consider the Nash bargaining game between the airline serving the reliever airport and the airline serving the major airport connected to the reliever airport, and the cooperation of the two airlines is under Nash game with the airline serving the other major airport. The results show that both the optimal airfares and airline profits are affected by the passenger flow interdependencies between the two paths with regard to the two airlines under Nash bargaining game. Taking the airlines' decision on the investments in the ground connection between the major airport and the reliever airport, it is established that an airline is more willing to invest in ground connection services when its served airport is in congestion while the connected airport is less congested under a non-cooperative game. However, given the cooperation between airlines serving the reliever airport and the major airport connected to it, the two airlines are willing to invest more in ground connection services when the major airport experiences congestion.

We carried out a numerical study in the context of the MAS in the Great Bay Area, comprising Zhuhai Jinwan Airport, Guangzhou Baiyun International Airport, and Hong Kong International Airport. Our numerical experiments account for varying structures of the international air travel passenger market, differing impacts of passenger flows on airport congestion, and diverse bargaining powers of cooperating airlines. The findings demonstrate that cooperation between the airline serving the major airport and the airline serving the reliever airport (connected to the major airport) benefits not only the cooperating airlines but also the non-cooperative airline within the MAS. Improved ground connection services lead to increased profits for all airlines in the MAS and higher demand on the path including cross-airport transfer under both cooperative games and non-cooperative games. Furthermore, comparisons of results under different impact coefficients of passenger flows on airport congestion highlight the importance of greater congestion relief provided by the minor airport and its ground connection to the major airport. Such relief drives higher profits, attracts increased investments from the major airport, and strengthens the competitiveness of the cooperation between the minor airport and its connected major airport. Based on insights from our numerical results, we provide recommendations for the operations and improvements of MAS with structures similar to our stylized framework. Firstly, the airline serving the connected major and reliever airports should engage in cooperation to maximize the profitability derived from the collaborative efforts of airlines within the MAS. Furthermore, the airline serving a relatively independent major airport should actively seek out potential collaborators to mitigate potential profit losses, particularly when there is cooperation between the airlines serving other airports within the MAS. Last, under the cooperation among airlines serving airports with ground connections, the airline with greater bargaining power not only receives a higher payoff but also invests more in developing these ground connections.

This chapter has several limitations that should be acknowledged. Firstly, we have focused on a stylized MAS network consisting of three airports, which models the GBA MAS composed of Hong Kong International Airport, Zhuhai Jinwan Airport, and Guangzhou Baiyun Airport. However, the GBA has more than three airports, and the cooperation and competition relationships among airlines and airports in GBA expect to further evolve. Future study may further examine more general and realistic MAS settings (e.g., considering MAS configurations involving multiple reliever airports or more complex connections between reliever airports and major airports) Besides, the competition and cooperation among airlines serving different airports and the interaction between airlines and airports are worth studying in the future. Secondly, we have assumed homogeneity in air passengers' travel preferences. However, it is crucial to recognize that the travel preferences of multi-class passenger groups play a significant role in understanding diverse air travel demands. These preferences are fundamental to the strategic considerations of airlines' operations and airports' decision-making processes (Ma et al., 2023a), which should be considered in future studies. Thirdly, this chapter did not explicitly model the ground connection services between the major and reliever airport. However, optimizing such connection services and exploring the seamless connection between separate air journeys of passengers is a valuable and meaningful topic for future research. Fourthly, this chapter examines the market structure within a MAS consisting of airports in close geographic proximity. Exploring aviation markets that include distant airports also presents a compelling area for future research.

Moreover, in this chapter, we have primarily focused on the investments in ground connection services from the perspective of airlines. However, it is important to recognize that airports, as integral components of a MAS, may invest in ground connections to fulfill specific objectives. Exploring the investments made by airports is a crucial area of research for gaining a deeper understanding of their operational dynamics within the MAS framework. Therefore, in future studies, investigating investments from airports will be an essential and valuable topic to further comprehend the role and impact of airports in the MAS context. Our study stylized a MAS structure, which represents today's GBA MAS and provides some analytical analysis with tractable models. Building on this MAS framework, there is significant potential for future operational research aimed at enhancing profitability. By optimizing decisions related to capacity allocation, pricing strategies, and investments in ground connections, airline operators can significantly improve their operational efficiency. Incorporating real-world data into these optimization models can yield actionable insights, which are crucial for refining the operational strategies of the GBA MAS.

Chapter 4

Air cargo transportation by passenger flights considering cargo demand and capacity uncertainties

Air cargo transportation with the unused belly capacity of passenger flights can improve transportation efficiency and reduce operational costs. To realize these potential benefits, we propose a framework to efficiently manage unused capacity on passenger flights, comprehensively accommodating uncertainties in flight capacity and cargo demand. A two-stage stochastic program is proposed to model our studied problem, with the first stage introducing a mid-term capacity reservation scheme while the second stage focuses on profitable short-term cargo-to-flight allocations. Sample Average Approximation is applied to handle various uncertainties in this program, while the Progressive Hedging algorithm is used for problem decomposition. A Lagrangian relaxed model is derived to provide lower bounds of operating cost. We design a modified heuristic algorithm that overperforms other baselines in cargo allocation tasks. Extensive numerical experiments on both medium- and large-scale instances demonstrate the effectiveness of the proposed model and solution approach. In addition, a sensitivity analysis is conducted, which emphasizes the importance of efficiently managing capacity in passenger flights and establishing partnerships with providers offering low-cost and abundant alternative resources. A comparison between a conservative benchmark by reserving all available capacities in flights and the proposed two-stage capacity management framework demonstrates that, even under the most challenging market conditions, the proposed approach can achieve substantial cost savings. The cost-saving potential becomes even more significant when cargo time-sensitivity is lower and ad hoc service options are more economically viable.

4.1 Introduction

This chapter explores a scenario in which the cargo forwarder utilizes the available belly space in passenger flights (obtained through long-term contract with airlines) to provide same-day shipment services to the identical destinations, aiming to minimize operational costs during the considered period. In this context, a cargo forwarder need to use the accessible capacity efficiently, therefore, excess capacity in passenger flights can be allocated for air cargo transportation and resold for commercial purposes to generate revenue after cargo capacity reservation. The forwarder can also engage in ad hoc capacity from external carriers/airlines, which typically incur higher unit costs if the reserved capacity is insufficient.

In an ideal deterministic situation where airline operators have complete information and face no uncertainties in the cargo transportation process, they could minimize transportation costs by perfectly matching capacity on passenger flights with daily cargo demand and then selling any remaining space to maximize additional revenue. However, the reality of transporting air cargo via passenger flights is filled with uncertainties that make these decisions challenging. It is often difficult for operators to determine in advance the precise cargo capacity to reserve on specific passenger flights.

The uncertainties considered in our research can be concluded into two key aspects, i.e., time and loading, which both impact air cargo and flights significantly. Specifically, our research focuses on the uncertainties from two key aspects, i.e., time and loading, which both impact air cargo and flights significantly. For instance, passenger flight schedules may change daily due to unpredictable factors like weather, affecting cargo loading time and scheduled departures. Additionally, packages' arrival times at origin airports may vary, and the time requirements of these packages may change from day to day (Azadian et al., 2012). Packages are typically transported to origin airports by buses from express collection points or other transfer airports, and any delays in these proceedings can lead to uncertain arrival times of air cargo. Uncertainty in cargo arrival times at the origin airport and in flight schedule execution affects cargo-to-flight assignments, introducing uncertainty in loading. Two capacity gaps illustrate uncertainty in available belly cargo space (Figure 4.1). Given the fixed total belly capacity of specific aircraft, Capacity Gap 1 is the difference between the total belly capacity and the space reserved for passengers' baggage, typically available for cargo, but sometimes smaller than expected when baggage usage reaches or exceeds allowances (Tang et al., 2008). Capacity Gap 2 is the sum of the unused portion of passengers' baggage allowance and Capacity gap 1, representing the actual cargo space. Because actual baggage weights are hard to predict, Capacity Gap 2 is highly variable and uncertain.

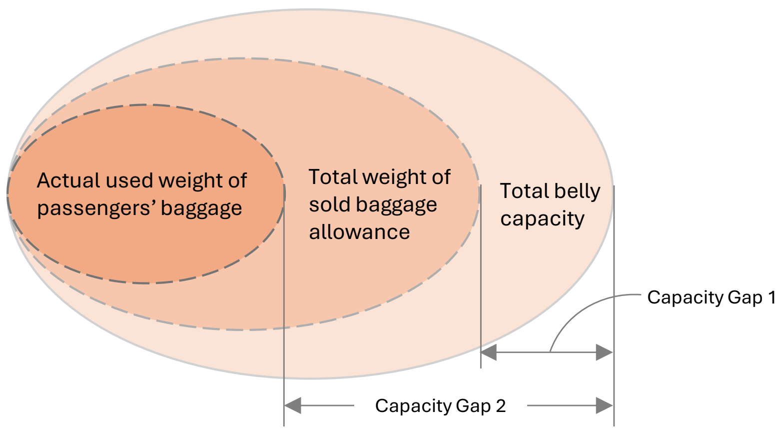

Figure 4.1: The usage of belly capacities in passenger flights (dashed lines shape the uncertain parts)

Given these complexities, it is crucial for air cargo operators to develop effective capacity management strategies to optimize resource allocation and minimize operational costs. These strategies should address uncertainties from both capacity users (i.e., air cargo) and capacity providers (i.e., passenger flights), and such uncertainties can be solved by operators dividing capacity management into two stages. In the first stage, operators develop a capacity reservation strategy for a mid-term period (e.g., one month). This involves determining reserved capacities on each flight based on predetermined flight schedules for the upcoming mid-term period. These first-stage decisions remain fixed throughout all short-term phases (e.g., one day) within the examined mid-term period. The objective is to secure sufficient capacity to meet daily cargo demands while maximizing the available capacity for selling to enhance potential revenue. Following the mid-term capacity reservation, the second stage focuses on the short-term cargo-to-flight allocation, typically on a daily basis within the defined mid-term period. Based on the first-stage decisions, cargo packages are allocated either to regular transportation using the pre-reserved capacity or to ad hoc services provided by other carriers. Decisions in the second stage should be made before every short-term period to handle daily fluctuations in cargo demand and variations in available capacities on flights. The goal is to minimize short-term operating costs by avoiding/reducing potential time penalties from delivery timing mismatches and avoiding the higher costs associated with ad hoc resources. This two-stage approach provides a comprehensive framework for efficiently managing flight capacity in air cargo transportation and finally minimizing the total operating cost generated in the above process, considering both capacity and demand uncertainty.

This chapter advances the field of air cargo transportation by addressing the role of passenger flights in cargo logistics under uncertainty. First, we introduce a novel capacity management framework that strategically combines mid-term capacity reservation with short-term cargo allocation. This two-stage approach enhances flexibility and cost-effectiveness, enabling more adaptive decision-making in air cargo operations. Second, to translate real-world considerations into a mathematical model, we develop a two-stage stochastic mixed-integer linear program that captures temporal demand variations while incorporating the operational constraints of passenger flights. Solving this problem efficiently poses significant computational challenges. To address this, we employ the Progressive Hedging (PH) algorithm for decomposition and design tailored heuristic algorithms. Specifically, we apply the Sample Average Approximation (SAA) method to approximate the expected value of the second-stage objective function and introduce a modified greedy regret algorithm for effective cargo allocation. Our proposed solution framework serves as a valuable reference for obtaining high-quality solutions to similar two-stage stochastic optimization problems. Third, beyond methodological and computational advancements, we validate our framework through extensive numerical experiments, demonstrating its ability to generate high-quality feasible solutions within practical time limits across diverse demand-supply scenarios. Additionally, our sensitivity analysis provides insights by examining how factors such as ad hoc service pricing and cargo time sensitivity influence system performance. By quantifying trade-offs between capacity reservation costs and overall operational expenses, our findings highlight the importance of strategic capacity management and the role of cost-effective alternative capacities in optimizing air cargo logistics.

The rest of this chapter is organized as follows. Section 4.2 discusses the problem settings and the mathematical formulation of our proposed two-stage stochastic program. Section 4.3 presents the overall solution framework for solving the studied problem. Section 4.4 details the computational experiments conducted using generated demand-supply datasets. Finally, Section 4.5 concludes the study and discusses potential future research topics.

4.2 Problem statement and mathematical formulation

4.2.1 Problem description

This section introduces the air cargo transporting cost minimization problem with the unused belly capacity in passenger flights. In this chapter, we focus on the operational decision-making of combination airlines that provide both passenger and cargo services. The operator of the combined airline applies the unused belly space of passenger aircraft for air cargo transportation. This operation is significant to diversify the revenue streams so that operators can minimize financial loss when one stream is disrupted[1]. The cargo transportation mode considered in our study is not an emerging concept, but rather a real and operationally established freight model.

Cargo transported via passenger aircraft often consists of time-sensitive and high-value

[1]The benefits brought by the application of capacities in passenger flights for cargo transportation were detailed introduced in the article `https://www.reedsmith.com/en/perspectives/global-air-freight/2022/01/carrying-the-load-use-of-passenger-aircraft-to-haul-cargo-during-covid19?`

goods that require timely response and repid delivery, such as pharmaceuticals, electronics, fashion items, and perishables. These shipments are typically initiated by cargo forwarders, logistics providers, and e-commerce platforms, whose requests may range from advance bookings to short-notice demands, depending on the urgency and variability of their supply chains. Cargo forwarders, therefore, serve a diverse customer base, including third-party logistics companies, multinational manufacturers, and cross-border e-commerce retailers. In this context, cargo forwarders act as service providers that offers reliable, time-critical transportation by routing shipments directly to destination airports, avoiding transfers and minimizing delay and possible time penalty.

Under the two-stage planning process modeled in this paper, forwarders make the mid-term operation plan by reserving capacity in each flights towards various destinations according to the known fleet assignment and flight schedules in the planning period. Given the reserved capacities in flights, cargo forwarders typically receive the collected cargo parcels from diverse customers and then conduct a pre-screening process to filter out cargo demands that is unsuitable for passenger aircraft and to prevent accepting more cargo than can be transported, thereby avoiding delayed response to demands. Carriers are supposed to exclude dangerous goods not authorized for passenger transport, shipments exceeding passenger-belly dimensional or weight constraints, and cargo from entities that do not meet Known Shipper (or equivalent) security requirements. The excluded cargo will be transported by other ways, i.e., dedicated cargo flights or trucks. This screening process is supposed to be independetly completed before the short-term cargo-to-flight assignment, and the passenger flights only response to the subset of cargo that is operationally feasible. Correspondingly, the cargo information regarding to the amount and characteristics of cargo demands are supposed to be known before assigning them to flights. This assumption aligns with current industry practices and ensures that the optimization model focuses on capacity allocation decisions within the reseasonable operational scope.

Prior to the two-stage planning process modeled in this chapter, airlines typically receive the collected cargo demand from diverse customers and then conduct a pre-screening process to filter out freight that is unsuitable for passenger aircraft (e.g., oversized or restricted cargo) and and to prevent accepting more cargo than can be transported, thereby avoiding unmet cargo demands. The excluded cargo will be transported by other ways. In our modeling framework, we assume that this screening process has already been completed, and the airline is managing only the subset of freight that is operationally feasible for transport via passenger aircraft. This assumption aligns with current industry practices and ensures that the optimization model focuses on capacity allocation decisions within the relevant operational scope.

To clarify the structure of our focused problem and the sequence of decision-making processes, Figure 4.2 illustrates the operational framework for managing cargo transportation via passenger flights. The framework is shown along the time axis and distinguishes between mid-term planning phases and short-term operational phases, corresponding to different levels of decision-making and information availability.

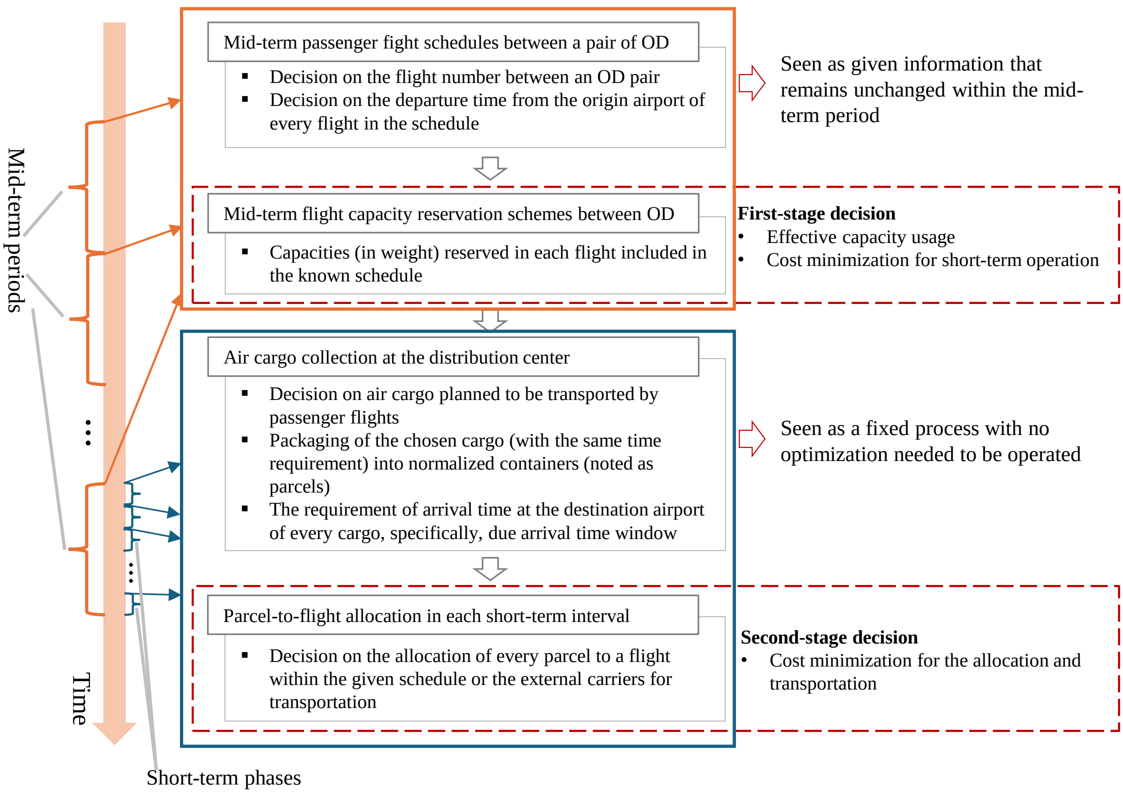

Figure 4.2: The decision-making process of the proposed two-stage capacity management

Although the identical flight schedules is implemented under each short-term planning period, uncertainties may arise, leading to variations in the actual departure times of flights compared to the predetermined schedule. Considering the uncertainties in each short-term period, capacity reservation decided in the first stage aims at efficiently using available belly space and to minimize the expected transportation costs occurred in all short-term periods. In each short-term phases included in the mid-term planning, air cargo begins to arrive at the origin airport and needs to be transported directly to their destination airports. In each short-term operational interval, air cargo parcels are collected, packaged into standardised containers, often known as unit load devices (ULDs), and associated with specific delivery time requirements. This packing and sorting is supposed to be exogenously completed before forwarders making cargo to flight assignments and it is not optimized in our setting. Once destination specific ULDs are ready, the forwarder needs to allocate each ULD to the reserved flight capacity for its destination or, if necessary, to external carriers. The ULD-to-flight allocation decisions forms the second-stage decision in our model. The goal here is to minimize the actual operational cost, which includes transportation costs, potential penalties for late deliveries and the use of ad hoc services.

4.2.2 Problem assumptions

Several assumptions are established in this section to shape the applicable context of our studied problem and thus facilitate the model development.

Assumption 1. *Capacities in passenger flights are more than sufficient for carrying passengers' baggage.*

Under Assumption 1, the belly space of passenger flights holds sufficient unused capacity applicable for cargo transportation. Conversely, without this assumption, cases may exist where the capacity is only adequate for passengers' baggage, making the study of using unused capacity for cargo meaningless. In this context, operators should pursue capacities from other carriers to guarantee that passengers' baggage can be transported to the destination airports rather than applying for cargo transportation. Thus, in the air transportation network, each origin-destination (OD) pair of airports has associated scheduled flights and corresponding unused capacities, which can be applied in air cargo transportation or other commercial ways after deciding the capacity reservation schemes. In other words, our analysis is restricted to OD pairs for which the scheduled passenger flights have surplus belly capacity available after accommodating all checked passenger baggage. In practice, such flights are typically operated by wide-body aircraft, which offer substantial cargo space in their belly spaces. However, this assumption does not imply that the overall cargo demand between the OD pair, including that handled by other airlines, is lower than the total available cargo capacity, which includes both dedicated cargo flights and passenger belly space. On the contrary, we assume that the capacity provided by dedicated cargo flights alone can be insufficient or ineffective to meet total demand or not suitable for transporting time-sensitive goods. This insufficiency justifies the necessity and significance to utilize belly capacities on passenger flights. If the dedicated cargo capacity were fully sufficient, the integration of passenger flight belly space into cargo operations would be unnecessary and irrelevant to the problem we aim to address. Here, another assumption should be introduced:

Assumption 2. *Cargo-to-flight assignments for distinct destination airports pairs do not interfere with one another and can be executed in parallel.*

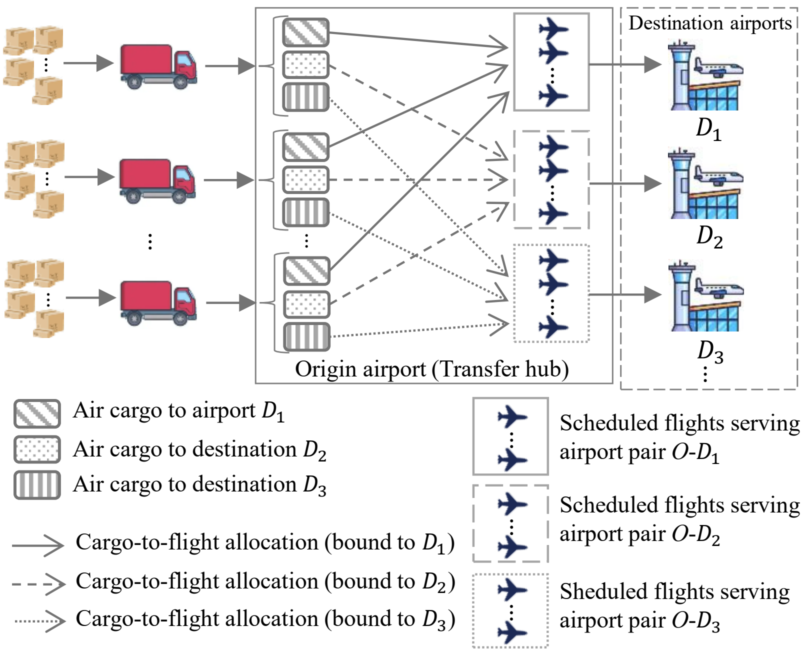

Figure 4.3: The considered process of cargo transportation from a transfer airport to multiple destination directly

Figure 4.3 depicts the operational setting in which a transfer airport consolidates outbound shipments and dispatches them directly to multiple destination airports using scheduled passenger flights. The analysis concentrates on the ground-handling and assignment process at a large transfer node, where dedicated ground vehicles deliver unit load devices (ULDs) to departure gates corresponding to their destinations.

The study targets customized, time-sensitive cargo for which direct flights from origin to destination are operationally preferred. As noted in Section 6.2, these shipments are pre-packed into destination-specific ULDs prior to the assignment stage. Because ULDs are assembled by destination, the operational rule is to load each destination's ULDs only onto flights serving that destination. Consequently, the ULD-to-flight assignment for one destination does not consume capacity or handling resources from flights serving other destinations within the decision horizon, and the corresponding assignment decisions do not interfere with one another.

This separability is further supported by how passenger operations and ground handling are organized. Aircraft type and scheduled belly capacity for passenger flights are predetermined at the timetable level, and baggage allowances are managed independently per flight. Forecasting, booking, and gate-level loading plans are executed per route or market, so realized demand on one OD pair does not typically alter aircraft assignment or available belly capacity on an unrelated pair within the relevant horizon.

Standardized ULD practice reinforces operational modularity. Certified ULD dimensions and fittings enable pre-loading, accurate weight-and-balance planning, and faster turn-around on both wide-body and, where applicable, narrow-body aircraft. Because ULDs are prepared, reconciled, and dispatched per flight and per destination, ground-handling workflows are naturally partitioned by OD pair, which limits coupling across destinations.

Under these conditions, modeling ULD-to-flight assignments for different destination airports as independent and executable in parallel is both operationally realistic and methodologically advantageous. If exceptional circumstances introduce strong coupling, for example, dynamic aircraft swaps across routes or binding, shared ULD pools—these can be addressed by extending the model with explicit coupling constraints; such cases lie outside the present scope.

To preserve feasibility under stochastic variations in belly capacity on passenger flights, we posit the following assumption:

Assumption 3. *Ad hoc cargo services are sufficiently available to cover unmet transportation needs, although at a higher unit cost than reserved passenger-flight capacity.*

Within each short-term operational period nested in the mid-term planning horizon, flights carry a predetermined amount of reserved cargo capacity. However, realized capacity is stochastic. Late passenger behavior—such as last-minute ticketing or the purchase of additional baggage allowances—can reduce the effective cargo space below the reserved level, because passenger baggage loading is strictly prioritized. In addition, capacity allocated and sold in the mid-term plan is not fungible across departures ex post, which limits reallocation flexibility when mismatches occur between realized capacity and cargo ready times.

Assumption 3 ensures that, when reserved passenger-flight capacity is infeasible or time-incompatible for some cargo, an external recourse option exists. In this study, ad hoc services denote on-demand capacity sourced from external carriers in the spot market, as well as operational recourse such as refunding or rescheduling shipments. These services are available at a higher per-unit cost relative to reserved belly capacity. Consequently, the assumption guarantees operational feasibility, since every shipment can be assigned a viable transport option, while preserving meaningful cost trade-offs. The optimization explicitly seeks to minimize reliance on ad hoc services because they carry a higher marginal cost.

The assumption is also consistent with industry practice. Airlines and forwarders forecast cargo demand and publish schedules sufficiently in advance to reserve baseline belly capacity, thereby reducing the likelihood of widespread unserved shipments. Residual uncertainty is addressed through recourse mechanisms such as spot market procurement and contingency agreements that provide a credible safeguard while preserving the economic value of pre reserved capacity.

Taken together, Assumptions 1 and 3 define the capacity environment of the problem. They justify the use of scheduled passenger flights for baseline cargo movement, support mid-term reservation decisions aligned with published timetables, and guarantee the existence of feasible recourse for stochastic shortfalls. This yields a realistic and tractable operating context that aligns with contemporary air cargo practices while preserving the essential cost–feasibility trade-off in the model.

Before presenting the detailed assumptions and model formulation, we summarize the key notations used throughout the paper in Table 4.1.

Table 4.1: Notations for the cargo transportation problem

Notation	Description
Sets&Indices	
$\mathcal{D}$	Set of destination airports connected to the origin(transfer) airport
$\mathcal{M}_d$	Set of air cargo (ULD) numbers, defined as $\mathcal{M}_d = \{1, 2, ..., \lvert\mathcal{M}_d\rvert\}$, $d \in \mathcal{D}$.
$\mathcal{K}_d$	Set of passenger flights to destination d, defined as $\mathcal{K}_d = \{1, 2, ..., \lvert\mathcal{K}_d\rvert\}$, $d \in \mathcal{D}$
$\mathcal{G}_d$	Set of possible capacity scenarios of flights serving the transfer airport and destination d, $d \in \mathcal{D}$
$\mathcal{H}_d$	Set of possible scenarios of air cargo demand to destination d, $d \in \mathcal{D}$.
d	Index of cargo destination, $d \in \mathcal{D}$
k	Index of passenger flights, $k \in \mathcal{K}_d$, $d \in \mathcal{D}$
m	Index of cargo packages, $m \in \mathcal{M}_d$, $d \in \mathcal{D}$
g	Index of flight capacity scenarios, $g \in \mathcal{G}_d$, $d \in \mathcal{D}$
h	Index of air cargo demand scenarios, $h \in \mathcal{H}_d$, $d \in \mathcal{D}$
Parameters	
$t_{m,h}$	The arrival time of cargo package m at the origin(transfer) airport under cargo demand scenario h, $m \in \mathcal{M}_d$, $h \in \mathcal{H}_d$, $d \in \mathcal{D}$
$T_{k,g}$	The departure time of flight k from the origin(transfer) airport under capacity scenario h, $k \in \mathcal{K}_d$, $g \in \mathcal{G}_d$, $d \in \mathcal{D}$

Notation	Description
$[l_{k,g}, u_{k,g}]$	Loading time window of flight k under capacity scenario g, $k \in \mathcal{K}_d$, $g \in \mathcal{G}_d$, $d \in \mathcal{D}$
$Y_{k,g}$	Maximum available capacity of flight k under flight capacity scenario g, $k \in \mathcal{K}_d$, $d \in \mathcal{D}$
$w_{m,h}$	Weight of package m under cargo scenario h, $h \in \mathcal{H}_d$, $d \in \mathcal{D}$
$[v_{m,h}, b_{m,h}]$	The due departure time window of package m from the origin airport under demand scenario h, $m \in \mathcal{M}_d$, $h \in \mathcal{H}_d$, $d \in \mathcal{D}$
$[r_{m,h}, q_{m,h}]$	The acceptable time window of package m from the origin airport under cargo scenario h, where $r_{m,h}$ and $q_{m,h}$ respectively indicate the earliest and latest departure time of package m from the origin airport under cargo demand scenario h, $m \in \mathcal{M}_d$, $d \in \mathcal{D}$. For every possible realised cargo scenario h, $v_{m,h} \geq r_{m,h}$ and $b_{m,h} \leq q_{m,h}$
$f_{mk,h}$	Time penalty cost for transporting package m by flight k under cargo scenario h
τ	Unit cost of using ad hoc services to deliver air cargo with unit weight that is taken as a constant
ξ	Unit transporting cost for delivering unit-weight air cargo that is taken as a constant
σ	Extra unit cost of using ad hoc services compared to the regular services for transporting a unit-weight cargo package, i.e., $\sigma = \tau - \xi$
ε	Unit revenue by selling unit capacity for carrying unit weight in flight k, assumed to be constant and decided exogenously
α_1	Time penalty rate for early departure
α_2	Time penalty rate for late departure
L	A sufficient large number
Decision variables	

Notation	Description
$\mathbf{y}$	Capacity reservation strategies, $\mathbf{y} = (..., \mathbf{y}_d, ...) = (..., (..., y_k, ...), ...)$, where y_{dk}'s are continuous decision variables, indicating how much capacity is reserved on flight k for air cargo transportation. $k \in \mathcal{K}_d$, and $d \in \mathcal{D}$
$\mathbf{x}$	Cargo-to-flight allocation schemes, $\mathbf{x} = (..., \mathbf{x}_d, ...) = (..., (..., x_{mk,g,h}, ...), ...)$, where $x_{dmk,g,h}$'s are binary decision variables that are decided scenario based, $x_{dmk,g,h} \in \{0, 1\}$, indicating whether package m is delivered by flight k under demand scenario h given realised flight capacity under scenario g. $m \in \mathcal{M}_d$, $k \in \mathcal{K}_d$, $g \in \mathcal{G}_d$, $h \in \mathcal{H}_d$, and $d \in \mathcal{D}$
$\mathbf{z}$	Binary decision variable, $\mathbf{z} = (..., \mathbf{z}_d, ...) = (..., (..., z_{m,g,h}, ...), ...)$, $z_m \in \{0, 1\}$, indicating whether package m is delivered by ad hoc services under demand scenario h given realised flight capacity under scenario g. $m \in \mathcal{M}_d$, $g \in \mathcal{G}_d$, $h \in \mathcal{H}_d$, and $d \in \mathcal{D}$

4.2.3 Notation introduction and model assumptions

We adopt a two-stage stochastic programming approach to formulate the cargo transportation cost minimization problem under the proposed two-stage capacity management framework. This section introduces the key modeling assumptions and associated notations, building on the problem setting defined earlier.

4.2.3.1 Two-stage decision framework

The adopted decision-making process is structured into two stages:

- First-stage (mid-term) decisions involve determining the reserved cargo capacity on scheduled passenger flights for mid-term planning of each OD airport pair, i.e., the origin airport to multiple destination airports. These decisions are made at the start of the mid-term planning horizon, when only probabilistic information about future conditions is available, represented by:

$$\mathbf{y} = (..., \mathbf{y}_d, ...), \text{where } \mathbf{y}_d = (..., y_k, ...), k \in \mathcal{K}_d, d \in \mathcal{D}.$$

where y_k is the reserved cargo capacity on flight k. In practice, the time horizon of the mid-term planning aligns with the operational cycle of airlines, depending on data availability.

- Second-stage (short-term) decisions involve allocating cargo packages or the use of ad hoc services to ensure that all cargo demand is fulfilled. These scenario-specific decisions are made before the short-term period begins when the uncertainties of flight capacities are realized, denoted by:

$$\mathbf{x} = (..., \mathbf{x}_d, ...), \text{where } \mathbf{x}_d = (..., \mathbf{x}_{d,g,h}, ...), g \in \mathcal{G}_d, h \in \mathcal{H}_d, d \in \mathcal{D}$$

$$\mathbf{z} = (..., \mathbf{z}_d, ...), \text{where } \mathbf{z}_d = (..., \mathbf{z}_{d,g,h}, ...), g \in \mathcal{G}_d, h \in \mathcal{H}_d, d \in \mathcal{D}$$

where $g \in \mathcal{G}_d$ indexes flight capacity scenarios and $h \in \mathcal{H}_d$ indexes cargo demand scenarios under destination d. Therefore, for a specific destination airport $d \in \mathcal{D}$, the combination (g, h), where $g \in \mathcal{G}_d$ and $h \in \mathcal{H}_d$, represents a joint realization of the uncertainties of flight capacities and cargo demand for a specific destination airport $d \in \mathcal{D}$. Given $m \in \mathcal{M}_d$ and $k \in \mathcal{K}_d$, $\mathbf{x}_{d,g,h}$ indicates the scenario-based cargo-to-flight allocation decisions and is defined as $\mathbf{x}_{d,g,h} = (..., x_{mk,g,h}, ...)$, where the binary variable $x_{mk,g,h}$ indicates whether cargo package m is allocated to flight k under scenario (g, h) ($x_{mk,g,h} = 1$) or not ($x_{mk,g,h} = 0$). $\mathbf{z}_{d,g,h} = (..., z_{m,g,h}, ...)$ where the binary variable $z_{m,g,h}$ indicates whether cargo package m is transported using ad hoc services ($z_{m,g,h} = 1$) or not ($z_{m,g,h} = 0$). For each destination airport $d \in \mathcal{D}$, mid-term capacity reservations $\mathbf{y}_d$ are determined before the planning horizon and are fixed across all scenarios. In contrast, cargo allocation decisions $\mathbf{x}_{d,g,h}$ and $\mathbf{z}_{d,g,h}$ are made after demand-capacity scenarios (g, h) are realized.

4.2.3.2 Scenario-based uncertainty

In our model, each scenario represents a potential realisation of daily cargo demand or flight capacities and a realised schedule. Under every realized scenario in short-term period, the included information of demand and capacities can be demonstrated by the following:

- For each destination airport d, capacity scenario $g \in \mathcal{G}_d$ includes the following information:
  - **Flight capacity**: $\mathbf{Y_{d,g}} = (..., Y_{k,g}, ...)$ where $Y_{k,g}$ indicates the realized available cargo capacity in flight k under scenario g. $k \in \mathcal{K}_d$.
  - **Flight departure time**: $\mathbf{T}_d = \left(T_{1,g}, T_{2,g}, ..., T_{|\mathcal{K}_d|,g}\right)$ where $T_{k,g}$ indicates the departure time of flight k under scenario g. $k \in \mathcal{K}_d$.
  - **Loading time window**: $(\left[l_{1,g}, u_{1,g}\right], \left[l_{2,g}, u_{2,g}\right], ..., \left[l_{|\mathcal{K}_d|,g}, u_{|\mathcal{K}_d|,g}\right])$ where $l_{k,g}$ and $u_{k,g}$ represent the earliest and latest time that cargo can be loaded onto flight k under scenario g, respectively. $k \in \mathcal{K}_d$.
- Demand scenario $h \in \mathcal{H}_d$ includes the following data:
  - **Package weights**: $\mathbf{w}_h = (w_{1,h}, w_{2,h}, ..., w_{|\mathcal{M}_d|,h})$ where $w_{m,h}$ is the weight of package m. $m \in \mathcal{M}_d$.
  - **Arrival time at the origin airport**: $\mathbf{t}_h = (..., t_{m,h}, ...)$. $m \in \mathcal{M}_d$
  - **Due departure windows**: $\left(\left[v_{1,h}, b_{1,h}\right], \left[v_{2,h}, b_{2,h}\right], ..., \left[v_{|\mathcal{M}_d|,h}, b_{|\mathcal{M}_d|,h}\right]\right)$. $m \in \mathcal{M}_d$.
  - **Acceptable departure time windows**: $\left(\left[r_{1,h}, q_{1,h}\right], \left[r_{2,h}, q_{2,h}\right], ..., \left[r_{|\mathcal{M}_d|,h}, q_{|\mathcal{M}_d|,h}\right]\right)$. $m \in \mathcal{M}_d$.

The specific rules and procedures for scenario generation employed in this study will be discussed in detail in Section 4.4.1.

The index $m \in \mathcal{M}_d$ denotes a randomly generated integer, between 1 and $|\mathcal{M}_d|$, of a cargo package within a specific scenario but does not correspond to a unique item across scenarios. $\mathcal{M}_d = \{1, 2, ..., |\mathcal{M}_d|\}$. A cargo package labeled $m = 1$ in scenario 1 is not the same physical parcel as $m = 1$ in scenario 2. The two parcels are each labeled with the index "1" in their respective scenarios. Instead, each $w_{m,h}$ represents the weight of a distinct cargo request that may arise under scenario h, reflecting the natural variability of cargo weights that arrive in practice. This consideration aligns with real-world operations where the set of shipments varies from day to day rather than representing uncertain attributes of fixed items. As assumed before, the departure sequence of flights serving a destination airport $d \in \mathcal{D}$ is predetermined. The flight index k shows the order of departure of flight k where $k = 1, 2, ..., |\mathcal{K}_d|$. Therefore, flights with the same index across different scenarios do not represent the same physical flights, but rather flights occupying the same position in the departure sequence.

In our model, the arrival time of a cargo package is defined as the moment it reaches the unloading point at the origin airport. This point represents the designated location within the terminal where cargo is transferred from the inbound delivery vehicles to airport ground handling services. The cargo to the same destination airport have been packed in the unit loaded devices (ULDs) before delivering to the origin airport, therefore, the ULDs can be loaded to the corresponding flights once they arrive at the airport.

4.2.4 Model formulation

4.2.4.1 The objective function

this chapter optimizes capacity management to minimize the total operating cost, including possible costs generated in two separate decision stages. The goal is to jointly optimize the mid-term capacity plan $\mathbf{y}$, and the scenario-specific allocation decisions $\mathbf{x}$ and $\mathbf{z}$, in order to minimize the total expected operating cost, while balancing mid-term stability and short-term adaptability in air cargo transportation planning. When operators make the mid-term decision on capacity reservations, opportunity costs are considered as the loss of revenue that should have been obtained by applying the unused capacities in other commercial ways. During the air cargo allocation, possible time penalties caused by earlier/late transportation of packages and extra fees for utilization of ad hoc capacities should be included in the total cost calculation. The minimization of the total operating cost in the cargo transportation process can be formulated as

$$\min_{\mathbf{x},\mathbf{y},\mathbf{z}} \sum_{d\in\mathcal{D}} \sum_{g\in\mathcal{G}_d} \left[\varphi_g \left(\mathbb{E}\left[Q_{d,g}\left(\mathbf{y}_d\right)\right] - B_{d,g}\left(\mathbf{y}_d, \mathbf{Y}_{d,g}\right)\right)\right]. \tag{4.1}$$

The practical meaning of the objective function can be explained as the total cost of air cargo transportation by passenger flight on a typical day within the examined mid-term period. In Eq. (4.1), φ_g indicates the probability that flight capacity scenario g happens and $\mathbb{E}[.]$ is the expectation operator (Khassiba et al., 2020; Ramirez-Pico et al., 2023). Given the mid-term capacity reservation strategies $\mathbf{y}$ and a specific capacity scenario g between (i, j), $\mathbb{E}\left[Q_g\left(\mathbf{y}\right)\right]$ is the expected cost across all possible cargo demand scenarios and the corresponding cargo-to-flight allocations during the short-term phases. $-B_g\left(\mathbf{y}, \mathbf{Y}_g\right)$ represents the opportunity cost resulting from inefficient capacity utilization. This term depends solely on capacity scenarios, not on demand scenarios. It can be computed using Eq. (4.5), which will be explained later. Given η_h denoting the probability of cargo demand scenario h occurring, $\mathbb{E}\left[Q_g\left(\mathbf{y}\right)\right]$ can be formulated as the average value going through all possible cargo scenarios, represented by

$$\mathbb{E}\left[Q_g\left(\mathbf{y}\right)\right] = \sum_{h\in\mathcal{H}} \eta_h Q_{g,h}\left(\mathbf{y}\right). \tag{4.2}$$

Under the realized capacity-demand scenario (g, h), the total operating cost $Q_{d,g,h}\left(\mathbf{y}_d\right)$ for transporting cargo to destination d is composed of costs by using ad hoc service $\sum_{m\in\mathcal{M}_d} \tau w_{m,h} z_{m,h}$, the fuel cost for carrying cargo packages that are allocated to regular services $\sum_{m\in\mathcal{M}_d} \xi w_{m,h} \sum_{k\in\mathcal{K}_d} x_{mk,h}$, and possible time penalty when packages are not delivered in due time window $\sum_{m\in\mathcal{M}_d} \sum_{k\in\mathcal{K}_d} f_{mk,h} x_{mk,h}$, which is formulated as

$$Q_{g,h}\left(\mathbf{y}\right) = \min_{\mathbf{x},\mathbf{z}} \sum_{m\in M_h} \left(\tau w_{m,h} z_{m,h} + \xi w_{m,h} \sum_{k\in K} x_{mk,g,h} + \sum_{k\in K} f_{mk,g,h} x_{mk,g,h}\right). \tag{4.3}$$

In Eq. (4.3), τ indicates the unit cost of ad hoc services for transporting cargo packages with unit weight. It should be noted that the weights of packages under different scenarios may be different to account for the uncertainty of cargo demand. $w_{m,h}$ indicates the weight of package m under scenario h. $z_{m,h}$ is a binary variable showing whether package m is delivered by ad hoc services under scenario h. $\sum_{k\in\mathcal{K}_d} x_{mk,h}$ determines whether package m is dealt with by regular services provided by one of the available flights. ξ indicates the unit marginal cost for carrying air cargo with the unit weight. The parameters τ and ξ are treated as exogenous and remain constant throughout the planning horizon. This simplification is widely adopted in transportation and logistics planning models, especially when the goal is to evaluate high-level resource allocation decisions rather than detailed operational pricing strategies. $f_{mk,g,h}$ is the time penalty of package m if it is allocated to flight k under scenario (g, h), defined as a point-wise function in

$$f_{mk,g,h} = \begin{cases} L & T_{k,g} < r_{m,h} \\ \alpha_1 \left(v_{m,h} - T_{k,g}\right) & r_{m,h} \leq T_{k,g} < v_{m,h} \\ 0 & v_{m,h} \leq T_{k,g} \leq b_{m,h} \\ \alpha_2 \left(T_{k,g} - b_{m,h}\right) & b_{m,h} < T_{k,g} \leq q_{m,h} \\ L & T_{k,g} > q_{m,h} \end{cases}. \tag{4.4}$$

The variable $T_{k,g}$ represents the departure time of flight k under scenario g. Each package m assigned to a flight k departs at the same time as the flight. The penalty cost generated from the allocation of a package is then determined based on its departure time, its due departure time window $\left[v_{m,h}, b_{m,h}\right]$, and its acceptable departure time window $\left[r_{m,h}, q_{m,h}\right]$. Penalty parameters α_1 and α_2 are applied for the calculation of time penalty when package m's departure time is earlier than $v_{m,h}$ or later than $b_{m,h}$, respectively, when the departure time falls within $\left[r_{m,h}, q_{m,h}\right]$. Additionally, L is a very large positive number to represent the unacceptable scenario in which a package is transported earlier than $r_{m,h}$ or later than $q_{m,h}$.

We consider the uncertainty in flight capacity as scenario-based fluctuation through different short-term planning phases. Under scenario g, available capacities on flights between each OD pair of airports (i, j) is known as $\mathbf{Y}_g$. After reserving flight capacity, there may be instances where not all of the reserved capacity is utilized. This unused capacity represents a lost opportunity, as it could have been allocated to other cargo shipments or used for alternative revenue-generating activities. Ignoring this cost would underestimate the true economic impact of over-reserving capacity. To accurately model this effect, we introduce an opportunity cost $-B_g\left(\mathbf{y}, \mathbf{Y}_g\right)$ for unused capacity. By assigning a unit opportunity cost $f^b \geq 0$ to reflect the potential value lost for each unit of unused capacity, $-B_g\left(\mathbf{y}, \mathbf{Y}_g\right)$ can be modeled as the unit opportunity cost f^b multiplying the exceeded capacity in flights after reservations, formulated as:

$$-B_g\left(\mathbf{y}, \mathbf{Y}_g\right) = -\sum_{k \in \mathcal{K}_g} f^b \times \max\left\{0, Y_{k,g} - y_k\right\}. \tag{4.5}$$

$-B_g\left(\mathbf{y}, \mathbf{Y}_g\right)$ is a nonlinear function of $\mathbf{y}_k$ and is minimized in the objective function. This consideration ensures that the optimization framework properly accounts for the trade-off between reserving sufficient capacity to meet uncertain demand and the risk of incurring costs from excess, unutilized capacity. f^b is assumed to be a constant in Eq. (4.5). This consideration simplifies the model and reflects a scenario where the marginal value of alternative uses for excess capacity does not diminish as the volume increases. In other words, the impact of the excessed capacity $\max\left\{0, Y_{k,g} - y_k\right\}$ on the demand-supply imbalance in the cargo transportation is negligible.

After a detailed introduction of the composed items in the objective function defined in Eq. (4.1), it can be inferred that reserving more cargo capacity (larger y_k values) reduces costs associated with ad hoc service utilization but increases opportunity costs, i.e., lost revenue in our study. In contrast, reserving lower cargo capacities (smaller y_k values) on passenger flights allows for greater revenue generated through the use of excess capacity (i.e., $\max\left\{0, Y_{k,g} - y_k\right\}$). However, this approach may result in insufficient capacity for cargo transportation, leading to higher costs for utilizing additional ad hoc capacity. Therefore, it is crucial to strike a balance between these two types of costs by optimizing mid-term capacity reservations.

4.2.4.2 Constraints

In this section, constraints adopted in the model are introduced to ensure that the mid-term capacity reservations and short-term package-to-flight allocations are optimized within feasible domains.

(Cargo flow conservation constraints): On each specific day with capacity-demand scenario (h, g), every package m arriving at its origin airport must be handled, either by utilizing passenger flights (when $\sum_{k\in K} x_{mk,g,h} = 1$) or through ad hoc capacities provided by other carriers (when $z_{m,g,h} = 1$). Since ad hoc services are not tied to specific scheduled flights, the flight index k does not apply to this variable and is therefore omitted. These constraints ensure that operators complete the transportation of every cargo package in daily tasks, either by regular services provided by the flight capacities or ad hoc services from the spot market. The cargo flow conservation constraints can be formulated as

$$\sum_{k\in\mathcal{K}_d} x_{mk,g,h} + z_{m,g,h} = 1, \forall d \in \mathcal{D}, h \in \mathcal{H}_d, g \in \mathcal{G}_d, m \in \mathcal{M}_d. \tag{4.6}$$

By substituting Constraint (4.6) into the objective function and subtracting a constant item regarding the fixed fuel costs for carrying all packages, i.e. $\sum_{m\in\mathcal{M}_d} \xi w_{m,h}$, Eq. (4.3) can be rewritten as

$$Q_{g,h}(\mathbf{y}_d) = \min_{\mathbf{x},\mathbf{z}} \sum_{m\in\mathcal{M}_d} \left(\sigma w_{m,h} z_{m,g,h} + \sum_{k\in\mathcal{K}_d} f_{mk,g,h} x_{mk,g,h} \right), \tag{4.7}$$

where $\sigma = \tau - \xi$ indicates the extra unit fee paid for the usage of ad hoc services apart from the unit operating cost (fuel cost) for the air cargo transportation.

(Capacity constraints): For each destination airport d, when we allocate packages to the scheduled passenger flights, the total weight of all loaded cargo in a flight k should not exceed the maximum cargo capacity that flight k can provide (Vancroonenburg et al., 2014). The provided capacity for air cargo transportation in flight k is determined by the lower limit between the reserved capacity (y_k) on the flight and the maximum available capacity remaining after the loading of passengers' baggage $(Y_{k,g})$. Then capacity constraints for each flight serving destination d can be represented by

$$\sum_{m \in \mathcal{M}_d} w_{m,h} x_{mk,g,h} \leq y_k, \forall d \in \mathcal{D}, g \in \mathcal{G}_d, h \in \mathcal{H}_d, k \in \mathcal{K}_d. \tag{4.8a}$$

$$\sum_{m \in \mathcal{M}_d} w_{m,h} x_{mk,g,h} \leq Y_{k,g}, \forall d \in \mathcal{D}, g \in \mathcal{G}_d, h \in \mathcal{H}_d, k \in \mathcal{K}_d, \tag{4.8b}$$

(Loading time constraints): During each short-term phase, the arrival time of a cargo is considered as the time that the cargo is ready for loading. Then, the arrival time of cargo m must be within the available loading time period of flight k to ensure that cargo m can be loaded onto flight k, formulated as

$$\sum_{k \in \mathcal{K}_d} x_{mk,g,h} l_{k,g} - z_{m,g,h} L \leq t_{m,h} \leq \sum_{k \in \mathcal{K}_d} x_{mk,g,h} u_{k,g} + z_{m,g,h} L, \forall d \in \mathcal{D}, g \in \mathcal{G}_d, h \in \mathcal{H}_d, m \in \mathcal{M}_d. \tag{4.9}$$

In our model, the arrival time of a cargo package $t_{m,h}$ is when it reaches the unloading point at the origin airport, i.e., the designated area where cargo is handed over from delivery vehicles to ground handling. The loading time window of flight k, i.e., $[l_{k,g}, u_{k,g}]$, is the period during which a package must leave the unloading point to make sure it can be loaded onto this flight. Since both events occur at the same location, we assume the transfer time between unloading and loading is negligible. This simplifies the model by focusing on the timing of cargo arrival and flight loading, without complicating intra-terminal logistics, and maintains model tractability while reflecting operational constraints.

L is taken as a sufficiently large number to ensure that the loading time constraints are satisfied, regardless of whether package m is transported by scheduled flight capacities or ad hoc services. For a specific destination d, if a package m is transported by the regular transportation services provided by flights, i.e., $\sum_{k \in \mathcal{K}_d} x_{mk,g,h} = 1$ while $z_{m,g,h} = 0$, $\sum_{k \in \mathcal{K}_d} x_{mk,g,h} l_{k,g}$ and $\sum_{k \in \mathcal{K}_d} x_{mk,g,h} u_{k,g}$ correspond to the earliest and latest loading times of the assigned flight, respectively. Conversely, if package m is transported via ad hoc services, i.e., $\sum_{k \in \mathcal{K}_d} x_{mk,g,h} = 0$ and $z_{m,g,h} = 1$, Eq. (4.9) is always satisfied.

(Reservation rationality constraints): In the short-term allocation process, the cargo capacity utilized on a passenger flight is determined by the minimum of the reserved capacity and the actual available belly capacity, which may vary across different short-term scenarios. Therefore, it is essential that the reserved capacity on each flight does not exceed the maximum possible belly capacity that could be realized in any scenario. While Constraint (4.8b) ensures feasibility by limiting the allocated capacity to what is available in each scenario, Constraint (4.10) ensures that the reservation itself remains meaningful and potentially usable across all scenarios. Reserving more capacity than the maximum attainable would result in an allocation that is always reduced at the operational level, rendering a portion of the reservation ineffective and leading to suboptimal strategic decisions. The constraint to ensure the rationality of capacity reservation schemes can be proposed as

$$0 \leq y_k \leq \max_g \left\{Y_{k,g}\right\}, \forall d \in \mathcal{D}, g \in \mathcal{G}_d, k \in \mathcal{K}_d. \tag{4.10}$$

(Variable constraints): In the proposed optimization problem, we take the variables indicating short-term allocation schemes of each package as binary variables and the variables representing mid-term capacity reservations as continuous variables, which can be concluded as

$$x_{mk,g,h}, z_{m,g,h} \in \{0,1\}, \forall d \in \mathcal{D}, h \in \mathcal{H}_d, g \in \mathcal{G}_d, m \in \mathcal{M}_d, k \in \mathcal{K}_d \tag{4.11}$$

and

$$y_k \geq 0, \forall d \in \mathcal{D}, k \in \mathcal{K}_d. \tag{4.12}$$

Table 4.2 summarizes the key features of the proposed two-stage stochastic programming model (Eqs. (4.1)-(4.12)). In this table, second-stage variables, $x_{mk,g,h}$ and $z_{m,g,h}$ are binary variables while the first-stage variables, i.e., y_k's for different d and k, are continuous variable. Constraints (4.10), as well as the objective function in Eq. (4.1), involve non-linearity. However, by defining the calculation of expected value in Eq. (4.2), the objective function in Eq. (4.1) can be taken as linear. Similarly, Constraint (4.10) can be treated as linear constraints since the expected maximum capacity of flights can be considered as constants. The complexity of the proposed model is influenced by the number of packages, flights, and OD pairs, as well as the fluctuations in flight capacity and the uncertainties in air cargo demand.

Table 4.2: Characteristics of the proposed two-stage stochastic programming model

Variables	**Size**	**Type**
Short-term package-to-passenger flight allocation: $x_{mk,g,h}$	$\sum_{d\in\mathcal{D}} \lvert\mathcal{G}_d\rvert\lvert\mathcal{H}_d\rvert\lvert\mathcal{K}_d\rvert\lvert\mathcal{M}_d\rvert$	Binary
Mid-term capacity reservation schemes: y_k	$\sum_{d\in\mathcal{D}} \lvert\mathcal{G}_d\rvert\lvert\mathcal{K}_d\rvert$	Continuous
Short-term package-to-ah hoc service allocation: $z_{m,g,h}$	$\sum_{d\in\mathcal{D}} \lvert\mathcal{G}_d\rvert\lvert\mathcal{H}_d\rvert\lvert\mathcal{M}_d\rvert$	Binary
Objective function	**Size**	**Type**
Objective Function for the first stage defined in (4.1)	1	Nonlinear
Objective Function for a specific destination defined in Eq. (4.2)	$\lvert\mathcal{D}\rvert$	Linear
Objective Function under a given capacity-demand scenario (4.3) (under each given scenario (g, h))	$\sum_{d\in\mathcal{D}} \lvert\mathcal{G}_d\rvert\lvert\mathcal{H}_d\rvert$	Linear
Constraints	**Size**	**Type**
Cargo flow conservation constraints (4.6)	$\sum_{d\in\mathcal{D}} \lvert\mathcal{G}_d\rvert\lvert\mathcal{K}_d\rvert\lvert\mathcal{M}_d\rvert$	Linear
Capacity constraints (4.8)	$\sum_{d\in\mathcal{D}} \lvert\mathcal{G}_d\rvert\lvert\mathcal{K}_d\rvert\lvert\mathcal{M}_d\rvert$	Nonlinear
Loading time constraints (4.9)	$2\sum_{d\in\mathcal{D}} \lvert\mathcal{G}_d\rvert\lvert\mathcal{K}_d\rvert\lvert\mathcal{M}_d\rvert$	Linear
Reservation rationality constraints (4.10)	$\sum_{d\in\mathcal{D}} \lvert\mathcal{G}_d\rvert\lvert\mathcal{K}_d\rvert$	Linear

4.3 Solution approach

This section outlines approaches applied to solve the proposed two-stage stochastic program, enabling the attainment of high-quality solutions within an acceptable time. Applicable approaches for solving stochastic programs include analytic or deterministic reformulations that replace the expectation with closed forms or convex approximations (fast but seldom applicable to mixed-integer second-stage decisions), Benders/L-shaped and multicut decompositions that are effective for linear second-stage models but often degrade with integrality, branch-and-Benders that strengthens cuts within mixed-integer linear program (MILP) trees at increased algorithmic complexity and runtime, stochastic dual dynamic programming which is particularly well suited to multistage linear settings rather than two-stage mixed-integer non-linear program (considered in our study), distributionally robust optimization (DRO) that enhances robustness via ambiguity sets but is more conservative and computationally demanding (Wiesemann et al., 2014; Cherukuri & Cortés, 2019; Löhndorf & Shapiro, 2019; van Ackooij & Warin, 2020; Branda & Matoušková, 2024; Hasan & Kargarian, 2024). Apart from the above mentioned methods, SAA and PHA are both been considered as mature methods for dealing with uncertainties to solve stochastic programming problems Dong et al. (2015). In our study, the objective function in the first-stage and the fight capacity constraints are non-linear, making it necessary and essential to decompose the origin problem to deterministic sampled scenario. Given the fixed parameters and the inclusion of first-stage variables in the second stage, every separated scenario-specific optimization can be seen as deterministic MILP. Therefore, we combine SAA with PH because our uncertainty does not produce tractable analytic expectations and our model exhibits strong scenario separability with mixed-integer second-stage decisions. SAA converts the nonlinear problem into a finite-scenario MILP amenable to deterministic optimization methods Verweij et al. (2003), while PHA decomposes the SAA model by scenario, enforces nonanticipativity through simple penalties, and exploits parallel computation of scenario-specific optimization.

4.3.1 Handling uncertainties based on Sample Average Approximation

The management of passenger flight capacity and air cargo demand involves various uncertainties, complicating the solving process for the proposed two-stage stochastic program designed to optimize capacity management and cargo allocation in two separate stages. SAA is particularly effective in this context, as it generates high-quality solutions by focusing on a representative subset of scenarios, thereby avoiding the difficulty of evaluating the entire set (Kenan et al., 2018). In our study, SAA operates by generating a typical sample of capacity-cargo scenarios, each indexed by s, from a total sample size of S that captures potential variations in uncertain parameters relevant to the model. In SAA, the index s

represents a specific scenario, similar to the given scenario indicated by (g, h) discussed above. By incorporating these sampled scenarios into the stochastic model, SAA reduces computational complexity while maintaining solution feasibility and high quality, making it well-suited for complex real-world stochastic optimization applications.

To simplify and enhance the solvability of the model, we assume that air cargo demand and flight capacities for each OD pair are independent. This assumption allows us to decompose the comprehensive program for optimizing air cargo transportation across the entire network into a series of more manageable distinct optimization tasks for each OD pair. Consequently, by applying SAA, the optimization model for an OD pair (noted as (i, j)) can be formulated as P 1. Under each generated scenario s, the considered uncertainty factors of flights and cargo demand are treated as given information.

P 1.

$$\min_{\mathbf{x},\mathbf{y},\mathbf{z}} Q = \sum_{d\in\mathcal{D}} \sum_{s\in\mathcal{S}_d} \left(\frac{1}{|\mathcal{S}_d|} \sum_{s\in\mathcal{S}_d} Q_{d,s} \right) \tag{4.13}$$

where

$$Q_{d,s} = \left(\sum_{m\in\mathcal{M}_d} \sigma w_{m,s} z_{m,s} + \sum_{m\in\mathcal{M}_d} \sum_{k\in\mathcal{K}_d} f_{mk,s} x_{mk,s} - \sum_{k\in\mathcal{K}_d} \varepsilon \times \max\left\{0, Y_{k,s} - y_k\right\} \right) \tag{4.14}$$

$$f_{mk,s} = \begin{cases} L & t^d_{k,s} < r_{m,s} \\ \alpha_1 \left(v_{m,s} - d_{k,s}\right) & r_{m,s} \le d_{k,s} < v_{m,s} \\ 0 & v_{m,s} \le d_{k,s} \le b_{m,s} \\ \alpha_2 \left(d_{k,s} - u_{m,s}\right) & b_{m,s} < d_{k,s} \le q_{m,s} \\ L & d_{k,s} > q_{m,s} \end{cases} \tag{4.15}$$

s.t.

$$\sum_{k\in\mathcal{K}_d} x_{mk,s} + z_{m,s} = 1, \forall d \in \mathcal{D}, s \in \mathcal{S}_d, m \in \mathcal{M}_d \tag{4.16}$$

$$\sum_{m\in\mathcal{M}_d} w_m x_{mk,s} \le \min\left\{y_k, Y_{k,s}\right\}, \forall d \in \mathcal{D}, s \in \mathcal{S}_d, k \in \mathcal{K}_d \tag{4.17}$$

$$\sum_{k\in\mathcal{K}_d} x_{mk,s}l_{k,s} - z_{m,s}L \le t_{m,s} \le \sum_{k\in\mathcal{K}_d} x_{mk,s}u_{k,s} + z_{m,s}L, \forall d \in \mathcal{D}, s \in \mathcal{S}_d, m \in \mathcal{M}_d, k \in \mathcal{K}_d \tag{4.18}$$

$$0 \le y_k \le \max_s \left\{Y_{k,s}\right\}, \forall d \in \mathcal{D}, s \in \mathcal{S}_d, k \in \mathcal{K}_d \tag{4.19}$$

$$x_{mk,s}, z_{m,s} \in \{0,1\}, \forall d \in \mathcal{D}, s \in \mathcal{S}_d, m \in \mathcal{M}_d, k \in \mathcal{K}_d \tag{4.20}$$

$$y_{k,s} \ge 0, \forall d \in \mathcal{D}, s \in \mathcal{S}_d, k \in \mathcal{K}_d \tag{4.21}$$

4.3.2 Optimization of capacity reservation scheme - Progressive Hedging algorithm

The objective function formulated in Eq. (4.13) includes decision variables for the first and second stages of the studied program. To address the complexity of this formulation, we employ the Progressive Hedging (PH) algorithm (Rockafellar & Wets, 1991), a scenario decomposition technique (Rajan et al., 2022), which is particularly well-suited for solving stochastic programming problems as it addresses the nonanticipativity constraints inherent in such formulations, i.e., ensuring that decisions made before the realization of uncertainty remain consistent across all scenarios (Listes & Dekker, 2005; Fan & Liu, 2010; Watson & Woodruff, 2011; Atakan & Sen, 2018). PH achieves this by decomposing the original two-stage stochastic problem into independent scenario subproblems under realized scenario s, which can be solved in parallel. The PH algorithm applied in our study assigns a distinct set of first-stage decision variables to each scenario, enabling parallel computations. For instance, for each scenario $s \in S$, the algorithm introduces decision variables $y_{k,s}$ and enforces a non-anticipativity constraint defined as

$$y_{k,s} = y_k, \forall d \in \mathcal{D}, s \in \mathcal{S}_d, k \in \mathcal{K}_d. \tag{4.22}$$

The constraint is essential as it ensures the first-stage decision vector across separate sampled scenarios (represented by $\mathbf{y_s}$) are identical and equal to $\mathbf{y}$. Furthermore, to ensure convergence to the optimal solution, the PH algorithm incorporates the penalty items into the objective function under each individual scenario s, which can be formulated as follows:

$$Q'_{d,s} = \sum_{m\in\mathcal{M}_d}\left(\sigma w_{m,s}z_{m,s} + \sum_{k\in\mathcal{K}_d} f_{mk,s}x_{mk,s}\right) - \sum_{k\in\mathcal{K}_d}\varepsilon\times\max\left\{0, Y_{k,s} - y_{k,s}\right\} + \sum_{k\in\mathcal{K}_d}\left(\lambda_{k,s}y_k + \frac{\rho}{2}\left\|y_{k,s} - y_k\right\|^2\right). \quad (4.23)$$

These subproblem solutions are then coordinated through an iterative process that updates a consensus (or aggregated) solution using dual variable adjustments. This decomposition-based approach not only improves computational efficiency because of the parallel solving process of separate scenarios but also facilitates scalability when dealing with large-scale, scenario-based models. The corresponding program by applying the PH algorithm is depicted as P 2.

P 2.

$$\min_{\mathbf{x}_s,\mathbf{y}_s,\mathbf{z}_s} Q'_{d,s} \quad (4.24)$$

s.t.

$$\lambda_{k,s} > 0, \forall d\in\mathcal{D}, s\in\mathcal{S}_d, k\in\mathcal{K}_d \quad (4.25)$$

$$\rho > 0 \quad (4.26)$$

$$Constraints (4.16) - (4.18), (4.20), (4.21)$$

and

$$\sum_{m\in\mathcal{M}_d} w_m x_{mk,s} \leq \min\left\{y_{k,s}, Y_{k,s}\right\}, \forall d\in\mathcal{D}, s\in\mathcal{S}_d, k\in\mathcal{K}_d \quad (4.27)$$

$$0 \leq y_{k,s} \leq \max_s \left\{Y_{k,s}\right\}, \forall d\in\mathcal{D}, s\in\mathcal{S}_d, k\in\mathcal{K}_d \quad (4.28)$$

In the PH algorithm, y_k in Eq. (4.17) and Eq. (4.19) is replaced by $y_{k,s}$ in Eq. (4.27) and Eq. (4.28) to distinguish y_k under different sample scenarios in the PH algorithm. Two parameters are required in the PH algorithm: i) a penalty factor, $\rho > 0$ and ii) a termination threshold represented by ϵ. Given ρ and ϵ, the pseudo-code for the PH algorithm for solving capacity management problems under each scenario is shown as Algorithm 1.

In the step **Decomposition** of Algorithm 1, the update of capacity reservation scheme $\mathbf{y}_s$

follows the Gradient Descent Algorithm idea by Eq. (4.29). δ is the learning rate shaping the step size of $y_{k,s}$ moving for the next iteration.

$$y_{k,s}^{(n+1)} = y_{k,s}^{(n)} - \delta \left[\lambda_{k,s}^{(n)} + \rho \left(y_{k,s}^{(n)} - y_{k}^{(n)}\right)\right] \tag{4.29}$$

In this chapter, we introduce an additional termination criterion based on the changes in the first-stage variables between consecutive iterations, which is quantified by the change between $\mathbf{y}^{(n)}$ and $\mathbf{y}^{(n-1)}$. When the change falls below the threshold in the termination criterion (ϵ), we infer that the first-stage variables have converged. This criterion is particularly effective in our analysis because the penalty associated with the non-anticipativity constraint in Eq. (4.22) actively drives $\mathbf{y}_s^{(n)}$ towards $\mathbf{y}^{(n-1)}$ with each iteration, ensuring consistent convergence across iterations.

Algorithm 1 Progressive Hedging for solving first-stage variables for a destination d: a pseudo-code

Initialization:
For every destination $d \in \mathcal{D}$, set $n \leftarrow 0$ ▷ iteration count
For every scenario $s \in S_d$, $\mathbf{y}_s^{(n)} = \left(..., y_{k,s}^{(n)}, ...\right) \leftarrow \arg\min_{\mathbf{x}_s,\mathbf{y}_s,\mathbf{z}_s} Q_s$
$\mathbf{y}^{(n)} := \left(..., y_k^{(n)}, ...\right) \leftarrow \frac{1}{S} \sum_{s\in\mathcal{S}_d} \mathbf{y}_s^{(n)}$ ▷ initial capacity reservation scheme
For every $s \in \mathcal{S}_d$, $\lambda_s^{(n)} := \rho \cdot \left(\mathbf{y}_s^{(n)} - \mathbf{y}^{(n)}\right)$ ▷ initial weight vector computation
Iteration update:
$n \leftarrow n + 1$
Decomposition:
For every $s \in \mathcal{S}_d$, $\mathbf{y}_s^{(n)} = \left(..., y_{k,s}^{(n)}, ...\right) \leftarrow \arg\min_{\mathbf{x}_s,\mathbf{y}_s,\mathbf{z}_s} Q_s'$
Aggregation:
$\mathbf{y}^{(n)} = \left(..., y_k^{(n)}, ...\right) \leftarrow \frac{1}{|\mathcal{S}_d|} \sum_{s\in\mathcal{S}_d} \mathbf{y}_s^{(n)}$
Weight update:
For every $s \in \mathcal{S}_d$, $\lambda_s^{(n)} := \lambda_s^{(n-1)} + \rho \cdot \left(\mathbf{y}_s^{(n)} - \mathbf{y}^{(n)}\right)$
Termination criterion check:
$\epsilon^{(n)} := \frac{1}{|\mathcal{S}_d|} \sum_{s\in\mathcal{S}_d} \left\|\mathbf{y}_s^{(n)} - \mathbf{y}^{(n)}\right\|$
$\omega^{(n)} := \left\|\mathbf{y}^{(n)} - \mathbf{y}^{(n-1)}\right\|$
if $(\epsilon^{(n)} > \epsilon)|(\omega^{(n)} > \omega)$ **then**
    Go to **Iteration update**
else
    Terminate with the first-stage strategies $\mathbf{y}^{(n)}$ (i.e., capacity reservation scheme)
end if

Once the capacity reservation scheme is updated, the cargo-to-flight allocation in the second stage is a generalized assignment problem (GAP), which is hard to obtain exact solutions, especially when numerous passenger flights and a large number of packages are involved. Haddadi (1999) employed Lagrangian relaxation to derive the lower bound of a minimization program, which served as a baseline for developing outperformed heuristic algorithms to achieve good-quality solutions. The gaps between the lower bounds from the relaxed model and the upper bounds provided by feasible solutions from heuristic algorithms demonstrate the performance of these algorithms. The outperformed heuristic algorithm is applied to achieve high-quality solutions for every sampled scenario under the SAA frame.

In the **Decomposition** step, following each update of $\mathbf{y}_s$, the operating costs under each scenario (within the scenario set generated in SAA) are calculated, along with the associated penalty items. Thus, the value of $Q_s^{'}$ can be obtained. Combined Eqs. (4.29) and (**??**), δ can be understood as the step size used in the Gradient Descent Algorithm to iteratively update the decision variables. The step size controls the magnitude of each update in the direction of the negative gradient and plays a critical role in determining the convergence of operating costs under each scenario as well as the quality of solutions. Based on adjustments to the system parameters, the initial value of δ is set to be 1 and then follows a dynamic step size strategy. When $Q_s^{'}$ decreases compared to the last iteration after updating $\mathbf{y}_s$, the update of $\mathbf{y}_s$ is repeated according to Eq. (4.29). Else δ halves. Once $Q_s^{'}$ decreases, δ goes back to the initialized value. The iterative process stops when δ is smaller than the threshold or the number of iterations is larger than the maximum iteration number, at which $\mathbf{y}_s^n$ is reported as the final solution to P 2. The key characteristics of P 2 are concluded in Table 4.3. It is evident that the scale of the problem is significantly smaller than that presented in Eqs. (4.1)-(4.12). The complexity of the program P 2 mainly depends on the amount of cargo demand, the number of passenger flights, and the number of generated sample scenarios by SAA.

Table 4.3: Characteristics of P 2

Variables/Objective functions	Size	Type
$x_{mk,s}$	$\sum_{d\in\mathcal{D}} \lvert\mathcal{S}_d\rvert \lvert\mathcal{M}_d\rvert \lvert\mathcal{K}_d\rvert$	Binary
$y_{k,s}$	$\sum_{d\in\mathcal{D}} \lvert\mathcal{S}_d\rvert \lvert\mathcal{K}_d\rvert$	Continuous
$z_{m,s}$	$\sum_{d\in\mathcal{D}} \lvert\mathcal{S}_d\rvert \lvert\mathcal{M}_d\rvert$	Binary
Objective function in the PH algorithm (4.24)	1	Quadratic
Constraints	**Size**	**Type**
Cargo flow conservation constraints (4.16)	$\sum_{d\in\mathcal{D}} \lvert\mathcal{S}_d\rvert \lvert\mathcal{M}_d\rvert$	Linear
Capacity constraints (4.17)	$\sum_{d\in\mathcal{D}} \lvert\mathcal{S}_d\rvert \lvert\mathcal{M}_d\rvert \lvert\mathcal{K}_d\rvert$	Linear
Loading time constraints (4.18)	$2\sum_{d\in\mathcal{D}} \lvert\mathcal{S}_d\rvert \lvert\mathcal{M}_d\rvert \lvert\mathcal{K}_d\rvert$	Linear
Reservation rationality constraints (4.19)	$\sum_{d\in\mathcal{D}} \lvert\mathcal{S}_d\rvert \lvert\mathcal{K}_d\rvert$	Linear
Weight vector positivity constraints (4.25)	$\sum_{d\in\mathcal{D}} \lvert\mathcal{S}_d\rvert \lvert\mathcal{K}_d\rvert$	Linear
Penalty factor positivity constraints (4.26)	$\lvert\mathcal{S}_d\rvert$	Linear

4.3.3 Optimization of capacity management and cargo-to-flight allocation in each sampled scenario

Within the SAA framework, the optimization problems associated with individual sample scenarios can be solved in parallel to generate candidate solutions, denoted by $\mathbf{x}_{d,s}$, $\mathbf{z}_{d,s}$ and $\mathbf{y}_{d,s}$, , together with the corresponding objective values $Q_s^{'}$. For small-scale instances, each iteration solves the scenario-specific subproblems with a standard solver. After obtaining updated first-stage variables $\mathbf{y}_{d,s}$ for all scenarios, the aggregated first-stage decision $\mathbf{y}_d$ is updated by averaging across scenarios, i.e., $\mathbf{y}_{d,s} = \frac{1}{|\mathcal{S}_d|}\sum_{s\in\mathcal{S}_d} \mathbf{y}_s^{(n)}$.

$$\sum_{m\in\mathcal{M}_d} w_m x_{mk,s} \le Y_{k,s}, \forall d \in \mathcal{D}, s \in \mathcal{S}_d, k \in \mathcal{K}_d \tag{4.30a}$$

$$\sum_{m\in\mathcal{M}_d} w_m x_{mk,s} \le y_{k,s}, \forall d \in \mathcal{D}, s \in \mathcal{S}_d, k \in \mathcal{K}_d \tag{4.30b}$$

$$Y_{k,s} \ge y_{k,s} + \left(\delta_{k,s} - 1\right) L, \forall d \in \mathcal{D}, s \in \mathcal{S}_d, k \in \mathcal{K}_s \tag{4.31a}$$

$$y_{k,s} + \delta_{k,s} L \ge Y_{k,s}, \forall d \in \mathcal{D}, s \in \mathcal{S}_d, k \in \mathcal{K}_d \tag{4.31b}$$

For medium-scale instances with more flights and greater cargo demand, obtaining both first- and second-stage decisions within acceptable time using a solver may be infeasible. In this case, first-stage capacity reservations are updated exogenously, and the allocation (second-stage) decisions are optimized by the solver. For large-scale instances with many destinations and high cargo volumes, the problem is solved using heuristic algorithms.

Several heuristic algorithms are tested to identify high-quality cargo allocations under each scenario s in the decomposition step of Algorithm 1. Specifically, we examine five different algorithms: i) random allocation, ii) lower bound replication (LBR), iii) greedy regret (RGT), iv) a combination of LBR and RGT, and v) modified RGT. While the application of LBR and RGT in package allocation follows the main ideas proposed in Jeet & Kutanoglu (2007), the specific implementation details have been adjusted to suit our specific problem. The main concepts of these algorithms are discussed in this subsection, while detailed steps and pseudo-code for the tested heuristic algorithms are provided in 8.2. In numerical studies, we compare the performance of these algorithms and apply the outperformed one to derive solutions for every sampled scenario in the PH algorithm.

4.3.3.1 Initialization

The heuristic algorithms for solving the decomposed problems defined in P **??** share similar preliminary steps, including data input, notation establishment, and the realized capacity level updating according to the reservation schemes. The initialization steps applicable to the analyzed heuristic algorithms are summarized in Algorithm 2. Following the collection of data on flights and packages, along with the initialization of parameters and sets, the allocation process is carried out by applying various heuristic algorithms. In this chapter, we consider a fixed number of flights between every OD pair of airports, as airline operators typically determine the number of flights based on extensive historical data and stakeholder experience before a mid-term planning period, as claimed in Assumption **??**. Additionally, the daily quantity of air cargo packages delivered to the origin airport is predetermined, implying that while the number of delivery instances is fixed, the weight of packages delivered each time may vary, introducing demand uncertainty, as assumed in Assumption **??** and explained in

Section 4.2.1.

Algorithm 2 Initialization steps in heuristic algorithms for OD pair (i, j)

Notation definition:

Calculate $\mu_{k,s}$ for all (m, k) pairs under scenario s.

Let $\mathbf{x}_s$ be the vector of cargo transportation problem, i.e., $\mathbf{x}_s = (x_{mk,s})_{m=1,..,|\mathcal{M}_d|,k=1,...,|\mathcal{K}_d|}$.

Let $\mathcal{M}_d = \{1, ...m, ...|\mathcal{M}_d|\}$ be the set of packages to be delivered to the destination d under scenario s.

Let $\mathcal{K}_d = \{1, ...k, ...|\mathcal{K}_d|\}$ be the set of passenger flights serving the destination d under scenario s.

Data input:

Read package data and flight schedule between the origin airport and the destination d under scenario s including:

package information (taking package m as an example): package weights $w_{m,s}$, arrival time at the origin airport $t_{m,s}$, due departure time window at the origin airport $\left[v_{m,s}, b_{m,s}\right]$ and acceptable departure time window at the origin airport $\left[r_{m,s}, q_{m,s}\right]$.

Flight information (taking flight k as an example): Loading/unloading time window $\left[l_{k,s}, u_{k,s}\right]$, maximum capacity for air cargo transportation $Y_{k,s}$, and departure time from origin airports $d_{k,s}$.

Capacity realization

Initialize realized capacity of flight k under scenario s: $y'_{k,s} := \min\left\{Y_{k,s}, y_k\right\}$, for all $k \in \mathcal{K}_d$.

Given the capacity reserved scheme (i.e., $\mathbf{y}$), the cargo-to-flight allocation decided in the second stage is formulated as a generalized assignment problem (GAP). Since the GAP is NP-hard and has a strictly positive duality gap, solutions to the relaxed problem are seldom capacity-feasible, much less optimal. With more flights serving destinations and larger amount of cargo demands, it is difficult to get solutions within effective time expense.

4.3.3.2 Random Allocation

Random allocation is a straightforward method that randomly selects cargo packages from the package set and assigns them to delivery services—either by regular capacity in passenger flights or ad hoc services based on the lowest cost criteria. Given a set of cargo packages, the algorithm initiates by randomly choosing a package and identifying alternative flights with sufficient capacity to transport it. Acceptable penalty costs are incurred, which are lower than those associated with using ad hoc services. The identified flights must align with the package's arrival time at its origin airport within suitable loading time windows.

If a flight meets the specified time and capacity conditions and offers the lowest penalty cost, it is selected to transport the chosen package. If no flight can accommodate the package at a lower cost than using ad hoc capacities, operators tend to use ad hoc services instead. Every time a chosen package has been allocated, the package set is updated by removing the package. This allocating process introduced above repeats until all packages have been allocated to their respective delivery services. While the Random Allocation algorithm is straightforward, the random nature of package selection can introduce variability in performance, rendering the results somewhat less predictable. Detailed steps in the random allocation are illustrated in 8.2.1.

4.3.3.3 Lower bound replication

The main idea of the Lower Bound Replication (LBR) algorithm is to repeatedly verify whether the package allocations obtained from Algorithm **??** remain feasible when considering the capacity constraints (4.17). Even if we follow the main idea introduced by Jeet & Kutanoglu (2007), our investigated problem is different from that because ad hoc services are applied in our study to deal with cases where no regular services can be feasible. It is important to note that flight capacities are not updated by subtracting the weight of allocated packages in Algorithm **??**, as the capacity constraints are relaxed in the Lagrangian relaxation model. However, the LBR algorithm is applied to find good-quality feasible solutions. Thus, capacity constraints should be taken into account. In the LBR algorithm, for each selected package-flight pair, if the allocation in the lower bound solution is still feasible under the capacity constraints (i.e., it meets all delivery requirements), the allocation is retained. Otherwise, an alternative feasible flight (with the lowest penalty cost) is identified for delivering the package according to the same identifying criterion introduced in the random allocation algorithm in Section 4.3.3.2. If regular services are inapplicable for the package, ad hoc services will be utilized for its delivery. The steps of the LBR algorithm are detailed in 8.2.2.

4.3.3.4 Greedy regret (RGT)

In the Greedy Regret (RGT) algorithm, the concept of “regret” is used to quantify the cost difference between the second-best delivery service (with the second-lowest-cost) and the most preferred flight (with the lowest cost) (Jeet & Kutanoglu, 2007). The RGT algorithm prioritizes the allocation of packages with higher “regret” values to avoid suboptimal and potentially costly assignments.

Given specific cargo demand data, the RGT algorithm assigns a “regret” value to each cargo package and ranks them accordingly. It selects the package with the highest “regret” value for allocation to its most preferred delivery service (either by passenger flight capacity or ad hoc capacity). After each allocation, the available capacity of the corresponding flight is updated and the “regret” values of all remaining packages are recalculated. The allocating process is repeated until all cargo packages have been assigned. The detailed steps of the RGT algorithm are outlined in Section 8.2.3.

In each iteration, the RGT algorithm selects packages based on their “regret” values, potentially outperforming algorithms that rely on random selections, such as random allocation and the LBR algorithm. However, “regret” values for all remaining packages are necessarily updated every time when the package with the highest “regret” has been allocated. More computational time will be caused by the repeated calculation of “regret” values, which is a trade-off for the potential achievement of more cost-effective package allocation decisions.

4.3.3.5 Algorithm combining LBR and RGT

As introduced above, LBR saves time but yields lower-quality solutions, whereas RGT, although more time-consuming, delivers higher-quality results. Therefore, we are exploring whether combining the two could result in an algorithm that efficiently achieves high-quality solutions. The algorithm combines the LBR and RGT algorithms to allocate the packages through two consecutive operations. First, all the packages that can be transported by the same flights as those in the lower-bound solution remain in the same allocation, following the operations of the LBR algorithm. Then, the remaining packages are assigned to passenger flights/ad hoc services following the steps of the RGT algorithm. The detailed steps of the algorithm combining the LBR and RGT algorithms are shown in 8.2.4. We evaluate the integration of the LBR and RGT algorithms to determine whether it successfully combines the speed of the LBR algorithm with the superior solution quality of the RGT algorithm.

4.3.3.6 Simplified RGT

The primary distinction between the modified RGT algorithm and its original version lies in the frequency of recalculating "regret" values. In the original RGT algorithm, as described in Section 4.3.3.4, "regret" values for all remaining packages are recalculated with each allocation of a package with the highest "regret". This necessity arises because changes in the available capacities of flights can alter the "regret" values, which largely depend on the limited available capacity of the packages' preferred flights. However, in our study, based on Assumption 1, we can infer that the change of "regret" values might not be substantial enough to affect the subsequent choice of packages. In other words, packages' "regret" values often remain consistent before and after a package has been allocated.

In our study, the abundant unused capacity in passenger flights allows the application of the modified RGT algorithm with less frequent recalculation of the "regret" values. In the modified RGT algorithm, prioritize the allocation of packages with high "regret" values to their most favourable flights, provided there is enough capacity on those flights. If not, the packages remain in the set and await allocation in the subsequent iteration.

The "regret" values are only recalculated when no more packages can be allocated to the most cost-effective flight. This process repeats until all packages are assigned to an appropriate service. Therefore, the frequency of "regret" value calculations is significantly reduced in the modified RGT algorithm compared to the original version. This adjustment not only simplifies the allocation process but also significantly reduces the computational time associated with recalculating "regret" values, thereby enhancing the efficiency of the algorithm. Detailed operations of the modified RGT algorithm are concluded in Section 8.2.5.

4.4 Numerical experiments

Hong Kong International Airport (HKIA) has been the world's busiest international cargo airport since 1996, providing a representative and data-rich setting. In 2024, HKIA handled 4.9 million tonnes of cargo, underscoring the scale required to test capacity allocation and scheduling models. That volume accounted for about 45% of the value of Hong Kong's external trade, roughly HK$4,300 billion, highlighting HKIA's centrality to high-value, time-sensitive flows[2]. In the numerical study, we choose HKIA as the origin airport of cargo demands. Correspondingly, we choose the most closest connected destination airports with HKIA[3], including Narita International Airport (NRT), Taiwan Taoyuan International Airport (TPE), Shanghai Pudong International Airport (PVG), Suvarnabhumi Airport (BKK), Kansai International Airport (KIX), Ninoy Aquino International Airport (MNL), Singapore Changi Airport (SIN), and London Heathrow Airport (LHR). The detailed flight schedules to the selected destination airports are listed in Table 8.2. The degree of uncertainty in both cargo and flight is set at a high level to ensure that the experimental results adequately demonstrate the application of our proposed solution and the effectiveness of the framework. All computational experiments were conducted on a 1.70 GHz Intel Core i7 processor with 16 GB of RAM.

We assume the cargo demands are packed as ULDs with type LD-3-45 (IATA code: AKH), a reduced-height, narrower variant designed primarily for certain narrowbody aircraft with containerized holds. It is compatible with many Airbus A320 family aircraft but does not fit in most Boeing narrowbodies (e.g., 737). Therefore, we summarize the considered flight schedules in Table 4.4.

Flight-side data are generated to remain closely aligned with the real-world schedule in Table 4.4, while accommodating realistic stochastic variability. Starting the predetermined flight timetable, specifying destination, scheduled departure and arrival times, and nominal weight capacities implied by aircraft type, we construct destination-specific flight sets and introduce possible delays to departure times and fluctuation to available belly-hold capacity.

[2] `https://www.hongkongairport.com/en/the-airport/air-cargo/`
[3] `https://www.airportinformation.com/HKG/destinations`

Table 4.4: Selected passenger flights to TPE, SIN, ICN, NRT, PVG, BKK, MNL, and LHR (times in decimal hours)

Flight No.	dep	arr	dest	cap	Flight No.	dep	arr	dest	cap	Flight No.	dep	arr	dest	cap
CX488	8.000	9.750	TPE	44.8	CX564	8.500	10.250	TPE	25.2	CX530	9.083	11.000	TPE	44.8
CX450	10.000	11.833	TPE	25.2	CX494	10.417	12.333	TPE	44.8	CX400	13.000	14.833	TPE	11.5
CX420	14.000	15.833	TPE	25.2	CX402	18.583	20.250	TPE	44.8	CX464	19.667	21.333	TPE	11.5
CX408	22.917	24.583	TPE	44.8	CX659	1.667	5.667	SIN	17.0	CX759	9.000	13.083	SIN	11.5
CX739	11.667	15.750	SIN	17.0	CX791	12.833	16.833	SIN	17.0	CX635	15.167	19.250	SIN	25.2
CX657	16.083	20.167	SIN	44.8	CX715	20.417	24.417	SIN	44.8	CX434	8.250	12.750	ICN	11.5
CX410	9.333	13.917	ICN	25.2	CX416	16.833	21.417	ICN	44.8	CX524	1.417	6.500	NRT	44.8
CX526	8.250	13.167	NRT	25.2	CX504	9.083	14.167	NRT	25.2	CX520	10.500	15.583	NRT	25.2
CX500	15.417	20.333	NRT	17.0	CX316	8.833	11.583	PVG	17.0	CX368	9.750	12.500	PVG	17.0
CX376	10.750	13.500	PVG	44.8	CX360	13.583	16.250	PVG	44.8	CX380	15.083	17.750	PVG	44.8
CX364	17.500	20.250	PVG	44.8	CX362	19.250	22.000	PVG	25.2	CX302	21.250	23.917	PVG	25.2
CX705	8.500	10.667	BKK	25.2	CX615	9.917	12.083	BKK	25.2	CX653	12.000	14.083	BKK	11.5
CX789	13.750	15.917	BKK	44.8	CX751	14.500	16.667	BKK	44.8	CX701	16.083	18.250	BKK	25.2
CX907	7.500	9.667	MNL	11.5	CX901	9.000	11.333	MNL	25.2	CX919	14.333	16.583	MNL	25.2
CX903	16.250	18.500	MNL	25.2	CX913	20.333	22.583	MNL	44.8	CX939	22.083	24.333	MNL	25.2
CX257	8.167	15.000	LHR	17.0	CX239	10.667	17.333	LHR	17.0	CX253	13.500	20.167	LHR	25.2
CX251	23.000	29.417	LHR	25.2	CX255	23.917	30.500	LHR	25.2					

dep: Departure time (times in decimal hours); arr: Arrival time (times in decimal hours); dest: Destination airport; cap: Capacity in weight (tons)

For each destination, these adjusted schedules define the service-time horizon within which cargo can be accepted and loaded. Conditional on a given flight-side scenario, the cargo-side dataset is produced by sampling cargo arrivals over the admissible service window and sizing total collected cargo with respect to the aggregate capacity of the corresponding flight group. Individual shipment weights are drawn to be consistent with the LD-3-45 unit load device, the assumed ULD standard in our setting. This procedure yields paired flight–cargo scenarios that preserve the structure of the real-world operation while reflecting operational uncertainty in both timing and capacity.

In this section, Section 4.4.1 outlines the detailed consideration in data generation in sample scenarios and numerical settings for system parameters. Section 4.4.2 evaluates the performance of our heuristic algorithms. The heuristic algorithm with the best performance in terms of solution quality and time expense is selected for solving the program under each parallel scenario in the PH algorithm because good-quality cargo-to-flight allocation helps optimize capacity reservations. Section 4.4.3 illustrates the convergence of operating costs, proving the effectiveness and efficiency of our proposed solving frame on the studied problem. Finally, Section 4.4.4 conducts a sensitivity analysis to examine how changes in system parameters impact operators' decisions on capacity reservations and corresponding operating costs.

4.4.1 Scenario generation and parameter setting

For each destination-specific scenario, flight-side variability is introduced by adding an independent and identically distributed delay to both departure and arrival times. The delay is sampled from a uniform distribution on [0, 1.5] hours and is applied symmetrically to preserve the original gate-to-gate travel time. Given the delayed departures, each flight's ground handling window is defined as the interval from 2.5 hours to 0.8 hours before departure, which represents the feasible period for accepting and loading cargo.

Available belly-hold capacity for cargo is modeled as a proportion of the flight's nominal weight capacity determined by aircraft type. This proportion is drawn independently from a uniform distribution on [0.26, 0.30], producing a realizable cargo capacity for each flight. The total available cargo capacity across all passenger flights is benchmarked as 30 percent of their designed weight capacity.

To translate capacity into discrete units, we compute the maximum number of LD-3-45 unit load devices (ULDs) by dividing the total available cargo capacity by the maximum allowable mass per LD-3-45 (1.2 tons). In each scenario, the realized number of ULDs is then sampled within a tighter operational range, specifically between 70 percent and 90 percent of this maximum, reflecting scenario-to-scenario variation in actual consolidation levels.

As shipment-level records are commercially sensitive, publicly accessible cargo datasets are scarce. In this study, cargo-side data are generated using the real-world flight schedule as the basis while incorporating uncertainty in weights and timing that is consistent with each destination's service window. For a given destination, cargo destined for that airport is assumed to arrive at the origin (HKIA) within a broad acceptance horizon that begins six hours before the earliest scheduled departure and ends two hours after the latest scheduled departure. Each arriving unit load device is assigned a weight drawn uniformly between 1.0

and 1.2 tons, matching the operating range of LD-3-45 containers.

Temporal flexibility is encoded through the due and acceptable time windows constructed directly from the arrival time and the maximum observed flight travel time to the destination in the schedule. For each cargo index by m in a specific cenario s, the earlier due arrival time ($v_{m,s}$) equals its arrival time plus the maximum travel time, augmented by a 5-hour offset and a small integer noise term that takes values 0, 1, or 2 with equal probability. The later due arrival time ($b_{m,s}$) extends the earlier bound by 7 hours plus an independent integer noise term with the same support. The earliest acceptable arrival time ($r_{m,s}$) is set to the larger of the arrival time plus the maximum travel time and u_1 minus 5 hours minus an independent small integer noise term, and the latest acceptable arrival time ($q_{m,s}$) extends $b_{m,s}$ by 5 hours plus an independent small integer noise term (0, 1, or 2). Cargo units are generated sequentially and appended to the dataset until a capacity-based cap, determined from the corresponding destination-specific flight scenario, is reached. This procedure produces scenario-specific demand streams that align with the flight service horizon and reflect uncertainty in both arrival timing and load.

4.4.2 Performance of heuristic algorithms in assigning cargo to flights

We adopt the following parameterization. The unit fee for ad hoc transport services is 5 HKD per kilogram, the unit revenue attributed to flight capacity is 0.5 HKD per kilogram, and the time-penalty rate is 100 HKD per hour per ULD. For ULDs arriving at HKIA, unloading and loading require 2 hours; consequently, a ULD is eligible for assignment to a flight only if it can reach HKIA at least 2 hours before the flight's latest loading time. Under this specification, 300 independent scenarios are generated to evaluate the exact solver against the selected, purpose-built heuristic algorithms. To isolate routing and assignment effects, first-stage capacity management is deactivated, so all available belly-hold capacity is reserved for cargo transport. Transportation costs are realized endogenously during the cargo-to-flight assignment. Given 300 randomly generated scenarios for each selected destination, the distributions of total transportation cost across the generated sample scenarios for the solver and the heuristics are presented in Figure 4.4, and summary statistics are reported in Table 4.5.

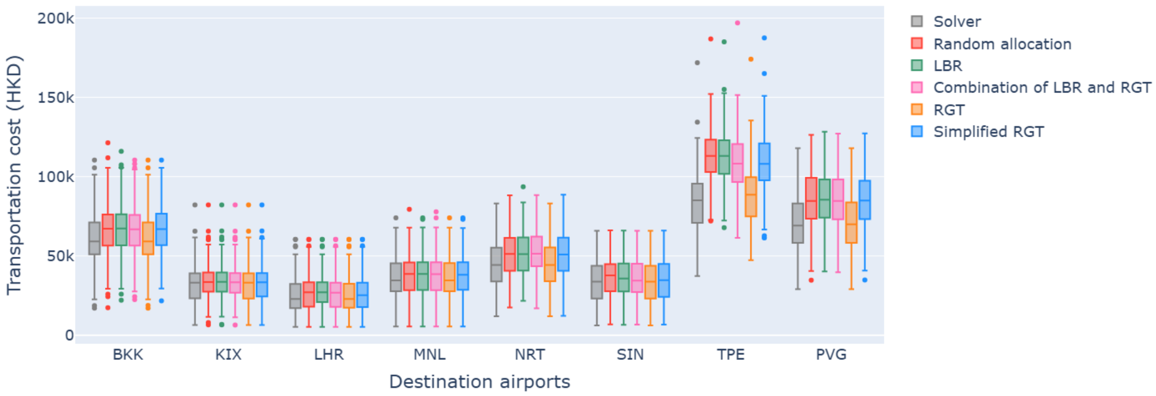

Figure 4.4: Results from solver and heuristic algorithms (assuming all available capacities are used for cargo transportation)

Table 4.5: Distributions of transportation costs from cargo-to-flight assignment by Solver and heuristic algorithms

	BKK						KIX					
Statistic ($\times 10^3$ HKD)	Solver	RA	LBR	RGT	LBR+RGT	SRGT	Solver	RA	LBR	RGT	LBR + RGT	SRGT
Maximum	110.46	121.39	115.99	110.46	110.46	110.46	82.17	82.17	82.17	82.17	82.17	82.17
Third quartile	71.14	76.17	76.30	75.85	71.14	76.65	39.04	39.52	39.54	39.25	39.07	39.25
Median	59.13	67.19	67.29	66.85	59.13	66.90	33.15	33.50	33.62	33.37	33.19	33.46
Mean	60.58	66.90	67.21	60.61	66.49	66.67	32.32	33.67	33.67	32.36	33.29	33.16
First quartile	50.96	56.57	56.70	56.54	50.96	56.83	23.22	27.48	27.53	26.78	23.29	24.41
Minimum	17.04	17.30	22.16	22.51	17.04	21.69	6.41	6.62	6.52	6.41	6.41	6.41
	LHR						MNL					
Statistic ($\times 10^3$ HKD)	Solver	RA	LBR	RGT	LBR+RGT	SRGT	Solver	RA	LBR	RGT	LBR+RGT	SRGT
Maximum	60.48	60.48	60.48	60.48	60.48	60.48	74.00	79.37	74.04	77.84	74.00	74.05
Third quartile	32.33	33.42	33.34	33.20	32.53	33.20	45.37	45.88	45.96	46.00	45.48	46.06
Median	22.88	27.04	27.13	26.79	22.86	25.25	34.52	38.72	38.61	38.50	34.52	38.16
Mean	24.68	26.77	26.81	24.94	26.34	26.14	35.97	37.85	37.91	35.99	37.95	38.00
First quartile	17.15	18.05	20.96	17.92	17.30	17.70	27.73	28.44	28.57	28.43	27.73	28.65
Minimum	5.26	5.26	5.26	5.26	5.26	5.26	5.59	5.59	5.59	5.59	5.59	5.59
	NRT						SIN					
Statistic ($\times 10^3$ HKD)	Solver	RA	LBR	RGT	LBR+RGT	SRGT	Solver	RA	LBR	RGT	LBR+RGT	SRGT
Maximum	83.04	88.28	93.57	88.38	83.04	88.59	65.90	66.15	66.04	65.91	65.91	65.98
Third quartile	55.24	61.37	61.63	62.17	55.33	61.49	43.80	44.89	45.27	45.09	43.80	45.03
Median	44.30	51.32	51.17	51.37	44.32	50.87	33.86	37.79	35.73	34.47	33.86	34.75
Mean	44.60	52.28	52.35	44.89	52.46	51.98	33.83	36.09	36.24	36.00	35.55	35.50
First quartile	34.00	40.65	40.75	43.49	34.04	40.61	23.20	27.70	27.61	27.17	23.20	23.24
Minimum	12.02	17.47	21.71	17.01	12.02	12.24	6.16	6.81	6.63	6.77	6.16	6.70
	TPE						PVG					
Statistic ($\times 10^3$ HKD)	Solver	RA	LBR	RGT	LBR+RGT	SRGT	Solver	RA	LBR	RGT	LBR+RGT	SRGT
Maximum	171.91	186.80	185.07	196.98	174.15	187.46	118.00	126.39	128.40	127.18	118.00	127.34
Third quartile	96.65	123.31	122.89	120.65	99.72	120.92	83.08	99.32	98.22	98.23	83.71	97.39
Median	85.04	113.04	113.09	120.65	88.68	108.04	69.11	84.73	85.42	84.63	70.02	85.00
Mean	83.94	112.97	112.80	88.23	108.33	108.56	70.63	86.05	86.54	70.86	85.50	85.85
First quartile	70.89	102.98	101.82	96.67	74.98	97.75	58.24	73.54	74.11	73.10	58.29	73.26
Minimum	37.38	72.11	67.89	61.36	47.35	61.36	29.04	34.77	40.31	39.77	29.04	34.87

Across the eight destinations, the heuristic algorithms consistently produce higher transportation costs than the solver, but the magnitude and distribution of the gaps vary by destination. In KIX, MNL, and SIN, the differences in mean and median costs are small, and the quartiles align closely with the solver's benchmarks, indicating that the rules applied in heuristic algorithms can produce cost-effective cargo-to-flight assignments compare to the exact optimal solutions obtained by the solver. By contrast, BKK and TPE exhibit the largest divergences across central and upper-tail statistics. In the two markets, mean and median costs under the heuristics rise by roughly one order of magnitude relative to the solver's gains elsewhere, and the third quartile and maximum values are noticeably higher, suggesting that more complex timing and consolidation trade-offs amplify the cost of local optimal choices. LHR, NRT, and PVG fall between these two ends of the spectrum: the heuristics remain serviceable but exhibit moderate inflation in mean and median costs, along with some widening of the upper tails.

Algorithmically, simpler rules such as RA and LBR tend to cause larger penalties in challenging markets, reflecting missed opportunities to consolidate loads or defer assignments to more advantageous departures, whereas guidance by load balance or routing time reduces these penalties and combined variants (LBR+RGT and SRGT) further improve central tendencies and mitigate extreme outcomes. However, even these strengthened heuristics do not fully match the solver in markets such as BKK and TPE, where coordinated, system-wide allocation has higher marginal value, and the remaining gap is concentrated in the upper tail under late arrivals, or tight loading windows. In this context, RGT provides a well-justified choice for the second-stage cargo-to-flight assignment. In destinations where heuristics closely track the solver (KIX, MNL, SIN), it delivers near-optimal means and medians with stable tail behavior, and in more demanding markets (BKK, TPE) it performs comparably to the strongest heuristic variants while remaining faster and easier to calibrate. These properties make RGT a cost-effective and broadly applicable option within the two-stage framework, enabling timely solution of large scenario sets and seamless integration with flight-side data generation and capacity management, thereby achieving competitive cost performance across heterogeneous markets without incurring the computational burden of the exact solver.

4.4.3 Convergence of the objective value and performance of the PH algorithm with modified RGT

In the PH algorithm, the residual of capacity reservation schemes and the difference between capacity reservation schemes in two consecutive iterations are formulated as Eq. (4.32) and Eq. (4.33), respectively. Here, the subscript n denotes the number of iterations completed by the PH algorithm. These two indicators are compared against predetermined termination thresholds to determine whether the termination criterion has been satisfied.

The PH algorithm for the proposed two-stage stochastic program is implemented to decompose the problem, and the SRGT algorithm was used to solve the cargo allocation that occurs in each iteration of the PH algorithm. As mentioned in the pseudo-code for the PH algorithm, ϵ^n and ω^n are calculated concurrently with each update of $\mathbf{y}^n$, which is used to check the convergence of the first-stage variable vector (i.e., the capacity reservation scheme). Figure 4.5 illustrates the convergence behavior of the three key indicators, ϵ, ω, and the total reserved capacity, i.e., $\left(\sum_{k\in\mathcal{K}_d} y_k\right)$, over successive iterations, using Kansai International Airport (KIX) as a representative destination airport.

$$\epsilon^{(n)} := \frac{1}{S}\sum_{s\in S}\left\|\mathbf{y}_s^{(n)} - \mathbf{y}^{(n)}\right\| \tag{4.32}$$

$$\omega^{(n)} := \left\|\mathbf{y}^{(n)} - \mathbf{y}^{(n-1)}\right\| \tag{4.33}$$

The evolution of these indicators demonstrates the effectiveness and stability of the proposed solution approach. Specifically, the indicator ϵ exhibits a rapid decrease during the initial iterations, followed by a gradual stabilization, indicating that the primal feasibility and solution accuracy improve steadily as the algorithm progresses. Similarly, ω, which reflects the magnitude of capacity adjustments between consecutive iterations, decreases monotonically and converges toward zero. This behavior suggests that the solution updates become increasingly small, implying that the algorithm approaches a fixed point and that oscillations are effectively eliminated. In contrast, the total reserved capacity $\sum_{k\in\mathcal{K}_d} y_k$ increases progressively and converges to a stable value as the iterations proceed. This trend indicates that the resource allocation decisions stabilize once convergence is achieved, reflecting consistency in the final capacity assignment. The smooth convergence of all three indicators confirms that the algorithm terminates with a stable and reliable solution. Overall, the convergence patterns of ϵ, ω, and the total reserved capacity collectively validate the robustness and numerical stability of the proposed method. The transportation costs to the chosen destinations obtained by different sizes of sampled scenarios are summarized in Table 4.6. The results demonstrate that the algorithm converges efficiently and produces consistent solutions for realistic large-scale airport scenarios.

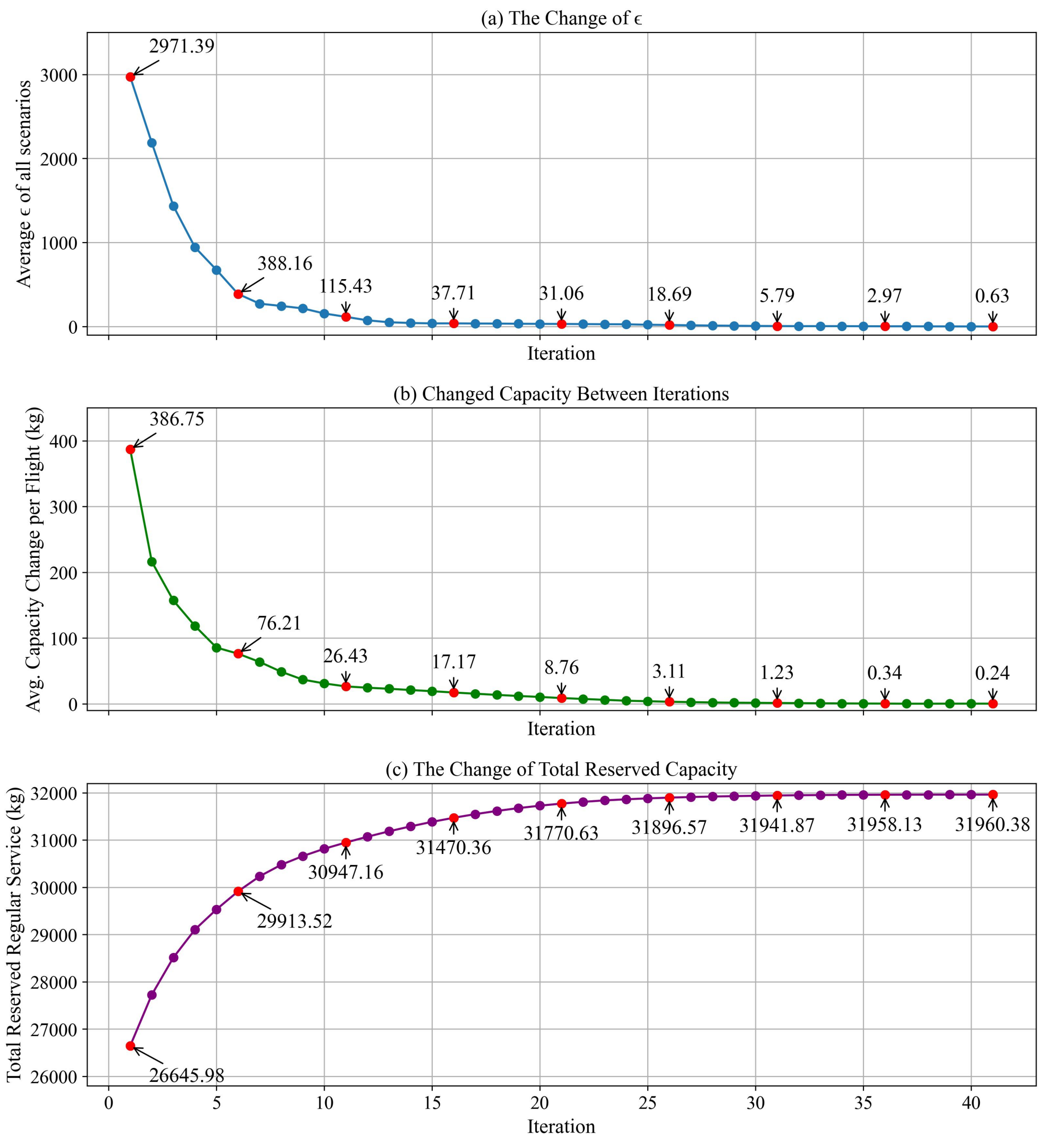

Figure 4.5: The change of ϵ, ω and the total reserved capacity, illustrated using Kansai International Airport (KIX) as an example

For each destination, we compute the in-sample operating cost by applying the capacity reservations derived from the training scenario set. The out-of-sample operating cost is evaluated by applying the same reservations to an independent set of 300 scenarios. Table 4.6 reports in-sample and out-of-sample operating costs across destinations and varying training sample sizes. Figure 4.6 illustrates (i) the stability of reserved capacity at the flight level and (ii) the convergence of in-sample and out-of-sample costs as the training sample size increases. Table 4.6 and Figure 4.6 jointly demonstrate convergence and out-of-sample validity of the proposed solving framework. Quantitatively, in-sample costs stabilize rapidly and approach out-of-sample values as the scenario set grows. For KIX, the in-sample cost falls from 31,085.5 HKD at $|S_d|$=10 to 27,523.8 HKD at $|S_d|$=300 (-11.5%), then changes by ¡3% between 300 and 500 (to 28,349.7 HKD). At $|S_d|$=500, the in–out gaps are small across destinations, 1.8% (KIX), 2.1% (LHR), 1.4% (MNL), 0.6% (NRT), 5.2% (SIN), 3.7% (BKK), 1.5% (PVG), 0.2% (TPE), whereas with $|S_d|$=10 they can be large and volatile (e.g., NRT +21.9%). The median absolute in–out gap declines from roughly 5-7% at $|S_d|$=50 to 1-3% at $|S_d|$=300, and aligns closely by $|S_d|$=400–500.

Figure 4.6 complements these results at the flight level, taking KIX as an representative example destination. Panel (a) shows reserved capacities converging to stable levels as scenarios increase. For KIX, flight capacities change markedly from 10 to 100 scenarios and then adjust only marginally through 500. Panel (b) shows the total cost curve flattening, with out-of-sample cost essentially unchanged beyond 300 scenarios. Consistent with Table 4.6, out-of-sample changes from $|S_d|$=400 to 500 are small (e.g., KIX +0.06%, LHR −1.3%, MNL −0.7%, NRT +0.3%, PVG −0.1%, TPE +0.2%), and remain within about ±2% relative to $|S_d|$=300. These patterns indicate that the framework has captured the salient demand–capacity structure, i.e., capacity reservations are stable, in–out gaps are low, and marginal benefits of additional scenarios beyond 300–400 are minimal. Choosing $|S_d|$=500 is therefore a conservative and sufficient setting that yields convincing capacity reservation schemes and reliable transportation cost estimates without unnecessary computational overhead.

Table 4.6: In-sample and out-of-sample operating cost of the chosen destination airports under different sample sizes

		Operating cost							
$\|S_d\|$		**KIX**	**LHR**	**MNL**	**NRT**	**SIN**	**BKK**	**PVG**	**TPE**
10	In sample	31085.5	24000.2	33048.3	32151.3	28461.4	50415.9	64744.9	58003.0
	Out of sample	27946.4	21778.8	30227.9	39199.0	29918.4	50300.4	62795.5	55362.3
50	In sample	26547.7	24959.7	30377.8	36679.6	33088.7	47883.1	61220.5	55869.6
	Out of sample	28627.0	24010.4	29456.2	35808.9	32834.8	50752.9	62323.1	54374.2
100	In-sample	26775.7	26219.4	30782.1	38077.6	26439.5	53489.6	61888.7	55610.2
	Out of sample	28625.7	25604.2	29518.4	38077.9	29229.0	50611.4	62649.2	54607.8
200	In-sample	27075.0	22638.2	30965.0	39906.1	29638.0	52514.3	59877.9	55130.6
	Out of sample	28530.9	22458.5	29537.6	39887.4	31189.9	51220.7	62532.4	54295.1
300	In-sample	27523.1	23315.4	29355.8	39913.5	29970.4	50098.2	60952.4	55088.6
	Out of sample	28649.4	22808.2	29464.2	39841.9	30961.3	51161.2	62444.7	54360.3
400	In-sample	27695.1	23688.8	29437.0	38444.9	29653.6	49831.8	62291.4	54402.1
	Out of sample	28585.8	22779.6	29433.6	39691.6	29644.8	50354.4	62619.0	54073.1
500	In-sample	28349.7	23122.0	28852.1	39562.6	32252.8	52259.1	61549.2	54690.5
	Out of sample	28602.5	22477.8	29267.1	39810.8	30650.8	50408.3	62400.2	54399.7

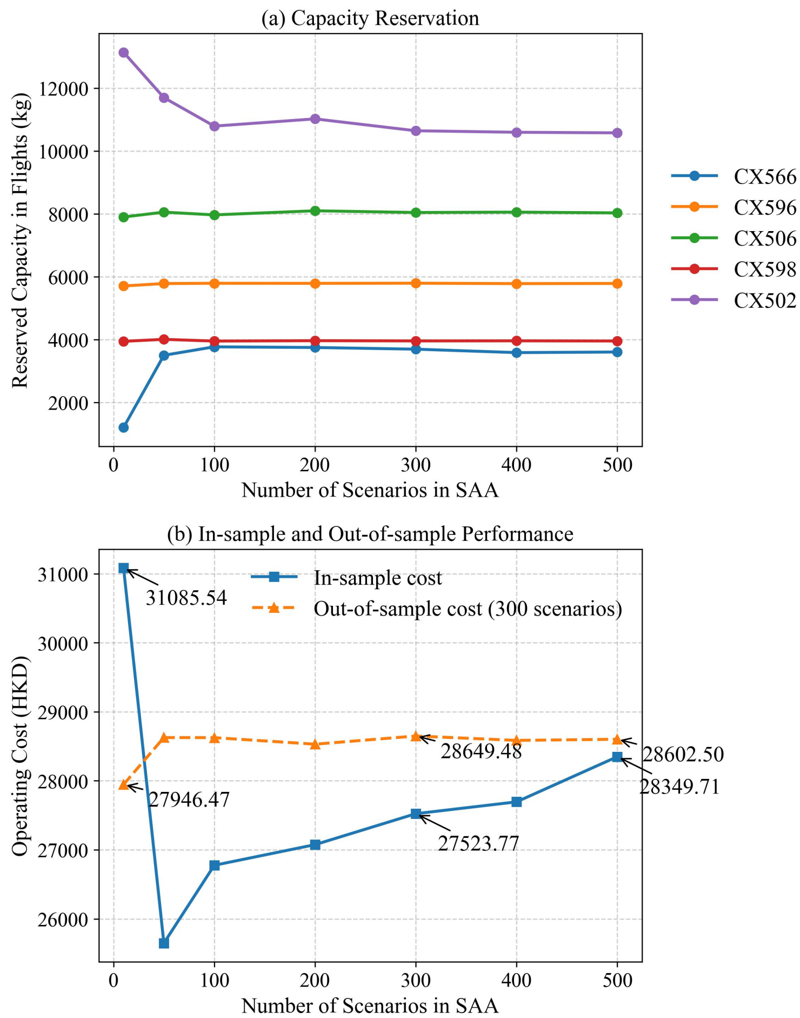

Figure 4.6: The change of reserved capacity of each flight serving HKG-KIX and the in-sample and out-of-sample results

4.4.4 Sensitivity Analysis

In this subsection, we conduct a sensitivity analysis to evaluate the impact of varying unit revenue for unit-weight capacity (i.e., ε) on the final objective value and the total reserved capacity in the first stage. The results are concluded as Table 4.8. In Table 4.8, negative operating costs indicate that the revenue generated from capacity sales can not only cover the operational expenses incurred during the cargo transportation process but also generate a profit.

To interpret Table 9 under the clarified benchmarking, we distinguish two $\varepsilon = 0.5$ HKD/kg cases: (i) the baseline with no capacity reservation, in which all unused belly capacity is allocated to cargo and generates no offsetting revenue; and (ii) the proposed two-stage framework with capacity reservation at $\varepsilon = 0.5$ HKD/kg, in which only the residual (post-reservation) capacity is used and the associated revenue partially covers downstream allocation costs. Cost-saving rates (CSR) are therefore computed as the percentage reduction in operating cost when moving from the baseline (no reservation, $\varepsilon = 0.5$ HKD/kg) to the two-stage solution at a given ε, including $\varepsilon = 0.5$ HKD/kg. It should be noted that the total reserved capacity is determined by our solution framework using 500 randomly generated sample scenarios (training set) for every selected destination. Operating costs (OCs) are then evaluated by applying the resulting capacity reservations to an independent set of 300 newly generated scenarios (test set). Cost-saving rates (CSRs) are computed by comparing these OCs to baseline costs evaluated on the same 300 test scenarios.

Under this interpretation, the $\varepsilon = 0.5$ HKD/kg two-stage solutions already yield nontrivial savings relative to the no-reservation baseline, despite keeping the same unit revenue rate. For example, operating costs decline by 13.7% at BKK (from 58,441.9 to 50,408.3 HKD), 14.4% at KIX (33,428.5 to 28,602.5 HKD), 7.3% at LHR (24,538.1 to 22,747.8 HKD), 16.2% at MNL (34,929.1 to 29,267.1 HKD), 11.4% at NRT (44,132.5 to 39,108.4 HKD), 13.8% at SIN (33,908.5 to 30,650.8 HKD), 30.3% at TPE (83,547.7 to 58,230.0 HKD), and 13.3% at PVG (71,987.9 to 62,400.2 HKD). These reductions arise because reserving capacity prevents capacity waste and lets the remaining capacity earn revenue to offset later handling and assignment costs.

Increasing ε above 0.5 further strengthens this effect. At $\epsilon = 1.0$, savings rise to 28.8% at BKK, 32.2% at KIX, 30.4% at LHR, 36.9% at MNL, 26.4% at NRT, 31.6% at SIN, 57.0% at TPE, and 49.0% at PVG. At $\epsilon = 2.0$, the corresponding CSRs are 63.4% (BKK), 73.9% (KIX), 67.7% (LHR), 77.5% (MNL), 53.8% (NRT), 83.4% (SIN), 166.8% (TPE, the revenue from selling capacity can cover the operational costs of cargo transportation and still leave a profit.), and 57.8% (PVG). Across destinations, total reserved capacity (TRC) decreases as ε increases, indicating that the framework systematically reduces capacity reservations when the revenue-per-kg threshold rises and concentrates on effective capacity utilization. the corresponding fall in operating cost reflects both reduced processing/allocation volumes and greater revenue coverage of remaining costs.

Table 4.8: Total reserved capacity and corresponding operating costs for selected destinations under various market conditions

	BKK			KIX		
ε (HKD/kg)	TRC (kg/day)	OC (HKD)	CSR	TRC (kg/day)	OC (HKD)	CSR
0.5 (baseline)	49538.2	58441.9	/	40154.9	33428.5	/
0.5	32945.9	50408.3	13.7%	31960.3	28602.5	14.4%
1	29164.3	41613.0	28.8%	28929.3	22650.6	32.2%
2	28546.4	21400.1	63.4%	24897.5	8704.0	73.9%
	LHR			MNL		
ε (HKD/kg)	TRC (kg/day)	OC (HKD)	CSR	TRC (kg/day)	OC (HKD)	CSR
0.5 (baseline)	30711.8	24538.1	/	44024.1	34929.1	/
0.5	26337.8	22747.8	7.3%	31334.5	29267.1	16.2%
1	22813.8	17085.8	30.4%	29841.4	22042.8	36.9%
2	20309.3	7918.1	67.7%	29829.5	7852.8	77.5%
	NRT			SIN		
ε (HKD/kg)	TRC (kg/day)	OC (HKD)	CSR	TRC (kg/day)	OC (HKD)	CSR
0.5 (baseline)	38507.2	44132.5	/	49637.1	33908.5	/
0.5	30269.5	39108.4	11.4%	43254.2	30650.8	13.8%
1	26770.2	32490.1	26.4%	34863.1	23203.7	31.6%
2	24327.3	20391.8	53.8%	32746.3	5639.9	83.4%
	TPE			PVG		
ε (HKD/kg)	TRC (kg/day)	OC (HKD)	CSR	TRC (kg/day)	OC (HKD)	CSR
0.5 (baseline)	90295.3	83547.7	/	73761.7	71987.9	/
0.5	66576.5	58230.0	30.3%	45918.0	62400.2	13.3%
1	54614.4	35903.5	57.0%	41127.4	36719.2	49.0%
2	44579.5	-13980.8	166.8%	37896.3	3043.6	57.8%

TRC: Total reserved capacity; OC: Operating cost; CSR: Cost-saving rate; ε: Ad hoc fee for transporting unit-weight cargo

The cost-saving rates are calculated by subtracting the operating costs of our proposed two-stage framework from the costs of the baseline settings and dividing by the the costs of the baseline settings.

These results have two managerial implications for carriers seeking to apply unused passenger-belly capacity in cargo services. First, capacity reservation delivers value even when unit revenue remains much smaller than the ad hoc service fee, by expanding possible utilization of residual capacity and then obtaining revenue to subsidize downstream costs. This cost-saving results justify adopting the two-stage framework as a default operating policy. Second, route-specific tuning of ε can materially improve economics with limited operational disruption: markets such as TPE, PVG, MNL, and KIX exhibit strong cost elasticity with respect to ε and benefit from higher revenue targets and more assertive reservation levels, whereas NRT and LHR respond more moderately and may require a balanced approach that pairs modest ε increases with consolidation and schedule coordination. In summary, the two-stage capacity management approach yields different levels of cost savings across freight markets. Carriers should therefore assess expected savings against implementation costs to ensure that the scheme is economically justified on each cargo market. To maximize benefits brought by the two-stage management approach, carriers can commercialize residual belly capacity that tends to remain unused for extended periods, converting it into stable revenue that helps cover transportation costs.

4.5 Conclusion and future study

Applying the unused belly capacity in passenger flights for air cargo transportation provides significant advantages, such as cost efficiency and operational flexibility. this chapter presents a framework to effectively manage this unused capacity, considering uncertainties in cargo demand and flight capacity. We examined various uncertainties, including fluctuations in cargo weights, arrival times of cargo at airports, available flight capacities, and flight schedules.

Our approach models the problem as a two-stage stochastic program and divides the capacity management into mid-term capacity reservations and short-term cargo-to-flight allocations. To make the stochastic model tractable and solvable with standard optimization tools, we employed the SAA method to approximate the expectation using a finite set of generated scenarios. The Progressive Hedging algorithm was then used to decompose the problem by optimizing first-stage variables within the context of second-stage decisions, ensuring consistency across both stages. Additionally, we utilized a Lagrangian relaxation model to provide lower bounds for operating costs across different scenarios. Various heuristic algorithms were employed to secure tight upper bounds compared to the lower bounds from the relaxed model, facilitating good-quality solutions in each candidate scenario in the PH algorithm. This comprehensive approach ensures that our capacity reservation and cargo allocation strategies are both efficient and stable under various uncertainties.

Through a series of numerical experiments, taking HKIA as the origin and 8 selected destination airports, we investigated the convergence of the objective values of our modelled program. Our approach successfully identified high-quality, feasible solutions. Specifically, the objective value exhibited less than a 2% fluctuation when using 500 sample scenarios, compared to results from 400 sample scenarios. The gaps between in-sample and out-of-sample results varies from 0.6% to 5.2%, showing the stability of our proposed framework in obtaining reliable capacity reservations. Additionally, we conducted a sensitivity analysis on the unit revenue associated with post-reserved (additional) belly capacity, examining how solution performance varies with changes in this parameter. Compared with baseline cases that do not employ our two-stage capacity management, the proposed approach delivers consistently high cost savings, with particularly obvious gains when the marginal revenue per unit weight of additional capacity is higher. These results demonstrate the effectiveness and economic value of the two-stage framework across a range of revenue conditions.

There are several limitations to this chapter. First, we assume that passenger flight capacities and cargo demands are independent across OD pairs. This assumption implicitly treats multi-leg routes as disjoint segments, modeling them as independent transportation processes between individual airport pairs. Future studies could relax the independence assumption and adopt network flow models that consider cargo flow interdependence between OD pairs. This would enable a more holistic understanding of capacity allocation and cargo flow dynamics. Furthermore, extending the model to allow for cargo transfers across multiple OD pairs could provide more accurate representations of real-world logistics, especially for long-distance or low-frequency shipments. Since belly cargo shares capacity with passenger baggage, future studies could aim to jointly optimize passenger and cargo operations in a unified framework, especially in the context of integrated airline planning. this chapter focuses on the operational decisions of airlines in cargo transportation, while the role of airports receives comparatively less attention. Future research can extend the scope of this work by further investigating the management of unused passenger flight capacity for cargo transportation across multiple airports (Hou et al., 2025). This expansion will aim to achieve broader capacity management and examine the dynamics of collaboration and competition among airports and airlines in the cargo transportation market.

There are several limitations to this study. First, we assume that passenger flight capacities and cargo demands are independent across OD pairs. Although we considered various cargo transportation routes to different destinations, the optimization is conducted independently. Future studies could relax the independence assumption and adopt network flow models that consider cargo flow interdependence between OD pairs. This would enable a more holistic understanding of capacity allocation and cargo flow dynamics. Furthermore, extending the model to allow for cargo transfers across multiple OD pairs could provide more accurate representations of real-world logistics, especially for long-distance or low-frequency shipments. Since belly cargo shares capacity with passenger baggage, future studies could aim to jointly optimize passenger and cargo operations in a unified framework, especially in the context of cooperation between cargo forwarders and airlines. This study focuses on the operational decisions of cargo forwarders in cargo transportation, while the role of airports and airlined receives comparatively less attention. Future research can extend the scope of this work by further investigating the management of unused passenger flight capacity for cargo transportation across multiple airports (Hou et al., 2025). This expansion will aim to achieve broader capacity management and examine the dynamics of collaboration and competition among airports, airlines and forwarders in the cargo transportation market.

In the calculation of the opportunity cost in the objective function, it is assumed that the economic value forgone for each additional unit of unused capacity remains the same, regardless of the total volume of excess capacity. This assumption may not always be realistic, particularly in markets where total demand is less than the total available supply. In future work, the opportunity cost parameter could be made demand-dependent or capped based on market absorption capacity, ensuring that the calculation does not overstate the benefit from unused capacity when market conditions are unfavorable. The study of specific ad hoc service providers, such as dedicated cargo flights that supplement capacity when passenger flight capacity is insufficient, is a critical area for further exploration. Exploring pricing strategies for capacity sales and the utilization of ad hoc services also presents a promising topic for further research, offering insights into economic and operational optimizations within the air cargo industry. Lastly, due to the unavailability of real-world cargo demands, we were unable to directly validate our proposed capacity management framework using actual operational cases. Although we have made efforts to ensure the realism of our numerical settings by employing the real-world flight schedules and airport pairs, the absence of empirical cargo data limits the practical validation of our model. In future work, access to real-world cargo demand data would enable a more robust assessment of the framework and facilitate the derivation of practical, data-driven insights.

Chapter 5

On the competition between air transport and high-speed rail considering inherent heterogeneous travel mode preferences

With the expansion of high-speed rail (HSR) networks, the competitive dynamics between established air transport (AT) systems and the ever-growing HSR services have undergone significant transformation. This study explores the evolving competitive relationships between the established AT system and the HSR services by explicitly considering travelers' heterogeneous preferences towards the two modes. In particular, we firstly analyze how travelers' choices vary with system parameters or operation decisions (e.g., service fare and service capacity). Then, the optimal operation decisions of both HSR and AT operators are examined under two objectives, i.e., profit-maximization and weighted welfare-profit maximization. Our findings include: (i) We identify four possible market equilibria, in which the HSR and AT operators may either compete with each other or not (with each case corresponding to two distinct equilibria); (ii) In the weighted welfare-profit maximization scenario, increasing the weight with HSR operator's profit can shift demand from air to HSR and intensify price competition under mild conditions. Furthermore, with the increment of the weight for social welfare, both airfares and HSR fares intend to decrease; (iii) When travelers exhibit a strong preference for one specific mode, the respective service operator is inclined to raise fares to increase profits. The derived results will be helpful to understand the impact of traveler's heterogeneous preference on the service operation and system performance, and provide valuable insights for the design of effective transportation policies and management strategies.

5.1 Introduction

In the competition between HSR and AT in short- and medium-haul cross-city travel markets, individual heterogeneity in travel mode preferences is an essential factor influencing system revenue and market outcomes, making it a noteworthy subject in transport planning (Park & Ha, 2006; Zhang et al., 2019; Wang et al., 2021). Although many theoretical studies have addressed HSR-AT competition (Roman et al., 2007; Ivaldi & Vibes, 2008; Adler et al., 2010; Dobruszkes, 2011; D'Alfonso et al., 2015; Xia & Zhang, 2016; Jiang et al., 2017; Tsunoda, 2018; Wang et al., 2018; Ma et al., 2019; Li et al., 2021), these often assume homogeneous travelers to maintain analytical tractability, thereby downplaying the impact of heterogeneous subjective perceptions. Empirical studies, on the other hand, have used survey-based data to establish influential relationships between various trip characteristics and travelers' mode choices (Roman et al., 2007; Behrens & Pels, 2012; Dobruszkes et al., 2014; Castillo-Manzano et al., 2015; Wan et al., 2016; Liu et al., 2019), but generally lack a systematic analysis of how operators should adapt strategies to accommodate preference heterogeneity. The significance of accounting for individual taste heterogeneity is further highlighted by studies such as Greene & Hensher (2003, 2013); Zhou et al. (2020), which emphasize its policy implications. In the context of Air-HSR competition, both objective service attributes and subjective attitudes, including unobserved preferences and psychological factors, jointly shape travel behavior (Abenoza et al., 2017). Despite this, there remains a gap in the literature: a few existing research directly link travelers' heterogeneous mode preferences with the operational strategy adjustments made by HSR or AT operators in a competitive market, as shown in Figure 5.1.

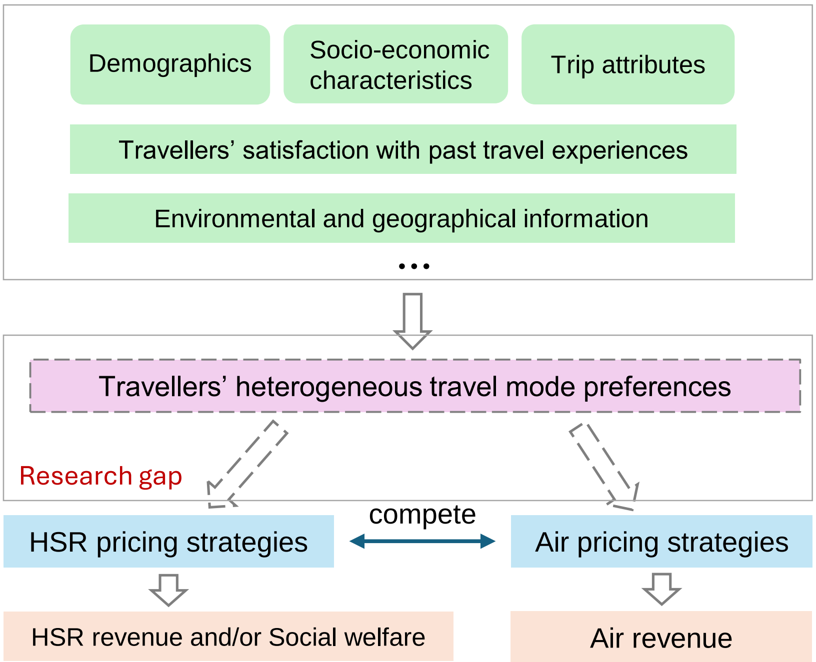

Figure 5.1: The missing link between travelers' heterogeneous mode preferences and transport pricing strategies

To address this gap, this study develops a bi-level framework to examine the competition between AT and HSR. In particular, for the lower-level model, we characterize travelers' mode choices by implementing the Hotelling model to explicitly incorporate travelers' preference heterogeneity. The upper-level model optimizes operational decisions for AT and HSR operators by maximizing either profit or a weighted profit-welfare objective.

The primary contributions of this study are threefold. First, this paper analytically and systematically bridges the gap between passenger preference heterogeneity and the competitive relationships between high-speed rail (HSR) and air transport (AT) using a tractable analytical framework. This work innovatively extends the Hotelling model by interpreting travelers' positions on the Hotelling axis as expressions of their subjective mode preferences, different from the traditional interpretation of geographic location. Second, the study develops a bi-level modeling structure that explicitly links travelers' mode choices at the lower level with operators' strategic decisions at the upper level. This framework enables an exploration of how the distribution of traveler preferences influences the equilibrium demand for each mode, as well as the optimal pricing strategies made by operators under either profit-maximization or weighted sum of profit and welfare objectives. Third, by applying this tractable analytical approach, the study proposes a generalizable framework for assessing the impact of travelers' mode preference heterogeneity on overall transport system performance. The framework's generality is demonstrated through analytical examples, such as replacing the commonly assumed uniform distribution of preferences with alternative forms, and through comprehensive numerical experiments. These experiments reveal how varying preference distributions affect operators' optimal pricing, profitability, and the resulting consumer surplus. In summary, these contributions provide new theoretical insights and practical guidance for both policymakers and transport operators seeking to account for passenger heterogeneity in a competitive, two-modal context.

The remainder of this paper is organized as follows. Section 5.2 introduces our studied context and corresponding model formulations. Section 5.3 provides numerical studies to show the impact of passengers' travel-mode-preference distribution on the Air-HSR competition with some assumptions on the function forms. Section 5.4 conclude the work and findings of this study and discuss some future research topics.

5.2 Problem statement and mathematical formulation

5.2.1 Problem description

This study investigates the heterogeneous mode preferences of travelers in markets jointly served by AT and HSR systems. These two modes differ in travel time, comfort, boarding procedures, and other service attributes. Travelers perceive and value these differences uniquely, leading to varied preferences between the two options. In our analysis, mode preference is quantified as a comprehensive monetary indicator, representing the perceived cost associated with choosing a particular mode. We model the distribution of these preferences across the traveler population as a continuous function. For origin-destination (OD) pairs where both air and HSR are available, travelers make mode choices based on ticket prices, system crowding, and their individual preferences. In response, operators can strategically adjust pricing to align with the preference distribution, aiming to achieve operational goals. This section explores traveler behaviour under equilibrium conditions and examines corresponding pricing strategies for different preference distributions.

5.2.1.1 Travelers

We consider a fixed travel demand, denoted as D, within the study region, and travelers exhibit heterogeneous preferences for HSR and AT services. Specifically, we assume travelers' preference of HSR is distributed in the interval $[0, 1]$, where 0 denotes the lowest preference for HSR, 1 denotes the highest, and $x \in [0, 1]$ denotes individual passenger's preference for HSR. As illustrated in Figure 5.2, we define $f(x) \geq 0$ as the density function, which denotes the number of travelers with HSR preference x. Further let $F(x)$ represent the cumulative number of travelers with a preference for HSR less than x, which is expressed as:

$$F(x) = \int_0^x f(x)dx. \tag{5.1}$$

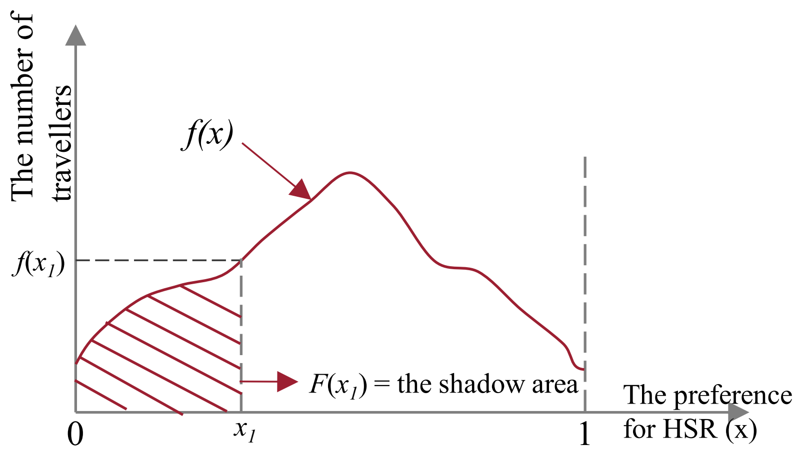

Figure 5.2: An example of density function showing travelers' preference distribution

Travelers choose travel modes according to travel cost including monetary cost and disutility. In a travel mode choice equilibrium state, no travelers can further reduce the travel cost by changing their travel mode choice. Based on the density function $f(x)$, the individual travel cost of a travelers whose preference of taking HSR is x can be formulated as (denoted as c_a) and HSR (denoted as c_h) can be formulated as follows:Specifically, for a traveler with a preference for HSR represented by x, the individual travel costs for AT (denoted as c_a) and

HSR (denoted as c_h) can be expressed as follows:

$$c_a(x) = p_a + \kappa_a(n_a) + d_a(x), \tag{5.2}$$

$$c_h(x) = p_h + \kappa_h(n_h) + d_h(1 - x), \tag{5.3}$$

where p_a and p_h are the service fare for the AT and HSR service respectively. $\kappa_a(n_a)$, and $\kappa_h(n_h)$ represent the additional costs or inconveniences (often referred to as crowding costs) incurred by travelers to secure a ticket for their chosen mode. We consider it may cost more time or efforts for the travelers to purchasing the ticket with more travelers choosing the mode, and assume $\frac{\partial \kappa_i}{\partial n_i} = \kappa_i' > 0, i = a, h$. Moreover, we assume the marginal crowding cost will increase when the number of passengers is increased, i.e., $\kappa_i'' > 0, i = a, h$. $d_a(x)$ and $d_h(1 - x)$ represent the disutility experienced by a passenger with HSR preference x when choosing AT or HSR service. $d_a(\cdot)$ is assumed to be strictly increasing with x, and $d_h(\cdot)$ is decreasing with x, i.e., $d_a' > 0$ and $d_h' > 0$. This is because travelers with a relatively higher preference for HSR (i.e., larger x) are more satisfied with HSR services and will experience lower disutility when choosing HSR, while incurring higher disutility when opting for AT.

We assume that passengers have an expected cost for travel, noted as c_o, which can be considered as the cost for cancelling this trip. When the minimal cost between the travel costs of the two available modes is larger than the acceptable cost c_o, i.e., $\min\{c_a(x), c_h(x)\} > c_o$ then the passenger is supposed to cancel travelling (or choose other modes, like driving a car). Considering the three choices, passengers are assumed to choose the one with the minimum cost, formulated as follows:

$$c(x) = \min\{c_a(x), c_h(x), c_o\}. \tag{5.4}$$

Denote the demand for AT and HSR by n_a and n_h, it can be easily inferred that $n_a + n_h \le D$ where D means the total number of potential travelers in the competitive market. Furthermore, with given capacities of both modes (i.e., the number of seats in flights/HSR trains), m_a and m_h, the capacity constraints should be satisfied as $n_a \le m_a$ and $n_h \le m_h$.

The total travel cost of all travelers can be calculated as

$$TC\left(n_a, n_h\right) = \int_0^{y_a} c_a\left(x\right) f\left(x\right) dx + \int_{y_h}^{1} c_h\left(x\right) f\left(x\right) dx + c_o \cdot \left(D - n_a - n_h\right), \qquad (5.5)$$

where the first term $\int_0^{y_a} c_a\left(x\right) f\left(x\right) dx$ and the second term $\int_{y_h}^{1} c_h\left(x\right) f\left(x\right) dx$ represent the total cost of travelers choosing AT and HSR, respectively. The third term $c_o \cdot \left(D - n_a - n_h\right)$ is the total cost of travelers who cancel the trip or choose alternative. Further let y_a and y_h represent maximum/minimum HSR preference value of travelers who choosing AT and HSR. Based on the definition of the cumulative number of travelers in Eq. (5.1), we can easily derive $y_a = F^{-1}\left(n_a\right)$ and $y_h = F^{-1}\left(D - n_h\right)$, where $F^{-1}\left(\cdot\right)$ is the inverse function of $F(\cdot)$.

5.2.1.2 Operators' profit and social welfare

Given the number of passengers choosing AT and HSR, n_a and n_h, the ticket price p_a and p_h, the net benefit of AT and HSR can be calculated as the revenue getting from the passengers minus the operating costs and capacity maintaining costs, formulated as follows:

$$\pi_a\left(p_a\right) = n_a \cdot p_a - w_a\left(n_a\right), \qquad (5.6)$$

$$\pi_h\left(p_h\right) = n_h \cdot p_h - w_h\left(n_h\right), \qquad (5.7)$$

where $n_i \cdot p_i,\ i = a, h$ denotes the revenue for AT and HSR operator. $w_i\left(n_i\right),\ i = a, h$ represents the operating cost for AT and HSR modes, respectively. It is assumed that $w_i\left(n_i\right),\ i = a, h$ is increasing and convex, i.e., $w_i' > 0$ and $w_i'' > 0$.[1]

Further, the consumer surplus of HSR passengers (CS_h) is formulated by

$$CS_h = \int_{y_h}^{1} \left(c_o - c_h\left(x\right)\right) f\left(x\right) dx. \qquad (5.8)$$

[1]Note that the operating cost is related to the capacity of each mode in reality, and the general form of operation cost can be expressed as $w_i\left(\frac{n_i}{m_i}\right),\ i = a, h$, where the cost is expressed as a function of the seat occupancy rate for both AT and HSR modes.

Following Yang & Zhang (2012) and we can calculate social welfare in the HSR system (SW_h) as

$$SW_h = CS_h + \pi_h. \tag{5.9}$$

5.2.2 Travel mode choice equilibrium

5.2.2.1 User equilibrium

Accurately understanding how passenger flow is distributed between the two competing travel modes is essential for policymakers to formulate effective strategies for future development. The total market demand, denoted by D, represents the pool of potential travelers and is assumed to be fixed. However, even with a constant potential demand within a city, the actual demand for AT and HSR remains elastic. This elasticity arises from the introduction of c_o, which accounts for travelers' outside options, such as choosing not to travel. The equilibrium passenger flows for AT and HSR must satisfy the following conditions:

$$n_i \left(c_i(y_i) - c_i^*\right) = 0, i = a, h, o, \tag{5.10a}$$

$$c_i \geq c^*, i = a, h, o, \tag{5.10b}$$

$$n_i \geq 0, x \in (0, 1), \tag{5.10c}$$

$$n_i \leq m_i, i = a, h, \tag{5.10d}$$

$$n_o + n_a + n_h = D, \tag{5.10e}$$

where c_i^* means the minimum travel cost of travelers with the lowest preference for their chosen mode. With the widespread adoption of telecommunication technology, it is expected that all travelers have precise knowledge of the travel prices for each option. Therefore, it is easy to understand that passengers with the identical HSR preference experience identical and the minimum cost among the three options, i.e., $c_i(y_i) = c_i^*, i = a, h, o$, formulated as Eqs. (5.10a). Eq. (5.10b) show that travel prices associated with feasible solutions should be larger than the minimum travel price between the OD pair. Eq. (5.10c) is the non-negative constraint of the equilibrium flow for each option. Eq. (5.10d) denotes that the passengers of each mode cannot exceed the maximum seats provided by the transport system.

Proposition 1. *At the travel mode choice equilibrium, the numbers of air passengers and HSR passengers, i.e., n_a^* and n_h^*, are both unique.*

The existence and uniqueness of UE solution to Eq. (5.10) can be proved, where the details are omitted here to save space.

5.2.2.2 Various equilibrium scenarios given different system conditions

Before we discuss the possible solutions to the travel mode choice equilibrium, some important HSR preference points should be defined. Let x_1 and x_2 represent the travelers' HSR preference values, where travelers with x_1 HSR preference are indifferent from AT and canceling, and travelers with x_2 HSR preference are indifferent from HSR and canceling, i.e., $c_a(x_1) = c_o$ and $c_h(x_2) = c_o$. When $x_1 \leq x_2$, there are separate captive markets of AT and HSR, i.e., no competition exist between the two modes. Let x_a and x_h represent the travelers' HSR preference points, where the two modes' capacity can serve, i.e., $\int_0^{x_a} f(x)dx = m_a$, $\int_{x_h}^1 f(x)dx = m_h$. Besides, we use $\tilde{x}$ to indicate the preference for HSR of indifferent passengers that have equal costs by the two modes, i.e., $c_a(\tilde{x}) = c_h(\tilde{x}) \leq c_o$. It can be inferred that the demands for the two modes can be formulated as the integral of $f(x)$, i.e.,

$$n_a = \int_0^{\min\{x_1,\tilde{x}\}} f(x)dx, \tag{5.11}$$

$$n_h = \int_{\max\{x_2,\tilde{x}\}}^1 f(x)dx. \tag{5.12}$$

Given system parameters including p_a, p_h, $d_a(\cdot)$, $d_h(\cdot)$, $\kappa_a(\cdot)$, $\kappa_h(\cdot)$ and $f(x)$, then we can derive the upper limit in Eq. (5.11) and the lower limit in Eq. (5.12) thus the unique UE solution (n_a, n_h). Even we have proved that the UE solution exists and is unique, the solution varies under various (p,m) pairs and system parameters including $f(x)$, $d(\cdot)$ and c_o. Then we discuss the possible scenarios and simultaneously use figures (Figure 5.3) to help intuitively understand the various cases by assuming linear functions in the travel price formulation. Before we discuss the possible passenger distribution under equilibrium state, an extreme scenario should be introduced where $p_a \geq c_o$ or $p_h \geq c_o$, as a result, $n_a = 0$ ($n_h = D$) or $n_a = D$ ($n_h = 0$). In this unusual scenario, all travelers choose neither AT nor HSR. We mention it solely for completeness and will not explore it further. The following discussed scenarios are much more likely to happen in real-world cases given $0 < p_a < c_0$ and $0 < p_h < c_0$.

(***Scenario I: Captive markets without competition***) In this scenario, $x_1 + x_2 \leq 1$, $0 < n_a < m_a$, $0 < n_h < m_h$, $m_a + m_h \geq D$, that is, both AT and high-speed rail (HSR) serve their respective captive passenger markets without competition. The capacity of each mode is sufficient to accommodate its potential travelers, and the total seats available can meet the overall travel demand. The demand for the two modes can be formulated as $n_a = F\left(c_a^{-1}(c_o)\right)$ and $n_h = D - F\left(c_h^{-1}(c_o)\right)$. Compared to the extreme case with very high ticket prices, this scenario may result from i) a higher acceptable travel cost (larger c_0), ii) lower travel prices (p_a and p_h) or iii) reduced sensitivity to preference dissonance (i.e., a slower increase in $d(\cdot)$ with decreasing preference for the chosen mode). Scenario I often represents real-world cases with excess transport capacity and low travel demand among residents. Assuming linear $d_i(\cdot)$ and $r_i(\cdot)$ functions, the travel prices for both modes can be illustrated in Figure 5.3a. We can infer the equivalent conditions of Scenario I:

$$c_a^{-1}(c_o) < c_h^{-1}(c_o), \tag{5.13a}$$

$$F^{-1}(m_a) > F^{-1}(D - m_h). \tag{5.13b}$$

(***Scenario II: Insufficient transport capacity and high crowding cost***) In this scenario, $x_1 + x_2 < 1$, $0 < n_a = m_a$ and/or $0 < n_h = m_h$, furthermore, $m_a + m_h < D$ that is, the transport capacity of both modes is insufficient to meet the total demand, leading to high crowding costs for travelers. x_a and x_h are defined as the locations making $\int_0^{x_a} f(x)\, dx = m_a$ and $\int_{x_h}^{1} f(x)\, dx = m_h$. There is still no competition between AT and HSR in this case. Compared to Scenario I, this scenario may show i) higher ticket prices for both transport modes (p_a

and p_h), ii) increased sensitivity to travel preference dissonance (d_a and d_h), iii) reduced transport capacity (m_a and m_h), or iv) higher crowding costs (r_a and r_h). Assuming linear $d_i(\cdot)$ and $r_i(\cdot)$ functions, the comparison of travel prices for both modes under this scenario and those under Scenario I is shown in Figure 5.3b. This scenario satisfy the condition that $\min\left\{c_a^{-1}(c_o), F^{-1}(m_a)\right\} < \max\left\{c_h^{-1}(c_o), F^{-1}(D-m_h)\right\}$.

(***Scenario III: Sufficient capacity for both competitive travel modes***) The main conditions for this scenario include $x_1 + x_2 \geq 1$, $0 < n_a < m_a$, $0 < n_h < m_h$, and $m_a + m_h > D$. In this case, the total transport capacity is greater than the overall demand. As a result, all travelers can use their preferred travel modes, since both AT and HSR have enough seats to accommodate their respective potential users. $\tilde{x}$ indicate the preference for HSR of indifferent passengers who experience equal travel costs for both air and HSR, i,e, $c_a(\tilde{x}) = c_h(\tilde{x})$. In this case, air travelers and HSR travelers can be calculated by $n_a = F(\tilde{x}) = F\left(c_a^{-1}(c_o - \eta)\right)$ and $n_h = D - F(\tilde{x}) = D - F\left(c_h^{-1}(c_o - \eta)\right)$, respectively. Compared to cases where no competition exists between the two modes, this scenario may see i) lower ticket prices (p_a and p_h), ii) reduced sensitivity to preference dissonance (d_a and d_h), iii) lower crowding costs as capacity is sufficient, or iv) a higher acceptable maximum cost (c_o). Typically, given linear forms of crowding costs, the travel prices under this scenario can be shown as Figure 5.3c. This scenario satisfy the condition that $\min\left\{c_a^{-1}(c_o), F^{-1}(m_a)\right\} > \max\left\{c_h^{-1}(c_o), F^{-1}(D-m_h)\right\}$.

(***Scenario IV: Competitive Market with Mode Shifts***) Building upon Scenario III, this scenario introduces possible shifts in traveler choices. In this case, a higher air travel cost shifts the location of indifferent travelers rightward (favouring HSR), while a higher HSR travel cost shifts the location of indifferent travelers leftward (favouring air travel). It can be inferred that if one mode becomes less attractive due to higher ticket prices, reduced capacity, or increased crowding costs, travelers with lower loyalty to that mode will shift to the alternative mode. When $m_a + m_h < D$, there is no competition between the two modes, and the capacity constraints still hold as $n_a \leq m_a$ and $n_h \leq m_h$. Assuming r_a, r_h, d_a and d_h as linear functions, travel prices under various ticket prices and crowding costs in this case can be represented by Figure 5.3d. This scenario satisfy the condition that $\min\left\{c_a^{-1}(c_o), F^{-1}(m_a)\right\} = \max\left\{c_h^{-1}(c_o), F^{-1}(D-m_h)\right\}$.

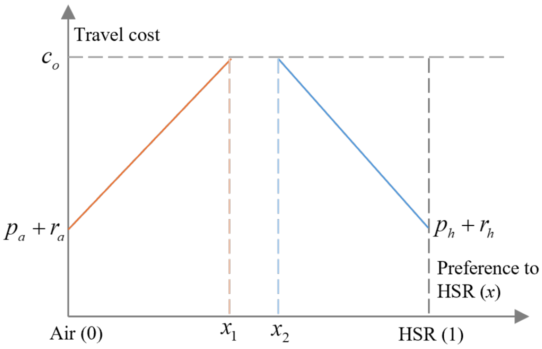

(a) Sufficient capacity of both modes (no competition)

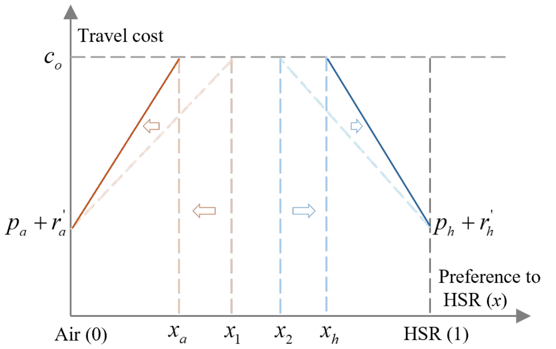

(b) Insufficient capacity of both modes (no competition)

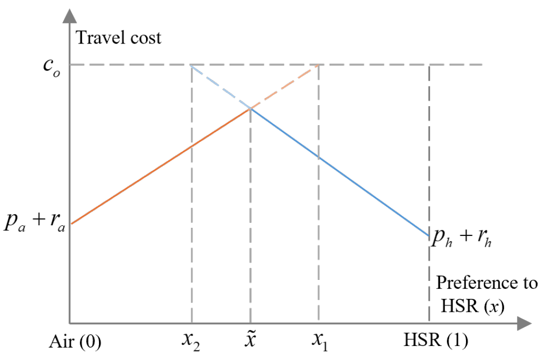

(c) Sufficient capacity of both modes

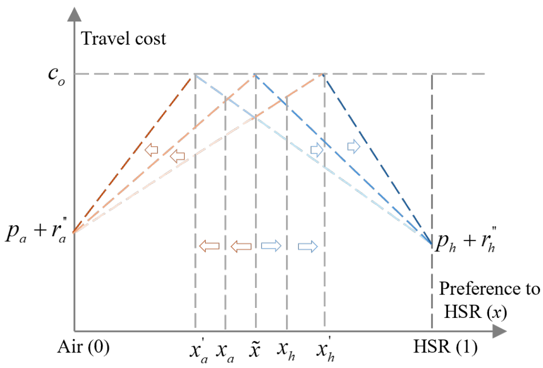

(d) Insufficient capacity of both modes

Figure 5.3: Possible travel mode choice equilibrium scenarios

5.2.2.3 Comparative statics

In this subsection, we examine how transport capacities and ticket prices of the two modes influence the demand for air travel and HSR under equilibrium conditions. As previously discussed, AT and HSR can operate in either captive markets or a competitive market. Therefore, we derive the results separately for these two market structures.

(Separate captive markets): When there is no competition between AT and HSR (as illustrated as Scenario I and II in Section 5.2.2.2), indicating the separate captive markets of the two modes, we can get that $n_a = \int_0^{x_1} f(x)\, dx = F(x_1)$ and $n_h = \int_{x_2}^{1} f(x)\, dx = D - F(x_2)$, where $x_1 + x_2 \leq 1$. In this case, we can have

$$p_a + \kappa_a \left(\int_0^{x_1} f(x)\, dx \right) + d_a(x_1) = c_o, \tag{5.14a}$$

$$p_h + \kappa_h \left(\int_{x_2}^{1} f(x)\, dx \right) + d_h(1 - x_2) = c_o. \tag{5.14b}$$

Based on the above formulations, the first-order derivatives of x_1 and x_2 with respect to various system parameters including the prices (p_a and p_h) and the transport capacity (m_a and m_h) can be calculated as:

$$\frac{\partial x_1}{\partial p_a} = -\frac{1}{\kappa_a^{'}\left(F\left(x_1\right)\right)\times f\left(x_1\right)+d_a^{'}\left(x_1\right)}, \tag{5.15a}$$

$$\frac{\partial x_2}{\partial p_h} = \frac{1}{\kappa_h^{\prime}\left(D-F\left(x_2\right)\right)\times f\left(x_2\right)+d_h^{'}\left(1-x_2\right)}, \tag{5.15b}$$

$$\frac{\partial x_1}{\partial m_a} = \frac{\kappa_a^{\prime}\left(F\left(x_1\right)\right)\times F\left(x_1\right)}{\kappa_a^{\prime}\left(F\left(x_1\right)\right)f\left(x_1\right)+d_a^{'}\left(x_1\right)}, \tag{5.16a}$$

$$\frac{\partial x_2}{\partial m_h} = -\frac{\kappa_h^{\prime}\left(D-F\left(x_2\right)\right)\times\left(D-F\left(x_2\right)\right)}{\kappa_h^{\prime}\left(D-F\left(x_2\right)\right)f\left(x_2\right)+d_h^{'}\left(1-x_2\right)}. \tag{5.16b}$$

From the above formulation, it can be easily investigated that $\frac{\partial x_1}{\partial p_a} < 0$, $\frac{\partial x_2}{\partial p_h} > 0$, $\frac{\partial x_1}{\partial m_a} > 0$, and $\frac{\partial x_2}{\partial m_h} < 0$, so we can further understand that $\frac{\partial n_a}{\partial p_a} = f\left(x_1\right)\times\frac{\partial x_1}{\partial p_a} < 0$, $\frac{\partial n_h}{\partial p_h} = -f\left(x_2\right)\times\frac{\partial x_2}{\partial p_h} < 0$, $\frac{\partial n_a}{\partial m_a} = f\left(x_1\right)\times\frac{\partial x_1}{\partial m_a} > 0$, and $\frac{\partial n_h}{\partial m_h} = -f\left(x_2\right)\times\frac{\partial x_2}{\partial m_h} > 0$. The above formulations indicate that the lower ticket price and higher transport capacity of a travel mode tend to attract more demand for the mode. Besides, it can be inferred that $\frac{\partial n_a}{\partial p_h} = 0$, $\frac{\partial n_h}{\partial p_a} = 0$, $\frac{\partial n_a}{\partial m_h} = 0$, and $\frac{\partial n_h}{\partial m_a} = 0$, indicating that the ticket price and transport capacity of a travel mode have no effect on the demand for another mode when there is no competition between them.

(Competitive market): Then we discuss the case where there is competition between the two travel modes, where $y_a = y_h = \tilde{x}$. The the derivatives of $\tilde{x}$ with respect to the ticket prices can be derived by setting:

$$p_a + d_a\left(\tilde{x}\right) + \kappa_a\left(\frac{F\left(\tilde{x}\right)}{m_a}\right) = p_h + d_h\left(1-\tilde{x}\right) + \kappa_h\left(\frac{D-F\left(\tilde{x}\right)}{m_h}\right). \tag{5.17}$$

Then the derivatives of $\tilde{x}$ with respect to ticket prices and transport capacities can be calculated as:

$$\frac{\partial\tilde{x}}{\partial p_a} = -\frac{1}{d_a^{'}\left(\tilde{x}\right)+d_h^{'}\left(1-\tilde{x}\right)+\kappa_a^{'}\left(F\left(\tilde{x}\right)\right)\times\times f\left(\tilde{x}\right)+\kappa_h^{'}\left(D-F\left(\tilde{x}\right)\right)\times f\left(\tilde{x}\right)}, \tag{5.18a}$$

$$\frac{\partial\tilde{x}}{\partial p_h} = \frac{1}{d_a^{'}\left(\tilde{x}\right)+d_h^{'}\left(1-\tilde{x}\right)+\kappa_a^{\prime}\left(F\left(\tilde{x}\right)\right)\times f\left(\tilde{x}\right)+\kappa_h^{\prime}\left(D-F\left(\tilde{x}\right)\right)\times f\left(\tilde{x}\right)}, \tag{5.18b}$$

$$\frac{\partial\tilde{x}}{\partial m_a} = \frac{\kappa_a^{\prime}\left(F\left(\tilde{x}\right)\right)\times F\left(\tilde{x}\right)}{d_a^{'}\left(\tilde{x}\right)+d_h^{'}\left(1-\tilde{x}\right)+\kappa_a^{\prime}\left(F\left(\tilde{x}\right)\right)\times f\left(\tilde{x}\right)+\kappa_h^{'}\left(D-F\left(\tilde{x}\right)\right)\times f\left(\tilde{x}\right)}, \tag{5.19a}$$

$$\frac{\partial \tilde{x}}{\partial m_h} = -\frac{\kappa_h' \left(D - F\left(\tilde{x}\right)\right) \times \left(D - F\left(\tilde{x}\right)\right)}{d_a'\left(\tilde{x}\right) + d_h'\left(1 - \tilde{x}\right) + \kappa_a'\left(F\left(\tilde{x}\right)\right) \times f\left(\tilde{x}\right) + \kappa_h'\left(D - F\left(\tilde{x}\right)\right) \times f\left(\tilde{x}\right)}. \tag{5.19b}$$

Based on the above formulations, it can be further inferred that $\frac{\partial n_a}{\partial p_a} = f\left(\tilde{x}\right) \times \frac{\partial \tilde{x}}{\partial p_a} < 0$, $\frac{\partial n_h}{\partial p_h} = -f\left(\tilde{x}\right) \times \frac{\partial \tilde{x}}{\partial p_h} < 0$, $\frac{\partial n_a}{\partial m_a} = f\left(\tilde{x}\right) \times \frac{\partial \tilde{x}}{\partial m_a} > 0$, and $\frac{\partial n_h}{\partial m_h} = -f\left(\tilde{x}\right) \times \frac{\partial \tilde{x}}{\partial m_h} > 0$. The investigation indicates a similar conclusions as those under captive markets, that is, more demand for a travel mode is likely to be attracted by lower ticket price and higher transport capacity of the travel mode. Furthermore, it can be inferred that $\frac{\partial n_a}{\partial p_h} = f\left(\tilde{x}\right) \times \frac{\partial \tilde{x}}{\partial p_h} > 0$, $\frac{\partial n_a}{\partial m_h} = f\left(\tilde{x}\right) \times \frac{\partial \tilde{x}}{\partial m_h} < 0$, $\frac{\partial n_h}{\partial p_a} = f\left(\tilde{x}\right) \times \frac{\partial \tilde{x}}{\partial p_a} > 0$, and $\frac{\partial n_h}{\partial m_a} = f\left(\tilde{x}\right) \times \frac{\partial \tilde{x}}{\partial m_a} < 0$, indicating that the demand of a travel mode will increase given a higher ticket price and lower transport capacity of its competitive travel mode.

Based on the above results, it is evident that regardless of whether competition exists between AT and HSR, higher ticket prices and lower capacity for a travel mode will reduce its demand while increasing demand for the alternative mode. Conversely, lower ticket prices and expanded capacity will attract more travelers from the competing mode.

5.2.3 Pricing strategies

5.2.3.1 Revenue Maximization

We now investigate the pricing strategies made by revenue-maximizing operators of both travel modes given the transport capacities are exogenously given. As this study emphasizes the impact of travelers' choice between AT and HSR, here and after captive markets of the two modes without competition will not be discussed. The operators make pricing strategies aiming to maximise their net revenue (or profit), we can separately derive the optimal ticket prices of AT and HSR under a competitive market (noted as p_a^{RM*} and p_h^{RM*}) by solving program:

$$\max: \pi_a\left(p_a\right) = p_a \times F\left(y_a\right) - w_a\left(F\left(y_a\right)\right), \tag{5.20a}$$

$$\max: \pi_h\left(p_h\right) = p_h \times \left(D - F\left(y_h\right)\right) - w_h\left(D - F\left(y_h\right)\right). \tag{5.20b}$$

Given the derived optimal pricing strategies, the profits of the two modes under the competitive market can be calculated. The general-form formulation of optimal ticket prices and profit of the two modes under different market structures are shown as follows:

$$p_a^{RM*} = \frac{F(\tilde{x}^{RM})}{f(\tilde{x}^{RM})} \times \left[d'_a\left(\tilde{x}^{RM}\right) + d'_h\left(1 - \tilde{x}^{RM}\right)\right] + F\left(\tilde{x}^{RM}\right) \times \left[\kappa'_a\left(n_a^{RM}\right) + \kappa'_h\left(n_h^{RM}\right)\right] + w'_a\left(n_a^{RM}\right), \tag{5.21a}$$

$$p_h^{RM*} = \frac{D-F(\tilde{x}^{RM})}{f(\tilde{x}^{RM})} \times \left[d'_a\left(\tilde{x}^{RM}\right) + d'_h\left(1 - \tilde{x}^{RM}\right)\right] + \left(D - F\left(\tilde{x}^{RM}\right)\right) \times \left[\kappa'_a\left(n_a^{RM}\right) + \kappa'_h\left(n_h^{RM}\right)\right] + w'_h\left(n_h^{RM}\right), \tag{5.21b}$$

$$\begin{aligned} \pi_a^{RM} = & \frac{\left(F\left(\tilde{x}^{RM}\right)\right)^2}{f\left(\tilde{x}^{RM}\right)} \times \left[d'_a\left(\tilde{x}^{RM}\right) + d'_h\left(1 - \tilde{x}^{RM}\right)\right] + \left(F\left(\tilde{x}^{RM}\right)\right)^2 \times \left[\kappa'_a\left(n_a^{RM}\right) + \kappa'_h\left(n_h^{RM}\right)\right] \\ & + F\left(\tilde{x}^{RM}\right) \times w'_a\left(n_a^{RM}\right) - w_a\left(q_a^{RM}\right), \end{aligned} \tag{5.22a}$$

$$\begin{aligned} \pi_h^{RM} = & \frac{\left(D - F\left(\tilde{x}^{RM}\right)\right)^2}{f\left(\tilde{x}^{RM}\right)} \times \left[d'_a\left(\tilde{x}^{RM}\right) + d'_h\left(1 - \tilde{x}^{RM}\right)\right] \\ & + \left(D - F\left(\tilde{x}^{RM}\right)\right)^2 \times \left[\kappa'_a\left(n_a^{RM}\right) + \kappa'_h\left(n_h^{RM}\right)\right] + \left(D - F\left(\tilde{x}^{RM}\right)\right) \times w'_h\left(n_h^{RM}\right) - w_h\left(n_h^{RM}\right). \end{aligned} \tag{5.22b}$$

In the first term in both pricing equations, $\frac{F(\tilde{x})}{f(\tilde{x})}$ or $\frac{D-F(\tilde{x})}{f(\tilde{x})}$, represents the inverse of demand elasticity. This term highlights how the sensitivity of demand to price changes is influenced by the distribution of travelers' mode preferences. When a larger proportion of travelers exhibit neutral preferences between the two modes, i.e., $f(\tilde{x})$ is high, even small price changes can lead to significant shifts in demand. As a result, operators must set lower optimal prices to remain competitive and attract more passengers. Conversely, if demand is inelastic, meaning $f(\tilde{x})$ is low due to travelers having strong and distinct preferences for either air or rail, price changes will have a weaker effect on demand shifts. In this case, operators can charge higher prices without experiencing substantial reductions in passenger numbers, maximizing revenue from travelers who are less sensitive to price variations. The second term in the pricing formulations, i.e., $\kappa'_a(q_a)$ or $\kappa'_h(q_h)$, accounts for marginal crowing costs. If crowding costs increase (e.g., due to high passenger density), optimal prices should increase to reflect the added cost burden. $w'_a(q_a)$ and $w'_h(q_h)$ represent marginal capacity maintenance costs. Higher maintenance costs lead to higher ticket prices, ensuring that infrastructure upkeep is financially sustainable. The pricing structure reflects a revenue management approach, where optimal prices are dynamically set based on demand sensitivity.

Profits are proportional to the square of demand $(F(\tilde{x}))^2$ and $(D - F(x))^2$. This implies that modest demand increases can lead to disproportionately higher profits, especially when travelers' preference distributions are less centralized, i.e., lower $f(\tilde{x})$. Higher marginal crowding costs $\kappa_a'(q_a)$ and $\kappa_h'(q_h)$ lead to weak attraction of modes to demands, thus reducing profits unless compensated by higher prices. The terms $g_a(m_a)$ and $g_h(m_h)$ represent fixed costs (e.g., fleet maintenance, infrastructure expenditures).

5.2.3.2 Maximization of a weighted sum of welfare and profit by HSR

In the literature, a case is often observed where the airline maximizes its own profit whereas the HSR operator maximizes a weighted sum of profit and social welfare due to the government regulation (Yang & Zhang, 2012; Tsunoda, 2018). In this section, we consider a scenario in which the airline seeks to maximize its profit, while the HSR operator maximizes a weighted sum of profit and social welfare. It can be easily inferred that, in this case, AT operators propose airfare p_a^{SW*} identical to p_a^{RM*} formulated in Eq. (5.21a). $\tilde{x}^{SW}$ indicates preference for HSR of indifferent passengers given the pricing strategy (p_a^{SW*}, p_a^{RM*}). The HSR operator determines the optimal ticket price by maximizing a weighted sum of system social welfare and operator profit:

$$\max : Q_h\left(p_h\right) = \alpha SW_h + (1-\alpha)\,\pi_h = \alpha CS_h + \pi_h, \tag{5.23}$$

$$\max : \pi_a\left(p_a\right) = p_a \times F\left(y_a\right) - w_a\left(F\left(y_a\right)\right), \tag{5.24}$$

where $\alpha \in (0, 1)$ is the weight on the social welfare within HSR system. The equilibrium ticket prices for HSR and air travel, under competition, are then derived as:

$$p_a^{SW*} = \frac{F(\tilde{x}^{SW})}{f(\tilde{x}^{SW})} \times \left[d_a'\left(\tilde{x}^{SW}\right) + d_h'\left(1-\tilde{x}^{SW}\right)\right] + F\left(\tilde{x}^{SW}\right) \times \left[\kappa_a'\left(n_a^{SW}\right) + \kappa_h'\left(n_h^{SW}\right)\right] + w_a'\left(n_a^{SW}\right) \tag{5.25}$$

$$\begin{aligned} p_h^{SW*} = & -\alpha\left(c_o - c_h\left(\tilde{x}^{SW}\right)\right) + \frac{D - F\left(\tilde{x}^{SW}\right)}{f\left(\tilde{x}^{SW}\right)} \times \left[d_a'\left(\tilde{x}^{SW}\right) + d_h'\left(1-\tilde{x}^{SW}\right)\right] \\ & + \left(D - F\left(\tilde{x}^{SW}\right)\right) \times \left[\kappa_a'\left(n_a^{SW}\right) + \kappa_h'\left(n_h^{SW}\right)\right] + w_h'\left(n_h^{SW}\right). \end{aligned} \tag{5.26}$$

At equilibrium, the indifferent passenger satisfies:

$$p_a^{SW*} + d_a(\tilde{x}^{SW}) + \kappa_a(n_a) = p_h^{SW*} + d_h(1 - \tilde{x}^{SW}) + \kappa_h(n_h). \tag{5.27}$$

By comparing the formulations of p_h^{SW*} and p_h^{RM*}, we observe that while both are influenced by the same fundamental factors, p_h^{SW*} is additionally affected by the term $-\alpha\left(c_o - c_h\left(\tilde{x}^{SW}\right)\right)$. The greater the weight placed on the welfare of the HSR system, the stronger the impact of $c_o - c_h\left(\tilde{x}^{SW}\right)$ on pricing strategies. This term represents the consumer surplus of indifferent travelers. Moreover, for all $x \leq \tilde{x}$, we have $c_o - c_h(x) \geq c_o - c_h\left(\tilde{x}^{SW}\right)$, indicating that $c_o - c_h\left(\tilde{x}^{SW}\right)$ reflects the lowest level of consumer surplus within the HSR traveler group.

By substituting the ticket prices (Eqs. (5.25)-(5.26)) into profit formulations, we can obtain the air profit and HSR profit as follows:

$$\begin{aligned}\pi_a^{SW} = & \frac{\left(F\left(\tilde{x}^{SW}\right)\right)^2}{f\left(\tilde{x}^{SW}\right)}\left[d_a'\left(\tilde{x}^{SW}\right) + d_h'\left(1 - \tilde{x}^{SW}\right)\right] + \left(F\left(\tilde{x}^{SW}\right)\right)^2\left[\kappa_a'\left(n_a^{SW}\right) + \kappa_h'\left(n_h^{SW}\right)\right] \\ & + F\left(\tilde{x}^{SW}\right) w_a'\left(n_a^{SW}\right) - w_a\left(n_a^{SW}\right),\end{aligned} \tag{5.28a}$$

$$\begin{aligned}\pi_h^{SW} = & \frac{\left(D - F\left(\tilde{x}^{SW}\right)\right)^2}{f\left(\tilde{x}^{SW}\right)}\left[d_a'\left(\tilde{x}^{SW}\right) + d_h'\left(1 - \tilde{x}^{SW}\right) - \alpha\left(c_o - c_h\left(\tilde{x}^{SW}\right)\right)\right] \\ & + \left(D - F\left(\tilde{x}^{SW}\right)\right)^2\left[\kappa_a'\left(n_a^{SW}\right) + \kappa_h'\left(n_h^{SW}\right)\right] + \left(D - F\left(\tilde{x}^{SW}\right)\right) w_h'\left(n_h^{SW}\right) - w_h\left(n_h^{SW}\right).\end{aligned} \tag{5.28b}$$

5.2.3.3 How social welfare weighting in HSR shapes pricing strategies

The examination of how social welfare weighting in the HSR systems influences the pricing strategies and subsequent profits of both HSR and air is a critical way to make an ex-ante assessment of welfare implications across different policy interventions. Travelers' heterogeneous mode preferences significantly affect cross-elasticities of demand between modes and consequently shape the strategic pricing responses of both HSR operators and airlines. The incorporation of preference heterogeneity into welfare-weighted models enables more specific analysis of market segmentation strategies, revealing how different welfare weights might disproportionately affect certain traveler groups based on their inherent mode preference distributions. The analytical insights can help policymakers make more targeted interventions that can simultaneously address efficiency objectives and equity considerations.

In our study, we use α to represent the social welfare weighting in the HSR system. To study the effect of α, we differentiate the above optimality conditions, i.e., Eqs. (5.26)-(5.27), with respect to α, yielding expressions for the sensitivities of the demand split $\tilde{x}^{SW}$ and prices (p_a^{SW*}, p_h^{SW*}) to changes in the social welfare weight:

$$\frac{\partial x^{SW}}{\partial \alpha} = \frac{-\left(c_o - c_h\left(\tilde{x}^{SW}\right)\right)}{\frac{\left[(1-\alpha)F\left(\tilde{x}^{SW}\right) - \left(D - F\left(\tilde{x}^{SW}\right)\right)\right]M\left(\tilde{x}^{SW}\right)}{f\left(\tilde{x}^{SW}\right)}\left(\frac{M'\left(\tilde{x}^{SW}\right)}{M\left(\tilde{x}^{SW}\right)} - \frac{f'\left(\tilde{x}^{SW}\right)}{f\left(\tilde{x}^{SW}\right)}\right) + (3-2\alpha)M\left(\tilde{x}^{SW}\right) + \left[(1-\alpha)w_a''\left(n_a^{SW}\right) + w_h''\left(n_h^{SW}\right) + 2\alpha\kappa_h'\left(n_h^{SW}\right)\right]f\left(\tilde{x}^{SW}\right) + 2\alpha d_h'\left(1-\tilde{x}^{SW}\right)} \tag{5.29a}$$

$$\frac{\partial p_a^{SW*}}{\partial \alpha} = \left[\frac{F\left(\tilde{x}^{SW}\right)M\left(\tilde{x}^{SW}\right)}{f\left(\tilde{x}^{SW}\right)}\left(\frac{M'\left(\tilde{x}^{SW}\right)}{M\left(\tilde{x}^{SW}\right)} - \frac{f'\left(\tilde{x}^{SW}\right)}{f\left(\tilde{x}^{SW}\right)}\right) + M\left(\tilde{x}^{SW}\right) + w_a''\left(n_a^{SW}\right)f\left(\tilde{x}^{SW}\right)\right]\frac{\partial \tilde{x}^{SW}}{\partial \alpha} \tag{5.29b}$$

$$\frac{\partial p_h^{SW*}}{\partial \alpha} = \left[\frac{F\left(\tilde{x}^{SW}\right)M\left(\tilde{x}^{SW}\right)}{f\left(\tilde{x}^{SW}\right)}\left(\frac{M'\left(\tilde{x}^{SW}\right)}{M\left(\tilde{x}^{SW}\right)} - \frac{f'\left(\tilde{x}^{SW}\right)}{f\left(\tilde{x}^{SW}\right)}\right) + 2M\left(\tilde{x}^{SW}\right) + w_a''\left(q_a^{SW}\right)f\left(\tilde{x}^{SW}\right)\right]\frac{\partial \tilde{x}^{SW}}{\partial \alpha} \tag{5.29c}$$

Let $M\left(\tilde{x}^{SW}\right)$ denote the derivative of the difference in non-monetary costs (disutility costs plus crowding costs) between air and HSR with respect to $\tilde{x}^{SW}$, defined as Eq. (5.30a). The first-order derivative of $M\left(\tilde{x}^{SW}\right)$ with respected to $\tilde{x}^{SW}$ is calculated as Eq. (5.30b).

$$\begin{aligned} M\left(\tilde{x}^{SW}\right) &= \frac{\partial}{\partial \tilde{x}^{SW}}\left[d_a\left(\tilde{x}^{SW}\right) + \kappa_a\left(n_a^{SW}\right) - d_h\left(\tilde{x}^{SW}\right) - \kappa_h\left(n_h^{SW}\right)\right] \\ &= d_a'\left(\tilde{x}^{SW}\right) + d_h'\left(1-\tilde{x}^{SW}\right) + \kappa_a'\left(n_a^{SW}\right)f\left(\tilde{x}^{SW}\right) + \kappa_h'\left(n_h^{SW}\right)f\left(\tilde{x}^{SW}\right) \end{aligned} \tag{5.30a}$$

$$\begin{aligned} M'\left(\tilde{x}^{SW}\right) &= d_a''\left(\tilde{x}^{SW}\right) - d_h''\left(1-\tilde{x}^{SW}\right) + \kappa_a'\left(n_a^{SW}\right)\times f'\left(\tilde{x}^{SW}\right) + \kappa_h'\left(n_h^{SW}\right)\times f'\left(\tilde{x}^{SW}\right) \\ &\quad + \kappa_a''\left(n_a^{SW}\right)\times\left(f\left(\tilde{x}^{SW}\right)\right)^2 - \kappa_h''\left(n_h^{SW}\right)\times\left(f\left(\tilde{x}^{SW}\right)\right)^2 \end{aligned} \tag{5.30b}$$

As previously stated, we have $d_a' > 0$, $d_h' > 0$, $f(x) > 0$, $\kappa_a' > 0$, $\kappa_h' > 0$, $\kappa_a'' > 0$, $\kappa_h'' > 0$, $w_a'' > 0$, and $w_h'' > 0$. It follows directly that $M\left(\tilde{x}^{SW}\right) > 0$. We define

$$\Phi(M, f)\left(\tilde{x}^{SW}\right) = \frac{M'\left(\tilde{x}^{SW}\right)}{M\left(\tilde{x}^{SW}\right)} - \frac{f'\left(\tilde{x}^{SW}\right)}{f\left(\tilde{x}^{SW}\right)} \tag{5.31}$$

as the difference in these proportional rates of change, which captures how the marginal non-monetary advantage of HSR evolves relative to the distribution of traveler preferences.

$f(\tilde{x}^{SW})$ indicates the density of travelers in the indifferent location. $f'(\tilde{x}^{SW})$ is the derivative of this density, showing how the number of travelers with preference near $\tilde{x}^{SW}$ changes with increasing preference for HSR. $\frac{f'\left(\tilde{x}^{SW}\right)}{f\left(x^{SW}\right)}$ is the relative (or proportional) rate of change of the density of travelers at preference $\tilde{x}^{SW}$. $\frac{f'\left(\tilde{x}^{SW}\right)}{f\left(\tilde{x}^{SW}\right)}$ measures how rapidly the concentration of travelers with a given HSR preference is changing at point x^{SW}, relative to the current density at that preference. Therefore, $\frac{f'\left(\tilde{x}^{SW}\right)}{f\left(x^{SW}\right)}$ tells us how sensitive the market is to shifts in the "indifferent" point between HSR and air.

$M\left(\tilde{x}^{SW}\right)$ measures how the non-monetary advantage of choosing HSR over air travel changes as passenger preference for HSR increases. $M'\left(\tilde{x}^{SW}\right)$ is the rate at which this change itself is changing, a second derivative in effect. $\frac{M'\left(\tilde{x}^{SW}\right)}{M\left(\tilde{x}^{SW}\right)}$ is the relative (proportional) rate of change of the marginal non-monetary benefit of HSR over air travel, at a given preference $\tilde{x}^{SW}$. $\frac{M'\left(\tilde{x}^{SW}\right)}{M\left(\tilde{x}^{SW}\right)}$ quantifies how quickly the incremental (marginal) "non-monetary benefit of HSR over air" changes, relative to its current value, as passenger preference for HSR increases. The ratio $\frac{M'\left(\tilde{x}^{SW}\right)}{M\left(\tilde{x}^{SW}\right)}$ tells how sensitive the perceived extra non-monetary benefits of HSR are to changes in traveler preferences at the tipping point between modes.

The expressions for the partial derivatives of equilibrium prices with respect to α, in Eq. (5.29a)-(5.29c) are functions of $M\left(\tilde{x}^{SW}\right)$, $f\left(\tilde{x}^{SW}\right)$ and their derivatives, and the second-order derivatives of operating costs in the two transport systems, i.e., $w''_a(n_a^{SW})$ and $w''_h(n_h^{SW})$. We introduce auxiliary terms Π_1, Π_2, and Π_3, defined by Eq. (5.32), to facilitate classification of the possible market outcomes, depending on the relative demand for each mode.

$$\Pi_1 = -\frac{f\left(\tilde{x}^{SW}\right)}{\left(F\left(\tilde{x}^{SW}\right)-\frac{D-F\left(\tilde{x}^{SW}\right)}{(1-\alpha)}\right)} \times \left[\left(2+\frac{1}{(1-\alpha)}\right)+\frac{w''_a\left(q_a^{SW}\right)f\left(\tilde{x}^{SW}\right)}{M\left(\tilde{x}^{SW}\right)}+\frac{\left(w''_h\left(n_h^{SW}\right)+2\alpha\kappa'_h\left(n_h^{SW}\right)\right)f\left(\tilde{x}^{SW}\right)+2\alpha d'_h\left(1-\tilde{x}^{SW}\right)}{(1-\alpha)M\left(\tilde{x}^{SW}\right)}\right] \tag{5.32a}$$

$$\Pi_2 = -\frac{f\left(\tilde{x}^{SW}\right)}{F\left(\tilde{x}^{SW}\right)} \times \left(1+\frac{w''_a\left(n_a^{SW}\right)f\left(\tilde{x}^{SW}\right)}{M\left(\tilde{x}^{SW}\right)}\right) \tag{5.32b}$$

$$\Pi_3 = -\frac{f\left(\tilde{x}^{SW}\right)}{F\left(\tilde{x}^{SW}\right)} \times \left(2+\frac{w''_a\left(n_a^{SW}\right)f\left(\tilde{x}^{SW}\right)}{M\left(\tilde{x}^{SW}\right)}\right) \tag{5.32c}$$

It is clear that when $n_a^{SW} = F\left(\tilde{x}^{SW}\right) > \frac{\left(D-F\left(\tilde{x}^{SW}\right)\right)}{(1-\alpha)} = \frac{n_h^{SW}}{(1-\alpha)}$, we can have $\Pi_1 < \Pi_3 < \Pi_2 < 0$. In contrast, when $n_a^{SW} = F\left(\tilde{x}^{SW}\right) < \frac{\left(D-F\left(\tilde{x}^{SW}\right)\right)}{(1-\alpha)} = \frac{n_h^{SW}}{(1-\alpha)}$, it can be inferred that $\Pi_3 < \Pi_2 < 0 < \Pi_1$. Table 5.1 summarizes the impacts of increasing α (i.e., giving more weight to social welfare in the HSR system) on the equilibrium prices (p_a^{SW*} and p_h^{SW*}) and demand distribution for various demand conditions.

Table 5.1: Different cases about changes of pricing strategies and demand distribution

Demand regime	Conditions on Φ	Results of partial derivatives	Price changes	Demand shift
$n_a^{SW} > \frac{n_h^{SW}}{(1-\alpha)}$	$\Phi > \Pi_2$	$\frac{\partial \tilde{x}^{SW}}{\partial \alpha} < 0$, $\frac{\partial p_a^{SW*}}{\partial \alpha} < 0$, $\frac{\partial p_h^{SW*}}{\partial \alpha} < 0$	↓ both	HSR gains demand (leftward $\tilde{x}^{SW}$)
	$\Pi_3 < \Phi < \Pi_2$	$\frac{\partial \tilde{x}^{SW}}{\partial \alpha} < 0$, $\frac{\partial p_a^{SW*}}{\partial \alpha} > 0$, $\frac{\partial p_h^{SW*}}{\partial \alpha} < 0$	HSR ↓, Air ↑	HSR gains demand
	$\Pi_1 < \Phi < \Pi_3$	$\frac{\partial \tilde{x}^{SW}}{\partial \alpha} < 0$, $\frac{\partial p_a^{SW*}}{\partial \alpha} > 0$, $\frac{\partial p_h^{SW*}}{\partial \alpha} > 0$	↑ both	HSR gains demand
	$\Phi < \Pi_1$	$\frac{\partial \tilde{x}^{SW}}{\partial \alpha} > 0$, $\frac{\partial p_a^{SW*}}{\partial \alpha} < 0$, $\frac{\partial p_h^{SW*}}{\partial \alpha} < 0$	↓ both	Air regains demand (rightward $\tilde{x}^{SW}$)
$n_a^{SW} < \frac{n_h^{SW}}{(1-\alpha)}$	$\Phi > \Pi_1$	$\frac{\partial \tilde{x}^{SW}}{\partial \alpha} > 0$, $\frac{\partial p_a^{SW*}}{\partial \alpha} > 0$, $\frac{\partial p_h^{SW*}}{\partial \alpha} > 0$	↑ both	Air gains demand
	$\Pi_2 < \Phi < \Pi_1$	$\frac{\partial \tilde{x}^{SW}}{\partial \alpha} < 0$, $\frac{\partial p_a^{SW*}}{\partial \alpha} < 0$, $\frac{\partial p_h^{SW*}}{\partial \alpha} < 0$	↓ both	HSR gains demand
	$\Pi_3 < \Phi < \Pi_2$	$\frac{\partial \tilde{x}^{SW}}{\partial \alpha} < 0$, $\frac{\partial p_a^{SW*}}{\partial \alpha} > 0$, $\frac{\partial p_h^{SW*}}{\partial \alpha} < 0$	HSR ↓, Air ↑	HSR gains demand
	$\Phi < \Pi_3$	$\frac{\partial \tilde{x}^{SW}}{\partial \alpha} < 0$, $\frac{\partial p_a^{SW*}}{\partial \alpha} > 0$, $\frac{\partial p_h^{SW*}}{\partial \alpha} > 0$	↑ both	HSR gains demand

The thresholds Π_1, Π_2, and Π_3 are essential benchmarks for the relative strength of HSR's (versus air's) marginal non-monetary advantage ($M(\tilde{x}^{SW*})$ and $M'(\tilde{x}^{SW*})$) compared to the "thickness" and sensitivity of the passenger market at the margin ($f(\tilde{x}^{SW*})$, $f'(\tilde{x}^{SW*})$). In practice, Π_1, Π_2, and Π_3 quantify how the effectiveness of welfare-driven HSR policy depends on both the strength of HSR's service improvements and the concentration of preference among marginal travelers. If many travelers hold indifferent preference between air and HSR, and HSR's advantage is growing, policy can "tip" the market dramatically. If not, even large interventions may have muted or perverse effects.

Proposition 2. *If the difference between the relative rate of change of HSR marginal non-monetary benefit, $\frac{M'(x^{SW})}{M(x^{SW})}$), and the relative rate of change of traveler density at the indifferent preference point, $\frac{f'(x^{SW})}{f(x^{SW})}$, lies within a specific range, namely $\Pi_3 < \Phi < \Pi_2$, then increasing the weight assigned to HSR social welfare will result in a lower HSR ticket price and a higher airfare, resulting in increased demand for HSR and reduced demand for air travel.*

Proof. When $\Pi_3 < \Phi < \Pi_2$, no matter whether $n_a^{SW} > \frac{n_h^{SW}}{1-\alpha}$ or not, it can be obtained that $\frac{\partial \tilde{x}^{SW}}{\partial \alpha} < 0$, $\frac{\partial p_a^{SW*}}{\partial \alpha} > 0$, $\frac{\partial p_h^{SW*}}{\partial \alpha} < 0$. Furthermore, $\frac{\partial n_a^{SW}}{\partial \alpha} = f\left(\tilde{x}^{SW}\right) \frac{\partial \tilde{x}^{SW}}{\partial \alpha} < 0$ and $\frac{\partial n_h^{SW}}{\partial \alpha} = -f\left(\tilde{x}^{SW}\right) \frac{\partial \tilde{x}^{SW}}{\partial \alpha} > 0$. □

When the demand distribution between air and HSR satisfies $n_a^{SW} > \frac{n_h^{SW}}{1-\alpha}$, as the difference $\frac{M'(\tilde{x}^{SW})}{M(\tilde{x}^{SW})} - \frac{f'(\tilde{x}^{SW})}{f(\tilde{x}^{SW})}$ makes $\Pi_3 < \Phi < \Pi_2$, when α increases, indifference point still shifts left

(HSR gains demand). HSR price drops, but air price rises, indicating that air reduces competition and targets more loyal passengers. Under the market where $n_a^{SW} < \frac{n_h^{SW}}{1-\alpha}$, if $\Pi_3 < \Phi < \Pi_2$, the increasing α causes that HSR price drops while air price rises. HSR continues to attract marginal demand, while air targets remaining loyalists.

Proposition 3. *In an air-dominant market, specifically when $n_a^{SW} > \frac{n_h^{SW}}{1-\alpha}$, if the difference between the relative rate of change of the HSR marginal non-monetary advantage, $\frac{M'(x^{SW})}{M(x^{SW})}$, and the relative rate of change of traveler density at the indifferent preference point, $\frac{f'(x^{SW})}{f(x^{SW})}$, is either sufficiently large ($\Phi > \Pi_2$) or sufficiently small ($\Phi < \Pi_1$), then the ticket prices for both air and HSR services will decrease.*

Proof. From Table 5.1, given $n_a^{SW} > \frac{n_h^{SW}}{1-\alpha}$, when $\Phi > \Pi_2$ or $\Phi < \Pi_1$, it can be derived that $\frac{\partial p_a^{SW*}}{\partial \alpha} < 0$ and $\frac{\partial p_h^{SW*}}{\partial \alpha} < 0$. □

When $n_a^{SW} > \frac{n_h^{SW}}{1-\alpha}$, there are more travelers choosing AT than HSR in the market, i.e., air travel currently holds a greater market share. The condition $\Phi > \Pi_2$ indicates that HSR's advantage is growing faster than the market thins out. In that case, increasing social welfare weight (α) leads to lower prices for both modes and a leftward shift of the indifference point x^{SW}, meaning more travelers switch from air to HSR. HSR becomes more attractive, aggressively lowering its price to draw demand. Air lowers price too, but HSR's reduction has a stronger effect. $\Phi > \Pi_2$ When $\Phi < \Pi_1$, the equilibrium indifference point moves right (air regains demand as HSR's perceived benefit diminishes sharply). Both prices drop, but air benefits more, potentially attracting more demand by lowering its price more aggressively.

Proposition 4. *In a market with a relatively balanced demand distribution, that is, when $n_a^{SW} < \frac{n_h^{SW}}{1-\alpha}$, if the difference between the relative rate of change of the HSR marginal non-monetary advantage, $\frac{M'(x^{SW})}{M(x^{SW})}$, and the relative rate of change of traveler density at the indifferent preference point, $\frac{f'(x^{SW})}{f(x^{SW})}$, is either sufficiently large ($\Phi > \Pi_1$) or sufficiently small ($\Phi < \Pi_3$), then the ticket prices for both air and HSR services will increase.*

Proof. From Table 5.1, given $n_a^{SW} < \frac{n_h^{SW}}{1-\alpha}$, when $\Phi > \Pi_1$ or $\Phi < \Pi_3$, it can be derived that $\frac{\partial p_a^{SW*}}{\partial \alpha} > 0$ and $\frac{\partial p_h^{SW*}}{\partial \alpha} > 0$. □

If the demand distribution between air and HSR satisfies $n_a^{SW} < \frac{n_h^{SW}}{1-\alpha}$, the market is not dominated by air. If $\Phi > \Pi_1$, all quantities increase, higher α pushes prices and the indifference point rightward (air regains demand). HSR less focused on attracting marginal passengers, so both raise prices. When $\Phi < \Pi_3$, both prices increase, but more travelers still move to HSR due to other (non-price) factors shifting the market.

Suppose HSR's advantage is growing faster than the market thins out (i.e., $\Phi > \Pi_2$). In that case, a small promotion for increasing the social welfare weight, can shift a large number of travelers to HSR, and both operators will feel pressure to lower prices. If the density of travelers near the margin is low or decreasing quickly (i.e., $\Phi < \Pi_1$ when $\Pi_1 < 0$), even a bigger policy push may barely move the market, and operators may actually raise prices since there are few "swing" customers left to compete for.

Proposition 5. *In a market where air demand is not significantly higher than HSR demand, specifically, when $n_a^{SW} < \frac{n_h^{SW}}{1-\alpha}$, an increase in the weight assigned to HSR social welfare will lead to a decrease in air ticket prices only if the difference between the relative rate of change of the HSR marginal non-monetary advantage, $\frac{M'(x^{SW})}{M(x^{SW})}$, and the relative rate of change of traveler density at the indifferent preference point, $\frac{f'(x^{SW})}{f(x^{SW})}$, falls within a specific range, namely* $\Pi_2 < \Phi < \Pi_1$.

Proof. Given the market demand distribution satisfying $n_a^{SW} > \frac{n_h^{SW}}{1-\alpha}$, it can be derived that $\frac{\partial p_a^{SW*}}{\partial \alpha} < 0$ only when $\Pi_2 < \Phi < \Pi_1$. □

Proposition 6. *When there are more air passengers than HSR, i.e., $n_a^{SW} > \frac{n_h^{SW}}{1-\alpha}$, an increase in the weight assigned to HSR social welfare will lead to a increase in HSR ticket prices only if the difference between the relative rate of change of the HSR marginal non-monetary advantage, $\frac{M'(x^{SW})}{M(x^{SW})}$, and the relative rate of change of traveler density at the indifferent preference point, $\frac{f'(x^{SW})}{f(x^{SW})}$, falls within a specific range, namely* $\Pi_1 < \Phi < \Pi_3$.

Proof. Under the condition that $n_a^{SW} > \frac{n_h^{SW}}{1-\alpha}$ in the market, it can be derived that $\frac{\partial p_h^{SW*}}{\partial \alpha} > 0$ only when $\Pi_1 < \Phi < \Pi_3$. □

In the market where $n_a^{SW} < \frac{n_h^{SW}}{1-\alpha}$, when $\Pi_2 < \Phi < \Pi_1$, both prices decrease, more travelers shift to HSR. HSR aggressively maximizes welfare, lowering prices to capture further demand. Given $\Pi_1 < \Phi < \Pi_3$ and $n_a^{SW} > \frac{n_h^{SW}}{1-\alpha}$, both prices increase as HSR's non-monetary advantage becomes less significant, but preference still shifts toward HSR (leftward $\tilde{x}^{SW}$). The market is less price-sensitive and both operators increase prices as competition between modes weakens.

When most travelers are clustered near the indifference point (high $f\left(\tilde{x}^{SW}\right)$), policy can be highly effective, i.e., a welfare push for HSR will trigger strong price competition and a big modal shift. When the distribution is flat or most travelers are far from the margin (low $f\left(\tilde{x}^{SW}\right)$), price competition weakens and policy effectiveness drops. If the distribution is sharply changing at the margin (high $|f'(\tilde{x}^{SW})|$), the sensitivity of the market to HSR advantage also changes rapidly, making outcomes more volatile and dependent on precise policy calibration.

The findings indicate that increasing the weight on social welfare in the HSR operator's objective (α) can be an effective lever for shifting demand from air to HSR and intensifying price competition, but only under specific market conditions. In particular, the policy is most effective when the marginal advantage of HSR in non-monetary terms is increasing rapidly and when a substantial portion of travelers are located near the indifference point between modes. Policymakers should therefore complement welfare weighting with targeted improvements in HSR service quality or traveler experience, especially in market segments where HSR's advantage is not yet remarkable. Otherwise, simply raising (α) may have muted or even counterproductive effects, such as simultaneous fare increases by both operators or a shift of demand back to AT. Using market analysis to identify traveler preference distributions and sensitivity is essential for maximizing the modal shift and consumer surplus gains from social welfare-driven policies.

5.2.3.4 How social welfare weighting in HSR impacts air and HSR profits

We differentiate the resulting profits of air and HSR systems, formulated in Eqs (5.28a)-(5.28b), with respect to α, and get the partial derivatives as follows:

$$\frac{\partial \pi_a^{SW}}{\partial \alpha} = \left[\frac{F(\tilde{x}^{SW}) M(\tilde{x}^{SW})}{f(\tilde{x}^{SW})} \left(\frac{M'(\tilde{x}^{SW})}{M(\tilde{x}^{SW})} - \frac{f'(\tilde{x}^{SW})}{f(\tilde{x}^{SW})} \right) + 2M\left(\tilde{x}^{SW}\right) + w_a''\left(q_a^{SW}\right) f\left(\tilde{x}^{SW}\right) \right] F\left(\tilde{x}^{SW}\right) \frac{\partial x^{SW}}{\partial \alpha}, \tag{5.33a}$$

$$\frac{\partial \pi_h^{SW}}{\partial \alpha} = \left[\frac{F(\tilde{x}^{SW}) M(\tilde{x}^{SW})}{f(\tilde{x}^{SW})} \left(\frac{M'(\tilde{x}^{SW})}{M(\tilde{x}^{SW})} - \frac{f'(\tilde{x}^{SW})}{f(\tilde{x}^{SW})} \right) + M\left(\tilde{x}^{SW}\right) + w_a''\left(q_a^{SW}\right) f\left(\tilde{x}^{SW}\right) + \frac{\alpha\left(c_o - c_h(\tilde{x}^{SW})\right) f(\tilde{x}^{SW})}{\left(D - F(\tilde{x}^{SW})\right)} \right] \left(D - F\left(\tilde{x}^{SW}\right)\right) \frac{\partial x^{SW}}{\partial \alpha}. \tag{5.33b}$$

We can further define a balance point for discussing the practical meaning from the derivatives:

$$\Pi_4 = -\frac{f\left(\tilde{x}^{SW}\right)}{F\left(\tilde{x}^{SW}\right)} \left[1 + \frac{w_a''\left(q_a^{SW}\right) f\left(\tilde{x}^{SW}\right)}{M\left(\tilde{x}^{SW}\right)} + \frac{\alpha\left(c_o - c_h\left(\tilde{x}^{SW}\right)\right)}{\alpha\left(c_o - c_h\left(\tilde{x}^{SW}\right)\right) + p_h^{SW*} - w_h'\left(n_h^{SW}\right)} \right]. \tag{5.34}$$

It is clear that $c_o - c_h\left(\tilde{x}^{SW}\right) \geq 0$. $p_h^{SW*} - w_h'\left(n_h^{SW}\right)$ can be interpreted as $\frac{\partial \pi_h^{SW}}{\partial n_h^{SW}}$, with its sign showing the phases of pricing strategy adjustments of HSR. When $\frac{\partial \pi_h^{SW}}{\partial n_h^{SW}} < 0$, HSR decides to sacrifice profit for pursuing higher social welfare in HSR system. Otherwise, $\frac{\partial \pi_h^{SW}}{\partial n_h^{SW}} > 0$ indicates that HSR decision makers improve profits to achieve the operational goal. In this study, we only discuss the cases where $p_h^{SW*} - w_h'\left(n_h^{SW}\right) > -\frac{1}{2}\alpha\left(c_o - c_h\left(\tilde{x}^{SW}\right)\right)$, i.e., we exclude the extreme case where a marginal increase of HSR demand will cause much higher marginal operating costs (under highly crowding in HSR system) than the marginal ticket revenue.

The condition $p_h^{SW*} - w_h'\left(n_h^{SW}\right) > 0$ is commonly observed in privately owned high-speed rail systems, where the primary objective is profit maximization. In contrast, in state-owned or public utility HSR systems, it is more likely that $p_h^{SW*} - w_h'\left(n_h^{SW}\right) < 0$ will hold. In these cases, the costs associated with constructing and operating high-speed rail are considerably higher and often exceed the revenue generated from ticket sales. This reflects the broader social and public service objectives that often motivate government investment in HSR, even when it is not immediately profitable from an operational standpoint.

When $p_h^{SW*} - w_h'\left(n_h^{SW}\right) > 0$, then $\Pi_3 < \Pi_4 < 0$. It also indicates that $\alpha\left(c_o - c_h\left(\tilde{x}^{SW}\right)\right) <$

$\frac{\left(D-F\left(\tilde{x}^{SW}\right)\right)}{f\left(\tilde{x}^{SW}\right)}M\left(\tilde{x}^{SW}\right)$, showing the narrow margin between the travel price of indifferent passengers and the maximum acceptable cost. The inequality also represents the lower intention for passengers to travel by either mode. Then, when $n_a^{SW} < \frac{n_h^{SW}}{(1-\alpha)}$, we can have that $\Pi_3 < \Pi_4 < 0 < \Pi_1$, while when $n_a^{SW} > \frac{n_h^{SW}}{(1-\alpha)}$, it can be inferred that $\Pi_1 < \Pi_3 < \Pi_4 < 0$. Otherwise, if $-\frac{1}{2}\alpha\left(c_o - c_h\left(\tilde{x}^{SW}\right)\right) < p_h^{SW*} - w_h'\left(n_h^{SW}\right) < 0$, we can derive $\Pi_4 < \Pi_3 < 0$. Furthermore, in this case, we can have that $\Pi_4 < \Pi_3 < 0 < \Pi_1$ when $n_a^{SW} < \frac{n_h^{SW}}{(1-\alpha)}$, while $\Pi_1 < \Pi_4 < \Pi_3 < 0$ when $n_a^{SW} > \frac{n_h^{SW}}{(1-\alpha)}$.

We use Table 5.2 to systematically summarize how increasing the weight on social welfare in the HSR system (α) affects both air and HSR profits under varying market regimes, market outcome conditions, and demand distributions. By systematically comparing different cases across various threshold conditions, several distinct patterns emerge regarding the impact of increasing the social welfare weight in the HSR system.

Table 5.2: Different cases about changes of pricing strategies and demand distribution

$p_h^{SW*} - w_h'\left(n_h^{SW}\right) > 0$			
Demand regime	**Conditions on Φ**	**Results of partial derivatives**	**Demand and profit changes**
$n_a^{SW} > \frac{n_h^{SW}}{(1-\alpha)}$	$\Phi > \Pi_4$	$\frac{\partial \tilde{x}^{SW}}{\partial \alpha} < 0$, $\frac{\partial \pi_a^{SW}}{\partial \alpha} < 0$, $\frac{\partial \pi_h^{SW}}{\partial \alpha} < 0$	Air demand ↓, HSR demand ↑, Air profit ↓, HSR profit ↓
	$\Pi_3 < \Phi < \Pi_4$	$\frac{\partial \tilde{x}^{SW}}{\partial \alpha} < 0$, $\frac{\partial \pi_a^{SW}}{\partial \alpha} < 0$, $\frac{\partial \pi_h^{SW}}{\partial \alpha} > 0$	Air demand ↓, HSR demand ↑, Air profit ↓, HSR profit ↑
	$\Pi_1 < \Phi < \Pi_3$	$\frac{\partial \tilde{x}^{SW}}{\partial \alpha} < 0$, $\frac{\partial \pi_a^{SW}}{\partial \alpha} > 0$, $\frac{\partial \pi_h^{SW}}{\partial \alpha} > 0$	Air demand ↓, HSR demand ↑, Air profit ↑, HSR profit ↑
	$\Phi < \Pi_1$	$\frac{\partial \tilde{x}^{SW}}{\partial \alpha} > 0$, $\frac{\partial \pi_a^{SW}}{\partial \alpha} < 0$, $\frac{\partial \pi_h^{SW}}{\partial \alpha} < 0$	Air demand ↑, HSR demand ↓, Air profit ↓, HSR profit ↓
$n_a^{SW} < \frac{n_h^{SW}}{(1-\alpha)}$	$\Phi > \Pi_1$	$\frac{\partial \tilde{x}^{SW}}{\partial \alpha} > 0$, $\frac{\partial \pi_a^{SW}}{\partial \alpha} > 0$, $\frac{\partial \pi_h^{SW}}{\partial \alpha} > 0$	Air demand ↑, HSR demand ↓, Air profit ↑, HSR profit ↑
	$\Pi_4 < \Phi < \Pi_1$	$\frac{\partial \tilde{x}^{SW}}{\partial \alpha} < 0$, $\frac{\partial \pi_a^{SW}}{\partial \alpha} < 0$, $\frac{\partial \pi_h^{SW}}{\partial \alpha} < 0$	Air demand ↓, HSR demand ↑, Air profit ↓, HSR profit ↓
	$\Pi_3 < \Phi < \Pi_4$	$\frac{\partial \tilde{x}^{SW}}{\partial \alpha} < 0$, $\frac{\partial \pi_a^{SW}}{\partial \alpha} < 0$, $\frac{\partial \pi_h^{SW}}{\partial \alpha} > 0$	Air demand ↓, HSR demand ↑, Air profit ↓, HSR profit ↑
	$\Phi < \Pi_3$	$\frac{\partial \tilde{x}^{SW}}{\partial \alpha} < 0$, $\frac{\partial \pi_a^{SW}}{\partial \alpha} > 0$, $\frac{\partial \pi_h^{SW}}{\partial \alpha} > 0$	Air demand ↓, HSR demand ↑, Air profit ↑, HSR profit ↑
$0 > p_h^{SW*} - w_h'\left(n_h^{SW}\right) > -\frac{1}{2}\alpha\left(c_o - c_h\left(\tilde{x}^{SW}\right)\right)$			
Demand regime	**Conditions on Φ**	**Results of partial derivatives**	**Demand and profit changes**
$n_a^{SW} > \frac{n_h^{SW}}{(1-\alpha)}$	$\Phi > \Pi_3$	$\frac{\partial \tilde{x}^{SW}}{\partial \alpha} < 0$, $\frac{\partial \pi_a^{SW}}{\partial \alpha} < 0$, $\frac{\partial \pi_h^{SW}}{\partial \alpha} < 0$	Air demand ↓, HSR demand ↑, Air profit ↓, HSR profit ↓
	$\Pi_4 < \Phi < \Pi_3$	$\frac{\partial \tilde{x}^{SW}}{\partial \alpha} < 0$, $\frac{\partial \pi_a^{SW}}{\partial \alpha} > 0$, $\frac{\partial \pi_h^{SW}}{\partial \alpha} < 0$	Air demand ↓, HSR demand ↑, Air profit ↑, HSR profit ↓
	$\Pi_1 < \Phi < \Pi_4$	$\frac{\partial \tilde{x}^{SW}}{\partial \alpha} < 0$, $\frac{\partial \pi_a^{SW}}{\partial \alpha} > 0$, $\frac{\partial \pi_h^{SW}}{\partial \alpha} > 0$	Air demand ↓, HSR demand ↑, Air profit ↑, HSR profit ↑
	$\Phi < \Pi_1$	$\frac{\partial \tilde{x}^{SW}}{\partial \alpha} > 0$, $\frac{\partial \pi_a^{SW}}{\partial \alpha} < 0$, $\frac{\partial \pi_h^{SW}}{\partial \alpha} < 0$	Air demand ↑, HSR demand ↓, Air profit ↓, HSR profit ↓
$n_a^{SW} < \frac{n_h^{SW}}{(1-\alpha)}$	$\Phi > \Pi_1$	$\frac{\partial \tilde{x}^{SW}}{\partial \alpha} > 0$, $\frac{\partial \pi_a^{SW}}{\partial \alpha} > 0$, $\frac{\partial \pi_h^{SW}}{\partial \alpha} > 0$	Air demand ↑, HSR demand ↓, Air profit ↑, HSR profit ↑
	$\Pi_3 < \Phi < \Pi_1$	$\frac{\partial \tilde{x}^{SW}}{\partial \alpha} < 0$, $\frac{\partial \pi_a^{SW}}{\partial \alpha} < 0$, $\frac{\partial \pi_h^{SW}}{\partial \alpha} < 0$	Air demand ↓, HSR demand ↑, Air profit ↓, HSR profit ↓
	$\Pi_4 < \Phi < \Pi_3$	$\frac{\partial \tilde{x}^{SW}}{\partial \alpha} < 0$, $\frac{\partial \pi_a^{SW}}{\partial \alpha} > 0$, $\frac{\partial \pi_h^{SW}}{\partial \alpha} < 0$	Air demand ↓, HSR demand ↑, Air profit ↑, HSR profit ↓
	$\Phi < \Pi_4$	$\frac{\partial \tilde{x}^{SW}}{\partial \alpha} < 0$, $\frac{\partial \pi_a^{SW}}{\partial \alpha} > 0$, $\frac{\partial \pi_h^{SW}}{\partial \alpha} > 0$	Air demand ↓, HSR demand ↑, Air profit ↑, HSR profit ↑

Proposition 7. *In a relatively* ***balanced*** *market, specifically, $n_a^{SW} < \frac{n_h^{SW}}{(1-\alpha)}$, increasing the weight placed on social welfare can lead to profit* ***increases*** *for both air and HSR operators, when either the strong HSR marginal non-monetary advantage or travelers' high sensitivity to this advantage presents, specifically, $\Phi > \Pi_1$ or $\Phi < \Pi_3$ when $p_h^{SW*} - w_h'(n_h^{SW}) > 0$ or $\Phi < \Pi_4$ when $0 > p_h^{SW*} - w_h'(n_h^{SW}) > -\frac{1}{2}\alpha(c_o - c_h(\tilde{x}^{SW}))$.*

Proof. We can derive $\frac{\partial \pi_a^{SW}}{\partial \alpha} > 0$ and $\frac{\partial \pi_h^{SW}}{\partial \alpha} > 0$, i.e., both air profit and HSR profit increase, given one of the following conditions holds:

- The HSR marginal non-monetary advantage is strong and travelers are relatively insensitive to this benefit, i.e., $\Phi > \Pi_1$; or

- The HSR marginal non-monetary advantage is weak and travelers are highly sensitive to this benefit, i.e.,
  - $\Phi < \Pi_3$ when $p_h^{SW*} - w_h'(n_h^{SW}) > 0$, or
  - $\Phi < \Pi_4$ when $0 > p_h^{SW*} - w_h'(n_h^{SW}) > -\frac{1}{2}\alpha(c_o - c_h(\tilde{x}^{SW}))$.

$\square$

Proposition 8. *In an **air-dominant** market, $n_a^{SW} > \frac{n_h^{SW}}{(1-\alpha)}$, increasing the weight placed on social welfare can lead to profit **decreases** for both air and HSR operators, when either the strong HSR marginal non-monetary advantage or travelers' high sensitivity to this advantage presents, specifically, $\Phi < \Pi_1$, or $\Phi > \Pi_4$ when $p_h^{SW*} - w_h'(n_h^{SW}) > 0$, or $\Phi > \Pi_3$ when $0 > p_h^{SW*} - w_h'(n_h^{SW}) > -\frac{1}{2}\alpha(c_o - c_h(\tilde{x}^{SW}))$.*

Proof. We can derive $\frac{\partial \pi_a^{SW}}{\partial \alpha} < 0$ and $\frac{\partial \pi_h^{SW}}{\partial \alpha} < 0$, i.e., both air profit and HSR profit increase, given one of the following conditions holds:

- The HSR marginal non-monetary advantage is strong and travelers are relatively insensitive to this benefit, i.e., $\Phi < \Pi_1$; or
- The HSR marginal non-monetary advantage is weak and travelers are highly sensitive to this benefit, i.e.,
  - $\Phi > \Pi_4$ when $p_h^{SW*} - w_h'(n_h^{SW}) > 0$, or
  - $\Phi > \Pi_3$ when $0 > p_h^{SW*} - w_h'(n_h^{SW}) > -\frac{1}{2}\alpha(c_o - c_h(\tilde{x}^{SW}))$.

$\square$

Proposition 9. *In an air-dominant market where $n_a^{SW} < \frac{n_h^{SW}}{(1-\alpha)}$, a higher density of neutral travelers at the point of indifference, i.e., higher $\frac{f'(\tilde{x}^{SW})}{f(\tilde{x}^{SW})}$, making $\Phi < \Pi_1$, is crucial for HSR to attract demand from the air mode. Conversely, in a market with a relatively balanced demand distribution, i.e., $n_a^{SW} > \frac{n_h^{SW}}{(1-\alpha)}$, greater sensitivity of travelers to the marginal non-monetary advantage of HSR becomes the key factor in shifting demand from air to HSR, specifically, higher $\frac{M'(\tilde{x}^{SW})}{M(\tilde{x}^{SW})}$ making $\Phi > \Pi_1$ when $p_h^{SW*} - w_h'(n_h^{SW}) > 0$ or $\Phi > \Pi_3$ when $0 > p_h^{SW*} - w_h'\left(n_h^{SW}\right) > -\frac{1}{2}\alpha\left(c_o - c_h\left(\tilde{x}^{SW}\right)\right)$.*

Proof. We can derive $\frac{\partial \tilde{x}^{SW}}{\partial \alpha} < 0$, i.e., the HSR demand increases while air demand decreases, given that one of the following conditions holds:

- $n_a^{SW} < \frac{n_h^{SW}}{(1-\alpha)}$ and $\Phi < \Pi_1$; or
- $n_a^{SW} > \frac{n_h^{SW}}{(1-\alpha)}$ and either of the following conditions:
  - $\Phi > \Pi_1$ when $p_h^{SW*} - w_h'(n_h^{SW}) > 0$; or
  - $\Phi > \Pi_3$ when $0 > p_h^{SW*} - w_h'\left(n_h^{SW}\right) > -\frac{1}{2}\alpha\left(c_o - c_h\left(\tilde{x}^{SW}\right)\right)$.

□

Propositions 7, 8 and 9 highlight two critical factors influencing demand shifts and profit outcomes for air and HSR modes: a sufficiently strong HSR marginal non-monetary advantage and high traveler sensitivity to this advantage. In a relatively balanced market where the number of air passengers does not significantly exceed that of HSR passengers, if these two factors are not simultaneously present (i.e., if Φ exceeds the upper threshold or falls below the lower threshold), an increased emphasis on HSR social welfare prompts both air and HSR operators to raise ticket prices and target their core customer base. This relaxation of competitive pressure leads to profit increases for both modes. Conversely, in an air-dominant market where air demand far surpasses that of HSR, a greater weight on HSR social welfare intensifies price competition, driving down HSR ticket prices and, in response, air ticket prices as well. This escalated competition ultimately results in reduced profits for both operators.

Proposition 10. *When the difference between the relative rate of change of the HSR marginal non-monetary advantage, $\frac{M'(x^{SW})}{M(x^{SW})}$, and the relative rate of change of traveler density at the indifferent preference point, $\frac{f'(x^{SW})}{f(x^{SW})}$, lies between Π_3 and Π_4, the effect of increasing the weight placed on HSR social welfare depends on the level of the HSR ticket price:*

- *If the HSR ticket price is relatively high ($p_h^{SW*} - w_h'(n_h^{SW}) > 0$): Increasing the social welfare weight for HSR will reduce air profit and increase HSR profit.*

- *If the HSR ticket price is relatively low ($0 > p_h^{SW*} - w_h'(n_h^{SW}) > -\frac{1}{2}\alpha(c_o - c_h(\tilde{x}^{SW}))$): Increasing the social welfare weight for HSR will increase air profit and decrease HSR profit.*

Proof. It follows that $\frac{\partial \pi_a^{SW}}{\partial \alpha} < 0$ and $\frac{\partial \pi_h^{SW}}{\partial \alpha} > 0$ whenever $\Pi_3 < \Phi < \Pi_4$, provided the HSR ticket price satisfies $p_h^{SW*} - w_h'(n_h^{SW}) > 0$, regardless of whether the market is demand-balanced or air-dominant. Conversely, if $0 > p_h^{SW*} - w_h'(n_h^{SW}) > -\frac{1}{2}\alpha\left(c_o - c_h(\tilde{x}^{SW})\right)$ and $\Pi_4 < \Phi < \Pi_3$, we have $\frac{\partial \pi_a^{SW}}{\partial \alpha} > 0$ and $\frac{\partial \pi_h^{SW}}{\partial \alpha} < 0$, again irrespective of the market demand structure. □

Proposition 11. *When the demand distribution in the market is relatively **balanced**, i.e., $n_a^{SW} < \frac{n_h^{SW}}{(1-\alpha)}$, a smaller difference between the relative rate of change of the HSR marginal non-monetary advantage, $\frac{M'(x^{SW})}{M(x^{SW})}$, and the relative rate of change of traveler density at the indifferent preference point, $\frac{f'(x^{SW})}{f(x^{SW})}$, implies that the increasing weight on the HSR social welfare will lead to profit **decrease** of both air and HSR. Specifically, the small difference makes $\Pi_4 < \Phi < \Pi_1$ when $p_h^{SW*} - w_h'(n_h^{SW}) > 0$ or $\Pi_3 < \Phi < \Pi_1$ when $0 > p_h^{SW*} - w_h'\left(n_h^{SW}\right) > -\frac{1}{2}\alpha\left(c_o - c_h\left(\tilde{x}^{SW}\right)\right)$.*

Proof. We can derive that $\frac{\partial \pi_a^{SW}}{\partial \alpha} < 0$ and $\frac{\partial \pi_h^{SW}}{\partial \alpha} < 0$ when either of the following conditions is satisfied:

- $\Pi_4 < \Phi < \Pi_1$ when $p_h^{SW*} - w_h'(n_h^{SW}) > 0$; or
- $\Pi_3 < \Phi < \Pi_1$ when $0 > p_h^{SW*} - w_h'\left(n_h^{SW}\right) > -\frac{1}{2}\alpha\left(c_o - c_h\left(\tilde{x}^{SW}\right)\right)$.

□

Proposition 12. *In an **air-dominant** market, where $n_a^{SW} < \frac{n_h^{SW}}{1-\alpha}$, a smaller difference between the relative rate of change of the HSR marginal non-monetary advantage, $\frac{M'(x^{SW})}{M(x^{SW})}$, and the relative rate of change of traveler density at the indifferent preference point, $\frac{f'(x^{SW})}{f(x^{SW})}$, fosters favorable profit outcomes for both modes. Specifically, when $\Pi_1 < \Phi < \Pi_3$ and the HSR ticket price satisfies $p_h^{SW*} - w_h'(n_h^{SW}) > 0$, or when $\Pi_1 < \Phi < \Pi_4$ and $0 > p_h^{SW*} - w_h'(n_h^{SW}) > -\frac{1}{2}\alpha\left(c_o - c_h(\tilde{x}^{SW})\right)$, increasing the weight placed on HSR social welfare will lead to a profit **increase** for both air and HSR operators.*

Proof. We can derive that $\frac{\partial \pi_a^{SW}}{\partial \alpha} > 0$ and $\frac{\partial \pi_h^{SW}}{\partial \alpha} > 0$ when either of the following conditions is satisfied:

- $\Pi_1 < \Phi < \Pi_3$ when $p_h^{SW*} - w_h'(n_h^{SW}) > 0$; or
- $\Pi_1 < \Phi < \Pi_4$ when $0 > p_h^{SW*} - w_h'\left(n_h^{SW}\right) > -\frac{1}{2}\alpha\left(c_o - c_h\left(\tilde{x}^{SW}\right)\right)$,

□

In the transitional zones, where Φ lies between the minimum and maximum thresholds, indicating a balance between HSR's service advantage and a significant presence of neutral travelers increasing the weight on HSR social welfare consistently drives demand from air to HSR, regardless of the prevailing demand regime. The impact on profits, however, depends on the ownership and operational objectives of the HSR system. If the HSR system is privately owned and profit-oriented ($p_h^{SW*} - w_h'\left(n_h^{SW}\right) > 0$), its profits are more likely to rise with increased welfare weighting. In contrast, when HSR operates as a state-owned, welfare-maximizing utility and the marginal cost is close to or slightly exceeds marginal revenue ($0 > p_h^{SW*} - w_h'\left(n_h^{SW}\right) > -\frac{1}{2}\alpha\left(c_o - c_h\left(\tilde{x}^{SW}\right)\right)$), air profit is more likely to increase due to softened competition as HSR prioritizes public service over profitability.

The above analysis provides several important insights for policymakers, regulators, and transport operators regarding how social welfare weighting in HSR affects market outcomes. Firstly, policy effectiveness depends on market structure. Increasing the social welfare weight in HSR's objective function does not guarantee universally positive outcomes. Its effectiveness is highly sensitive to the distribution of passenger preferences and the relative competitiveness of HSR versus air. Transport policies are most impactful when there is a substantial group of "swing" travelers who are open to switching modes in response to price or service changes and enough service advantages of HSR compared to air services. Secondly, the direction and magnitude of demand shifts and profit changes depend on whether the market regime is air-dominant or HSR-dominant, and whether HSR's marginal advantage is strong or weak. For example, in an air-dominant market with HSR holding a clear advantage, raising the welfare weight can intensify competition and reduce profits for both modes.

Conversely, under certain conditions, such as a dominant HSR market, both operators can experience profit increases as the competitive pressure moderates. Thirdly, the ownership and operational objectives of the HSR system significantly shape the profit outcomes. Privately owned HSR systems are more likely to benefit from increased welfare weighting when they can serve additional demand at a profit. In contrast, state-owned, welfare-oriented HSR systems may prioritize accessibility over profitability, which can soften competition and allow air operators to maintain or even increase their profits. Given the insights derived from the analysis, policymakers should ensures that social objectives, such as increased modal shift to HSR or greater public accessibility, are met without inadvertently undermining the financial sustainability of the transport systems involved based on the actual distribution of traveler preferences and the cost structures of each mode.

5.2.4 Analytical example with uniform preference distribution of travelers

5.2.4.1 Basic settings

In this section, we consider the potential travelers are distributed uniformly across the preference range $[0, 1]$ with identical density of traveler per unit of length. Then we assume the functions related to travel price formulation and profit calculation are linear and derive the corresponding results about pricing and profits. The settings applied in this section are summarised as Table. 5.3.

Table 5.3: Assumed functions in the analytical example

Functions	**Specifications**
Differential function	$f(x) = D$
Cumulative function	$F(x) = Dx$
Dissonance function	$d_a(x) = \omega_a x$, $d_h(1-x) = \omega_h(1-x)$
Crowding cost function	$\kappa_a(x) = \mu_a Dx/m_a$, $\kappa_h(x) = \mu_h(D - Dx)/m_h$
Operating cost function	$w_a(q_a) = \theta_a n_a/m_a = \theta_a D\tilde{x}/m_a$, $w_h(q_h) = \theta_h n_h/m_h = \theta_h D(1-\tilde{x})/m_h$

In Table 5.3, ω_a and ω_h, μ_a, μ_h, θ_a, θ_h are assumed to be constants. Capacities of air and HSR systems are considered to be given exogenously, i.e., m_a and m_h are taken as constants. Therefore, the capacity maintaining costs of the two modes are assumed to be fixed, noted as G_a and G_h. By substituting the above assumed functions into travel price formulation defined in Eq. (5.2) and Eq. (5.3), the preference of HSR of the indifferent travelers can be formulated as

$$\tilde{x}_u = \frac{\frac{\mu_h}{m_h} D + p_h - p_a + \omega_h}{(\omega_a + \omega_h) + D\left(\frac{\mu_a}{m_a} + \frac{\mu_h}{m_h}\right)}. \tag{5.35}$$

The above equation shows that the demand distribution across the two modes depends on (i) Price difference $p_a - p_h$: higher HSR prices shift more passengers to air, and vice versa; (ii) Dissatisfaction parameters (ω_a, ω_h): If passengers strongly prefer one mode, they are less sensitive to price differences; and (iii) Crowding costs (μ_a, μ_h): If congestion costs increase for one mode, more passengers switch to the alternative mode.

5.2.4.2 Pricing strategies of the two modes

Assuming a uniform distribution of travelers' preference, we use $p_{a,u}^{RM*}$ and $p_{h,u}^{RM*}$ to represent the optimal ticket prices for Air travel and HSR travel when both modes maximize their profits. The formulations of the above prices are shown as:

$$p_{a,u}^{RM*} = \frac{1}{3}\left((\omega_a + 2\omega_h) + \left(\frac{\mu_a}{m_a} + 2\frac{\mu_h}{m_h}\right) D + 2\frac{\theta_a}{m_a} + \frac{\theta_h}{m_h}\right), \tag{5.36a}$$

$$p_{h,u}^{RM*} = \frac{1}{3}\left((2\omega_a + \omega_h) + \left(2\frac{\mu_a}{m_a} + \frac{\mu_h}{m_h}\right) D + \frac{\theta_a}{m_a} + 2\frac{\theta_h}{m_h}\right). \tag{5.36b}$$

Here, ω_a and ω_h represent travelers' loyalty to air travel and HSR, respectively. The parameters μ_a and μ_h denote the marginal increase in crowding costs during travel, reflecting travelers' sensitivity to congestion. Similarly, θ_a and θ_h capture the marginal increase in operating costs due to higher occupancy rates resulting from increased demand, indicating the operators' capacity to manage congestion.

Several observations can be concluded. If travelers have a stronger preference for air travel ($\omega_a > \omega_h$), the optimal air price is higher than the HSR price, allowing airlines to capture more revenue from loyal customers. Conversely, if travelers prefer HSR more ($\omega_h > \omega_a$), HSR can set a higher price without losing much demand. Given that air travel experiences higher congestion costs ($\mu_a > \mu_h$), airlines must raise prices to manage demand and maintain profitability. Conversely, when HSR has lower crowding costs, it can keep prices lower, gaining a competitive advantage. The operating costs per unit of capacity (θ_a/m_a and θ_h/m_h) directly determine pricing. Airlines must charge more to remain profitable if air travel has higher operating costs.

Taking the first-order derivatives of $p_{a,u}^{RM*}$ and $p_{h,u}^{RM*}$ with respect to the related variables gives:

$$\frac{\partial p_{a,u}^{RM*}}{\partial \omega_a} = \frac{\partial p_{h,u}^{RM*}}{\partial \omega_h} = \frac{1}{3} = \frac{1}{2}\frac{\partial p_{h,u}^{RM*}}{\partial \omega_a} = \frac{1}{2}\frac{\partial p_{a,u}^{RM*}}{\partial \omega_h}, \tag{5.37}$$

$$\frac{\partial p_{a,u}^{RM*}}{\partial \mu_a} = \frac{1}{3m_a} = \frac{1}{2}\frac{\partial p_{h,u}^{RM*}}{\partial \mu_a}, \tag{5.38}$$

$$\frac{\partial p_{h,u}^{RM*}}{\partial \mu_h} = \frac{1}{3m_h} = \frac{1}{2}\frac{\partial p_{a,u}^{RM*}}{\partial \mu_h}, \tag{5.39}$$

$$\frac{\partial p_{a,u}^{RM*}}{\partial \theta_a} = \frac{2}{3m_a} = 2\frac{\partial p_{h,u}^{RM*}}{\partial \theta_a}, \tag{5.40}$$

$$\frac{\partial p_{h,u}^{RM*}}{\partial \theta_h} = \frac{2}{3m_h} = 2\frac{\partial p_{a,u}^{RM*}}{\partial \theta_h}. \tag{5.41}$$

The above results indicate that traveler's preferences and sensitivity to crowding affect the alternative mode more strongly, while their own operating costs have a stronger impact on pricing. Specifically, the impact of travelers' preference and sensitivity to the crowding for one mode on its own price is half that on the competing mode. For example, if passengers become more loyal to air travel (ω_a increases) or more sensitive to the crowding (μ_a increases), the HSR price decreases twice as much as the air price increases. Besides, the effect of a mode's operating cost on its own price is twice that on the competing mode. For example, if airline operating costs θ_a increase, air fares increase twice as much as HSR fares.

The optimal ticket prices of the two competitive modes (noted as $p_{h,u}^{SW*}$ and $p_{a,u}^{SW*}$) when HSR maximize a weighted sum of both its profit and social welfare in HSR system are formulated as follows:

$$p_{h,u}^{SW*} = \frac{1}{\frac{3}{2} - \left(1 - \frac{1}{2}k\right)\alpha}\left(-\alpha\left(c_o - kA\right) + A + \frac{\theta_h}{m_h}\right), \tag{5.42a}$$

$$p_{a,u}^{SW*} = \frac{1}{2}\left(\frac{\mu_h}{m_h}D + \frac{-\alpha\left(c_o - kA\right) + A + \frac{\theta_h}{m_h}}{\frac{3}{2} - \left(1 - \frac{1}{2}k\right)\alpha} + \omega_h + \frac{\theta_a}{m_a}\right), \tag{5.42b}$$

where

$$k = \frac{\left(\omega_h + \frac{\mu_h D}{m_h}\right)}{\left(\omega_a + \omega_h\right) + D\left(\frac{\mu_a}{m_a} + \frac{\mu_h}{m_h}\right)}, \tag{5.43}$$

$$A = \omega_a + \frac{\mu_a}{m_a}D + \frac{1}{2}\left(\frac{\mu_h}{m_h}D + \omega_h + \frac{\theta_a}{m_a}\right), \tag{5.44}$$

where $k \in (0,1)$ represents the relative weight of HSR preference and congestion costs compared to the total impact of both modes. Then we can derive the formulation of air and HSR profit as follows:

$$\pi_{a,u}^{SW} = \left(p_a^{SW*} - \frac{\theta_a}{m_a}\right) D\tilde{x}_u^{SW}, \tag{5.45a}$$

$$\pi_{h,u}^{SW} = \left(p_h^{SW*} - \frac{\theta_h}{m_h}\right) D\left(1 - \tilde{x}_u^{SW}\right). \tag{5.45b}$$

The first-order partial derivatives of $\tilde{x}_u^{SW*}$, $p_{h,u}^{SW*}$, $p_{a,u}^{SW*}$, and with respect to α can be calculated as:

$$\frac{\partial p_{h,u}^{SW*}}{\partial \alpha} = -\frac{1}{\left(\frac{3}{2} - \left(1 - \frac{1}{2}k\right)\alpha\right)^2}\left[\frac{3}{2}c_o - (k+1)\left(\omega_a + \frac{\mu_a}{m_a}D + \frac{1}{2}\left(\frac{\mu_h}{m_h}D + \omega_h + \frac{\theta_a}{m_a}\right)\right) - \left(1 - \frac{1}{2}k\right)\frac{\theta_h}{m_h}\right], \tag{5.46}$$

$$\frac{\partial p_{a,u}^{SW*}}{\partial \alpha} = \frac{1}{2}\frac{\partial p_{h,u}^{SW*}}{\partial \alpha} \tag{5.47}$$

$$\frac{\partial \tilde{x}_u^{SW}}{\partial \alpha} = \frac{\frac{1}{2}\frac{\partial p_{h,u}^{SW*}}{\partial \alpha}}{\omega_a + \omega_h + D\left(\frac{\mu_a}{m_a} + \frac{\mu_h}{m_h}\right)} \tag{5.48}$$

It is clear that when

$$c_0 > \frac{2}{3}(k+1)\left(\omega_a + \frac{\mu_a}{m_a}D + \frac{1}{2}\left(\frac{\mu_h}{m_h}D + \omega_h + \frac{\theta_a}{m_a}\right)\right) - \left(\frac{2}{3} - \frac{1}{3}k\right)\frac{\theta_h}{m_h}, \tag{5.49}$$

we can have $\frac{\partial p_{h,u}^{SW*}}{\partial \alpha} < 0$, $\frac{\partial \tilde{x}_u^{SW}}{\partial \alpha} < 0$ and $\frac{\partial p_{a,u}^{SW*}}{\partial \alpha} < 0$. Therefore, given the assumed uniform distribution of travelers' mode preference, when the maximum acceptable travel cost is large enough, specifically, satisfy the condition defined in Eq. (5.49), the demands shift from air to HSR. Both the optimal ticket prices of air travel and HSR travel decreases if a bigger weight is put on the welfare in HSR system. Even though air and HSR both reduce prices, HSR prices decrease more significantly due to its welfare-oriented considerations.

The above analysis on how the weight assigned to welfare in the HSR system affects optimal pricing aligns with the findings in Yang & Zhang (2012). In their study, it is also demonstrated that prices decrease as the emphasis on welfare increases, under an assumption about the value range of gross benefits. This assumption can be interpreted as analogous to the condition of maximum acceptable cost defined in Eq. (5.49) in our study.

Then the partial derivatives of air and HSR profit with respect to α can be formulated as:

$$\frac{\partial \pi_{a,u}^{SW}}{\partial \alpha} = D\left[\tilde{x}_u^{SW} + \frac{\left(p_a^{SW*} - \frac{\theta_a}{m_a}\right)}{\omega_a + \omega_h + D\left(\frac{\mu_a}{m_a} + \frac{\mu_h}{m_h}\right)}\right]\frac{\partial p_a^{SW*}}{\partial \alpha} \tag{5.50a}$$

$$\frac{\partial \pi_{h,u}^{SW}}{\partial \alpha} = \frac{D}{\omega_a+\omega_h+D\left(\frac{\mu_a}{m_a}+\frac{\mu_h}{m_h}\right)}\left(\frac{\mu_a}{m_a}D + \omega_a + \frac{1}{2}\frac{\theta_h}{m_h} + \frac{1}{2}\frac{\mu_h}{m_h}D + \frac{1}{2}\omega_h + \frac{1}{2}\frac{\theta_a}{m_a} - p_h^{SW*}\right)\frac{\partial p_h^{SW*}}{\partial \alpha} \tag{5.50b}$$

It is clear that, under the condition specified in Eq. (5.49), air operator profit and air ticket price move in tandem whenever $p_a^{SW*} > \frac{\theta_a}{m_a}$. This relationship is fundamental, as it reflects that positive pricing power. Thus, positive profit requires ticket prices to cover at least the marginal cost per unit demand. This condition should always be satisfied in any viable AT operation.

Turning to the HSR system, the effect of increasing the social welfare weight (α) on HSR profit can be interpreted through two complementary perspectives. First, when Eq. (5.49) holds and the HSR ticket price is relatively low, specifically satisfying the threshold in the condition

$$p_{h,u}^{SW*} < \frac{\mu_a}{m_a}D + \omega_a + \frac{1}{2}\frac{\theta_h}{m_h} + \frac{1}{2}\frac{\mu_h}{m_h}D + \frac{1}{2}\omega_h + \frac{1}{2}\frac{\theta_a}{m_a}, \tag{5.51}$$

raising the social welfare weight leads to further price reductions. This boosts consumer surplus for travelers but reduces the HSR operator's profit, illustrating the expected trade-off between HSR welfare objectives and financial sustainability. In this regime, HSR is effectively transferring HSR operator surplus to HSR passengers by pursuing affordability and higher ridership.

On the other hand, if the HSR ticket price exceeds the threshold in Eq. (5.51), the system enters a regime where lowering HSR fares (i.e., further increasing the social welfare weight) actually increases profitability. This counterintuitive result arises because the market is sufficiently robust, either due to higher base demand, favorable cost structures, or price inelasticity among potential HSR users, such that fare reductions stimulate enough additional demand to offset the lost revenue per ticket.

A deeper understanding comes from reformulating the condition for profitability, as shown in Eq.(5.52). Here, when the baseline travel intention (i.e., the maximum acceptable travel price c_0) is sufficiently high to satisfy both Eq.(5.49) and Eq. (5.52), increasing the social welfare weight in HSR leads to lower profits. This scenario characterizes a market where demand is so strong (or the trip is more compulsory) that further price reductions (motivated by welfare objectives) primarily weaken margins without generating enough incremental demand to compensate for the lost revenue.

$$c_o > \left(\left(1 + \frac{1}{2}k\right) - \frac{1}{2\alpha}\right)\left(\omega_a + \frac{\mu_a}{m_a}D + \frac{1}{2}\left(\frac{\mu_h}{m_h}D + \omega_h + \frac{\theta_a}{m_a}\right)\right) + \frac{1}{2}\left(1 + \frac{1}{2\alpha} - \frac{1}{2}k\right)\frac{\theta_h}{m_h} \tag{5.52}$$

In summary, the relationship between ticket pricing, profit, and social welfare weight in HSR is highly context-dependent. Effective policy must be responsive to market conditions and grounded in rigorous analysis of both demand and cost dynamics to achieve an optimal balance between public benefit and operator viability.

5.3 Numerical studies

5.3.1 Numerical setting

In this section, we conduct a numerical experiment to evaluate air and HSR demand, profitability, and overall social welfare under different distributions of passengers' mode preferences. We select Hong Kong and Shanghai as the origin and destination cities due to Shanghai's status as an international metropolis with numerous tourist attractions and a rich cultural heritage, making it a highly attractive destination for travelers from Hong Kong. Potential travelers between these two cities have two primary transport options: (i) Traveling by

HSR from Hong Kong's West Kowloon Station to Shanghai Hongqiao Station and (ii) Traveling by air from Hong Kong International Airport to either Shanghai Pudong International Airport or Shanghai Hongqiao International Airport.

To model the air travel market, we refer to flight schedules available on the Qunar website, which indicate that approximately 30 daily flights operate between Hong Kong and Shanghai, provided by multiple airlines. The majority of these flights utilize Airbus 330 and Airbus 320 aircraft, with economy fares ranging between 1,000 and 2,000 CNY. Given this pricing range, we set the airfare in our experiment at 1,500 CNY ($p_a = 1500$) and assume 2,000 available seats ($m_a = 2000$) based on an arbitrary but reasonable approximation of airline capacity. Similarly, for HSR services, we rely on train schedules from the official Chinese railway ticketing platform, 12306. Two Fuxing high-speed trains, G100 and G900, operate daily between Hong Kong and Shanghai, with second-class fares set at 951 CNY and 800 CNY, respectively. The travel times for these services are 8 hours and 6 minutes and 10 hours and 55 minutes, respectively. The 8-car Fuxing train, which is commonly used on this route, accommodates 1,023 second-class seats per train. Based on this information, we approximate the total available HSR capacity as 2,000 seats ($m_h = 2000$) and set an average ticket price of 850 CNY ($p_h = 850$).

To estimate demand, we reference statistical data[2], which indicates that from January 14 to January 24, 2025, cross-border passenger traffic from mainland China to Hong Kong reached 1.002 million, with a daily average of 91,000 passengers. Notably, 66.1% of these passengers travelled between Hong Kong and cities within Guangdong province, meaning they are unlikely to consider air travel as a viable alternative. Excluding these short-haul travelers, we focus on middle-haul passengers, who represent a fraction of the total cross-border traffic. Due to the lack of publicly available passenger flow data for this specific OD pair (Hong Kong–Shanghai), we estimate total demand at 3,000 passengers ($D = 3000$) based on proportional analysis and reasonable judgment.

Airlines typically provide baggage handling services, ensuring that even on flights with high occupancy rates, passengers experience minimal discomfort. In contrast, high-speed rail

[2]The report is published on the website: `https://www.dutenews.com/n/article/8660295`

(HSR) passengers often face space constraints due to limited baggage storage areas at the ends of train cars. Additionally, overhead bins have size restrictions, and when luggage racks are full, passengers must place oversized baggage in front of their seats, reducing their space and causing discomfort. As a result, the discomfort of HSR passengers increases significantly with higher occupancy rates. In contrast, air passengers are less affected by crowding, as their baggage can be managed separately, reducing space-related inconveniences. To accurately reflect these differences, we define different crowding cost functions for HSR and air passengers, incorporating distinct parameters to capture the varying rates at which discomfort increases with seat occupancy. Specifically, we define the crowding cost functions as $\kappa_a = 400\,(n_a/m_a)$ for air passengers and $\kappa_h = 600\,(n_a/m_a)$ for HSR passengers.

The disutility parameters in the dissonance functions represent the inconvenience experienced by travelers when they cannot use their preferred mode of transport. This reflects their loyalty to a particular travel mode. In this study, we model travelers' heterogeneous mode preferences as a distribution along a preference axis ranging from 0 to 1, where 0 represents HSR preference and 1 represents AT preference. The closer a traveler's position is to either end of the axis, the stronger their loyalty to the corresponding mode. Since travelers' positions on this axis inherently indicate their loyalty and mode preference, we do not analyze the impact of specific dissonance function parameters or functional forms on numerical results. Instead, our focus is on how the distribution of travelers' preferences influences these results. For simplicity, we represent dissonance functions for both air and HSR passengers using linear functions with identical parameters. Similar linear functions have been applied in the literature (Yang & Zhang, 2012; Wang et al., 2020b).

The disutility parameter is chosen based on the assumption that dissonance should constitute a meaningful but not overwhelming portion of total travel costs. This ensures that while dissonance affects mode choice, it does not entirely determine traveler behaviour. Other factors, such as ticket prices and congestion discomfort, are not explicitly incorporated into the dissonance function but are acknowledged as additional influences on mode choice. Specifically, the dissonance functions for air passengers and HSR passengers are defined as $d_a(x) = 400x$ and $d_h(x) = 400\,(1 - x)$, respectively.

In Section 5.2.1.2, we define the operating cost of a transport system as a function of the occupancy rate, aligning with the prevailing definition in the literature. Specifically, operating costs increase with rising demand and decrease as traffic capacity expands. To keep consistent with the previous analytical example, we assume linear operating cost functions for both air and HSR systems, expressed as $w_a(n_a, m_a) = 100000(n_a/m_a)$ and $w_a(n_a, m_a) = 80000(n_a/m_a)$. The difference in the coefficients in the function accounts for the fact that airplanes and high-speed trains offer different services to passengers. For example, most flights provide in-flight meals, whereas high-speed trains rarely offer such services.

In our study, the unit seat costs for air and HSR are set at 200 CNY and 150 CNY, respectively. These unit costs are influenced by multiple factors, and accurately incorporating initial investment costs into the unit cost is challenging. Therefore, in defining the maintenance cost functions, we follow numerical settings about unit costs per seat for air travel and HSR utilized in Yang & Zhang (2012). Yang & Zhang (2012) also noted that the fixed cost of operating an HSR train is higher than that of running a flight. However, our study does not consider the initial investment costs of air and HSR systems, as we focus on scenarios where both flight and HSR schedules are already established and remain unchanged. By assuming a fixed service schedule, our analysis isolates the impact of ticket pricing and traveler preferences on demand, profitability, and social welfare without the confounding effects of infrastructure investment decisions.

The differential function $f(x)$ is expected to incorporate not only travelers' subjective preferences for travel modes but also other factors influencing their mode choices, such as onboard time, access time, and level of comfort. Furthermore, we conduct a sensitivity analysis to examine the impact of system parameters on the optimal ticket prices for both modes, travelers' choices, and the profitability of AT and HSR. For the initial numerical experiment, the parameter and function settings are summarized in Table 5.4.

Table 5.4: Summary of numerical settings

Parameters and functions	Specifications
Airfare between the studied OD pair	$p_a = 1500$
Price of HSR ticket for the OD pair	Two considered values, i.e., $p_h = 850$ and $p_h = 951$
Total potential demand between the OD pair	$D = 3000$
Maximum seats provided by the AT system	$m_a = 2000$
Maximum seats can be provided by the HSR system	$m_h = 2000$
Crowding cost of travelers with preference x	$\kappa_a\left(\frac{n_a}{m_a}\right) = 400\left(\frac{n_a}{m_a}\right)$, $\kappa_h\left(\frac{n_h}{m_h}\right) = 600\left(\frac{n_h}{m_h}\right)$
Operating costs of travel mode i	$w_a\left(\frac{n_a}{m_a}\right) = 100000\left(\frac{n_a}{m_a}\right)$, $w_h\left(\frac{n_h}{m_h}\right) = 80000\left(\frac{n_h}{m_h}\right)$
Maintaining cost for reserving transporting capacity	$g_a(m_a) = 200m_a$, $g_h(m_h) = 150m_a$
Dissonance function of passengers with preference x for HSR	$d_a(x) = 400x$, $d_h(x) = 400(1-x)$

5.3.2 Results under different preference distributions with given ticket prices and transporting capacities

In this section, we compare the numerical results under different preference distributions of travelers by defining various forms of $f(x)$ with predetermined ticket prices of the two competitive modes. Specifically, in this case, we assume that operators do not adjust pricing strategies when operating with different traveler groups. Different forms are considered including symmetric distributions containing: i) strong bipolorized distribution with differential function defined in Eq. (5.53a) and cumulative function defined in Eq. (5.54a); ii) weak bipolorized distribution with differential function defined in Eq. (5.53b) and cumulative function defined in Eq. (5.54b); (iii) uniform distribution with differential function defined in Eq. (5.53c) and cumulative function defined in Eq. (5.54c); (iv) weak centralized distribution with differential function defined in Eq. (5.53d) and cumulative function defined in Eq. (5.54d); (v) strong centralized distribution with differential function defined in

Eq. (5.53e) and cumulative function defined in Eq. (5.54e); and asymmetric distributions including (vi) strong HSR-skewed distribution with differential function defined in Eq. (5.53f) and cumulative function defined in Eq. (5.54f); (vii) weak HSR-skewed distribution with differential function defined in Eq. (5.53g) and cumulative function defined in Eq. (5.54g); (viii) weak air-skewed distribution with differential function defined in Eq. (5.53h) and cumulative function defined in Eq. (5.54g); and (ix) strong air-skewed distribution with differential function defined in Eq. (5.53i) and cumulative function defined in Eq. (5.54f). Figures 5.4 and 5.5 show an intuitive understanding of the explored travel mode preference distribution.

$$f_1(x) = D\cos(2\pi x) + D \tag{5.53a}$$

$$f_2(x) = \frac{D}{2}\cos(2\pi x) + D \tag{5.53b}$$

$$f_3(x) = D \tag{5.53c}$$

$$f_4(x) = -\frac{D}{2}\cos(2\pi x) + D \tag{5.53d}$$

$$f_5(x) = -D\cos(2\pi x) + D \tag{5.53e}$$

$$f_6(x) = 2Dx \tag{5.53f}$$

$$f_7(x) = 0.5D + Dx \tag{5.53g}$$

$$f_8(x) = 1.5D - Dx \tag{5.53h}$$

$$f_9(x) = 2D - 2Dx \tag{5.53i}$$

$$F_1(x) = \frac{D}{2\pi}\sin(2\pi x) + Dx \tag{5.54a}$$

$$F_2(x) = \frac{D}{4\pi}\sin(2\pi x) + Dx \tag{5.54b}$$

$$F_3(x) = Dx \tag{5.54c}$$

$$F_4(x) = -\frac{D}{4\pi}\sin(2\pi x) + Dx \tag{5.54d}$$

$$F_5(x) = -\frac{D}{2\pi}\sin(2\pi x) + Dx \tag{5.54e}$$

$$F_6(x) = Dx^2 \tag{5.54f}$$

$$F_7(x) = 0.5Dx - 0.5Dx^2 \tag{5.54g}$$

$$F_8(x) = 1.5Dx - 0.5Dx^2 \tag{5.54h}$$

$$F_9(x) = 2Dx - Dx^2 \tag{5.54i}$$

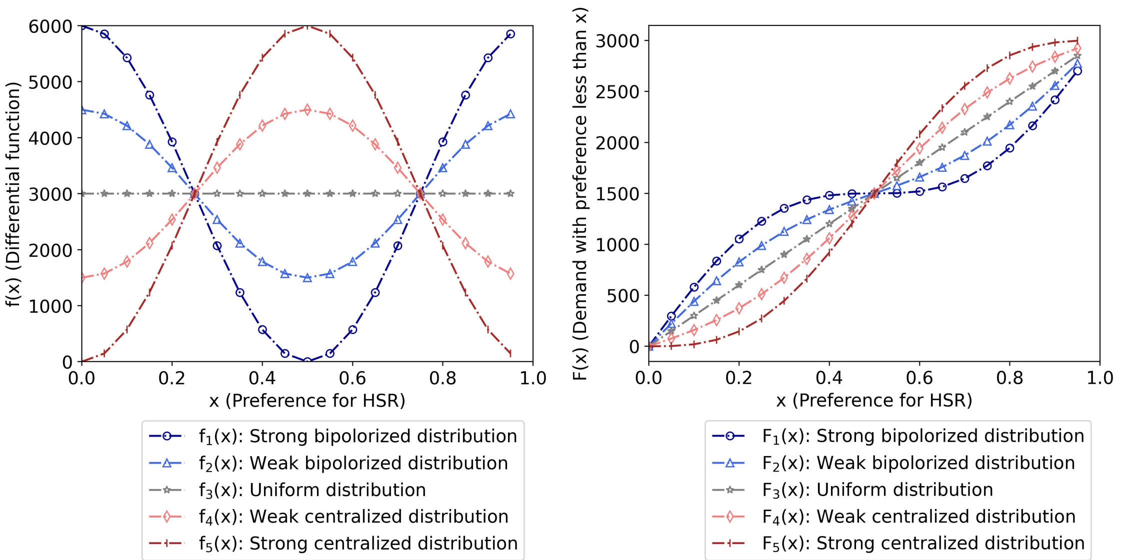

(a) Different mode preference symmetric distribution functions

(b) Cumulative demand functions of symmetric distribution

Figure 5.4: Considered symmetric travel mode preference distribution among travelers

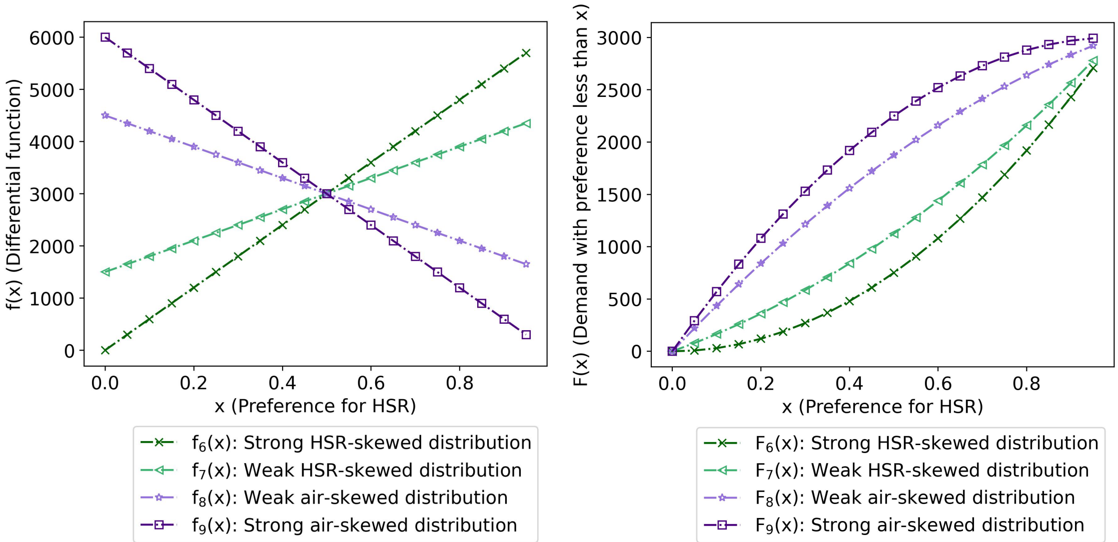

(a) Different mode preference asymmetric distribution functions

(b) Cumulative demand functions of asymmetric distribution

Figure 5.5: Considered asymmetric travel mode preference distribution among travelers

By substituting the above-considered differential functions into the formulations proposed in the prior sections, we can derive the numerical results regarding the demands and profits of the two modes and the corresponding consumer surplus of air and HSR passengers. The obtained results are concluded in Table 5.5.

Table 5.5: Results with given ticket prices and capacities ($m_a = m_h = 2000$)

$p_a = 1500$ and $p_h = 800$										
$f(x)$	$\tilde{x}$	n_a	n_h	π_a (10^6)	π_h (10^5)	$\pi_a + \pi_h$ (10^6)	CS_a (10^6)	CS_h (10^6)	$CS_a + CS_h$ (10^6)	Social welfare (10^6)
$f_1(x)$	0.469	1499	1501	1.774	8.408	2.614	1.935	2.875	4.811	7.425
$f_2(x)$	0.484	1477	1523	1.742	8.575	2.599	1.883	2.878	4.761	7.360
$f_3(x)$	0.491	1472	1528	1.734	8.613	2.596	1.847	2.855	4.703	7.298
$f_4(x)$	0.493	1467	1533	1.727	8.651	2.592	1.811	2.833	4.644	7.236
$f_5(x)$	0.495	1468	1532	1.729	8.643	2.593	1.781	2.801	4.582	7.175
$f_6(x)$	0.574	1357	1643	1.427	10.224	2.449	1.512	3.261	4.773	7.223
$f_7(x)$	0.648	1260	1740	1.568	9.487	2.516	1.677	3.077	4.754	7.270
$f_8(x)$	0.408	1585	1415	1.898	7.754	2.674	2.004	2.623	4.628	7.301
$f_9(x)$	0.336	1679	1321	2.035	7.040	2.739	2.131	2.410	4.541	7.280
$p_a = 1500$ and $p_h = 951$										
$f(x)$	$\tilde{x}$	n_a	n_h	π_a (10^6)	π_h (10^5)	$\pi_a + \pi_h$ (10^5)	CS_a (10^6)	CS_h (10^6)	$CS_a + CS_h$ (10^6)	Social welfare (10^6)
$f_1(x)$	0.560	1504	1496	1.781	10.629	2.844	1.941	2.641	4.582	7.426
$f_2(x)$	0.530	1545	1455	1.840	10.255	2.866	1.950	2.553	4.503	7.369
$f_3(x)$	0.520	1560	1440	1.862	10.118	2.874	1.934	2.501	4.436	7.309
$f_4(x)$	0.515	1568	1432	1.874	10.046	2.8780	1.912	2.459	4.371	7.249
$f_5(x)$	0.511	1567	1433	1.872	10.055	2.8776	1.880	2.430	4.310	7.188
$f_6(x)$	0.602	1447	1553	1.560	12.013	2.762	1.603	2.868	4.471	7.232
$f_7(x)$	0.671	1352	1648	1.698	11.148	2.813	1.765	2.704	4.468	7.281
$f_8(x)$	0.435	1674	1326	2.027	9.080	2.935	2.093	2.285	4.370	7.314
$f_9(x)$	0.362	1778	1222	2.178	8.132	2.991	2.232	2.071	4.303	7.294

Note: considered various travelers' preference distributions include: $f_1(x)$: Strong bipolorized distribution; $f_2(x)$: Weak bipolorized distribution; $f_3(x)$: Uniform distribution; $f_4(x)$: Weak centralized distribution; $f_5(x)$: Strong centralized distribution; $f_6(x)$: Weak HSR-skewed distribution; $f_7(x)$: Strong HSR-skewed distribution; $f_8(x)$: Weak air-skewed distribution; and $f_9(x)$: Strong air-skewed distribution.

$\tilde{x}$ is the preference of indifferent travelers; n_a and n_h are air travel demand and HSR demand, respectively; π_a and π_h are the profits of AT and HSR, respectively; CS_a and CS_h are consumer surplus of air passengers and HSR passengers, respectively. Social welfare of all participants (all travelers and operators of air and HSR) is calculated by $\pi_a + \pi_h + CS_a + CS_h$.

The values in the table are rounded to three decimal places, except for the total profit ($\pi_a + \pi_h$), which is given to four decimal places to maintain distinction. This exception applies when the differential functions $f_4(x)$ and $f_5(x)$ are considered, with $p_h = 951$.

The units of fares, profits, consumer surplus and welfare are all in Chinese currency (Chinese Yuan, CNY).

Observing the above results, we analyze how different preference distributions influence travelers' mode choices, profits of the two modes and social welfare under the two groups of given ticket prices. For symmetric preference distributions (i.e., $f_1(x)$, $f_2(x)$, $f_3(x)$, $f_4(x)$, and $f_5(x)$), where two equally sized groups of travelers prefer either air or HSR travel, if a larger proportion show a neutral preference toward the two modes, air travel demand increases when $p_h = 951$ while decrease when $p_h = 800$. Correspondingly, as the preference distribution becomes more centralized, HSR demand decreases at $p_h = 951$ while increases at $p_h = 800$. The observation indicates that travelers' neutral preferences within the market, i.e., when travelers demonstrate lower loyalty to their initially preferred mode coupled with price discounts offered by a particular mode, are two key factors in attracting increased demand for the mode with a price advantage.

For asymmetric preference distributions (i.e., $f_6(x)$, $f_7(x)$, $f_8(x)$, and $f_9(x)$), the results indicate that the mode with a greater number of initially inclined travelers tends to attract higher overall demand. Additionally, by analyzing the variation in demand between air and HSR under the two HSR ticket pricing scenarios, it can be inferred that the effect of HSR fare reductions on demand distribution remains relatively consistent across different asymmetric preference distributions. This suggests that when travelers favor one mode over the other, adjustments in ticket pricing have a limited impact on their mode choices.

The results about air and HSR profits indicate that, as an well-established mode for mid-haul trips, air travel consistently generates significantly higher profits compared to HSR. Examining the changes in air and HSR profits under symmetric preference distributions, it is observed that when the preference distribution becomes more centralized, HSR profits decline while air travel profits increase at $p_h = 951$. Conversely, when $p_h = 800$, HSR profits experience an increase while air travel profits decline. These trends suggest that when a larger proportion of travelers maintain neutral preferences between the two competing modes, only sufficiently strong pricing advantages for either mode can significantly enhance profitability.

Furthermore, it is evident that HSR achieves higher profits at $p_h = 951$ compared to $p_h = 800$ across the considered cases, the increased profits are more significantly when travelers' preference distributions are more centralized or HSR-skewed. This observation indicates that a moderate fare increase can lead to higher profitability, especially when a significantly segment of travelers remains strongly committed to a particular mode.

An analysis of consumer surplus among air and HSR passengers reveals that a reduction in HSR fares leads to an increase in the consumer surplus of HSR passengers, a corresponding decrease in the consumer surplus of air passengers, and an overall improvement of total consumer surplus for all travelers within markets served by both modes. Comparing social welfare across various preference distributions, the highest level of social welfare is observed when travelers are distinctly divided into groups with strong loyalty to their preferred modes, i.e., under a strongly bipolarized distribution. Furthermore, with a given preference distribution, the social welfare at $p_h = 951$ is higher than at $p_h = 800$. Additionally, the increase in social welfare resulting from a modest higher HSR fare is more apparent when a larger proportion of travelers hold neutral preferences between the two modes or a stronger preference for air travel. This observation suggests that, as a newly introduced mode for cross-board travel, HSR operators are more likely to realize increased profits and enhanced social welfare rather than significant gains in consumer surplus by setting a higher fare. Consequently, the profit-generating aspect of HSR should be prioritized over its welfare-enhancing attribute under such circumstances.

Overall, the analysis indicates that, given a fixed ticket price for the well-established mode in the market, the newly introduced mode can set a higher fare to achieve increased profits for both modes, greater social welfare for all stakeholders, and higher consumer surplus for the substitute mode. In this context, the profit-generating potential of the newly introduced mode is amplified. Furthermore, the profit gains for the new mode become more pronounced as a greater proportion of travelers prefer it, that is, when the preference distribution is highly polarized or skewed towards the newly introduced mode, whereas the enhancement of social welfare is more evident when the majority of passengers favor the incumbent mode.

Conversely, a lower fare for the newly introduced mode is likely to attract a larger share of demand, resulting in higher consumer surplus for both its own passengers and for travelers in the overall market, thereby highlighting the welfare, enhancing the welfare function of the new mode. When the newly introduced mode offers a price discount, it is particularly effective at attracting demand from the substitute mode among travelers who either have neutral preferences between the two modes or display loyalty towards the new mode. Notably, the improvement in social welfare resulting from price discounts is most significant when the preference distribution is more centralized or skewed towards the long-established mode.

5.3.3 Ticket prices as decision variables

In the above section, we investigate the impact of travelers' preference distribution on the mode choice equilibrium, air profits, HSR profit and consumer surplus of air passengers and HSR passengers given the ticket prices and transport capacities of the two modes. In other words, Section 5.3.2 tests the scenario where transport operators decide ticket prices from a static opinion. In this section, both ticket prices of air and HSR are taken as decision variables in the operations. The obtained airfares, HSR ticket prices, air demands, HSR demands, air profits, HSR profits, and consumer surplus of air and HSR passengers are concluded in Figures. 5.6-5.9.

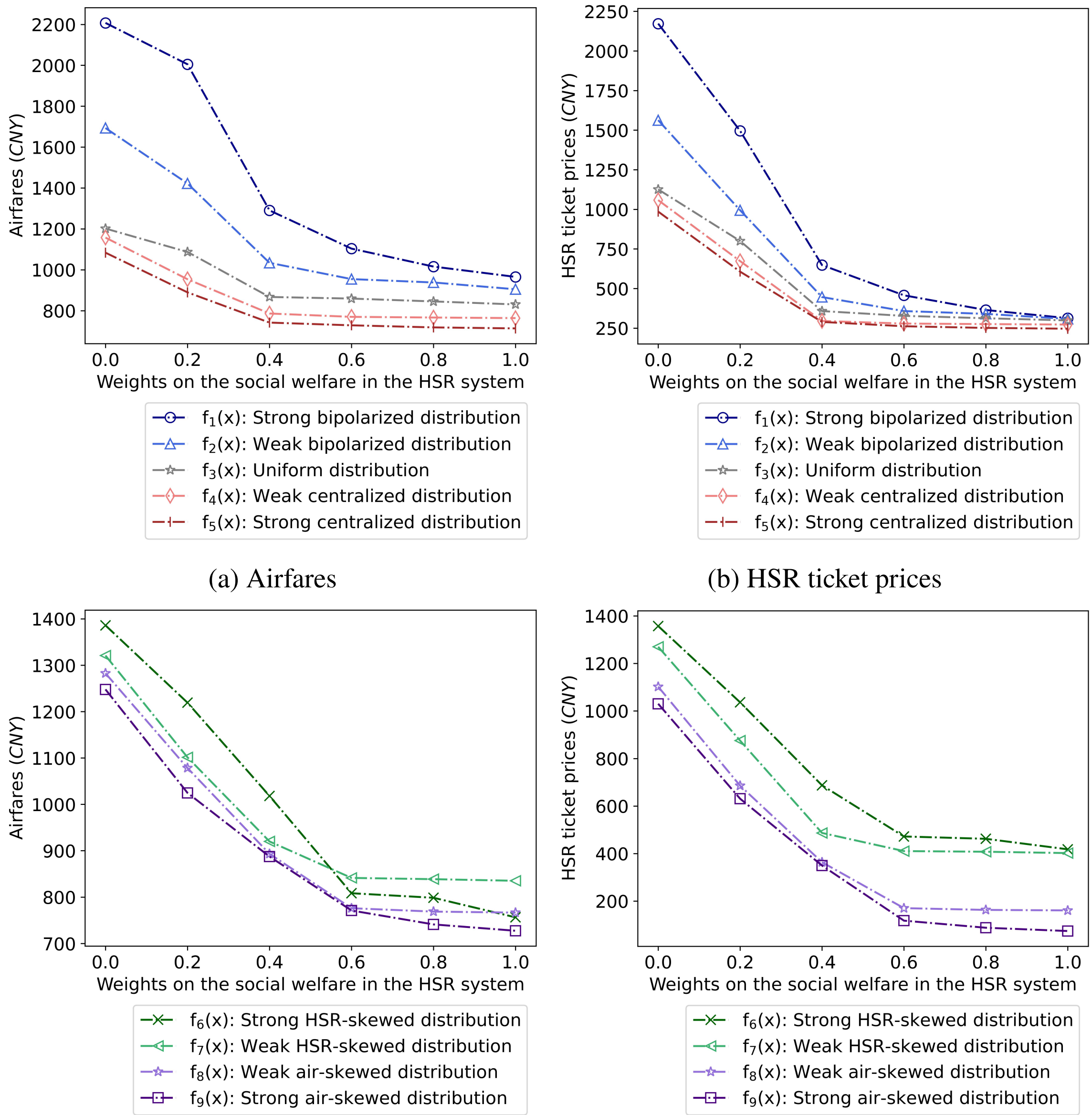

(a) Airfares

(b) HSR ticket prices

(c) Airfares

(d) HSR ticket prices

Figure 5.6: Results of ticket prices under various distributions of traveler's mode preference

Fig. 5.6 illustrates how airfares and HSR ticket prices evolve as the weight on social welfare in the HSR system increases. A consistent downward trend is observed for both air and HSR ticket prices across all traveler preference distributions, confirming that when HSR operators prioritise social welfare over profits, they set lower ticket prices to attract more passengers. However, the rate of price decline and the relative pricing levels vary depending on the distribution of traveler preferences.

In symmetric distributions ($f_1(x)$, $f_2(x)$, $f_3(x)$, $f_4(x)$, $f_5(x)$), where traveler preferences are more balanced between air and HSR, both airfares and HSR ticket prices start at higher levels when the social welfare weight is low. As the weight increases, HSR ticket prices drop sharply, especially in strong bipolarized ($f_1(x)$) and weak bipolarized ($f_2(x)$) markets, where two traveler groups are loyal to AT and HSR separately. Airfares also decline in response to lower HSR prices, but the rate of decrease is more gradual, suggesting that airlines adjust pricing strategically to remain competitive without completely undermining revenue.

In asymmetric distributions ($f_6(x)$, $f_7(x)$, $f_8(x)$, $f_9(x)$), where travelers initially favour either air or HSR, pricing trends reveal interesting differences. In HSR-skewed markets ($f_6(x)$, $f_7(x)$), where demand naturally favours HSR, HSR ticket prices start at higher levels but decrease rapidly, aligning with the strong demand shift toward HSR. Airfares in these markets also decrease, but the decline is less steep, indicating that airlines may rely on a niche market segment that remains loyal to air travel despite lower HSR fares. Conversely, in air-skewed markets ($f_8(x)$, $f_9(x)$), airfares are initially high but experience a sharp decline as HSR pricing becomes more competitive, showing that airlines must significantly lower fares to retain passengers in markets where HSR is aggressively priced.

A key insight observed from Figure 5.6 is that when the weight on social welfare is high (close to 1), both airfares and HSR ticket prices stabilize at lower levels, suggesting that further prioritization of social welfare in the HSR system has diminishing effects on price reductions. This implies that beyond a certain point, lowering HSR prices further may not dramatically change demand dynamics, as most price-sensitive passengers (or passengers with a weaker preference for air travel) have already shifted to HSR.

These findings indicate that HSR pricing policies should be carefully calibrated based on market characteristics. In balanced markets, gradual fare reductions can ensure smooth competition without destabilizing air travel. In HSR-dominated markets, maintaining financial sustainability while lowering fares is crucial, as excessive price cuts may lead to profitability challenges. Meanwhile, in air-dominated regions, airlines may need to implement aggressive pricing strategies or service differentiation to remain competitive. Additionally, integrated ticketing systems or multimodal transport policies could help reduce extreme fare competition and create a more sustainable pricing equilibrium between air and HSR.

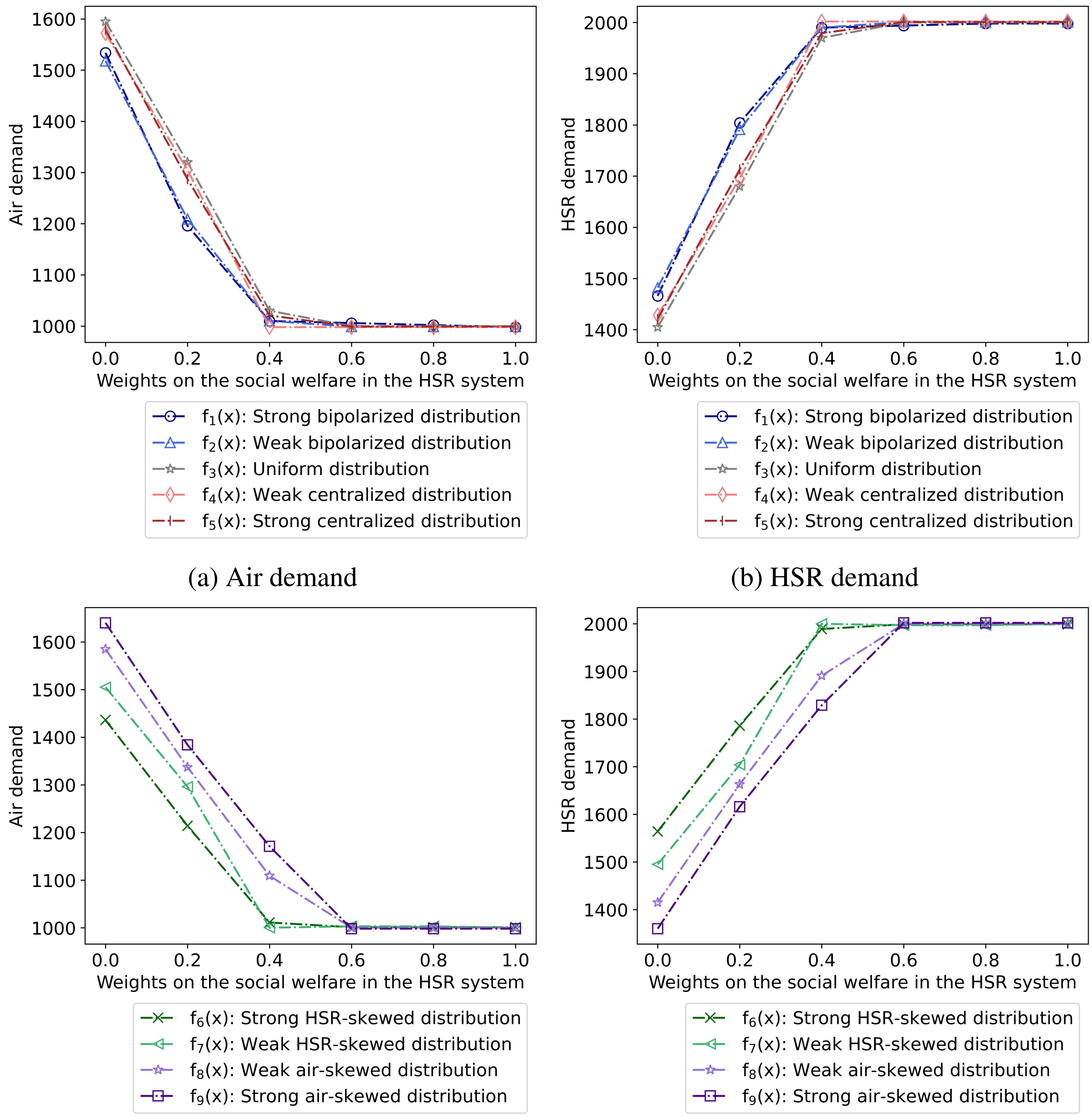

(a) Air demand

(b) HSR demand

(c) Air demand

(d) HSR demand

Figure 5.7: Results of demands of AT and HSR under various asymmetric preference distribution

Figure 5.7 illustrate how air and HSR demand evolve as the weight on social welfare in the HSR system increases. A clear inverse relationship is observed: as the social welfare weight increases, air demand decreases while HSR demand rises, indicating that prioritizing social welfare in HSR pricing leads to a significant shift of passengers from air to HSR. The magnitude and pattern of these changes vary across different traveler preference distributions, reflecting differences in market dynamics.

In symmetric distributions ($f_1(x)$, $f_2(x)$, $f_3(x)$, $f_4(x)$, $f_5(x)$), where travelers have more balanced preferences between air and HSR, the transition from air to rail happens gradually at first but accelerates as the social welfare weight increases. Notably, in strong bipolarized ($f_1(x)$) and weak bipolarized ($f_2(x)$) distributions, where travelers are more divided between air and HSR, air demand starts relatively high but declines sharply as HSR becomes more attractive. Meanwhile, in uniform ($f_3(x)$) and centralized distributions ($f_4(x)$, $f_5(x)$), the shift is smoother, suggesting that markets with more evenly distributed preferences experience a more stable transition between modes.

In asymmetric distributions ($f_6(x)$, $f_7(x)$, $f_8(x)$, $f_9(x)$), where travelers initially favour one mode over the other, the impact of increasing HSR's social welfare weight is more pronounced. In HSR-skewed distributions ($f_6(x)$, $f_7(x)$), where travelers already have a strong preference for HSR, air demand drops rapidly, and HSR demand increases significantly, showing that HSR-friendly markets respond quickly to fare reductions. Conversely, in air-skewed distributions ($f_8(x)$, $f_9(x)$), the attraction of air travel remains relatively strong at first but eventually declines sharply as HSR pricing becomes more competitive. This suggests that in air-dominated markets, passengers are more resistant to switching to HSR until fare reductions reach a critical threshold.

An important insight is that when the weight on social welfare in the HSR system is high (approaching 1), air demand converges towards a low, stable level across all distributions, while HSR demand reaches a plateau. This indicates that beyond a certain point, further prioritization of social welfare in HSR pricing has diminishing effects on demand shifts, as most passengers who are willing to switch from air to HSR have already done so.

Above observations suggest that policymakers should consider market-specific strategies when adjusting HSR pricing for social welfare optimization. In markets with balanced traveler preferences, a gradual approach to price reductions can ensure a smooth transition without disrupting air travel excessively. In HSR-friendly markets, investment in capacity expansion and service quality may be necessary to accommodate the rapid shift in demand. Meanwhile, in air-dominated markets, complementary policies such as multimodal integration and targeted incentives may be needed to encourage a more sustainable mode shift without severely impacting AT viability.

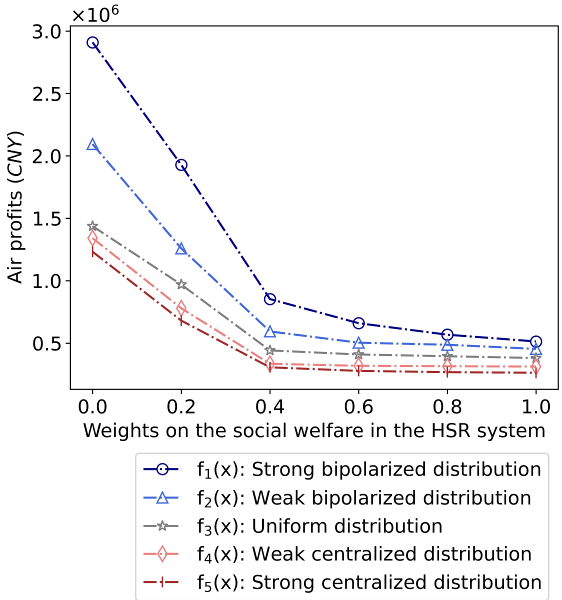

(a) Air profits

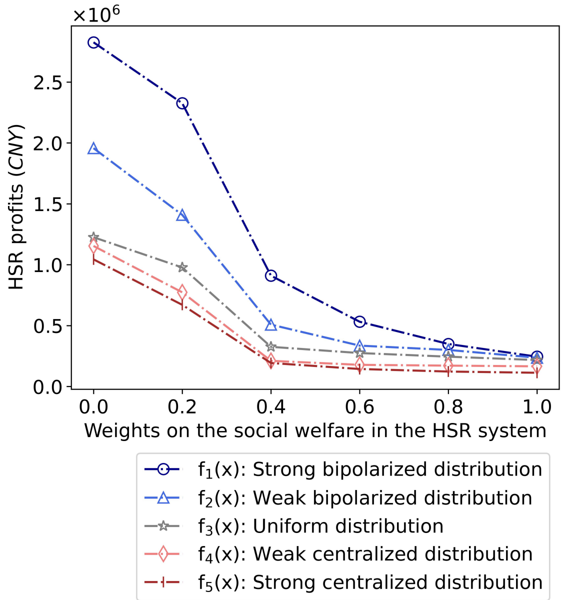

(b) HSR profits

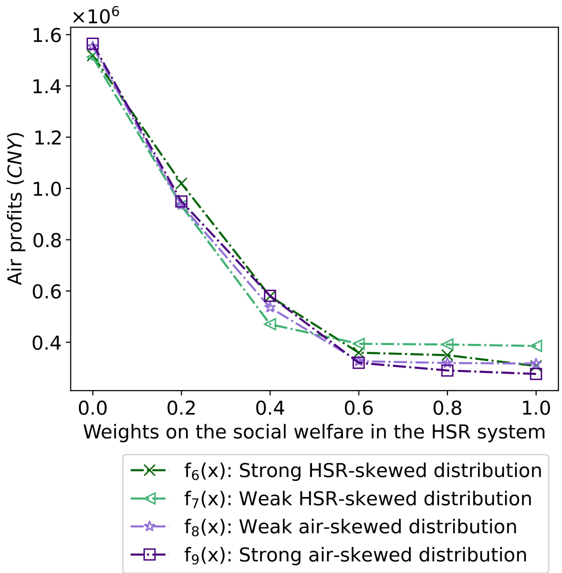

(c) Air profits

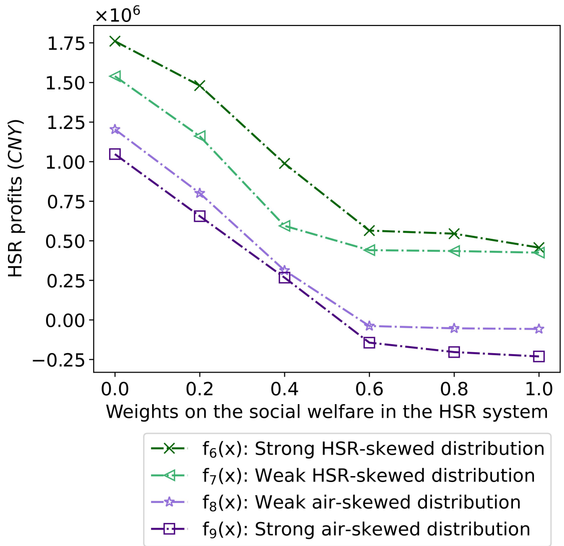

(d) HSR profits

Figure 5.8: Results of air profits and HSR profits under various distributions of traveler's mode preference

Fig. 5.8 illustrates how the profits of both air travel and high-speed rail (HSR) change as the weight on social welfare in the HSR system increases. As expected, both air and HSR profits decline as more emphasis is placed on social welfare in the optimization of HSR ticket prices. This trend is observed across all traveler preference distributions, though the magnitude of the decline varies. In strongly bipolarized distributions ($f_1(x)$, $f_2(x)$), where travelers are initially split between air and HSR, both air and HSR profits start at relatively high levels but experience sharp declines as HSR fares are reduced to attract more passengers. This suggests that in markets with strong mode competition, profitability is highly sensitive to pricing strategies, and aggressive fare reductions may undermine the financial viability of both air and HSR operators.

In uniform and centralized distributions ($f_3(x)$, $f_4(x)$, $f_5(x)$), where traveler preferences are more balanced, air and HSR profits decline more gradually. The initial profits are lower compared to bipolarized markets, and as the social welfare weight increases, both air and HSR experience steady but less dramatic financial losses. This indicates that in these markets, pricing adjustments can be more sustainable, as demand shifts occur more smoothly without drastically disrupting the profitability of either mode. However, in HSR-skewed markets ($f_6(x)$, $f_7(x)$), HSR profits decline significantly despite rising demand, suggesting that excessive fare reductions to maximize social welfare may lead to financial instability for HSR operators. Meanwhile, in air-skewed markets ($f_8(x)$, $f_9(x)$), air profits drop sharply as demand shifts to HSR, with some cases showing negative HSR profits, indicating that HSR operators may struggle to sustain operations solely based on low fares.

These insights suggest that a careful balance is needed between social welfare and profitability to ensure the long-term sustainability of both air and HSR systems. In markets where HSR has strong potential, subsidies or operational cost optimizations may be necessary to maintain financial stability while supporting affordable pricing. In air-dominated regions, policies should focus on gradual pricing transitions and service differentiation to allow both modes to coexist competitively. Additionally, multimodal cooperation and integrated ticketing strategies could help mitigate extreme profit losses and create a more sustainable, consumer-friendly transport network.

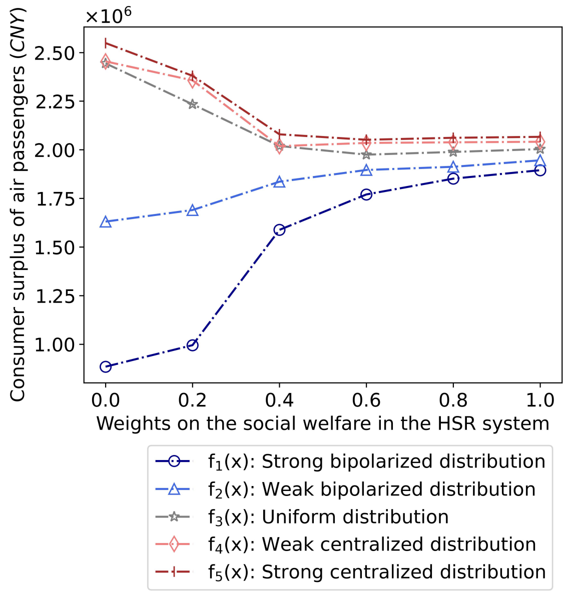

(a) Consumer surplus of air passengers

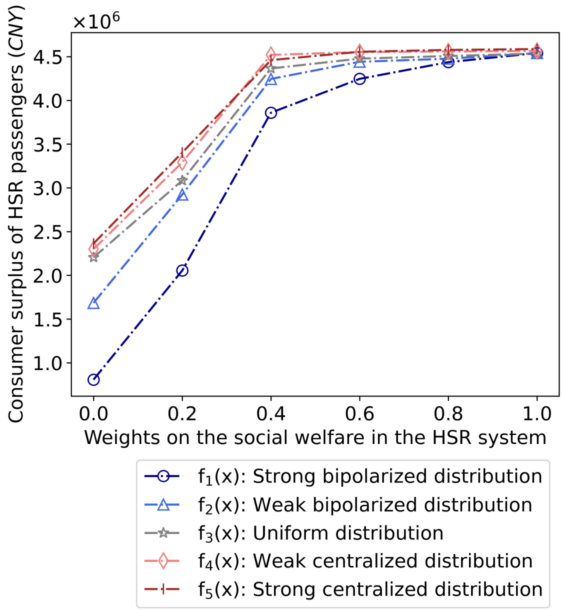

(b) Consumer surplus of HSR passengers

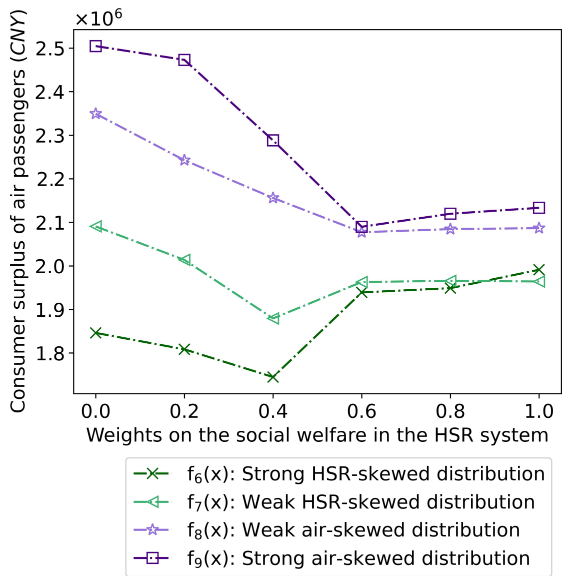

(c) Consumer surplus of air passengers

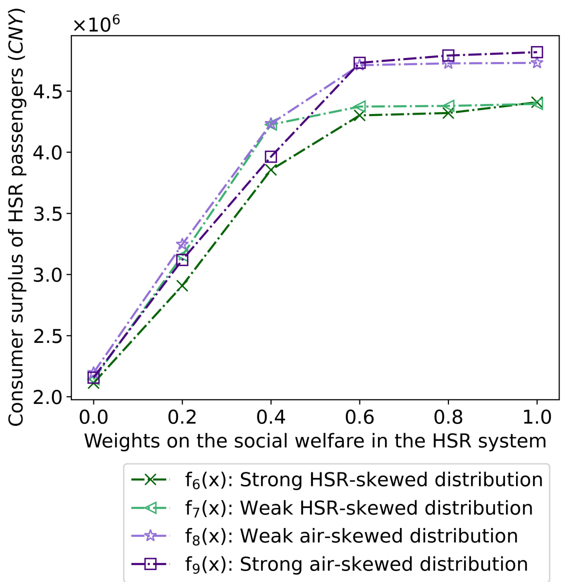

(d) Consumer surplus of HSR passengers

Figure 5.9: Results of consumer surplus under various symmetric preference distribution

Figure 5.9 illustrate how the consumer surplus of both air and HSR passengers changes as the weight on social welfare in the HSR system increases. A clear positive impact on HSR passenger surplus is observed, while the effects on air passenger surplus vary depending on the traveler preference distribution. This suggests that emphasizing social welfare in HSR pricing strategies improves overall consumer benefits, but the distribution of those benefits differs across markets.

For HSR passengers, consumer surplus increases steadily as the social welfare weight rises, reflecting the benefits of lower ticket prices and higher demand for rail travel. This trend is consistent across all traveler distributions, with a more rapid increase in strongly bipolarized ($f_1(x)$), weak bipolarized ($f_2(x)$), and centralized ($f_4(x)$, $f_5(x)$) markets, where travelers are more evenly split between air and HSR. In these cases, HSR passengers gain significantly from price reductions, leading to a substantial rise in consumer welfare. A similar pattern is observed in HSR-skewed distributions ($f_6(x)$, $f_7(x)$), where HSR already has a strong preference, but the increase in surplus is slightly less pronounced, indicating that passengers in these markets were already benefiting from rail options even before fare reductions.

For air passengers, the impact on consumer surplus is more complex. In balanced distributions ($f_1(x)$, $f_2(x)$, $f_3(x)$, $f_4(x)$, $f_5(x)$), air passenger surplus initially declines as HSR becomes more competitive, leading to reduced air travel demand and lower airfare revenues. However, in some cases, air passenger surplus stabilizes or even increases at higher social welfare weights, suggesting that airlines respond to competitive pressure by lowering fares, which benefits remaining air travelers. In air-skewed distributions ($f_8(x)$, $f_9(x)$), where air travel is more dominant, air passenger surplus remains relatively high but experiences a slight decline as HSR becomes more attractive. This suggests that while airlines still retain a significant market share, fare reductions and competitive adjustments reduce some of the consumer benefits that air travelers initially enjoyed.

A key insight is that as HSR prioritizes social welfare, the overall consumer surplus of HSR passengers rises significantly, while the air passenger surplus either remains stable or declines slightly in air-dominated markets. This implies that increasing the social welfare weight in HSR pricing benefits the majority of travelers, particularly those who prefer HSR. However, in air-dependent regions, policymakers may need to implement complementary policies to ensure that air passengers do not experience a disproportionate loss in consumer welfare.

These findings highlight the importance of market-specific policy considerations. In HSR-friendly markets, investment in rail infrastructure and service quality can further enhance consumer welfare. In air-dominated regions, policies should encourage fair competition between air and rail, while ensuring that air passengers continue to have viable travel options. Additionally, multimodal integration strategies, such as coordinated scheduling and fare harmonization between air and HSR, could help balance consumer benefits across both modes and create a more sustainable transport ecosystem.

All of the above analysis underscores that travelers' mode preference distribution plays a crucial role in shaping the pricing strategies, demand, profitability, and consumer surplus of both air and HSR systems. In balanced markets, where travelers are evenly distributed between air and HSR, fare reductions in HSR lead to a steady increase in rail demand, a corresponding decline in air travel, and a gradual shift in consumer surplus from air to HSR passengers. However, in HSR-skewed markets, the demand shift happens more rapidly, with HSR operators facing a challenge in maintaining profitability despite higher ridership. Conversely, in air-skewed markets, air demand remains relatively strong until HSR fares reach a critical low point, at which passengers start shifting modes, causing a sharper decline in air profitability. Across all distributions, as the weight on social welfare in the HSR system increases, both air and HSR profits decline, though the extent varies based on initial traveler preferences. While HSR passengers consistently benefit from fare reductions and experience rising consumer surplus, air passenger surplus fluctuates, declining in some cases due to reduced demands but stabilizing or even increasing in others due to competitive fare reductions by airlines.

In summary, pricing strategies in transport systems must be proposed according to the specific traveler preference distribution of each market. In markets where travelers have a strong preference for a single mode, aggressive fare reductions risk destabilizing the competing mode and could lead to long-term financial sustainability concerns. Meanwhile, in more balanced markets, gradual pricing adjustments can create a smoother transition between air and HSR while maintaining fair competition. Policymakers should consider strategies such as multimodal coordination, differentiated service offerings, and targeted subsidies to ensure that both air and HSR remain viable while maximizing overall consumer welfare. Understanding traveler preference distributions is therefore essential for designing efficient, sustainable, and passenger-centric transport policies that balance affordability, competition, and financial health across the system.

5.4 Conclusion

As connectivity between Hong Kong and Mainland China expands through a comprehensive HSR network, the competitive dynamics between established AT and newly introduced HSR services have garnered significant attention. A review of existing literature highlights a gap in research regarding competition between these modes, particularly in the context of travelers' diverse preferences. To address this issue, the present study introduces a framework grounded in the Hotelling model, explicitly incorporating heterogeneous mode preferences to examine the competitive interplay between AT and HSR.

We construct tractable bi-level models for two distinct optimization scenarios. For the upper-level model, we consider (i) both air and HSR operators aim to maximize their respective profits, and (ii) AT pursues profit maximization while HSR operators optimize a weighted sum of profit and social welfare. For the lower-level model, we characterizes travelers' mode preferences along a continuous spectrum, offering an intuitive and analytically tractable approach to individual travel choice behavior.

Our analytical results show: (i) Increasing ticket prices or reducing capacity for one mode diminishes its demand while boosting demand for the alternative mode; conversely, lowering prices or expanding capacity promotes mode switching in favor of the improved option; (ii) When both modes focus on profit maximization, the optimal ticket prices and resulting profitability are strongly affected by the heterogeneity in travelers' mode preferences; (iii) Overlooking this diversity or assuming uniform preferences may result in suboptimal pricing decisions and lost revenue potential.

Our numerical analysis shows: (i) For a competitive market, the effect of travelers' preferences and congestion sensitivity on a mode's optimal price is half as strong as the influence exerted by the competing mode, while a mode's own operating costs impact its optimal price twice as much as those of the alternative mode; (ii) Price competition is most effective when a substantial share of travelers remain neutral or flexible in their preferences. Proper increment of service fare may benefit a mode with a loyal customer base, whereas fare reductions enhance consumer surplus across all passengers; (iii) In markets dominated by strong loyalty to a particular mode, aggressive fare reductions may destabilize the competitor and threaten financial viability. Conversely, in balanced markets, gradual pricing adjustments support a smoother transition between air and HSR, fostering fair and sustainable competition.

This study has several limitations. The numerical results rely on assumed functional forms and parameters due to a lack of real-world passenger data, although efforts were made to incorporate reliable flight and HSR information sources to ensure robust conclusions. Additionally, while the study accounts for heterogeneous mode preferences, these preferences are influenced by numerous external factors that require further investigation. Future studies should incorporate survey data to better understand the determinants of travelers' mode choices and refine pricing strategies accordingly.

Future research should explore the interaction between travelers' mode choice behaviors and the underlying factors influencing their preferences. Additionally, price discrimination strategies, which have been studied in the context of heterogeneous passengers with different travel purposes, could be extended to analyze differentiated pricing structures for air and HSR based on travelers' mode preferences. Incorporating these elements would provide deeper insights into optimal pricing policies and enhance the competitiveness and sustainability of transport systems.

Chapter 6

MAS-RnR: Air cargo transfer management within a multi-airport system

This chapter formulates cargo routing in a multi-airport transfer hub as an integer linear program, aiming at minimizing the costs depending on intermediate transfer times. Heterogeneous values of time are applied to quantify transfer times in major and minor airports. A solving framework called MAS-Transfer Relax-and-Repair (MAS-RnR) for getting efficient cargo transfer operations is proposed, combining an linear programming relaxation for the multi-commodity flow with an assignment heuristic dealing with the non-integer assignment values. The multi-airport system in the Great Bay Area, with 3 major airports, 4 minor airports and 12 road connections between them, is considered as a real-world example in the numerical studies. Small-scale, medium-scale, and large-scale problems have all been separately observed, where different amounts of air cargo and flights are included. The results show that the proposed MAS-RnR can help find high-quality integer solutions within limited time expense. Even for problem sizes that solvers cannot solve within 24 hours, our proposed framework can obtain feasible integer solutions within 2 hours with only a 2% gap from the lower bound getting from the linear programming relaxation. The sensitivity analysis investigates the impact of the heterogeneity of values of time on the cargo routing results and capacity utilization across airports.

6.1 Introduction

The rapid globalization of trade and the increasing demand for just-in-time delivery of goods have raised the significance of air cargo transportation in modern supply chains (Huang & Chang, 2010; Lakew & Tok, 2015; Azadian et al., 2017; Bombelli et al., 2020; Rodbundith et al., 2021; Chen et al., 2024). Air cargo transportation offers extraordinary response speed and service reliability, making it irreplaceable for transporting high-value and time-sensitive cargo (Azadian et al., 2012; Kiraci, 2025). As the amount and diversity of global air cargo continue to rise, single hub airports are increasingly constrained in their ability to handle the cargo demands in the future. In this context, the multi-airport system (MAS) has becoming a promising and inevitable way for supporting the evolving needs of the air cargo industry, as an transfer hub with integrated transportation resources and higher operation flexibility.

In the air cargo market, efficient cargo shipment relies on three key players: shippers, carriers, and forwarders. Shippers, such as manufacturers and exporters, initiate shipments, prepare cargo, and choose suitable transport solutions. Carriers, typically airlines, physically transport goods between airports, ensuring safe and timely delivery. Forwarders serve as essential intermediaries, coordinating the logistics between shippers and carriers usually without operating their own aircraft. By integrating and utilizing transportation resources in a MAS, forwarders gain flexibility to optimize strategies, reduce costs, and offer customized service. MAS also enables more frequent feeder services and provides alternative routing options during congestion or disruptions at major hubs, thereby enhancing the reliability and resilience of the air cargo supply chain. As potential difficulties coexist with the benefits in air cargo transportation in a MAS, how to integrate the resources of multiple airports within the MAS for efficiently handling air cargo transportation tasks has become an important topic.

Much of the existing research on the optimization of air cargo transportation has focused on single-airport scenarios, which are inapplicable when considering the intricate interdependencies and shared resources characteristic of the MAS environment, and are restricted by the capacity limitations of a single airport. This paper seeks to address this gap by developing and analyzing optimization models customized to air cargo transportation within MASs. Our study focuses on the decision-making process of forwarders to make efficient transfer routing of each transshipment cargo in a MAS. Given the capacities and schedules of flights serving airports in the MAS and timetables of cargo trucks connecting each major-minor airport pair, the forwarder decides the customized transfer routing for each cargo according to its origin-destination (OD), arrival time at its origin, its weight and volume. Given the heterogeneous congestion levels across major and minor airports within a MAS, the objective should include not only the minimization of network-wide air-cargo transfer times but also the reduction of cargo dwell times, specifically at major airports.

This paper contributes to air cargo transportation research from theoretical, technical, and practical perspectives. Theoretically, we extend the literature by introducing a MAS as an integrated transfer hub and explicitly optimizing intra-MAS air cargo transfer operations. To the best of our knowledge, this is the first study to treat a MAS as a transfer hub and to formalize how cargo forwarders assign each shipment to efficient cross-airport transfer strategies so that cargo passes through the hub as quickly as possible before onward transportation to its destination. Technically, we formulate the intra-MAS cargo transfer problem as an integer linear program (ILP) and propose MAS-Transfer Relax-and-Repair (MAS-RnR), a Branch-and-Price–inspired solving framework that starts from the linear relaxation with continuous variables and employs column generation to obtain strong lower bounds. At each branching node, heuristic algorithms construct high-quality feasible integer solutions and corresponding upper bounds, and after every branching step the linear relaxation is re-solved to update the lower bound, while a greedy procedure iteratively tightens the upper bound, progressively closing the gap between bounds. This approach is efficient for finding high-quality feasible integer solutions to large-scale generalized assignment problems arising in air cargo transportation. Practically, we demonstrate the applicability and significance of the problem using the GBA as a real-world case. By instantiating the model with public data and information from official sources, supplemented with clearly stated assumptions for some parameters, we evaluate MAS-RnR against baseline heuristic algorithms and a commercial solver across different instance sizes. The results show that MAS-RnR generates high-quality near-optimal solutions with under 2% optimality gaps relative to the lower bounds from LP relaxations, even when baseline heuristics generate lower-quality solutions and the commercial solver fails to obtain any integer solution within 12 hours. To accommodate a wider range of market conditions, we conduct sensitivity analyses on varying levels of airport dwell-time heterogeneity and different ad hoc costs, compare the resulting cargo-to-strategy allocations, and show that the proposed method efficiently handles diverse cases by adjusting transfer management to efficiently use resources in MAS and simultaneously minimize the cargo transfer time inside the MAS.

The remainder of this chapter is organized as follows. Section 6.2 introduce our studied context, corresponding model formulations and the solving framework. Section 6.3 conducts numerical studies with different problem sizes and sensitivity analysis on the time parameters. Section 6.4 conclude this chapter and discuss limitations and possible related future research topics.

6.2 Problem statement, mathematical formulation and solution

6.2.1 Problem description

In this study, we propose a decision-support program for air cargo forwarders that aims to minimize operating costs while fulfilling international air cargo transportation tasks. Within the air cargo market, forwarders serve as intermediaries, delivering comprehensive transportation solutions to shippers (businesses or individuals) requiring the movement of goods to specified destinations. Upon receiving service price proposals from forwarders, shippers respond by placing cargo orders according to their logistical needs. This process generates a demand profile that the forwarder need to satisfy.

To address these demands, forwarders negotiate contractual agreements with carriers, entities that own and operate air transportation resources such as aircraft and ground handling facilities. Carriers, in turn, offer flight capacities at negotiated rates. It is assumed that all pricing and capacity agreements with both shippers (for transportation services) and carriers (for access to air cargo capacity) are established prior to the commencement of the transportation planning process modeled in this study. Given these established agreements, the forwarder's primary task becomes the design of an efficient transportation plan for the given cargo demands that minimizes total transportation costs, with the MAS acting as a central transfer hub.

We denote the set of airports within the MAS by $\mathcal{A} = \{1, 2, \ldots, |\mathcal{A}|\}$, where each airport is indexed by a. This set is partitioned into two disjoint subsets: $\mathcal{I}$, the set of minor airports providing only domestic cargo services, and $\mathcal{J}$, the set of major airports that handle both domestic and international cargo. Ground connections exist between minor and major airports. For each such connection between a minor airport $i \in \mathcal{I}$ and a major airport $j \in \mathcal{J}$, let $\mathcal{B}_{ij} = \left\{1, 2, \ldots, |\mathcal{B}_{ij}|\right\}$, indexed by b, denote the set of available buses. Each bus b has a capacity Y_b, departs from the minor airport at time t_b^1, and arrives at the corresponding major airport at t_b^2.

Regarding air transport, the cargo network includes three types of air links: from the origin airport to a minor airport (oi), from the origin airport to a major airport (oj), and from a major airport to the destination airport (jd). For each link, we define the corresponding set of available flights: K_{oi}, K_{oj}, and K_{jd}, respectively, all indexed by k. Each flight k has capacities (Y_k for weight, Q_k for volume) and times (departure t_k^1, arrival t_k^2), and each truck b has capacities (Y_b, Q_b) and times (departure t_b^1 from minor airports, arrival t_b^2 at major airports).

International air cargo demand is represented by multiple origin-destination (OD) airport pairs $(o, d) \in W$. For each OD pair, let $\mathcal{M}_{od} = \{1, 2, \ldots, |\mathcal{M}_{od}|\}$, indexed by m, represent the set of cargo shipments, with each shipment m having a weight w_m and a volume v_m and an arrival time at its origin airport t_m^0. The forwarder's objective is to minimize the total operating cost, encompassing both transportation and time-related costs for all shipments. These costs are calculated using flight- and airport-specific parameters, reflecting the possible variability in aircraft capacity and storage resources across different links and airports. Specifically, let μ_k denote the per-unit weight transportation cost for flight k, and let θ_o, θ_i, and θ_j represent the value of cargo dwell time at the origin, minor, and major airports, respectively. The monetary-form costs related to transferring in airports are calculated by the value of dwell time multiplying the staying time in airports. The parameter ρ represents the monetary value of on-board time and is used to calculate the time-related cost of the air transporting process, from the origin airport to the destination airport, by multiplying it by the separate on-board time on links.

To capture the operational realities of ad hoc services, f_o and f_a denote the average response times for utilizing ad hoc services at origin airports and transfer airports in the MAS, respectively. To ensure feasible loading and unloading operations, u_a represents the average handling time for cargo at airport a, accounting for transfers between storage points (or the previously loaded trucks/flights) and the loading space of flights or buses. For cargo assigned to regular scheduled flights, the departure and arrival times at each airport coincide with those of the respective flights. In contrast, for cargo transported via ad hoc services, the average transit time is used to represent temporal information. Specifically, let T_{oa}, T_{ij}, and T_{jd} denote the average transportation times for ad hoc services between the origin airport o and any airport a within the MAS, between minor and major airports within the MAS (airport link ij), and from major airports (denoted by j) to the destination airport d, respectively. For example, if a cargo m is allocated to ad hoc services between its origin airport o and a major airport j, then the arrival time of the cargo at airport j can be calculated as $t_m^0 + f_o + T_{oi}$. The parameter ρ represents the monetary value of time and is used to calculate the total time-related cost of the transportation process, from the origin airport to the destination airport, by multiplying it by the total transportation time.

Given these market conditions and the use of the MAS as a transfer hub, forwarders must allocate each cargo to appropriate strategies and corresponding flights or buses, ensuring sufficient time intervals for cargo handling and connections between consecutive legs. We introduce the following decision variables:

- $x_{mk} = 1$ if the cargo m is assigned to flight k, and 0 otherwise.
- $z_m^{oa} = 1$ if the cargo m is transported from the origin airport to a transfer airport $a \in \mathcal{A}$ via ad hoc air services, and 0 otherwise.
- $z_m^{jd} = 1$ if the cargo m is transported from a major transfer airport j to the destination airport via ad hoc air services, and 0 otherwise.
- $z_m^{ij} = 1$ if the cargo m is transported between minor airport i and major airport j via ad hoc road services, and 0 otherwise.

By allocating transfer strategies for every received air cargo and utilizing available resources efficiently within the framework of a MAS, our model provides a systematic approach for forwarders to complete shipments with minimum operating costs. The notations introduced above are summarized in Table 6.1.

Table 6.1: Notations in this chapter

Notation	**Description**
$\mathcal{A}$	Set of airports within the considered MAS in the air cargo network, where $\mathcal{A} = \mathcal{I} \cup \mathcal{J}$
$\mathcal{I}$	Set of minor airports in the MAS that do not provide direct transportation services to the destination airport.
$\mathcal{J}$	Set of major airports in the MAS that provide direct transportation services to the destination airport
$\mathcal{M}_{od}$	Set of parcel indices requiring transportation between OD airport pair (o, d), $(o, d) \in W$
$\mathcal{K}_{oa}$	Set of flight indices serving between the origin airport and airport a, for $a \in \mathcal{A}$
$\mathcal{K}_{ad}$	Set of flight indices serving between airport a and the destination airport d, for $a \in \mathcal{A}$

Notation	Description
$\mathcal{B}_{ij}$	Set of buses providing ground services between airport pair (i, j), where $i \in \mathcal{I}$, $j \in \mathcal{J}$
i	Index of minor airports in the MAS, $i \in \mathcal{I}$
j	Index of major airports in the MAS, $j \in \mathcal{J}$
m	Index of an air cargo to be transported between OD airport pair (o, d), $m \in \mathcal{M}_{od}$ for $(o, d) \in \mathcal{W}$
k	Index of a flight, $k \in \mathcal{K}_{oa} \cup \mathcal{K}_{jd}, a \in \mathcal{A}, j \in \mathcal{J}$
b	Index of ground buses serving ground connection between minor airports and major airports, $b \in \mathcal{B}_{ij}$ for $i \in \mathcal{I}$, $j \in \mathcal{J}$
Y_k	Maximum cargo capacity of flight k, $k \in \mathcal{K}_{oa} \cup \mathcal{K}_{jd}$, for $a \in \mathcal{A}$, $j \in \mathcal{J}$ and $(o, d) \in \mathcal{W}$
Y_b	Maximum weight capacity of truck b, for $i \in \mathcal{I}$, $j \in \mathcal{J}$ and $b \in \mathcal{B}_{ij}$
$\theta_o(\theta_a)$	Monetary cost per unit time interval for air cargo transferring in the origin airports (transfer airports in the MAS), reflecting the various scarcity level of resources in different airports
φ_{oa}	Unit cost for ad hoc services between the origin airport and transfer airports in the MAS, i.e., link oa, for $a \in \mathcal{A}$ and $o \in \mathcal{W}$
φ_{jd}	Unit cost for ad hoc services between major airports in the MAS and the destination airport, for $j \in \mathcal{J}$ and $d \in \mathcal{W}$
f_o, f_a	The average response times of ad hoc transportation services in the origin airport o and the transfer airport a in the MAS, respectively, for $(o, d) \in \mathcal{W}$, $a \in \mathcal{A}$
T_{oa}, T_{ij}, T_{jd}	Average transportation times of ad hoc services between link oa, ij, and jd, respectively, where $(o, d) \in W$, $j \in \mathcal{J}$, $i \in \mathcal{I}$
t_k^1	Scheduled departure time of flight k from its origin airport, $k \in \mathcal{K}_{oa} \cup \mathcal{K}_{ad}$, for $(o, d) \in \mathcal{W}$

Notation	Description
t_k^2	Scheduled arrival time of flight k at its destination airport, $k \in \mathcal{K}_{oa} \cup \mathcal{K}_{ad}$, for $(o, d) \in \mathcal{W}$ and $a \in \mathcal{A}$
t_b^1	Scheduled departure time of truck b from its origin minor airport, $b \in \mathcal{B}_{ij}$ for $i \in \mathcal{I}$, $j \in \mathcal{J}$
t_b^2	Scheduled arrival time of truck b from its origin minor airport, $b \in \mathcal{B}_{ij}$ for $i \in \mathcal{I}$, $j \in \mathcal{J}$
t_m^0	Scheduled arrival time of cargo m at the origin airports, $m \in \mathcal{M}_{od}$ for $(o, d) \in \mathcal{W}$
$S_{oa}/S_{ad}/S_{ij}$	The travel time of vehicles between link $oa/ad/ij$
$\mathbf{x} = (..., \mathbf{x}_m, ...)$	Binary variable vector indicating cargo-to-flight allocation, $\mathbf{x}_m = (..., x_{mk}, ...)$, $k \in \mathcal{K}_{oa} \cup \mathcal{K}_{jd}$ for $a \in \mathcal{A}$, $j \in \mathcal{J}$ and $(o, d) \in \mathcal{W}$
$\mathbf{z} = (..., \mathbf{z}_m, ...)$	Binary variable vector indicating whether ad hoc services are used between airports in the network, $\mathbf{z}_m = \left(..., z_m^{oa}, z_m^{jd}, z_m^{ij}...\right)$, for $(o, d) \in \mathcal{W}$, $i \in \mathcal{I}$, $j \in \mathcal{J}$ and $a \in \mathcal{A}$

6.2.2 Mathematical formulations

With the introduced problem setting and notations, the minimum program for air cargo transportation problem considering transfer at a MAS can be formulated as follows:

P 3.

$$\begin{aligned}
\min_{\mathbf{x},\mathbf{z}} \sum_{(o,d)\in\mathcal{W}} \sum_{m\in\mathcal{M}_{od}} & \left\{ \sum_{i\in\mathcal{I}} \theta_o \left[\sum_{k\in\mathcal{K}_{oi}} x_{mk} \left(t_k^1 - t_m^0\right) + z_m^{oi} T_{oi} \right] \right. \\
& + \sum_{i\in\mathcal{I}} \theta_i \left[\sum_{b\in\mathcal{B}_{ij}} x_{mb} t_b^1 - z_m^{oi} \left(t_m^0 + T_{oi} + f_{oi}\right) - \sum_{k\in\mathcal{K}_{oi}} x_{mk} t_k^2 + z_m^{ij} T_{ij} \right] \\
& + \sum_{j\in\mathcal{J}} \theta_o \left[\sum_{k\in K_{oj}} x_{mk} \left(t_k^1 - t_m^0\right) + z_m^{oj} T_{oj} \right] + \sum_{a\in\mathcal{A}} \left[\sum_{k\in\mathcal{K}_{oa}} \rho x_{mk} \left(t_k^2 - t_m^0\right) + z_m^{oa} \left(\rho f_{oa} + \varphi_{oa} S_{oa}\right) \right] \\
& + \sum_{i\in\mathcal{I}} \sum_{j\in J} \left[\sum_{b\in\mathcal{B}_{ij}} \rho x_{mb} \left(t_b^2 - t_b^1\right) + z_m^{ij} \left(\rho f_{ij} + \varphi_{ij} S_{ij}\right) \right] + \sum_{j\in\mathcal{J}} \left[\sum_{k\in\mathcal{K}_{jd}} \rho x_{mk} \left(t_k^2 - t_k^1\right) + z_m^{jd} \left(\rho f_{jd} + \varphi_{jd} S_{jd}\right) \right] \\
& + \sum_{j\in\mathcal{J}} \theta_j \left[z_m^{jd} T_{jd} + \sum_{k\in\mathcal{K}_{jd}} x_{mk} t_k^1 - z_m^{oj} \left(t_m^0 + T_{oj} + f_{oj}\right) \right] \Bigg\} \\
& + \sum_{j\in\mathcal{J}} \theta_j \left[- \sum_{k\in\mathcal{K}_{oj}} x_{mk} t_k^2 - \sum_{i\in I} \left(\sum_{b\in\mathcal{B}_{ij}} x_{mb} t_b^2 + z_m^{ij} \left(T_{ij} + f_{ij}\right) + z_m^{oi} \left(t_m^0 + T_{oi} + f_{oi}\right) + \sum_{k\in\mathcal{K}_{oi}} x_{mk} t_k^1 \right) \right] \Bigg\}
\end{aligned} \tag{6.1}$$

s.t.

$$\sum_{a\in\mathcal{A}} \left(\sum_{k\in\mathcal{K}_{oa}} x_{mk} t_k^1 + z_m^{oa} L \right) \geq t_m^0 + u_o, \forall (o,d) \in \mathcal{W}, m \in \mathcal{M}_{od} \tag{6.2}$$

$$\begin{aligned}
\sum_{b\in\mathcal{B}_{ij}} x_{mb} t_b^1 + \left(1 - z_m^{ij} - \sum_{b\in\mathcal{B}_{ij}} x_{mb}\right) L \geq z_m^{oi} \left(t_m^0 + T_{oi} + f_{oi}\right) + \sum_{k\in\mathcal{K}_{oi}} x_{mk} t_k^1 + u_i, \\
\forall (o,d) \in \mathcal{W}, m \in \mathcal{M}_{od}, i \in \mathcal{I}, j \in \mathcal{J}
\end{aligned} \tag{6.3}$$

$$\begin{aligned}
\sum_{k\in\mathcal{K}_{jd}} x_{mk} t_k^1 + z_m^{jd} L \geq \sum_{b\in\mathcal{B}_{ij}} x_{mb} t_b^1 + z_m^{ij} \left(T_{ij} + f_{ij}\right) + z_m^{oi} \left(t_m^0 + T_{oi} + f_{oi}\right) + \sum_{k\in\mathcal{K}_{oi}} x_{mk} t_k^1 \\
+ \sum_{k\in\mathcal{K}_{oj}} x_{mk} t_k^2 + z_m^{oj} \left(T_{oj} + f_{oj}\right) + u_j, \forall (o,d) \in \mathcal{W}, m \in \mathcal{M}_{od}, j \in \mathcal{J}
\end{aligned} \tag{6.4}$$

$$\sum_{a\in A} \left(z_m^{oa} + \sum_{k\in\mathcal{K}_{oa}} x_{mk} \right) = 1, \forall (o,d) \in \mathcal{W}, m \in \mathcal{M}_{od} \tag{6.5}$$

$$\sum_{j\in J} \left(z_m^{jd} + \sum_{k\in\mathcal{K}_{jd}} x_{mk} \right) = 1, \forall (o,d) \in \mathcal{W}, m \in \mathcal{M}_{od} \tag{6.6}$$

$$\sum_{k\in\mathcal{K}_{oi}} x_{mk} + z_m^{oi} - \sum_{j\in\mathcal{J}} \left(\sum_{b\in B_{ij}} x_{mb} + z_m^{ij} \right) = 0, \forall (o,d) \in \mathcal{W}, m \in \mathcal{M}_{od}, i \in I \tag{6.7}$$

$$\sum_{k\in\mathcal{K}_{oj}} x_{mk} + z_m^{oj} + \sum_{i\in I}\left(\sum_{k\in\mathcal{K}_{oi}} x_{mk} + z_m^{oi} + \sum_{b\in\mathcal{B}_{ij}} x_{mb} + z_m^{ij}\right) - \sum_{k\in\mathcal{K}_{jd}} x_{mk} - z_m^{jd} = 0, \quad \forall (o,d)\in\mathcal{W}, m\in\mathcal{M}_{od}, j\in\mathcal{J} \tag{6.8}$$

$$\sum_{(o,d)\in\mathcal{W}}\sum_{m\in\mathcal{M}_{od}} w_m x_{mb} \le Y_b, \forall (o,d)\in\mathcal{W}, i\in\mathcal{I}, j\in\mathcal{J}, b\in\mathcal{B}_{ij} \tag{6.9}$$

$$\sum_{(o,d)\in\mathcal{W}}\sum_{m\in\mathcal{M}_{od}} v_m x_{mb} \le Q_b, \forall (o,d)\in\mathcal{W}, i\in\mathcal{I}, j\in\mathcal{J}, b\in\mathcal{B}_{ij} \tag{6.10}$$

$$\sum_{(o,d)\in\mathcal{W}}\sum_{m\in\mathcal{M}_{od}} w_m x_{mk} \le Y_k, \forall (o,d)\in\mathcal{W}, i\in\mathcal{I}, j\in\mathcal{J}, k\in\mathcal{K}_{oi}\cup\mathcal{K}_{jd} \tag{6.11}$$

$$\sum_{(o,d)\in\mathcal{W}}\sum_{m\in\mathcal{M}_{od}} v_m x_{mk} \le Q_k, \forall (o,d)\in\mathcal{W}, i\in\mathcal{I}, j\in\mathcal{J}, k\in\mathcal{K}_{oi}\cup\mathcal{K}_{jd} \tag{6.12}$$

$$x_{mk}, z_m^{oa}, z_m^{ij}, z_m^{jd} \in \{0,1\}, \forall (o,d)\in\mathcal{W}, m\in\mathcal{M}_{od}, a\in\mathcal{A}, i\in\mathcal{I}, j\in\mathcal{J} \tag{6.13}$$

The objective function (6.1) aims at the total operating cost of the air cargo transportation by summing the transporting cost and time costs. Constraints (6.2), (6.3) and (6.4) ensure the sufficient time so that cargo can be loaded to the assigned flights/buses before the flights/buses leaving. Constraints (6.5), (6.6), (6.7), and (6.8) ensure the cargo flow conservation in origin airports, destination airports, minor airports, and major airports, respectively. Constraints (6.9), (6.10), (6.11), and (6.12) state the weight and volume capacity constraints of flights and buses, respectively. Constraints (6.13) put binary restriction on the cargo allocation variables. Table 6.2 summarizes the key features of the proposed integer linear program (ILP) for modeling the cargo transfer problem inside a MAS.

Table 6.2: Characteristics of the proposed ILP for cargo transportation problem

Variables	**Size**	**Type**
The cargo-to-vehicle assignment: x_{mk}	$\sum_{(o,d)\in\mathcal{W}}\left[\lvert\mathcal{M}_{od}\rvert\left(\sum_{i\in\mathcal{I}}\lvert\mathcal{K}_{oi}\rvert+\sum_{j\in\mathcal{J}}\lvert\mathcal{K}_{jd}\rvert+\sum_{i\in\mathcal{I},j\in\mathcal{J}}\lvert\mathcal{B}_{ij}\rvert\right)\right]$	Binary
The cargo-to-ad hoc service assignment, including z_m^{oa}, z_m^{jd}, and z_m^{ij}	$\sum_{(o,d)\in\mathcal{W}}\left[\lvert\mathcal{M}_{od}\rvert\left(\lvert\mathcal{I}\rvert+\lvert\mathcal{I}\rvert\lvert\mathcal{J}\rvert+\lvert\mathcal{J}\rvert\right)\right]$	Binary
Objective function	**Size**	**Type**
Objective function defined in (6.1)	1	Linear
Constraints	**Size**	**Type**
Origin Departure Readiness Constraints (6.2)	$\sum_{(o,d)\in\mathcal{W}}\lvert\mathcal{M}_{od}\rvert$	Linear
Inter-trip sequencing constraints in the minor airports (6.3)	$\sum_{(o,d)\in\mathcal{W}}\lvert\mathcal{M}_{od}\rvert\lvert\mathcal{I}\rvert\lvert\mathcal{J}\rvert$	Linear
Inter-trip sequencing constraints in the major airports (6.4)	$\sum_{(o,d)\in\mathcal{W}}\lvert\mathcal{M}_{od}\rvert\lvert\mathcal{J}\rvert$	Linear
Flow conservation constraints in the origin airports (6.5)	$\sum_{(o,d)\in\mathcal{W}}\lvert\mathcal{M}_{od}\rvert$	Linear
Flow conservation constraints in the destination airports (6.6)	$\sum_{(o,d)\in\mathcal{W}}\lvert\mathcal{M}_{od}\rvert$	Linear
Flow conservation constraints in the minor airports in the MAS (6.7)	$\sum_{(o,d)\in\mathcal{W}}\lvert\mathcal{M}_{od}\rvert\lvert\mathcal{I}\rvert$	Linear
Cargo flow conservation constraints in the major airports in the MAS (6.8)	$\sum_{(o,d)\in\mathcal{W}}\lvert\mathcal{M}_{od}\rvert\lvert\mathcal{J}\rvert$	Linear
Truck weight capacity constraints (6.9)	$\sum_{(o,d)\in\mathcal{W}}\left[\lvert\mathcal{M}_{od}\rvert\sum_{i\in\mathcal{I},j\in\mathcal{J}}\lvert\mathcal{B}_{ij}\rvert\right]$	
Truck volume capacity constraints (6.10)	$\sum_{(o,d)\in\mathcal{W}}\left[\lvert\mathcal{M}_{od}\rvert\sum_{i\in\mathcal{I},j\in\mathcal{J}}\lvert\mathcal{B}_{ij}\rvert\right]$	Linear
Flight weight capacity constraints (6.11)	$\sum_{i\in\mathcal{I},j\in\mathcal{J}}\lvert\mathcal{B}_{ij}\rvert$	Linear
Flight volume capacity constraints (6.12)	$\sum_{i\in\mathcal{I},j\in\mathcal{J}}\lvert\mathcal{B}_{ij}\rvert$	Linear
Binary integrality constraints (6.13)	$\sum_{(o,d)\in\mathcal{W}}\left[\lvert\mathcal{M}_{od}\rvert\left(\sum_{i\in\mathcal{I}}\lvert\mathcal{K}_{oi}\rvert+\sum_{j\in\mathcal{J}}\lvert\mathcal{K}_{jd}\rvert+\sum_{i\in\mathcal{I},j\in\mathcal{J}}\lvert\mathcal{B}_{ij}\rvert\right)\right]$ $+\sum_{(o,d)\in\mathcal{W}}\left[\lvert\mathcal{M}_{od}\rvert\left(\lvert\mathcal{I}\rvert+\lvert\mathcal{I}\rvert\lvert\mathcal{J}\rvert+\lvert\mathcal{J}\rvert\right)\right]$	Linear

6.2.3 Solving framework

In the solving framework, for the root node and each generated node after each branching step, the LP relaxation is applied to get the solution of the relaxed program of the node, including both integer and non-integer values, also noted as the lower-bound solution of lower-bound solution of **P** 3. For the non-integer values, i.e., the inapplicable cargo-to-strategy assignments, a greedy algorithm is designed to reconsider the cargo assignments by first choosing available strategies in the basic strategies with the lowest cost, if all included vehicles have sufficient weight and volume capacities. Otherwise, the strategy with the lowest cost from the non-basic strategy set is selected to handle the cargo. After all the cargo have been allocated to strategies by either the commercial solver or the greedy algorithm, the cargo-to-strategy assignments and the corresponding total transportation cost serves as the upper-bound solution and the upper bound value of the optimal objective function of **P** 3, respectively. The cargo with the highest non-integer variable value in the lower-bound solution is chosen to generate branching rules for child nodes. Figure 6.1 shows the process of the solving framework.

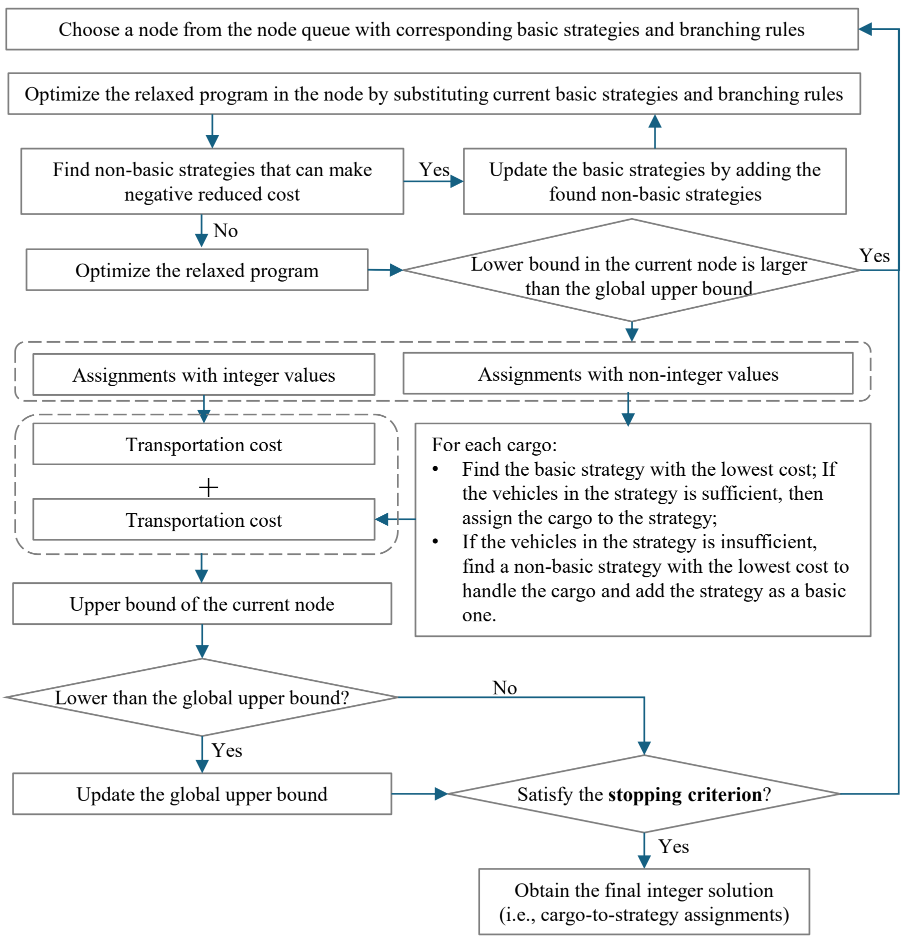

Figure 6.1: The process of the solving framework

6.2.3.1 Master problem and the reduced cost formulation

We use $\mathcal{G}_{od}$ to indicate all available strategies between OD pair (o, d) and divide it into $\mathcal{G}^1_{od}$ and $\mathcal{G}^2_{od}$ to represent the set of basic strategies and non-basic strategies, i.e., $\mathcal{G}_{od} = \mathcal{G}^1_{od} \cup \mathcal{G}^2_{od}$. It can be easily inferred that $|\mathcal{G}^1_{od}| < |\mathcal{G}_{od}|$ so that the only small fraction of the strategies between each OD pair is considered in the master problem. To efficiently solve the problem, we reformulate it as a cargo-to-strategy assignment (instead of cargo-to-vehicle assignment) and a strategy generation problem as **P** 4. Here, each strategy represents a column, comprising a specific combination of flights, buses, and possible ad hoc services between airports.

P 4.

$$\min_{\mathbf{x}} \sum_{(o,d)\in\mathcal{W}} \sum_{m\in\mathcal{M}_{od}} \sum_{g\in\mathcal{G}^1_{od}} C_{mg} x_{mg} \tag{6.14}$$

$$\sum_{g\in\mathcal{G}_m} x_{mg} = 1, \forall (o, d) \in \mathcal{W}, m \in \mathcal{M}_{od} \tag{6.15}$$

$$\sum_{(o,d)\in\mathcal{W}} \sum_{m\in\mathcal{M}_{od}} \sum_{g\in\mathcal{G}_m} w_m x_{mg} \delta_{gk} \leq Y_k, \forall k \in \mathcal{K} \tag{6.16}$$

$$\sum_{(o,d)\in\mathcal{W}} \sum_{m\in\mathcal{M}_{od}} \sum_{g\in\mathcal{G}_m} v_m x_{mg} \delta_{gk} \leq Q_k, \forall k \in \mathcal{K} \tag{6.17}$$

$$\sum_{(o,d)\in\mathcal{W}} \sum_{m\in\mathcal{M}_{od}} \sum_{g\in\mathcal{G}_m} w_m x_{mg} \delta_{gb} \leq Y_b, \forall b \in \mathcal{B} \tag{6.18}$$

$$\sum_{(o,d)\in\mathcal{W}} \sum_{m\in\mathcal{M}_{od}} \sum_{g\in\mathcal{G}_m} v_m x_{mg} \delta_{gb} \leq Q_b, \forall b \in \mathcal{B} \tag{6.19}$$

$$x_{mg} \in \{0, 1\}, \forall (o, d) \in \mathcal{W}, m \in \mathcal{M}_{od}, g \in \mathcal{G}^1_{od} \tag{6.20}$$

where

$$\begin{aligned}
C_{mg} = &\sum_{i\in\mathcal{I}} \left[\theta_o \left(\sum_{k\in\mathcal{K}_{oi}} x_{gk} \left(t^1_k - t^0_m\right) + z^{oi}_g T_{oi}\right) + \theta_i \left(\sum_{b\in\mathcal{B}_{ij}} x_{gb} t^1_b - z^{oi}_g \left(t^0_m + T_{oi} + f_{oi}\right) - \sum_{k\in\mathcal{K}_{oi}} x_{gk} t^2_k + z^{ij}_g T_{ij}\right) + w_m \left(\sum_{k\in\mathcal{K}_{oi}} \mu_k x_{gk} + \sum_{k\in\mathcal{K}_{jd}} \mu_k x_{gk}\right)\right] \\
&+ \sum_{j\in J} \left[\theta_o \left(\sum_{k\in\mathcal{K}_{oj}} x_{gk} \left(t^1_{k_1} - t^0_m\right) + z^{oj}_g T_{oj}\right)\right] \\
&+ \sum_{j\in J} \left[\theta_j \left(z^{jd}_m T_{jd} + \sum_{k\in\mathcal{K}_{jd}} x_{gk} t^1_k - z^{oj}_g \left(t^0_m + T_{oj} + f_{oj}\right) - \sum_{k\in\mathcal{K}_{oj}} x_{gk} t^2_k - \sum_{b\in B_{ij}} x_{gb} t^2_b - z^{ij}_g \left(T_{ij} + f_{ij}\right) - z^{oi}_g \left(t^0_m + T_{oi} + f_{oi}\right) - \sum_{k\in\mathcal{K}_{oi}} x_{gk} t^1_k\right)\right]
\end{aligned} \tag{6.21}$$

Let α_m be the dual variables of Constraints (6.15), β_k and β_b the dual variables of

Constraints (6.16) and (6.18), γ_k and γ_b the dual variables of Constraints (6.17) and (6.19). The reduced cost $\bar{C}_{mg}$ of the allocation of cargo m to strategy g can be formulated as:

$$\bar{C}_{mg} = C_{mg} - \alpha_m + \sum_{k \in \mathcal{K}} w_m \beta_k \delta_{gk} + \sum_{b \in \mathcal{B}} w_m \beta_b \delta_{gb} + \sum_{k \in \mathcal{K}} w_m \gamma_k \delta_{gk} + \sum_{b \in \mathcal{B}} w_m \gamma_b \delta_{gb} \tag{6.22}$$

6.2.3.2 Column generation

For every node generated from branching steps, the relaxed program with continuous variables between $[0, 1]$ is optimized by the commercial solver. Then for each OD pair, any strategy from the non-basic strategy set are added if the corresponding reduced cost of the assignment of any cargo to the strategy is negative. We use $\mathcal{G}_m$ to indicate the set of available transportation strategies of cargo m because not all strategies between the same OD pair as the cargo are applicable to carry cargo m. For instance, if the first flight in a strategy departs from the origin airport earlier than the arrival of a cargo, the strategy is obviously unavailable to handle the cargo. Therefore, in the column generation step, for each cargo, we focus only on a limited set of meaningful strategies rather than all options, when finding non-basic strategies that can make $\bar{C}_{mg} < 0$. For each OD pair, we use $\mathcal{G}^1_{od}$ and $\mathcal{G}^2_{od}$ to indicate the basic and non-basic strategy set between the OD pair. When applying the column generation, the number of non-basic strategies to search for a cargo m has been reduced from $\mathcal{G}^2_{od}$ to $\mathcal{G}_m \backslash \mathcal{G}^2_{od}$ which has obviously less elements. We define

$$\mathcal{G}^{'}_m = \left\{ g | g \in \mathcal{G}_m, \bar{C}_{mg} < 0 \right\} \tag{6.23}$$

and all found strategies $g \in \mathcal{G}^{'}_m$ are added to the basic strategy set of corresponding OD pair, i.e., $\mathcal{G}^1_{od} = \mathcal{G}^1_{od} \cup \mathcal{G}^{'}_m$. The relaxed program optimization and column generation are repeated until there are no more non-basic strategies can make the reduced cost be negative.

6.2.3.3 The root node generation and the global lower bound initialization

The solving framework in this study begins with generating a root node by utilizing a greedy algorithm and then branching it to child nodes. The basic strategy set in the root node is firstly generated by using a greedy algorithm by enumerate cargo and assign it to the most cost-saving strategy with sufficient vehicle capacities. We use the number "0" to represent the identity (id) of the root node. All chosen strategy in each OD pair compose the initial basic strategy set of the OD pair in the root node can be noted as $\mathcal{G}_{od}^{1,(0)}$. Those feasible strategies not included in $\mathcal{G}_{od}^{1,(0)}$ compose the non-basic strategy set, represented by $\mathcal{G}_{od}^{2,(0)}$. By substituting $\mathcal{G}_{od}^{1,(0)}$ into the relaxed program defined by Eqs.(6.14) - (6.19) and the relaxed binary integrality constraints (6.20) to the following constraints:

$$x_{mg} \in [0,1], \forall (o,d) \in \mathcal{W}, m \in \mathcal{M}_{od}, g \in \mathcal{G}_{od}, \tag{6.24}$$

and optimize the program by a commercial solver. The optimization of the relaxed master problem in the root node and column generation step are repeated until there is no new non-basic strategies can generate negative reduced costs and added to the basic strategy set. Then the relaxed program is optimized with the final version of basic strategies. The optimal objective value serves as the global lower bound (LB) of the ILP defined in **P** 3. If the values of variables in the optimal solution of the relaxed program are all integer, the objective value is also the upper bound as well as the optimal value of the original ILP defined in **P** 3. Otherwise, a greedy algorithm is applied to get the upper bound in the root node ($UB^{(0)}$). The details of the greedy algorithm is introduced in Section 6.2.3.5. The detailed in the root node generation are shown in the Algorithm 3.

Algorithm 3 The initialization of the root node and the global lower bound

Step 0: Initialization of global UB, LB and cargo-to-strategy assignments x

Set $UB = null$, $LB = null$, and $\mathbf{x} = null$.

Set $n = 0$ to indicate the identity(id) of the root node.

Step 1: Initialization of the root node

Set $BR^{(0)} \leftarrow$ empty List() to represent the branching rules in the root node.

Set $NQ \leftarrow$ empty Queue() to indicate the queue of node generated from branching.

Step 2: Initialization of basic strategies by a heuristic algorithm

for $(o, d) \in \mathcal{W}$ **do**

  Pick a cargo (denoted by $\hat{m}$) randomly from $\mathcal{M}_{od}$.

  Choose a strategy $g^* \leftarrow \arg\min_g \{C_{mg} | m \in \mathcal{M}_{od}, g \in \mathcal{G}_{od}\}$.

  if $g^* \notin \mathcal{G}_{od}^{1,(0)}$ **then**

    $\mathcal{G}_{od}^{1,(0)} = \mathcal{G}_{od}^{1,(0)} \cup g^*$.

  end if

end for

Step 3: Add new strategies between each OD pair to the basic strategy set (column generation)

Set $\mathcal{G}_{od}^{2,(0)} = \mathcal{G}_{od} \backslash \mathcal{G}_{od}^{1,(0)}$ for each $(o, d) \in \mathcal{W}$.

Set $\mathcal{G}' = \left\{g | \forall (o, d) \in \mathcal{W}, m \in \mathcal{M}_{od}, g \in \mathcal{G}_{od}^{2,(n)}, \bar{C}_{mg} < 0\right\}$.

while $|\mathcal{G}'| > 0$ **do**

  Optimize the relaxed program (Eqs. (6.14)-(6.19) and (6.24)) by substituting $\mathcal{G}_{od} := \mathcal{G}_{od}^{1,(0)}$.

  Update the dual variable values.

  for $(o, d) \in \mathcal{W}$ **do**

    for $m \in \mathcal{M}_{od}$ **do**

      Set $\mathcal{G}_m' = \{g | m \in \mathcal{M}_{od}, g \in \mathcal{G}_m, \bar{C}_{mg} < 0\}$

      if $|\mathcal{G}_m'| > 0$ **then**

        Update $\mathcal{G}_{od}^{1,(0)} = \mathcal{G}_{od}^{1,(0)} \cup \mathcal{G}_m'$

      end if

    end for

    Set $\mathcal{G}_{od}' = \{g | g \in \mathcal{G}_{od}^2, \exists m \in \mathcal{M}_{od}, \bar{C}_{mg} < 0\}$.

  end for

  Update $\mathcal{G}_{od}^{2,(n)} = \mathcal{G}_{od} \backslash \mathcal{G}_{od}^{1,(0)}$ for each $(o, d) \in \mathcal{W}$.

  Update $\mathcal{G}' = \left\{g | \forall (o, d) \in \mathcal{W}, m \in \mathcal{M}_{od}, g \in \mathcal{G}_{od}^{2,(n)}, \bar{C}_{mg} < 0\right\}$

end while

Step 4: Update the global upper bound and add the root node to the node queue

$LB \leftarrow$ the optimal value of the relaxed program defined in Eqs (6.14)-(6.19), (6.24) by substituting $\mathcal{G}_{od} := \mathcal{G}_{od}^{1,(0)}$.

Update $NQ \leftarrow [n] + NQ$

6.2.3.4 Branching steps

In the branching-and-price framework, we use a queue to include nodes with corresponding relaxed master problem, branching rules and upper bound values. We use integers $n \geq 0$ to represent the identity of nodes branching from the root nodes $BR^{(n)}$ is used to represent the branching rules in the node n, including the constraints of arbitrary values of variables indicate the branching rules of specific cargo-strategy pairs (assigned or not). The solving framework works beginning with adding the root node into the node queue.

Following the optimization of master problem in the root node with the final version of basic strategies in Section 6.2.3.3, the cargo-strategy pair with the non-integer variable value closest to 0.5 is chosen to branch to 3 child nodes. The child nodes include the branching rules setting (i) the cargo is assigned to the strategy; (ii) the cargo is assigned to the alternative strategy; and (iii) the cargo is assigned to neither the two strategies, respectively. The above 3 branched nodes are then added to the node queue.

6.2.3.5 The greedy algorithm for the upper bound update and cutting rules

When the linear relaxation produces fractional values for the binary assignment variables, we apply a greedy rounding heuristic. For each cargo within an OD pair, consider its basic strategies ordered by decreasing fractional value. Attempt to assign the cargo to the basic strategy with the largest fractional value, provided all vehicles in that strategy have sufficient residual capacity. If this strategy is infeasible, proceed to the basic strategy with the second-largest fractional value, and continue iteratively until a capacity-feasible basic strategy is identified.

If no basic strategy is feasible due to capacity limitations, we consider the non-basic strategies for the same OD pair, ordered by increasing cost, attempting to assign the cargo to the lowest-cost non-basic strategy with sufficient capacity. If this is infeasible, consider the second-lowest-cost non-basic strategy, and so forth, until a feasible option is identified. The selected non-basic strategy is then added into the basic strategy set for that OD pair. The ad hoc service is assumed to be sufficiently available, consequently, a feasible strategy can ultimately be found for every cargo.

After all cargo have been assigned (i.e., their corresponding binary variables are set to 1), the resulting cargo-to-strategy assignment constitutes a feasible solution. Its total transportation cost provides an upper bound (UB) on the objective value of problem **P** 3. Each time a node-specific UB is obtained, it is compared against the current best UB. If the UB of the node is smaller, the current best UB is updated to this value, and the best feasible integer solution is simultaneously updated to the node's cargo-to-strategy assignment. Otherwise, the current best UB remains unchanged, and the current best solution (i.e., the highest-quality feasible cargo-to-strategy assignment) is retained. In the subsequent branch-and-bound procedure, any node with corresponding relaxed master problem value (the node's lower bound) exceeding the current best UB is eliminated from further consideration.

6.2.3.6 Stopping criterion

The dimensionality of the proposed ILP for cargo transshipment within a MAS transfer hub is determined by the cargo throughput, the number of covered OD pairs, the flight frequencies for each airport pair, and the number of trucks on each minor–major airport link. When the instance size surpasses a practicable limit, the solution time for exact integer optimization exceeds the planning horizon (e.g., more than 24 hours for next-day operations), which materially reduces the operational relevance of exact solutions for day-ahead scheduling.

In view of the additional time required to prepare and complete downstream activities following generation of the cargo-to-strategy assignment (i.e., the mapping of consignments to specific transfer modes, flights, and truck movements), we impose a fixed computational budget of two hours. The best available integer solution at the termination of this time window is adopted as the finalized cargo-to-strategy assignment. More specifically, we employ a time-based termination criterion: if runtime exceeds a prescribed limit, the feasible solution associated with the current best upper bound is implemented as the definitive cargo-to-strategy assignment. The detailed steps in the solving framework is shown in Table 4.

Algorithm 4 The solving framework

while $|NQ| > 0$ **do**

Choose the first node with $id = n$ from NQ.

Set $UB^{(n)} = 0$ and $\mathbf{x} = \varnothing$.

Optimize the relaxed program (Eqs. (6.14)-(6.19) and (6.24)) by substituting $\mathcal{G}_{od} := \mathcal{G}_{od}^{1,(0)}$ and constraints included in $BR^{(n)}$.

Set $\mathcal{G}_{od}^{2,(0)} = \mathcal{G}_{od} \backslash \mathcal{G}_{od}^{1,(0)}$ for each $(o,d) \in \mathcal{W}$.

Set $\mathcal{G}^{'} = \left\{g|\forall(o,d) \in \mathcal{W}, m \in \mathcal{M}_{od}, g \in \mathcal{G}_{od}^{2,(n)}, \bar{C}_{mg} < 0\right\}$.

while $|\mathcal{G}^{'}| > 0$ or the computational time has not reached to 2 hours **do**

Optimize the relaxed program (Eqs. (6.14)-(6.19) and (6.24)) by substituting $\mathcal{G}_{od} := \mathcal{G}_{od}^{1,(0)}$ and constraints included in $BR^{(n)}$.

Update the dual variable values.

for $(o,d) \in \mathcal{W}$ **do**

Set $\mathcal{G}_{od}^{'} = \{g|g \in \mathcal{G}_{od}^{2}, \exists m \in \mathcal{M}_{od}, \bar{C}_{mg} < 0\}$.

if $|\mathcal{G}_{od}^{'}| > 0$ **then**

Update $\mathcal{G}_{od}^{1,(n)} = \mathcal{G}_{od}^{1,(n)} \cup \mathcal{G}_{od}^{'}$

end if

end for

Update $\mathcal{G}_{od}^{2,(n)} = \mathcal{G}_{od} \backslash \mathcal{G}_{od}^{1,(n)}$ for each $(o,d) \in \mathcal{W}$.

Update $\mathcal{G}^{'} = \left\{g|\forall(o,d) \in \mathcal{W}, m \in \mathcal{M}_{od}, g \in \mathcal{G}_{od}^{2,(n)}, \bar{C}_{mg} < 0\right\}$

end while

Set $\mathcal{MG}^{1,(n)} := \{(m,g)|x_{mg} = 1, \forall(o,d) \in \mathcal{W}, m \in \mathcal{M}_{od}, g \in \mathcal{G}_m\}$ to include cargo assignments with integer values.

Set $\mathcal{MG}^{2,(n)} := \{(m,g)|x_{mg} \in (0,1), \forall(o,d) \in \mathcal{W}, m \in \mathcal{M}_{od}, g \in \mathcal{G}_m\}$ to include cargo assignments with non-integer values.

for $(m,g) \in \mathcal{MG}^1$ **do**

$UB^{(n)} = UB^{(n)} + C_{mg}$; $\mathbf{x}^{(n)} = \mathbf{x}^{(n)} \cup x_{mg}$.

Set $x_{mg} = 1$ and $x_{mg'} = 0, \forall g \in \mathcal{G}_m, g' \neq g$.

end for

for $\hat{m} \in \left\{m|(m,g) \in \mathcal{MG}^{2,(n)}\right\}$ **do**

Let (o,d) denote the OD pair for cargo m.

Let $\mathcal{K}_g$ and $\mathcal{B}_g$ indicate the set of flights included in the strategy g.

if $\exists g \in \mathcal{G}_{od}^{1,(n)}$ that $\forall k \in \mathcal{K}_g, Y_k \geq w_{\hat{m}}, Q_k \geq v_{\hat{m}}$ and $\forall b \in \mathcal{B}_g, Y_b \geq w_{\hat{m}}, Q_b \geq v_{\hat{m}}$ **then**

Set $\hat{g} \leftarrow \arg\min_g \left\{C_{\hat{m}g}|g \in \mathcal{G}_{od}^{1,(n)}, \forall k \in \mathcal{K}_g, Y_k \geq w_{\hat{m}}, Q_k \geq v_{\hat{m}}, \forall b \in \mathcal{B}_g, Y_b \geq w_{\hat{m}}, Q_b \geq v_{\hat{m}}\right\}$

else

Set $\hat{g} \leftarrow \arg\min_g \left\{C_{\hat{m}g}|g \in \mathcal{G}_{od}^{2,(n)}, \forall k \in \mathcal{K}_g, Y_k \geq w_{\hat{m}}, Q_k \geq v_{\hat{m}}, \forall b \in \mathcal{B}_g, Y_b \geq w_{\hat{m}}, Q_b \geq v_{\hat{m}}\right\}$.

end if

Set $UB^{(n)} = UB^{(n)} + C_{\hat{m}\hat{g}}$; $x_{\hat{m}\hat{g}} = 1$ and $\mathbf{x} = \mathbf{x} \cup x_{\hat{m}\hat{g}}$.

end for

if $UB^{(n)} < UB$ **then**

Set $UB = UB^{(n)}$ and $\mathbf{x} = \mathbf{x}^{(n)}$

end if

Choose $(\hat{m}, \hat{g}) \leftarrow \arg\max_{m,g} \{(x_{mg} - 0.5)^2|(m,g) \in \mathcal{MG}^2\}$.

if $\{(\hat{m},g)|(\hat{m},g) \in \mathcal{MG}^2\}$ has more than two elements **then**

Choose $(\hat{m}, g') \in \mathcal{MG}^2, g' \neq \hat{g}$ that $x_{\hat{m}g'} > x_{\hat{m}g}, \forall g \in \{g|(m,g) \in \mathcal{MG}^2, m = \hat{m}\}$.

else

Choose $(\hat{m}, g') \in \mathcal{MG}^2, g' \neq \hat{g}$.

end if

Set $n_1 := n+1$, $BR^{(n_1)} = BR^{(n)} + [x_{\hat{m}\hat{g}} = 1, x_{\hat{m}g'} = 0]$.

Set $n_2 := n+2$, $BR^{(n_2)} = BR^{(n)} + [x_{\hat{m}\hat{g}} = 0, x_{\hat{m}g'} = 1]$.

Set $n_3 := n+3$, $BR^{(n_3)} = BR^{(n)} + [x_{\hat{m}\hat{g}} = 0, x_{\hat{m}g'} = 0]$.

Update $NQ \leftarrow [n_1, n_2, n_3] + NQ$

end while

6.3 Numerical studies

The Guangdong–Hong Kong–Macao Greater Bay Area (GBA) constitutes one of the world's densest MAS, integrating Guangzhou, Shenzhen, Foshan, Hong Kong, Macao, Huizhou and Zhuhai within a 1–2 hour ground travel catchment. The Hong Kong–Zhuhai–Macao Bridge (HZMB), together with high-speed rail and expressway corridors, enables time-reliable, short-haul inter-airport transfers of air cargo, effectively creating a connected air-side–landside network rather than isolated airport catchments. Hong Kong International Airport (HKIA) has been the world's busiest international cargo hub for decades and already has a certain level of market competitiveness. Despite commissioning the third runway in 2022, HKIA's capacity expansion remains constrained relative to the persistent growth of e-commerce, high-value manufacturing, and time-sensitive logistics. To avoid foregoing this rapidly expanding yet unmet cargo demand, HKIA should pursue cooperative arrangements with neighboring airports.

In this context, the GBA MAS is suited for a numerical study because it demonstrates: (i) multiple proximate international and secondary airports with complementary roles (HKIA, Guangzhou Baiyun International Airport, and Shenzhen Baoan International Airport serves as major airports while airports in Huizhou, Macau, Foshan, and Zhuhai are considered as minor airports); (ii) dedicated cross-boundary infrastructure (e.g., HZMB) that materially lowers transfer frictions; (iii) remarkable demand asymmetries (long-haul concentration at HKIA, regional capacity at Shenzhen/Guangzhou and limited international services at Zhuhai/Macao); and (iv) policy support (as introduced in Section 6.1) and regulatory and customs arrangements that increasingly facilitate intermodal and cross-airport cargo flows. These above-introduced features of the GBA MAS make it a realistic example in our study to test the performance of the proposed solving framework and investigate its applicability given heterogeneous values of transfer time in different airports.

6.3.1 Numerical settings

As the cargo demand for specific OD pairs are often not been published by the airports, we try to simulate the cargo demand to be transferred in the GBA MAS and flights serving these cargo demand according to some public data. In our study, the cargo is assume to be packed in unit load devices (ULD), so a cargo is refer to a ULD. Various ULD have different weight and volume range according to the specific transportation tasks. In this numerical experiment, we assume LD3/AKE as the ULD used in the air cargo transportation, whose max gross weight range from 1588-1700kg and volume range from 4.3-4.6m^3.

Most cargo between major airports is moved by standard semi-trailers (articulated trucks) due to their high capacity and compatibility with ULDs/pallets. Articulated trucks have volume range from 60-100m^3 and weight range from 20000-25000kg. Actual loaded weight may be less than the maximum payload if the cargo is bulky but light (volume-limited). With three parallel runways, HKIA aims to handle the maximum of 102 aircraft movements per hour[1]. For those cargo that cannot be handled by the scheduled flights/trucks, ad hoc services provided by third-party logistics companies can be used with a price of 0.02 USD/kg/hour. In summary, the system parameters are set as Table 6.3

[1]The data was published on https://www.info.gov.hk/gia/general/202102/24/P2021022400328.htm

Table 6.3: Parameter setting

System parameters	**Notations**	**Settings**
Ad-hoc service cost rate	φ	0.02 USD/kg/hour
Value of travel time	ρ	1 USD/hour
Value of dwell time in origin airports/minor airports	θ	0.5 USD/hour
Value of dwell time in origin/minor airports	θ_o, θ_i	0.5 USD/hour
Value of dwell time in major airports	θ_j	1 USD/hour
Flight time: origin airports → minor/major airports	T_{oi}, T_{oj}	3 hours
Flight time: major airports → destination airports	T_{jd}	5 hours
Flight time: minor airports → major airports	T_{ij}	3 hours
Ad-hoc response time: origin airports → minor airports	f_{oi}	4 hours
Ad-hoc response time: origin airports → major airports	f_{oj}	2 hours
Ad-hoc response time: minor airports → major airports	f_{ij}	1 hour
Ad-hoc response time: major airports → destination airports	f_{jd}	2 hours
Handling/loading time at origin/destination/minor/major airports	/	2 hours
Cargo demand Characteristics	**Notations**	**Settings**
Cargo weight	w_m	random integer in $[1000, 1500]kg$
Cargo volume	v_m	random real in $[4.3, 4.6]m^3$
Number of cargo per OD pair	/	Depends on specific scenarios, includes: 15, 20, 30, 40, 50
Cargo arrival time at origin airports	t_m^0	random integer in $[0, 15]$
Cargo flight characteristics	**Notations**	**Settings**
Aircraft weight capacity	Y_k	22000 kg
Aircraft volume capacity	Q_k	156 m^3
Headway between consecutive flights per OD pair	/	Depends on specific scenarios, includes: 6 h, 8 h and 12 h (daily, 00:00–24:00)
Truck characteristics	**Notations**	**Settings**
Truck weight capacity	Y_b	20000 kg
Truck volume capacity	Q_b	80 m^3
Truck headway (per minor–major airport pair)	/	Depends on specific scenarios, includes: 4 h, 6 h, 8 h

Apart from the above assumed parameters, some parameters will affect the results of transportation cost, including the number of cargo between each OD pair of airports and the frequency of flights and trucks between airports. Inspired by the cargo flights serving PVG and HKG[2], the flight frequency and capacity are assumed to abide by some reasonable distributions. As the demand data between specific OD pair is hard to obtain and sometimes refer to business privacy, we decide to assume the number of cargo demand according to the

[2]According to the cargo Cathy Pacific website (`https://www.cathaycargo.com/en-us/home.html`), There are 12 scheduled direct flights between the two cities with individual flights have varying days of operation. Different types of Boeing and Airbus aircraft are applied to serve the strategy. Various types of aircraft serve this route, the maximum capacity of weight and volume varies from 7000 to $24000kg$, and from 37 to $854m^3$.

total capacity of cargo flights in the system, i.e., we try to achieve that the cargo capacities will neither be excessively wasted nor obviously insufficient. We investigate the performance of our proposed solving framework under different scenarios defined by different cargo demand quantities and flight and truck frequencies.

6.3.2 Performance of the solving framework under different scenarios

6.3.2.1 Baselines: two heuristic algorithms

The transportation cost produced by MAS-Transfer Relax-and-Repair (MAS-RnR) is a valid upper bound on the optimal objective value of the original ILP formulation of the cargo transfer problem. We evaluate solution quality using the optimality gap between this upper bound and a lower bound which can be the exact ILP optimum or the result from the LP relaxation. Smaller (tighter) gaps indicate better performance.

To evaluate the upper bounds delivered by MAS-RnR, we compare against two heuristic allocation schemes that also generate feasible solutions (and hence upper bounds):

- **Random Allocation (RA).** Given the set of cargo demands to be transferred within the MAS, RA iteratively selects an unassigned cargo uniformly at random and assigns it to the feasible strategy (strategy-plan) with the lowest transportation cost under current capacities. The cumulative assignment cost provides an upper bound.

- **Greedy Regret (RGT)**. RGT differs from RA in its assignment order. For each unassigned cargo, it computes a regret score equal to the difference between the lowest-cost and second-lowest-cost feasible strategies (given current capacities) (Jeet & Kutanoglu, 2007). At each step, the cargo with the highest regret is selected and assigned to its lowest-cost feasible strategy. Regret scores are recomputed after every assignment. The resulting total cost is another upper bound.

The primary distinction between RA and RGT is the sequence in which cargo are allocated. Because transfer-strategy capacities within the MAS are limited, assignment order affects the availability of low-cost strategies and thus the quality of the final feasible solution. By comparing the upper bounds and corresponding optimality gaps obtained by RA, RGT, and MAS-RnR, we quantify the benefits of bound-aware, relax-and-repair decision-making under capacity constraints.

6.3.2.2 Numerical results under different instance sizes

Instance size is driven by the number of cargo demands and by the service frequencies of flights and cargo trucks. To assess MAS-RnR across diverse operating regimes, we construct scenarios that vary demand volume and flight/truck frequencies. Let Δt_1 denote the flight departure headway and Δt_2 the cargo-truck headway for each minor–major airport pair, and let N represent the number of cargo units (ULDs) to be transported per OD airport pair. We report UB_1 and UB_2 as the best upper bounds on total transportation cost obtained by MAS-RnR within 1 hour and 2 hours, respectively. Alongside the two heuristic baselines (RA and RGT), we employ the commercial solver Gurobi (Python API) to compute exact integer solutions when tractable. For all scenarios, we also solve the LP relaxation of the original ILP to obtain a lower bound used to benchmark optimality gaps. For each scenario, total transportation cost, computation time, and the resulting optimality gap are summarized in Table 6.4.

Table 6.4: Numerical results under different system settings

	Transportation cost (USD) (computaional time), gap[a]					
$(\Delta t_1, \Delta t_2, N)$	RA	RGT	Solver	LP relaxation	UB_1 (MAS-RnR)	UB_2 (MAS-RnR)
(12h, 8h, 10)	6086.7 (1s)	6086.7 (1s)	6086.7 (1s)	6086.7 (1s)	6086.7 (2s)	6086.7 (2s)
(12h, 8h, 15)	10349.6 (1s), 1.73%	10787.8 (2s) 6.04%	10173.2 (16s)	10171.2	10227.0, 0.53%	10226.0, 0.52%
(12h, 8h, 20)	17167.5 (1s), 3.20%	17009.3 (2s), 2.25%	/[b]	16635.5	16760.6, 0.75%	16760.6, 0.75%
(8h, 6h, 30)	20167.5 (7s), 4.04%	20145.0 (15s), 3.93%	/	19384.0	19624.1, 1.24%	19592.7, 1.08%
(8h, 6h, 40)	36033.2 (4s), 3.14%	35865.7 (10s), 2.67%	/	34935.7	35154.3, 0.63%	35106.2, 0.49%
(8h, 6h, 50)	52633.4 (16s), 2.53%	52370.8 (40s), 2.01%	/	51336.5	51607.4, 0.53%	51570.2, 0.46%
(6h, 4h, 30)	9692.6 (1.6s), 4.76%	10519.6 (5.7s), 13.7%	/	9252.0	9434.7, 1.97%	9416.2, 1.78%
(6h, 4h, 40)	23361.6 (0.4s) 6.04%	23361.6 (2.2s), 6.04%	/	22031.2	22381.7, 1.59%	22356.3, 1.48%
(6h, 4h, 50)	39015.5 (1.5s), 3.49%	39015.5 (18.2s), 3.49%	/	37701.4	38041.5, 0.90%	38041.5, 0.90%

[a] The optimality gap is computed as $(UB - LB)/LB \times 100\%$. If the commercial solver returns a integer solution within 12 hours, LB denotes the optimum reported by the solver. Otherwise, LB denotes the objective value of the LP relaxation, which is a valid lower bound but strictly less than or equal to the true optimal value of the original (integer) program.

[b] The symbol “/” means the commercial solver cannot come out a integer solution within 12 hours.

Based on the numerical results, MAS-RnR demonstrates strong performance in both solution quality and computational efficiency. Across the test scenarios, MAS-RnR method attains consistently small optimality gaps even on the largest and most structurally challenging instances. From a runtime perspective, MAS-RnR is competitive because it delivers near-optimal solutions within acceptable time, outperforming RA and RGT when they produce faster but lower-quality results, and providing high-quality feasible solutions in cases where the commercial solver fails to find any integer solution within 12 hours. This advantage is particularly valuable under strict time budgets. Taken together, these results indicate that MAS-RnR offers a reliable and scalable alternative in solving cargo transfer problem within MAS context to general-purpose solvers, delivering high-quality solutions rapidly and consistently across a wide range of problem instances.

6.4 Conclusion

This study examines cargo transfer within a MAS that integrates geographically adjacent minor and major airports into a coordinated transfer hub. Cargo can be strategyd either directly via major airports with international schedules or through air–ground–air itineraries that use inter-airport trucking between minor–major airport pairs. To reflect operational heterogeneity, we model distinct dwell time values at minor and major airports. The studied problem is formulated as an integer linear program that minimizes total transportation cost, comprising dwell-time-dependent transfer costs (i.e., monetary form of time costs) and costs associated with ad hoc capacity utilization. The program considers flight and truck weight/volume capacity limitations and time-feasibility constraints that preserve sequence consistency across air and ground legs.

The computational complexity is driven by the number of shipments and the frequency of flights and trucks. To solve large instances efficiently, we propose MAS-RnR, a branch-and-price-inspired framework with explicit algorithmic steps, including (1) Root node generation: A heuristic assigns each cargo to its lowest-cost strategy while temporarily ignoring capacity limits, creating a cost-efficient (but possibly capacity-violating) set of strategies that compose the initial basis; (2) Column generation: We iteratively solve a restricted master problem and find nonbasic strategies with negative reduced cost. Only a subset of candidate strategies is inserted each iteration to control problem size and accelerate solves; (3) Relaxation and repair: When no improving columns remain, we solve the restricted master as a linear relaxation. Fractional cargo-to-strategy assignments are repaired via a greedy reassignment to produce an integer solution and update the upper bound; (4) Branching: We branch on the cargo-to-strategy variable closest to 0.5. After each branching step, we repeat column generation, LP relaxation, and greedy repair to refine bounds per node; (5) Lower bounding: An LP relaxation of the full strategy model provides valid lower bounds for optimality-gap assessment.

Numerical experiments use scenarios informed by real-world data and controlled simulations that vary flight and truck frequencies and demand intensity. We benchmark MAS-RnR against two heuristic algorithms, RA and RGT, which differ in cargo selection order and strategy assignment logic while updating remaining capacities after each assignment. With 1-hour and 2-hour time limits, MAS-RnR consistently achieve smaller optimality gaps relative to commercial-solver optimum (when available) or LP-relaxation lower bounds, outperforming RA and RGT in solution quality while remaining computationally practical. In summary, the paper demonstrates the value of treating a MAS as a unified transfer hub for international air cargo and contributes a detailed optimization and algorithmic framework that integrates heterogeneous dwell times, joint air–ground routing, and scalable column generation with targeted branching and greedy repair. The results provide a guidance for designing and operating consolidated cargo hubs under capacity and time constraints.

This study has limitations. Firstly, we assume complete information, i.e., flight schedules and cargo demands are known and fixed during decision making. In practice, forwarders may lack full visibility into available flight capacity or shipment arrival time at origins, and operations are subject to unexpected disruptions. Extending the framework to explicitly model uncertainty, e.g., through stochastic programming, distributionally robust optimization, chance constraints, or robust column generation, may be more applicable to the real-world uncertain factors. We also focus on a single forwarder with unrestricted access to all feasible transfer strategies in the MAS. Homogeneity in resource access across airports, as well as contractual or slot constraints is assumed basically in this study. Future research could incorporate multi-agent settings with heterogeneous access rights and explore competition and cooperation among forwarders and airlines using bilevel and game-theoretic formulations. In addition, multi-stage decision processes could be introduced to handle sequential information revelation and interruptions (e.g., rolling-horizon re-optimization, and time-dependent ground congestion). These extensions would enhance the realism, and managerial relevance of MAS-based cargo transfer planning.

Chapter 7

Conclusion

7.1 Contributions and insights

This thesis advances the modeling and optimization of multi-airport systems (MAS) and intermodal competition by developing tractable analytical frameworks, scalable algorithms, and policy-relevant insights across four connected themes: passenger behavior and airline strategy in MAS with cross-airport transfers, stochastic management of unused belly capacity on passenger flights, competitive interactions between air transport and high-speed rail under heterogeneous traveler preferences, and integrated cargo transfer planning across minor–major airport pairs within a MAS. Collectively, these studies illuminate how pricing, capacity, congestion, ground connectivity, and uncertainty jointly shape system performance, and they provide decision support for airlines, airports, and policymakers seeking resilient and efficient operations.

This thesis investigates passenger behavior and airline decisions in a multi-airport system (MAS) comprising two major airports and a reliever airport linked to one of the majors via a ground connection, enabling cross-airport transfers. We develop tractable models to capture (i) passengers' route choices under elastic demand and (ii) airlines' airfare setting and investment in ground connections under both non-cooperative and cooperative game-theoretic settings.

On the demand side, passengers can: (1) fly directly via either major airport, (2) air travel via the reliever airport and transfer to the connected major airport through ground traffic, or (3) choose other modes (elastic demand). We characterize the passenger choice equilibrium and show that lower airfares, shorter travel times, and larger capacities on any path increase its flow, divert passengers away from alternatives, and reduce the market's minimum generalized travel price. Because congestion externalities are stronger on paths involving cross-airport transfers, the equilibrium is sensitive to capacity and time improvements on the ground connection: investments that shorten transfer times shift demand toward the reliever–major path.

On the supply side, we propose bi-level models to determine optimal airfares and ground-connection investments. Under a three-airline Nash game without ground-investment decisions, the airlines serving the unconnected major airport and the reliever airport operate on the elastic segment of their demand curves. Introducing cooperation via a Nash bargaining game between the airline serving the reliever airport, and the airline at the connected major airport and simultaneous Nash competition with the airline serving the other major airport, reveals that optimal fares and profits depend critically on the interdependence of passenger flows between the two competing paths. When ground-investment decisions are endogenous, non-cooperative airlines invest more in the ground connection when their own airport is congested and the linked airport is relatively uncongested. Under cooperation between the airlines serving the connected major and reliever airports, both invest more when the connected major airport becomes congested, applying the reliever–major connection to alleviate bottlenecks and accommodate additional demand.

A numerical study focused on the Greater Bay Area, Zhuhai Jinwan Airport (reliever), Guangzhou Baiyun International Airport (independent major), and Hong Kong International Airport (connected major), confirm these insights across different market structures, congestion sensitivities, and bargaining powers. Cooperation between the airlines serving connected major and reliever airports raises the profits of both cooperating partners and, through rebalanced competition, can also benefit the non-cooperating airline. Enhancing the ground connection consistently increases MAS-wide profits and boosts demand on the transfer route under both cooperative and non-cooperative regimes. Sensitivity analyses underscore the strategic value of congestion relief provided by the reliever airport and its ground link: stronger relief generates higher profits, attracts larger investments by the connected major, and strengthens the competitiveness of the cooperating airline pair.

Managerial implications are threefold. First, airlines serving a connected major–reliever airport pair should pursue cooperation to unlock joint gains from coordinated pricing and targeted ground investments. Second, airlines at relatively independent major airports should proactively explore partnerships to avoid profit loss when neighbor rival airports cooperate. Third, when cooperation exists, greater bargaining power not only secures a larger surplus share but also translates into stronger investment commitments to the ground connection, amplifying the cooperative advantage.

In managing unused belly capacity for cargo, this thesis develops a decision framework for exploiting unused belly capacity on passenger flights to transport air cargo, delivering cost and flexibility advantages while explicitly accounting for operational uncertainty. We model uncertainties in cargo weights, cargo arrival times, available flight capacity, and schedule disturbance, and we structure decisions across two timescales, i.e., mid-term capacity reservations and short-term cargo-to-flight allocations.

Methodologically, we formulate a two-stage stochastic program and employ Sample Average Approximation to approximate expectations with finite scenario sets. We solve the resulting problem using Progressive Hedging to coordinate first-stage reservation decisions with second-stage allocation responses, ensuring cross-scenario consistency. Several tailored heuristics furnish strong upper bounds within PH subproblems, obtaining high-quality solutions and practical computational times. This integrated approach produces capacity reservation and allocation policies that are both efficient and robust to the key sources of uncertainty faced by airlines.

Using HKIA as the origin and eight destinations, we tested convergence and solution quality. With 500 scenarios, objective values differed by under 2% from 400-scenario runs, and in-sample vs. out-of-sample gaps ranged from 0.6% to 5.2%, indicating stable, reliable capacity reservations. Sensitivity tests on post-reservation unit revenue show consistent cost savings over a no–two-stage baseline, with especially large gains when marginal revenue per unit of additional belly capacity is higher. Overall, the two-stage framework proves effective and economically robust across revenue conditions.

As high-speed rail (HSR) connectivity between Hong Kong and Mainland China expands, its interaction with established air transport (AT) is reshaping intercity travel markets. Although prior studies examine air–rail competition, they often overlook differences in travelers' inherent preferences. This study addresses that gap by developing a Hotelling-based framework that explicitly models preference diversity and analyzes strategic pricing and capacity decisions for AT and HSR within a tractable bi-level structure. The upper level covers two institutional settings, both operators maximizing profit, and a mixed setting in which AT maximizes profit while HSR optimizes a weighted objective combining profit and social welfare, while the lower level places travelers along a continuous preference spectrum to get intuitive, closed-form mode-choice results.

The analysis shows that price and capacity decisions have clear cross-modal effects: raising prices or limiting capacity for one mode reduces its demand and shifts travelers to the other, whereas lowering prices or expanding capacity attracts travelers toward the improved option. Under profit-maximizing competition, optimal fares and profits depend strongly on the distribution of traveler preferences. Ignoring this heterogeneity or assuming uniform tastes leads to systematically weaker pricing strategies and missed revenue. Capacity choices and congestion interact with preference diversity, strengthening or weakening the impact of pricing moves depending on market composition.

Numerical experiments support these findings and quantify the main drivers. In competitive settings, a mode's optimal price reacts more to the rival's parameters than to its own demand-side parameters, while its own operating costs matter much more than the competitor's costs. Price competition is most effective when a sizable neutral segment exists. Moderate fare increases can benefit modes with loyal customer bases, whereas fare reductions generally raise consumer surplus. In markets with strong loyalty to one mode, aggressive undercutting can destabilize the rival and threaten financial feasibility. In more balanced markets, gradual price adjustments enable smoother substitution between air and HSR and promote fair, sustainable competition.

This thesis investigates cargo transfers in a MAS that coordinates geographically proximate minor and major airports as a unified transfer hub. Shipments can move either directly via major airports with international schedules or through air–ground–air itineraries that include inter-airport trucking between minor–major pairs. To capture operational differences, we assign distinct dwell times to minor and major airports. We formulate the planning problem as an integer linear program that minimizes total transportation cost, combining dwell-time-dependent transfer costs, representing the monetary value of time and costs associated with ad hoc capacity usage. The model enforces weight and volume limits on flights and trucks and applied time-feasibility constraints that maintain sequence consistency across air and ground legs.

Because computational complexity scales with the number of shipments and the frequency of flights and trucks, we develop MAS-RnR, a branch-and-price-inspired solution framework tailored to large instances. The method constructs an initial basis by assigning each shipment to its lowest-cost strategy while temporarily ignoring capacities, then iteratively performs column generation to add promising strategies with negative reduced cost. When no improving columns remain, a linear relaxation is solved and fractional assignments are repaired via a targeted greedy procedure to obtain high-quality integer solutions and update upper bounds. Branching on near-fractional cargo-to-strategy variables, followed by repeated column generation and repair, refines bounds at each node, while an LP relaxation of the full strategy space provides valid lower bounds to assess optimality gaps. This combination of restricted master solves, selective column insertion, and structured repair maintains tractability without sacrificing solution quality.

Numerical experiments using data-informed and simulated scenarios—varying flight and truck frequencies and demand intensity—demonstrate that MAS-RnR delivers consistently smaller optimality gaps than benchmark heuristics that assign cargo sequentially with capacity updates. Within one- and two-hour time limits, MAS-RnR outperforms these baselines in solution quality while remaining computationally practical, and it compares favorably against commercial solver optima when available or against LP-relaxation lower bounds when exact solutions are out of reach. The results underscore the operational value of treating a MAS as a consolidated transfer hub for international air cargo and show the importance of modeling heterogeneous dwell times alongside joint air–ground routing.

Overall, the thesis advances theory and practice across passenger and cargo operations in multi-airport and multimodal systems. It develops a tractable framework for demand–supply interactions in multi-airport systems with cross-airport transfers, yielding testable predictions on fares, flows, and investment under alternative competitive structures and offering actionable guidance for integrated air–ground strategies to alleviate congestion and enhance system performance. It addresses uncertainty in belly cargo planning by modeling stochastic cargo demand and flight capacity, and proposes an efficient solution, combining decomposition methods and modified heuristics that delivers high-quality solutions and provides a substantive methodological and practical contribution to air cargo by passenger operations. It introduces an analytically air–rail competition model that considers heterogeneous traveler preferences to inform pricing and capacity decisions under varied market compositions and policy objectives, supporting evaluations that balance commercial outcomes with social welfare. Finally, it contributes an optimization and algorithmic framework for scalable planning of cargo flows across connected airports under tight capacity and time constraints, offering clear guidance on when air–ground–air strategies and targeted capacity deployment reduce costs and improve throughput relative to direct-air-only options.

7.2 Limitations and future study

Across the studies, several simplifying assumptions enable analytical tractability and scalable computation but limit external validity. Some models stylize the Greater Bay Area (GBA) multi-airport system as a three-airport network and treat traveler preferences as homogeneous. While this captures key mechanisms, the GBA contains more airports and more complex cooperation–competition patterns among airlines and airport authorities. Future work should examine richer MAS configurations with multiple reliever airports, denser inter-airport connections, and explicit modeling of ground access and air–ground service design. Incorporating multi-class passenger heterogeneity, price sensitivity, and schedule valuation—supported by stated-preference and revealed-preference data—would better reflect diverse travel behaviors and sharpen policy and operational insights. Extending the scope from proximate airports to markets that include more distant airports would also broaden applicability.

On the cargo side, several studies assume independence across origin–destination pairs, effectively decomposing multi-leg routes into disjoint segments and underrepresenting network effects such as consolidation, flow coupling, and re-routing. Relaxing this assumption via network flow formulations with interdependent OD flows and allowing transfers across multiple OD pairs would yield a more realistic view of capacity allocation and routing, especially for long-haul or low-frequency services. Because belly cargo shares capacity with passenger baggage, an integrated passenger–cargo planning framework—co-optimizing schedules, capacities, and allocations—merits attention. The current focus is primarily on airline/forwarder decisions. Future work should bring airports into the optimization loop, examining their roles in investing in ground connectivity, managing unused capacity across multiple airports, and coordinating with airlines under cooperative or competitive arrangements.

Several modeling choices can be refined to better align with market realities. The opportunity cost of unused capacity is treated as linear and constant at the margin, which may overstate benefits when supply exceeds demand. Future research could adopt demand-dependent, saturating, or capped opportunity-cost functions calibrated to market absorption. Likewise, the role of ad hoc capacity providers, e.g., chartered freighters that supplement belly capacity—deserves explicit treatment, including pricing, availability, and contracting mechanisms. Investigating dynamic pricing for capacity sales and the interaction with ad hoc services could uncover economically efficient and operationally robust policies.

Data availability remains a constraint. Some numerical experiments rely on assumed parameters and functional forms due to limited access to operational data on flight capacity, shipment arrivals, and traveler preferences. As data-sharing opportunities expand, assembling datasets that combine flight schedules, load factors, cargo demand traces, trucking schedules, and passenger survey evidence will enable empirical validation, structural estimation, and data-driven calibration. Such efforts can support external validity checks, counterfactual analyses, and the derivation of implementable planning rules.

Methodologically, several extensions can enhance realism and decision support. Many formulations assume complete information and deterministic inputs, whereas actual operations face shipment arrival uncertainty, capacity volatility, disruptions, and time-dependent ground congestion. Stochastic programming, distributionally robust optimization, chance constraints, robust column generation, and rolling-horizon re-optimization can represent uncertainty and sequential information revelation. Multi-agent settings with heterogeneous access rights, slot constraints, and contractual frictions would allow the study of competition and cooperation among forwarders, airlines, and airports using bi-level, equilibrium, and game-theoretic models. For passenger markets, advancing from representative-agent models to preference-segmented or continuous-distribution models, and exploring price discrimination by segment and itinerary, would yield richer pricing and investment implications. Finally, integrating the proposed optimization and algorithmic frameworks into decision-support tools, validated on real operations, is a practical next step to translate these research findings into operational impact.

Declaration of Generative AI and AI-assisted technologies in the writing process

During the preparation of this work, the authors used ChatGPT in order to polish some of the words, sentences, and grammar to improve the overall readability of the article. After using this tool/service, the authors reviewed and edited the content as needed and takes full responsibility for the content of the publication.

Chapter 8

Appendices

8.1 Proof of UE solution existence and uniqueness by proving the equivalent minimization program solution uniqueness

8.1.1 Proof of equivalent UE minimization program

We briefly show that the minimization program defined in Eq. (3.7) is equivalent to UE condition defined in Eq. (3.5) by proving that the first-order condition of the corresponding Lagrange function of Eq. (3.7) is the same as Eq. (3.5).

$$
\begin{aligned}
\mathcal{L}(q_1, q_2, q_3, q, \lambda) =& \frac{1}{2} \sum_{m,m' \in \{1,3\}, m \neq m'} \left(\int_0^{q_m} p_m(\omega, q_{m'}) d\omega + \int_0^{q_m} p_m(\omega, 0) d\omega \right) \\
&+ \int_0^{q_2} p_2(\omega) d\omega - \int_0^{q} F(\omega) d\omega + \lambda \left(q - \sum_{m=1,2,3} q_m \right)
\end{aligned} \tag{8.1}
$$

subject to

$$q_m \geq 0, m = 1, 2, 3 \tag{8.2a}$$

$$q \geq 0 \tag{8.2b}$$

where λ is the Lagrange multiplier associated with Constraint (3.5d); $F(\cdot)$ is inverse demand function, i.e., $F(\cdot) = q^{-1}(\cdot)$. The KKT conditions are as follows:

$$\frac{\partial \mathcal{L}}{\partial q_1} = p_1(q_1, q_3) - \lambda \geq 0; q_1 \geq 0; q_1(p_1(q_1, q_3) - \lambda) = 0; \tag{8.3a}$$

$$\frac{\partial \mathcal{L}}{\partial q_2} = p_2(q_2) - \lambda \geq 0; q_2 \geq 0; q_2(p_2(q_2) - \lambda) = 0; \tag{8.3b}$$

$$\frac{\partial \mathcal{L}}{\partial q_3} = p_3(q_3, q_1) - \lambda \geq 0; q_3 \geq 0; q_3(p_3(q_3, q_1) - \lambda) = 0; \tag{8.3c}$$

$$\frac{\partial \mathcal{L}}{\partial q} = \lambda - F(q) \geq 0; q \geq 0; q(\lambda - F(q)) = 0; \tag{8.3d}$$

$$\frac{\partial \mathcal{L}}{\partial \lambda} = q - \sum_{m=1,2,3} q_m = 0 \tag{8.3e}$$

Considering the λ as the minimum travel price, i.e., $\lambda = p^* = min\{p_m\}, m = 1, 2, 3$, and the total demand q between the given OD pair is positive, Eq. (8.3) is equivalent to Eq. (3.5). This completes the proof.

8.1.2 Proof of UE solution existence and uniqueness

To prove the existence of the UE solution, we prove (i) the domain for the objective function of the equivalent minimization program defined in Eq. (3.7) is compact and convex, and (ii) the objective function is continuous and quasi-concave with respect to each variable. First, it is readily seen that the domain space is $\omega = S_1 \times S_2 \times S_3 \times S_4$ is compact and convex as the set where $S_1 = \{q_1 : q_1 \geq 0\}$, $S_2 = \{q_2 : q_2 \geq 0\}$, $S_3 = \{q_3 : q_3 \geq 0\}$, and $S_4 = \{q : q \geq 0\}$ are all convex and compact, so is their Cartesian product ω. We rewrite the objective function as:

$$z(\boldsymbol{q}) = \frac{1}{2}\left(\int_0^{q_1} p_1(\omega, q_3)d\omega + \int_0^{q_1} p_1(\omega, 0)d\omega\right) + \frac{1}{2}\left(\int_0^{q_3} p_3(\omega, q_1)d\omega + \int_0^{q_3} p_3(\omega, 0)d\omega\right) + \int_0^{q_2} p_2(\omega)d\omega - \int_0^{q} F(\omega)d\omega \tag{8.4}$$

The objective function is continuous because the travel full prices and elastic demand are defined as continuous function.

The concavity of the objective function is proved by showing that the Hessian matrix of the objective function in Eq. (3.7) is positive definite. The Hessian matrix is as follows:

$$\mathbf{H} = \begin{bmatrix} 2d'_{i,q_1} + T'_{i,V_i} & 2d'_{i,q_3} + T'_{i,V_i} & 0 & 0 \\ d'_{i,q_1} + T'_{i,V_i} & d'_{i,q_3} + d'_{k,q_3} + T'_{i,V_i} + T'_{k,V_k} & 0 & 0 \\ 0 & 0 & 2d'_{j,q_2} + T'_{j,V_j} & 0 \\ 0 & 0 & 0 & -F'(q) \end{bmatrix} \tag{8.5}$$

As shown in Eq. (8.5), **H** is a block diagonal matrix, and can be readily shown to be positive definite if the following inequalities hold:

$$\begin{aligned} &\begin{vmatrix} 2d'_{i,q_1} + T'_{i,V_i} & 2d'_{i,q_3} + T'_{i,V_i} \\ d'_{i,q_1} + T'_{i,V_i} & d'_{i,q_3} + d'_{k,q_3} + T'_{i,V_i} + T'_{k,V_k} \end{vmatrix} \\ &= 2d'_{i,q_1}\left(d'_{k,q_3} + T'_{k,V_k}\right) + T'_{i,V_i}\left(d'_{k,q_3} + T'_{k,V_k} + d'_{i,q_1} - d'_{i,q_3}\right) > 0 \end{aligned} \tag{8.6a}$$

because it can be proved easily that

$$\begin{vmatrix} 2d'_{j,q_2} + T'_{j,V_j} & 0 \\ 0 & -F'(q) \end{vmatrix} = -F'(q)\left(4d'_{j,Q_j} + T'_{j,V_j}\right) > 0 \tag{8.6b}$$

Therefore, if Condition (8.7) holds, the objective function in Eq. (3.7) is strictly convex and has a unique optimal solution, indicating the UE condition defined at Eq. (3.5) has a unique solution. This completes the discussion of solution existence and uniqueness of UE condition defined in Eq. (3.5).

$$2d'_{i,q_1}\left(d'_{k,q_3} + T'_{k,V_k}\right) + T'_{i,V_i}\left(d'_{k,q_3} + T'_{k,V_k} + d'_{i,q_1} - d'_{i,q_3}\right) > 0 \tag{8.7}$$

8.1.3 Derivation of the comparative statics results

At an interior equilibrium, for path from O to D through Airport i, i.e., Path 1, we have

$$\tau_{oi} + \alpha t_{oi} + 2d_i\left(q_1, q_3, C_i\right) + T_i(q_1 + q_3) + \tau_{id} + \alpha t_{id} = p \tag{8.8}$$

For path from O to D through Airport j, i.e., Path 2, the travel price at equilibrium satisfies:

$$\tau_{oj} + \alpha t_{oj} + 2d_j(q_2, C_j) + T_j(q_2) + \tau_{jd} + \alpha t_{jd} = p \tag{8.9}$$

Travel price of Path 3, i.e. from O to D through Airport i and k at equilibrium satisfies:

$$\tau_{ok}+\alpha t_{ok}+d_k(q_3, C_k)+T_k(q_3)+\tau_{ki}+\alpha t_{ki}+T_i(q_1+q_3)+d_i(q_1, q_3, C_i)+\tau_{id}+\alpha t_{id} = p \tag{8.10}$$

Besides, the flow conservation at equilibrium can be denoted as:

$$q_1 + q_2 + q_3 = q \tag{8.11}$$

Based on the user equilibrium conditions above, we can derive the following equations related to the derivatives of passenger flows and minimum travel cost with regard to τ_{oi}:

$$1 + \left(2d^{'}_{i,q_1} + T^{'}_{i,V_i}\right)\frac{\partial q_1}{\partial \tau_{oi}} + \left(2d^{'}_{i,q_3} + T^{'}_{i,V_i}\right)\frac{\partial q_3}{\partial \tau_{oi}} = \frac{\partial p}{\partial \tau_{oi}} \tag{8.12a}$$

$$\left(2d^{'}_{j,q_2} + T^{'}_{j,V_j}\right)\frac{\partial q_2}{\partial \tau_{oi}} = \frac{\partial p}{\partial \tau_{oi}} \tag{8.12b}$$

$$\left(2d^{'}_{i,q_1} + T^{'}_{i,V_i}\right)\frac{\partial q_1}{\partial \tau_{oi}} + \left(d^{'}_{k,q_3} + T^{'}_{k,V_k} + d^{'}_{i,q_3} + T^{'}_{i,V_i}\right)\frac{\partial q_3}{\partial \tau_{oi}} = \frac{\partial p}{\partial \tau_{oi}} \tag{8.12c}$$

$$\frac{\partial q_1}{\partial \tau_{oi}} + \frac{\partial q_2}{\partial \tau_{oi}} + \frac{\partial q_3}{\partial \tau_{oi}} = q^{'}\frac{\partial p}{\partial \tau_{oi}} \tag{8.12d}$$

From the above equations, we can solve that

$$\frac{\partial p}{\partial \tau_{oi}} = \frac{\left(2d'_{j,q_2}+T'_{j,V_j}\right)\left(2d'_{i,q_1}+T'_{i,V_i}\right)\left(d'_{k,q_3}+T'_{k,V_k}+d'_{i,q_3}-d'_{i,q_1}\right)}{2d'_{i,q_1}\left\{\left(d'_{k,q_3}+T'_{k,V_k}+d'_{i,q_1}-d'_{i,q_3}\right)\left(2d'_{j,q_2}+T'_{j,V_j}\right)+\left[-q'\left(2d'_{j,q_2}+T'_{j,V_j}\right)+1\right]\left[2d'_{i,q_1}\left(d'_{k,q_3}+T'_{k,V_k}\right)+T'_{i,V_i}\left(d'_{k,q_3}+T'_{k,V_k}+d'_{i,q_1}-d'_{i,q_3}\right)\right]\right\}} \tag{8.13a}$$

$$\frac{\partial q_1}{\partial \tau_{oi}} = \frac{-2d'_{i,q_1}\left(d'_{k,q_3}+T'_{k,V_k}+d'_{i,q_1}-d'_{i,q_3}\right)\left(2d'_{j,q_2}+T'_{j,V_j}\right)+\left[q'\left(2d'_{j,q_2}+T'_{j,V_j}\right)-1\right]\left\{\left(d'_{k,q_3}+T'_{k,V_k}\right)\left[2d'_{i,q_1}\left(d'_{k,q_3}+T'_{k,V_k}\right)+T'_{i,V_i}\left(d'_{k,q_3}+T'_{k,V_k}+d'_{i,q_3}-d'_{i,q_1}\right)\right]\right\}}{2d'_{i,Q_i}\left(d'_{k,q_3}+T'_{k,V_k}+d'_{i,q_1}-d'_{i,q_3}\right)\left\{\left(d'_{k,q_3}+T'_{k,V_k}+d'_{i,q_1}-d'_{i,q_3}\right)\left(2d'_{j,q_2}+T'_{j,V_j}\right)+\left[-q'\left(2d'_{j,q_2}+T'_{j,V_j}\right)+1\right]\left[2d'_{i,q_1}\left(d'_{k,q_3}+T'_{k,V_k}\right)+T'_{i,V_i}\left(d'_{k,q_3}+T'_{k,V_k}+d'_{i,q_1}-d'_{i,q_3}\right)\right]\right\}} \tag{8.13b}$$

$$\frac{\partial q_2}{\partial \tau_{oi}} = \frac{\left(2d'_{i,q_1}+T'_{i,V_i}\right)\left(d'_{k,q_3}+T'_{k,V_k}+d'_{i,q_3}-d'_{i,q_1}\right)}{2d'_{i,q_1}\left\{\left(d'_{k,q_3}+T'_{k,V_k}+d'_{i,q_1}-d'_{i,q_3}\right)\left(2d'_{j,q_2}+T'_{j,V_j}\right)+\left[-q'\left(2d'_{j,q_2}+T'_{j,V_j}\right)+1\right]\left[2d'_{i,q_1}\left(d'_{k,q_3}+T'_{k,V_k}\right)+T'_{i,V_i}\left(d'_{k,q_3}+T'_{k,V_k}+d'_{i,q_1}-d'_{i,q_3}\right)\right]\right\}} \tag{8.13c}$$

$$\frac{\partial q_3}{\partial \tau_{oi}} = \frac{\left[-q'\left(2d'_{j,q_2}+T'_{j,V_j}\right)+1\right]\left[2d'_{i,q_1}\left(2d'_{i,Q_i}+T'_{i,V_i}\right)\right]+\left(d'_{k,q_3}+T'_{k,V_k}+d'_{i,q_1}-d'_{i,q_3}\right)\left(2d'_{j,q_2}+T'_{j,V_j}\right)}{\left(d'_{k,q_3}+T'_{k,V_k}+d'_{i,q_1}-d'_{i,q_3}\right)\left\{\left(d'_{k,q_3}+T'_{k,V_k}+d'_{i,q_1}-d'_{i,q_3}\right)\left(2d'_{j,q_2}+T'_{j,V_j}\right)+\left[-q'\left(2d'_{j,q_2}+T'_{j,V_j}\right)+1\right]\left[2d'_{i,q_1}\left(d'_{k,q_3}+T'_{k,V_k}\right)+T'_{i,V_i}\left(d'_{k,q_3}+T'_{k,V_k}+d'_{i,q_1}-d'_{i,q_3}\right)\right]\right\}} \tag{8.13d}$$

It can be easily get that $\frac{\partial q_1}{\partial \tau_{oi}} < 0$ and $\frac{\partial q_3}{\partial \tau_{oi}} > 0$ while $\frac{\partial q_2}{\partial \tau_{oi}}$ and $\frac{\partial p}{\partial \tau_{oi}}$ are positive only when

$$d'_{k,q_3} + T'_{k,V_k} + d'_{i,q_3} - d'_{i,q_1} > 0. \tag{8.14}$$

$d'_{k,q_3} + T'_{k,V_k} + d'_{i,q_3}$ means the marginal increase of congestion delay cost (d_k), transfer cost (T_k) in Airport k, and congestion delay cost in Airport i (d_i) caused by an additional passenger on Path 3. d'_{i,q_1} means the marginal increase of congestion delay cost (d_i) in Airport i caused by an additional passenger on Path 3. Condition [8.14] means that given the existing distribution of passenger flows, the inclusion of an additional passenger on Path 3 exerts a higher marginal increase of the overall travel cost of Path 3 compared to the increase of delay cost and transfer cost in Airport i caused by additional passenger on Path 1 on the total travel cost of Path 1.

For total airfare of travel link id, i.e., τ_{id},

$$\frac{\partial p}{\partial \tau_{id}} = \frac{\left(2d'_{j,q_2}+T'_{j,V_j}\right)\left(d'_{k,q_3}+T'_{k,V_k}+d'_{i,q_1}-d'_{i,q_3}\right)}{2d'_{i,Q_i}\left(2d'_{j,q_2}+T'_{j,V_j}\right)\left(d'_{k,q_3}+T'_{k,V_k}+d'_{i,q_1}-d'_{i,q_3}\right)+2d'_{i,Q_i}\left[1-q'\left(2d'_{j,q_2}+T'_{j,V_j}\right)\right]\left[2d'_{i,q_1}\left(d'_{k,q_3}+T'_{k,V_k}\right)+T'_{i,V_i}\left(d'_{k,q_3}+T'_{k,V_k}+d'_{i,q_1}-d'_{i,q_3}\right)\right]} \tag{8.15a}$$

$$\begin{aligned}\frac{\partial q_1}{\partial \tau_{id}} = & \frac{d'_{k,q_3} + T'_{k,V_k} + d'_{i,q_3} - d'_{i,q_1}}{2d'_{i,Q_i}\left(2d'_{k,q_3} + 2T'_{k,V_k} + T'_{i,V_i}\right) + T'_{i,V_i}\left(d'_{k,q_3} + T'_{k,V_k} + d'_{i,q_3} - d'_{i,q_1}\right)} \times \\ & \frac{\left[-1 + q'\left(2d'_{j,q_2} + T'_{j,V_j}\right)\right]\left[2d'_{i,q_1}\left(d'_{k,q_3} + T'_{k,V_k}\right) + T'_{i,V_i}\left(d'_{k,q_3} + T'_{k,V_k} + d'_{i,q_1} - d'_{i,q_3}\right)\right]}{2d'_{i,Q_i}\left(2d'_{j,q_2} + T'_{j,V_j}\right)\left(d'_{k,q_3} + T'_{k,V_k} + d'_{i,q_1} - d'_{i,q_3}\right) + 2d'_{i,Q_i}\left[1 - q'\left(2d'_{j,q_2} + T'_{j,V_j}\right)\right]\left[2d'_{i,q_1}\left(d'_{k,q_3} + T'_{k,V_k}\right) + T'_{i,V_i}\left(d'_{k,q_3} + T'_{k,V_k} + d'_{i,q_1} - d'_{i,q_3}\right)\right]}\end{aligned} \tag{8.15b}$$

$$\frac{\partial q_2}{\partial \tau_{id}} = \frac{\left(d'_{k,q_3}+T'_{k,V_k}+d'_{i,q_1}-d'_{i,q_3}\right)}{2d'_{i,Q_i}\left(2d'_{j,q_2}+T'_{j,V_j}\right)\left(d'_{k,q_3}+T'_{k,V_k}+d'_{i,q_1}-d'_{i,q_3}\right)+2d'_{i,Q_i}\left[1-q'\left(2d'_{j,q_2}+T'_{j,V_j}\right)\right]\left[2d'_{i,q_1}\left(d'_{k,q_3}+T'_{k,V_k}\right)+T'_{i,V_i}\left(d'_{k,q_3}+T'_{k,V_k}+d'_{i,q_1}-d'_{i,q_3}\right)\right]} \tag{8.15c}$$

$$\frac{\partial q_3}{\partial \tau_{id}} = \frac{1}{2d'_{i,Q_i}\left(2d'_{k,q_3}+2T'_{k,V_k}+T'_{i,V_i}\right)+T'_{i,V_i}\left(d'_{k,q_3}+T'_{k,V_k}-d'_{i,Q_i}\right)} \times \frac{-2d'_{i,Q_i}\left[1-q'\left(2d'_{j,q_2}+T'_{j,V_j}\right)\right]\left[2d'_{i,q_1}\left(d'_{k,q_3}+T'_{k,V_k}\right)+T'_{i,V_i}\left(d'_{k,q_3}+T'_{k,V_k}+d'_{i,q_1}-d'_{i,q_3}\right)\right]}{2d'_{i,Q_i}\left(2d'_{j,q_2}+T'_{j,V_j}\right)\left(d'_{k,q_3}+T'_{k,V_k}+d'_{i,q_1}-d'_{i,q_3}\right)+2d'_{i,Q_i}\left[1-q'\left(2d'_{j,q_2}+T'_{j,V_j}\right)\right]\left[2d'_{i,q_1}\left(d'_{k,q_3}+T'_{k,V_k}\right)+T'_{i,V_i}\left(d'_{k,q_3}+T'_{k,V_k}+d'_{i,q_1}-d'_{i,q_3}\right)\right]} \tag{8.15d}$$

For airfare of air travel Path 2, i.e., τ_2,

$$\frac{\partial p}{\partial \tau_2} = \frac{2d'_{i,q_1}\left(d'_{k,q_3}+T'_{k,V_k}\right)+T'_{i,V_i}\left(d'_{k,q_3}+T'_{k,V_k}+d'_{i,q_1}-d'_{i,q_3}\right)}{\left(2d'_{j,q_2}+T'_{j,V_j}\right)\left(d'_{k,q_3}+T'_{k,V_k}+d'_{i,q_1}-d'_{i,q_3}\right)+\left[1-q'\left(2d'_{j,q_2}+T'_{j,V_j}\right)\right]\left[2d'_{i,q_1}\left(d'_{k,q_3}+T'_{k,V_k}\right)+T'_{i,V_i}\left(d'_{k,q_3}+T'_{k,V_k}+d'_{i,q_1}-d'_{i,q_3}\right)\right]} \tag{8.16a}$$

$$\frac{\partial q_1}{\partial \tau_2} = \frac{d'_{k,q_3}+T'_{k,V_k}+d'_{i,q_3}-d'_{i,q_1}}{\left(2d'_{j,q_2}+T'_{j,V_j}\right)\left(d'_{k,q_3}+T'_{k,V_k}+d'_{i,q_1}-d'_{i,q_3}\right)+\left[1-q'\left(2d'_{j,q_2}+T'_{j,V_j}\right)\right]\left[2d'_{i,q_1}\left(d'_{k,q_3}+T'_{k,V_k}\right)+T'_{i,V_i}\left(d'_{k,q_3}+T'_{k,V_k}+d'_{i,q_1}-d'_{i,q_3}\right)\right]} \tag{8.16b}$$

$$\frac{\partial q_2}{\partial \tau_2} = \frac{q'\left[2d'_{i,q_1}\left(d'_{k,q_3}+T'_{k,V_k}\right)+T'_{i,V_i}\left(d'_{k,q_3}+T'_{k,V_k}+d'_{i,q_1}-d'_{i,q_3}\right)\right]-\left(d'_{k,q_3}+T'_{k,V_k}+d'_{i,q_1}-d'_{i,q_3}\right)}{\left(2d'_{j,q_2}+T'_{j,V_j}\right)\left(d'_{k,q_3}+T'_{k,V_k}+d'_{i,q_1}-d'_{i,q_3}\right)+\left[1-q'\left(2d'_{j,q_2}+T'_{j,V_j}\right)\right]\left[2d'_{i,q_1}\left(d'_{k,q_3}+T'_{k,V_k}\right)+T'_{i,V_i}\left(d'_{k,q_3}+T'_{k,V_k}+d'_{i,q_1}-d'_{i,q_3}\right)\right]} \tag{8.16c}$$

$$\frac{\partial q_3}{\partial \tau_{oj}} = \frac{2d'_{i,q_1}}{\left(2d'_{j,q_2}+T'_{j,V_j}\right)\left(d'_{k,q_3}+T'_{k,V_k}+d'_{i,q_1}-d'_{i,q_3}\right)+\left[1-q'\left(2d'_{j,q_2}+T'_{j,V_j}\right)\right]\left[2d'_{i,q_1}\left(d'_{k,q_3}+T'_{k,V_k}\right)+T'_{i,V_i}\left(d'_{k,q_3}+T'_{k,V_k}+d'_{i,q_1}-d'_{i,q_3}\right)\right]} \tag{8.16d}$$

For airfare of air travel link ok,

$$\frac{\partial p}{\partial \tau_{ok}} = \frac{2d'_{i,q_3}\left(2d'_{j,q_2}+T'_{j,V_j}\right)}{\left(2d'_{j,q_2}+T'_{j,V_j}+T'_{i,V_i}\right)\left(T'_{k,V_k}+d'_{k,q_3}+d'_{i,q_1}-d'_{i,q_3}\right)+2d'_{i,q_1}\left(T'_{k,V_k}+d'_{k,q_3}\right)-q'\left(2d'_{j,q_2}+T'_{j,V_j}\right)\left[2d'_{i,q_1}\left(T'_{k,V_k}+d'_{k,q_3}\right)+T'_{i,V_i}\left(T'_{k,V_k}+d'_{k,q_3}+d'_{i,q_1}-d'_{i,q_3}\right)\right]} \tag{8.17a}$$

$$\frac{\partial q_1}{\partial \tau_{ok}} = \frac{\left(2d'_{j,q_2}+T'_{j,V_j}\right)+\left[1-q'\left(2d'_{j,q_2}+T'_{j,V_j}\right)\right]\left(2d'_{i,q_1}+T'_{k,V_k}\right)}{\left(2d'_{j,q_2}+T'_{j,V_j}\right)\left(T'_{k,V_k}+d'_{k,q_3}+d'_{i,q_1}-d'_{i,q_3}\right)+\left[1-q'\left(2d'_{j,q_2}+T'_{j,V_j}\right)\right]\left[2d'_{i,q_1}\left(T'_{k,V_k}+d'_{k,q_3}\right)+T'_{i,V_i}\left(T'_{k,V_k}+d'_{k,q_3}+d'_{i,q_1}-d'_{i,q_3}\right)\right]} \tag{8.17b}$$

$$\frac{\partial q_2}{\partial \tau_{ok}} = \frac{2d'_{i,q_3}}{\left(2d'_{j,q_2}+T'_{j,V_j}+T'_{i,V_i}\right)\left(T'_{k,V_k}+d'_{k,q_3}+d'_{i,Q_i}\right)+2d'_{i,q_1}\left(T'_{k,V_k}+d'_{k,q_3}\right)-q'\left(2d'_{j,q_2}+T'_{j,V_j}\right)\left[2d'_{i,q_1}\left(T'_{k,V_k}+d'_{k,q_3}\right)+T'_{i,V_i}\left(T'_{k,V_k}+d'_{k,q_3}+d'_{i,q_1}-d'_{i,q_3}\right)\right]} \tag{8.17c}$$

$$\frac{\partial q_3}{\partial \tau_{ok}} = \frac{-\left(2d'_{j,q_2}+T'_{j,V_j}\right)-\left(2d'_{i,q_1}+T'_{i,V_i}\right)\left[1-q'\left(2d'_{j,q_2}+T'_{j,V_j}\right)\right]}{\left(2d'_{j,q_2}+T'_{j,V_j}\right)\left(T'_{k,V_k}+d'_{k,q_3}+d'_{i,q_1}-d'_{i,q_3}\right)+\left[1-q'\left(2d'_{j,q_2}+T'_{j,V_j}\right)\right]\left[2d'_{i,q_1}\left(T'_{k,V_k}+d'_{k,q_3}\right)+T'_{i,V_i}\left(T'_{k,V_k}+d'_{k,q_3}+d'_{i,q_1}-d'_{i,q_3}\right)\right]} \tag{8.17d}$$

For travel time in link oi,

$$\frac{\partial p}{\partial t_{oi}} = \frac{\alpha\left(2d'_{j,q_2}+T'_{j,V_j}\right)\left(d'_{k,q_3}+T'_{k,V_k}+d'_{i,q_3}-d'_{i,q_1}\right)}{\left(2d'_{j,q_2}+T'_{j,V_j}\right)\left(d'_{k,q_3}+T'_{k,V_k}+d'_{i,q_1}-d'_{i,q_3}\right)+\left[1-q'\left(2d'_{j,q_2}+T'_{j,V_j}\right)\right]\left[2d'_{i,q_1}\left(d'_{k,q_3}+T'_{k,V_k}\right)+T'_{i,V_i}\left(d'_{k,q_3}+T'_{k,V_k}+d'_{i,q_1}-d'_{i,q_3}\right)\right]} \tag{8.18a}$$

$$\frac{\partial q_1}{\partial t_{oi}} = \frac{-\alpha\left\{\left(2d'_{j,q_2}+T'_{j,V_j}\right)+\left(d'_{k,q_3}+T'_{k,V_k}+d'_{i,q_1}-d'_{i,q_3}+T'_{i,V_i}\right)\left[1-q'\left(2d'_{j,q_2}+T'_{j,V_j}\right)\right]\right\}}{\left\{\left(2d'_{j,q_2}+T'_{j,V_j}\right)\left(d'_{k,q_3}+T'_{k,V_k}+d'_{i,q_1}-d'_{i,q_3}\right)+\left[1-q'\left(2d'_{j,q_2}+T'_{j,V_j}\right)\right]\left[2d'_{i,q_1}\left(d'_{k,q_3}+T'_{k,V_k}\right)+T'_{i,V_i}\left(d'_{k,q_3}+T'_{k,V_k}+d'_{i,q_1}-d'_{i,q_3}\right)\right]\right\}} \tag{8.18b}$$

$$\frac{\partial q_2}{\partial t_{oi}} = \frac{\alpha\left(d'_{k,q_3}+T'_{k,V_k}+d'_{i,q_3}-d'_{i,q_1}\right)}{\left(2d'_{j,q_2}+T'_{j,V_j}\right)\left(d'_{k,q_3}+T'_{k,V_k}+d'_{i,q_1}-d'_{i,q_3}\right)+\left[1-q'\left(2d'_{j,q_2}+T'_{j,V_j}\right)\right]\left[2d'_{i,q_1}\left(d'_{k,q_3}+T'_{k,V_k}\right)+T'_{i,V_i}\left(d'_{k,q_3}+T'_{k,V_k}+d'_{i,q_1}-d'_{i,q_3}\right)\right]} \tag{8.18c}$$

$$\frac{\partial q_3}{\partial t_{oi}} = \frac{\alpha\left(2d'_{j,q_2}+T'_{j,V_j}\right)+\alpha\left(2d'_{i,q_1}+T'_{i,V_i}\right)\left[1-q'\left(2d'_{j,q_2}+T'_{j,V_j}\right)\right]}{\left(2d'_{j,q_2}+T'_{j,V_j}\right)\left(d'_{k,q_3}+T'_{k,V_k}+d'_{i,q_1}-d'_{i,q_3}\right)+\left[1-q'\left(2d'_{j,q_2}+T'_{j,V_j}\right)\right]\left[2d'_{i,q_1}\left(d'_{k,q_3}+T'_{k,V_k}\right)+T'_{i,V_i}\left(d'_{k,q_3}+T'_{k,V_k}+d'_{i,q_1}-d'_{i,q_3}\right)\right]} \tag{8.18d}$$

For travel time in link id, $\frac{\partial p}{\partial t_{id}}$, $\frac{\partial q_1}{\partial t_{id}}$, $\frac{\partial q_2}{\partial t_{id}}$ and $\frac{\partial q_3}{\partial t_{id}}$ equal to $\frac{\partial p}{\partial t_{oi}}$, $\frac{\partial q_1}{\partial t_{oi}}$, $\frac{\partial q_2}{\partial t_{oi}}$ and $\frac{\partial q_3}{\partial t_{oi}}$, respectively.

For the total air travel time of Path 2, i.e., t_2,

$$\frac{\partial p}{\partial t_2} = \frac{\alpha\left[2d'_{i,q_1}\left(d'_{k,q_3}+T'_{k,V_k}\right)+T'_{i,V_i}\left(d'_{k,q_3}+T'_{k,V_k}+d'_{i,q_1}-d'_{i,q_3}\right)\right]}{\left(2d'_{j,q_2}+T'_{j,V_j}\right)\left(d'_{k,q_3}+T'_{k,V_k}+d'_{i,q_1}-d'_{i,q_3}\right)+\left[1-q'\left(2d'_{j,q_2}+T'_{j,V_j}\right)\right]\left[2d'_{i,q_1}\left(d'_{k,q_3}+T'_{k,V_k}\right)+T'_{i,V_i}\left(d'_{k,q_3}+T'_{k,V_k}+d'_{i,q_1}-d'_{i,q_3}\right)\right]} \tag{8.19a}$$

$$\frac{\partial q_1}{\partial t_2} = \frac{\alpha\left(d'_{k,q_3}+T'_{k,V_k}+d'_{i,q_3}-d'_{i,q_1}\right)}{\left(2d'_{j,q_2}+T'_{j,V_j}\right)\left(d'_{k,q_3}+T'_{k,V_k}+d'_{i,q_1}-d'_{i,q_3}\right)+\left[1-q'\left(2d'_{j,q_2}+T'_{j,V_j}\right)\right]\left[2d'_{i,q_1}\left(d'_{k,q_3}+T'_{k,V_k}\right)+T'_{i,V_i}\left(d'_{k,q_3}+T'_{k,V_k}+d'_{i,q_1}-d'_{i,q_3}\right)\right]} \tag{8.19b}$$

$$\frac{\partial q_2}{\partial t_2} = \frac{-\alpha\left\{\left(d'_{k,q_3}+T'_{k,V_k}+d'_{i,q_1}-d'_{i,q_3}\right)-q'\left[2d'_{i,q_1}\left(d'_{k,q_3}+T'_{k,V_k}\right)+T'_{i,V_i}\left(d'_{k,q_3}+T'_{k,V_k}+d'_{i,q_1}-d'_{i,q_3}\right)\right]\right\}}{\left(2d'_{j,q_2}+T'_{j,V_j}\right)\left(d'_{k,q_3}+T'_{k,V_k}+d'_{i,q_1}-d'_{i,q_3}\right)+\left[1-q'\left(2d'_{j,q_2}+T'_{j,V_j}\right)\right]\left[2d'_{i,q_1}\left(d'_{k,q_3}+T'_{k,V_k}\right)+T'_{i,V_i}\left(d'_{k,q_3}+T'_{k,V_k}+d'_{i,q_1}-d'_{i,q_3}\right)\right]} \tag{8.19c}$$

$$\frac{\partial q_3}{\partial t_2} = \frac{2\alpha d'_{i,q_3}}{\left(2d'_{j,q_2}+T'_{j,V_j}\right)\left(d'_{k,q_3}+T'_{k,V_k}+d'_{i,q_1}-d'_{i,q_3}\right)+\left[1-q'\left(2d'_{j,q_2}+T'_{j,V_j}\right)\right]\left[2d'_{i,q_1}\left(d'_{k,q_3}+T'_{k,V_k}\right)+T'_{i,V_i}\left(d'_{k,q_3}+T'_{k,V_k}+d'_{i,q_1}-d'_{i,q_3}\right)\right]} \tag{8.19d}$$

For the travel time in link ok

$$\frac{\partial p}{\partial t_{ok}} = \frac{2\alpha d'_{i,q_1}\left(2d'_{j,q_2}+T'_{j,V_j}\right)}{\left(2d'_{j,q_2}+T'_{j,V_j}\right)\left(d'_{k,q_3}+T'_{k,V_k}+d'_{i,q_1}-d'_{i,q_3}\right)+\left[1-q'\left(2d'_{j,q_2}+T'_{j,V_j}\right)\right]\left[2d'_{i,q_1}\left(d'_{k,q_3}+T'_{k,V_k}\right)+T'_{i,V_i}\left(d'_{k,q_3}+T'_{k,V_k}+d'_{i,q_1}-d'_{i,q_3}\right)\right]} \tag{8.20a}$$

$$\frac{\partial q_1}{\partial t_{ok}} = \frac{\alpha\left(2d'_{j,q_2}+T'_{j,V_j}\right)+2\alpha d'_{i,q_1}\left[1-q'\left(2d'_{j,q_2}+T'_{j,V_j}\right)\right]\left(2d'_{i,q_1}+T'_{i,V_i}\right)}{\left(2d'_{j,q_2}+T'_{j,V_j}\right)\left(d'_{k,q_3}+T'_{k,V_k}+d'_{i,q_1}-d'_{i,q_3}\right)+\left[1-q'\left(2d'_{j,q_2}+T'_{j,V_j}\right)\right]\left[2d'_{i,q_1}\left(d'_{k,q_3}+T'_{k,V_k}\right)+T'_{i,V_i}\left(d'_{k,q_3}+T'_{k,V_k}+d'_{i,q_1}-d'_{i,q_3}\right)\right]} \tag{8.20b}$$

$$\frac{\partial q_2}{\partial t_{ok}} = \frac{2\alpha d'_{i,q_1}}{\left(2d'_{j,q_2}+T'_{j,V_j}\right)\left(d'_{k,q_3}+T'_{k,V_k}+d'_{i,q_1}-d'_{i,q_3}\right)+\left[1-q'\left(2d'_{j,q_2}+T'_{j,V_j}\right)\right]\left[2d'_{i,q_1}\left(d'_{k,q_3}+T'_{k,V_k}\right)+T'_{i,V_i}\left(d'_{k,q_3}+T'_{k,V_k}+d'_{i,q_1}-d'_{i,q_3}\right)\right]} \tag{8.20c}$$

$$\frac{\partial q_3}{\partial t_{ok}} = \frac{-\alpha\left[\left(2d'_{j,q_2}+T'_{j,V_j}\right)+\left(2d'_{i,q_1}+T'_{i,V_i}\right)-q'\left(2d'_{i,q_1}+T'_{i,V_i}\right)\left(2d'_{j,q_2}+T'_{j,V_j}\right)\right]}{\left(2d'_{j,q_2}+T'_{j,V_j}\right)\left(d'_{k,q_3}+T'_{k,V_k}+d'_{i,q_1}-d'_{i,q_3}\right)+\left[1-q'\left(2d'_{j,q_2}+T'_{j,V_j}\right)\right]\left[2d'_{i,q_1}\left(d'_{k,q_3}+T'_{k,V_k}\right)+T'_{i,V_i}\left(d'_{k,q_3}+T'_{k,V_k}+d'_{i,q_1}-d'_{i,q_3}\right)\right]} \tag{8.20d}$$

For travel time in link ki, the equations of $\frac{\partial p}{\partial t_{ki}}$, $\frac{\partial q_1}{\partial t_{ki}}$, $\frac{\partial q_2}{\partial t_{ki}}$ and $\frac{\partial q_3}{\partial t_{ki}}$ is similar to $\frac{\partial p}{\partial t_{ok}}$, $\frac{\partial q_1}{\partial t_{ok}}$,

$\frac{\partial q_2}{\partial t_{ok}}$ and $\frac{\partial q_3}{\partial t_{ok}}$, respectively, and the only difference is that α in equations about derivatives to t_{ok} should be replaced by β in equations about t_{ki}.

For Airport i's capacity C_i,

$$\frac{\partial p}{\partial C_i}=\frac{2d'_{i,C_i}\left(d'_{k,q_3}+T'_{k,V_k}\right)\left(2d'_{j,q_2}+T'_{j,V_j}\right)}{\left(2d'_{j,q_2}+T'_{j,V_j}\right)\left(d'_{k,q_3}+T'_{k,V_k}+d'_{i,q_1}-d'_{i,q_3}\right)+\left[1-q'\left(2d'_{j,q_2}+T'_{j,V_j}\right)\right]\left[2d'_{i,q_1}\left(d'_{k,q_3}+T'_{k,V_k}\right)+T'_{i,V_i}\left(d'_{k,q_3}+T'_{k,V_k}+d'_{i,q_1}-d'_{i,q_3}\right)\right]} \tag{8.21a}$$

$$\frac{\partial q_1}{\partial C_i}=\frac{-d'_{i,C_i}\left(2d'_{j,q_2}+T'_{j,V_j}\right)-d'_{i,C_i}T'_{i,V_i}-\left[d'_{i,C_i}T'_{i,V_i}q'\left(2d'_{j,q_2}+T'_{j,V_j}\right)\right]-2d'_{i,C_i}\left[1-q'\left(2d'_{j,q_2}+T'_{j,V_j}\right)\right]\left(d'_{k,q_3}+T'_{k,V_k}\right)}{\left(2d'_{j,q_2}+T'_{j,V_j}\right)\left(d'_{k,q_3}+T'_{k,V_k}+d'_{i,q_1}-d'_{i,q_3}\right)+\left[1-q'\left(2d'_{j,q_2}+T'_{j,V_j}\right)\right]\left[2d'_{i,q_1}\left(d'_{k,q_3}+T'_{k,V_k}\right)+T'_{i,V_i}\left(d'_{k,q_3}+T'_{k,V_k}+d'_{i,q_1}-d'_{i,q_3}\right)\right]} \tag{8.21b}$$

$$\frac{\partial q_2}{\partial C_i}=\frac{2d'_{i,C_i}\left(d'_{k,q_3}+T'_{k,V_k}\right)}{\left(2d'_{j,q_2}+T'_{j,V_j}\right)\left(d'_{k,q_3}+T'_{k,V_k}+d'_{i,q_1}-d'_{i,q_3}\right)+\left[1-q'\left(2d'_{j,q_2}+T'_{j,V_j}\right)\right]\left[2d'_{i,q_1}\left(d'_{k,q_3}+T'_{k,V_k}\right)+T'_{i,V_i}\left(d'_{k,q_3}+T'_{k,V_k}+d'_{i,q_1}-d'_{i,q_3}\right)\right]} \tag{8.21c}$$

$$\frac{\partial q_3}{\partial C_i}=\frac{d'_{i,C_i}\left(2d'_{j,q_2}+T'_{j,V_j}\right)+d'_{i,C_i}T'_{i,V_i}\left[1-q'\left(2d'_{j,q_2}+T'_{j,V_j}\right)\right]}{\left(2d'_{j,q_2}+T'_{j,V_j}\right)\left(d'_{k,q_3}+T'_{k,V_k}+d'_{i,q_1}-d'_{i,q_3}\right)+\left[1-q'\left(2d'_{j,q_2}+T'_{j,V_j}\right)\right]\left[2d'_{i,q_1}\left(d'_{k,q_3}+T'_{k,V_k}\right)+T'_{i,V_i}\left(d'_{k,q_3}+T'_{k,V_k}+d'_{i,q_1}-d'_{i,q_3}\right)\right]} \tag{8.21d}$$

For Airport j's capacity,

$$\frac{\partial p}{\partial C_j}=\frac{2d'_{j,C_j}\left[2d'_{i,q_1}\left(d'_{k,q_3}+T'_{k,V_k}\right)+T'_{i,V_i}\left(d'_{k,q_3}+T'_{k,V_k}+d'_{i,q_1}-d'_{i,q_3}\right)\right]}{\left(2d'_{j,q_2}+T'_{j,V_j}\right)\left(d'_{k,q_3}+T'_{k,V_k}+d'_{i,q_1}-d'_{i,q_3}\right)+\left[1-q'\left(2d'_{j,q_2}+T'_{j,V_j}\right)\right]\left[2d'_{i,q_1}\left(d'_{k,q_3}+T'_{k,V_k}\right)+T'_{i,V_i}\left(d'_{k,q_3}+T'_{k,V_k}+d'_{i,q_1}-d'_{i,q_3}\right)\right]} \tag{8.22a}$$

$$\frac{\partial q_1}{\partial C_j}=\frac{2d'_{j,C_j}\left(d'_{k,q_3}+T'_{k,V_k}+d'_{i,q_3}-d'_{i,q_1}\right)}{\left(2d'_{j,q_2}+T'_{j,V_j}\right)\left(d'_{k,q_3}+T'_{k,V_k}+d'_{i,q_1}-d'_{i,q_3}\right)+\left[1-q'\left(2d'_{j,q_2}+T'_{j,V_j}\right)\right]\left[2d'_{i,q_1}\left(d'_{k,q_3}+T'_{k,V_k}\right)+T'_{i,V_i}\left(d'_{k,q_3}+T'_{k,V_k}+d'_{i,q_1}-d'_{i,q_3}\right)\right]} \tag{8.22b}$$

$$\frac{\partial q_2}{\partial C_j}=\frac{-2d'_{j,C_j}\left(d'_{k,q_3}+T'_{k,V_k}+d'_{i,q_1}-d'_{i,q_3}\right)+2d'_{j,C_j}q'\left[2d'_{i,q_1}\left(d'_{k,q_3}+T'_{k,V_k}\right)+T'_{i,V_i}\left(d'_{k,q_3}+T'_{k,V_k}+d'_{i,q_1}-d'_{i,q_3}\right)\right]}{\left(2d'_{j,q_2}+T'_{j,V_j}\right)\left(d'_{k,q_3}+T'_{k,V_k}+d'_{i,q_1}-d'_{i,q_3}\right)+\left[1-q'\left(2d'_{j,q_2}+T'_{j,V_j}\right)\right]\left[2d'_{i,q_1}\left(d'_{k,q_3}+T'_{k,V_k}\right)+T'_{i,V_i}\left(d'_{k,q_3}+T'_{k,V_k}+d'_{i,q_1}-d'_{i,q_3}\right)\right]} \tag{8.22c}$$

$$\frac{\partial q_3}{\partial C_j}=\frac{2d'_{i,q_1}d'_{j,C_j}}{\left(2d'_{j,q_2}+T'_{j,V_j}\right)\left(d'_{k,q_3}+T'_{k,V_k}+d'_{i,q_1}-d'_{i,q_3}\right)+\left[1-q'\left(2d'_{j,q_2}+T'_{j,V_j}\right)\right]\left[2d'_{i,q_1}\left(d'_{k,q_3}+T'_{k,V_k}\right)+T'_{i,V_i}\left(d'_{k,q_3}+T'_{k,V_k}+d'_{i,q_1}-d'_{i,q_3}\right)\right]} \tag{8.22d}$$

For Airport k's capacity, C_k,

$$\frac{\partial p}{\partial C_k}=\frac{2d'_{k,C_k}d'_{i,q_1}\left(2d'_{j,q_2}+T'_{j,V_j}\right)}{\left(2d'_{j,q_2}+T'_{j,V_j}\right)\left(d'_{k,q_3}+T'_{k,V_k}+d'_{i,q_1}-d'_{i,q_3}\right)+\left[1-q'\left(2d'_{j,q_2}+T'_{j,V_j}\right)\right]\left[2d'_{i,q_1}\left(d'_{k,q_3}+T'_{k,V_k}\right)+T'_{i,V_i}\left(d'_{k,q_3}+T'_{k,V_k}+d'_{i,q_1}-d'_{i,q_3}\right)\right]} \tag{8.23a}$$

$$\frac{\partial q_1}{\partial C_k}=\frac{d'_{k,C_k}\left(2d'_{j,q_2}+T'_{j,V_j}\right)+d'_{k,C_k}\left[1-q'\left(2d'_{j,q_2}+T'_{j,V_j}\right)\right]\left(2d'_{i,q_1}+T'_{i,V_i}\right)}{\left(2d'_{j,q_2}+T'_{j,V_j}\right)\left(d'_{k,q_3}+T'_{k,V_k}+d'_{i,q_1}-d'_{i,q_3}\right)+\left[1-q'\left(2d'_{j,q_2}+T'_{j,V_j}\right)\right]\left[2d'_{i,q_1}\left(d'_{k,q_3}+T'_{k,V_k}\right)+T'_{i,V_i}\left(d'_{k,q_3}+T'_{k,V_k}+d'_{i,q_1}-d'_{i,q_3}\right)\right]} \tag{8.23b}$$

$$\frac{\partial q_2}{\partial C_k} = \frac{2d'_{k,C_k}d'_{i,q_1}}{\left(2d'_{j,q_2}+T'_{j,V_j}\right)\left(d'_{k,q_3}+T'_{k,V_k}+d'_{i,q_1}-d'_{i,q_3}\right)+\left[1-q'\left(2d'_{j,q_2}+T'_{j,V_j}\right)\right]\left[2d'_{i,q_1}\left(d'_{k,q_3}+T'_{k,V_k}\right)+T'_{i,V_i}\left(d'_{k,q_3}+T'_{k,V_k}+d'_{i,q_1}-d'_{i,q_3}\right)\right]} \tag{8.23c}$$

$$\frac{\partial q_3}{\partial C_k} = \frac{-d'_{k,C_k}\left(2d'_{j,q_2}+T'_{j,V_j}\right)+d'_{k,C_k}\left[-1+q'\left(2d'_{j,q_2}+T'_{j,V_j}\right)\right]\left(2d'_{i,q_1}+T'_{i,V_i}\right)}{\left(2d'_{j,q_2}+T'_{j,V_j}\right)\left(d'_{k,q_3}+T'_{k,V_k}+d'_{i,q_1}-d'_{i,q_3}\right)+\left[1-q'\left(2d'_{j,q_2}+T'_{j,V_j}\right)\right]\left[2d'_{i,q_1}\left(d'_{k,q_3}+T'_{k,V_k}\right)+T'_{i,V_i}\left(d'_{k,q_3}+T'_{k,V_k}+d'_{i,q_1}-d'_{i,q_3}\right)\right]} \tag{8.23d}$$

For investment from Airline O-i-D in ground connection services between Airport i and Airport k,

$$\frac{\partial p}{\partial h_1} = \frac{2T'_{k,h_1}d'_{i,q_1}\left(2d'_{j,q_2}+T'_{j,V_j}\right)}{\left(2d'_{j,q_2}+T'_{j,V_j}\right)\left(d'_{k,q_3}+T'_{k,V_k}+d'_{i,q_1}-d'_{i,q_3}\right)+\left[1-q'\left(2d'_{j,q_2}+T'_{j,V_j}\right)\right]\left[2d'_{i,q_1}\left(d'_{k,q_3}+T'_{k,V_k}\right)+T'_{i,V_i}\left(d'_{k,q_3}+T'_{k,V_k}+d'_{i,q_1}-d'_{i,q_3}\right)\right]} \tag{8.24a}$$

$$\frac{\partial q_1}{\partial h_1} = \frac{T'_{k,h_1}\left(2d'_{j,q_2}+T'_{j,V_j}\right)+T'_{k,hr}\left[1-q'\left(2d'_{j,q_2}+T'_{j,V_j}\right)\right]\left(2d'_{i,q_1}+T'_{i,V_i}\right)}{\left(2d'_{j,q_2}+T'_{j,V_j}\right)\left(d'_{k,q_3}+T'_{k,V_k}+d'_{i,q_1}-d'_{i,q_3}\right)+\left[1-q'\left(2d'_{j,q_2}+T'_{j,V_j}\right)\right]\left[2d'_{i,q_1}\left(d'_{k,q_3}+T'_{k,V_k}\right)+T'_{i,V_i}\left(d'_{k,q_3}+T'_{k,V_k}+d'_{i,q_1}-d'_{i,q_3}\right)\right]} \tag{8.24b}$$

$$\frac{\partial q_2}{\partial h_1} = \frac{2T'_{k,h_1}d'_{i,q_1}}{\left(2d'_{j,q_2}+T'_{j,V_j}\right)\left(d'_{k,q_3}+T'_{k,V_k}+d'_{i,q_1}-d'_{i,q_3}\right)+\left[1-q'\left(2d'_{j,q_2}+T'_{j,V_j}\right)\right]\left[2d'_{i,q_1}\left(d'_{k,q_3}+T'_{k,V_k}\right)+T'_{i,V_i}\left(d'_{k,q_3}+T'_{k,V_k}+d'_{i,q_1}-d'_{i,q_3}\right)\right]} \tag{8.24c}$$

$$\frac{\partial q_3}{\partial h_1} = \frac{-T'_{k,h_1}\left[\left(2d'_{j,q_2}+T'_{j,V_j}\right)-q'\left(2d'_{i,q_1}+T'_{i,V_i}\right)\left(2d'_{j,q_2}+T'_{j,V_j}\right)+\left(2d'_{i,q_1}+T'_{i,V_i}\right)\right]}{\left(2d'_{j,q_2}+T'_{j,V_j}\right)\left(d'_{k,q_3}+T'_{k,V_k}+d'_{i,q_1}-d'_{i,q_3}\right)+\left[1-q'\left(2d'_{j,q_2}+T'_{j,V_j}\right)\right]\left[2d'_{i,q_1}\left(d'_{k,q_3}+T'_{k,V_k}\right)+T'_{i,V_i}\left(d'_{k,q_3}+T'_{k,V_k}+d'_{i,q_1}-d'_{i,q_3}\right)\right]} \tag{8.24d}$$

For investment from Airline O-k in ground connection services between Airport i and Airport k, the equations of $\frac{\partial p}{\partial h_3}$, $\frac{\partial q_1}{\partial h_3}$, $\frac{\partial q_2}{\partial h_3}$ and $\frac{\partial q_3}{\partial h_3}$ is similar to $\frac{\partial p}{\partial h_1}$, $\frac{\partial q_1}{\partial h_1}$, $\frac{\partial q_2}{\partial h_1}$ and $\frac{\partial q_3}{\partial h_1}$, respectively.

8.1.4 Analytical example of passenger flow distribution between the OD pair served by the MAS

In Section 3.2.3.3, we emphasize the impact of system factors on the passenger flow distribution instead of getting close-form results about specific passenger flow. In this subsection, we assume that functions in the formulation of travel full prices, i.e. Eqs. (3.1)-(3.3) and Eq.(3.5e), are linearly function to get passenger flow in each air travel route under the linearity assumption. The functions are defined in Table. 8.1. It should be noted that all parameters defined in the linear functions are assumed to be positive constants. By substituting the above linear functions into the interior equilibrium conditions (Eqs. (3.6)), we can get the specified UE conditions in the MAS, shown in Eq. (8.25). By solving Eq. (8.25), we can get the passenger flow in each travel route through our stylized MAS as Eq. (8.26).

Table 8.1: Linear function definitions

Functions	Definitions	Specifications
Congestion delay function	$d_i = \xi_{i,1}q_1 + \xi_{i,3}q_3 - \eta_i C_i$ $d_j = \xi_j q_2 - \eta_j C_j$ $d_k = \xi_k q_3 - \eta_k C_k$	$d_i > 0, q_1 > 0, q_3 > 0$ $d_j > 0, q_2 > 0$ $d_k > 0, q_3 > 0$
Transfer cost function	$T_i = \zeta_i (q_1 + q_3) + T_{i,0}$ $T_j = \zeta_j q_2 + T_{j,0}$ $T_k = \zeta_k q_3 - \sigma (h_1 + h_3) + T_{k,0}$	$T_{i,0}$ is the minimum transfer cost in Airport i $T_{j,0}$ is the minimum transfer cost in Airport j $T_{k,0}$ is the minimum transfer cost in Airport k
Inverse elastic demand function	$p* = q_0 - \lambda q$	q_0 means the potential total demand between OD

$$\left(2\xi_{i,1} + \zeta_i + \lambda\right) q_1 + \lambda q_2 + \left(2\xi_{i,3} + \zeta_i + \lambda\right) q_3 = 2\eta_i C_i + q_0 - T_{i,0} - \tau_1 - \alpha(t_{oi} + t_{id}) \tag{8.25a}$$

$$\lambda q_1 + \left(2\xi_j + \zeta_j + \lambda\right) q_2 + \lambda q_3 = 2\eta_j C_j + q_0 - T_{j,0} - \tau_2 - \alpha(t_{oj} + t_{jd}) \tag{8.25b}$$

$$\begin{aligned}&\left(2\xi_{i,1} + \zeta_i + \lambda\right) q_1 + \lambda q_2 + \left(\xi_{i,3} + \xi_k + \zeta_i + \zeta_k + \lambda\right) q_3 = \eta_i C_i + \eta_k C_k \\ &+ \sigma (h_1 + h_3) + q_0 - T_{i,0} - T_{k,0} - \tau_{3,1} - \tau_{3,2} - \tau_{ki} - \alpha (t_{ok} + t_{id}) - \beta t_{ki}\end{aligned} \tag{8.25c}$$

From the above equations describing UE state under linearity assumption on functions, we can get the closed-form specific passenger flow as below:

$$q_1 = \frac{\left(\zeta_3 - \xi_{i,3} + \xi_k\right)\left[\Omega (q_0 - \Delta_1) - \xi_{i,1}\lambda (q_0 - \Delta_2) - \Psi (\Delta_3 - \Delta_1)\right] + \Gamma (\Delta_3 - \Delta_1)}{\xi_{i,1}\Gamma} \tag{8.26a}$$

$$q_2 = -\frac{\lambda\left(\zeta_3 - \xi_{i,3} + \xi_k + \xi_{i,1}\right)\left[\Omega(q_0 - \Delta_1) - \xi_{i,1}\lambda(q_0 - \Delta_2) - \Psi(\Delta_3 - \Delta_1)\right] + \Gamma(\Delta_3 - \Delta_1) + \xi_{i,1}\Gamma(q_0 - \Delta_2)}{\Omega\Gamma} \tag{8.26b}$$

$$q_3 = \frac{\Omega (q_0 - \Delta_1) - \xi_{i,1}\lambda (q_0 - \Delta_2) - \Psi (\Delta_3 - \Delta_1)}{\Gamma} \tag{8.26c}$$

where

$$\begin{aligned}\Gamma = \xi_{i,1}&\left[\left(2\xi_{i,3}+\zeta_1+\lambda\right)\left(2\xi_j+\zeta_2\right)+\left(2\xi_{i,3}+\zeta_1\right)\lambda\right]\\ &-\left(\xi_{i,3}-\xi_k-\zeta_3\right)\left[\left(2\xi_{i,1}+\zeta_1+\lambda\right)\left(2\xi_j+\zeta_2\right)+\left(2\xi_{i,1}+\zeta_1\right)\lambda\right]\end{aligned} \tag{8.27a}$$

$$\Delta_1 = \tau_1 + \alpha(t_{oi}+t_{id}) + T_{i0} - 2\eta_i C_i \tag{8.27b}$$

$$\Delta_2 = \tau_2 + \alpha(t_{oj}+t_{jd}) + T_{j0} - 2\eta_j C_j \tag{8.27c}$$

$$\Delta_3 = \tau_{3,1} + \tau_{3,2} + \tau_{ki} + \alpha\left(t_{ok}+t_{id}\right) + \beta t_{ki} + T_{k0} - \eta_k C_k - \delta\left(h_1+h_3\right) \tag{8.27d}$$

$$\Psi = \left(2\xi_{i,1}+\zeta_1+\lambda\right)\left(2\xi_j+\zeta_2\right)+\left(2\xi_{i,1}+\mu_1\right)\lambda \tag{8.27e}$$

$$\Omega = \xi_{i,1}\left(2\xi_j+\zeta_2+\lambda\right) \tag{8.27f}$$

The parameters in the linear function definitions are included in the above results. However, the exact values of these coefficients will not be discussed in this paper. It should be noted that it is also feasible to obtain closed-form specific passenger flow by assuming some elementary functions such as quadratic functions. In Eq. (8.27), it can be easily get that $\Gamma, \Psi, \Omega > 0$. To a certain degree, Δ_m indicates the expense associated with path m, which is directly linked to monetary and non-monetary costs and inversely related to the capacity of the airports and the service level of ground connection along path m (included for Path 3). Eq. (8.26) can be rewritten as:

$$\begin{aligned}&\begin{bmatrix}\frac{\left(\zeta_3-\xi_{i,3}+\xi_k\right)(\Psi-\Gamma-\Omega)}{\xi_{i,1}\Gamma} & \frac{\lambda\left(\zeta_3-\xi_{i,3}+\xi_k\right)}{\Gamma} & \frac{\left(\zeta_3-\xi_{i,3}+\xi_k\right)(\Gamma-\Psi)}{\xi_{i,1}\Gamma}\\ \frac{\lambda\left(\zeta_3-\xi_{i,3}+\xi_k+\xi_{i,1}\right)(\Omega-\Psi)-\Gamma}{\Omega\Gamma} & -\frac{\lambda^2\xi_{i,1}\left(\zeta_3-\xi_{i,3}+\xi_k+\xi_{i,1}\right)-\xi_{i,1}\Gamma}{\Omega\Gamma} & \frac{\lambda\left(\zeta_3-\xi_{i,3}+\xi_k+\xi_{i,1}\right)\Psi-\Gamma}{\Omega\Gamma}\\ \frac{\Psi-\Omega}{\Gamma} & \frac{\xi_{i,1}\lambda}{\Gamma} & -\frac{\Psi}{\Gamma}\end{bmatrix}\begin{bmatrix}\Delta_1\\ \Delta_2\\ \Delta_3\end{bmatrix}\\ &+\begin{bmatrix}\frac{\left(\zeta_3-\xi_{i,3}+\xi_k\right)\left(\Omega-\xi_{i,1}\lambda\right)q_0}{\xi_{i,1}\Gamma}\\ -\frac{\lambda\left(\zeta_3-\xi_{i,3}+\xi_k+\xi_{i,1}\right)\left(\Omega-\xi_{i,1}\lambda\right)q_0+\xi_{i,1}\Gamma q_0}{\Omega\Gamma}\\ \frac{\left(\Omega-\xi_{i,1}\lambda\right)q_0}{\Gamma}\end{bmatrix}=\begin{bmatrix}q_1\\ q_2\\ q_3\end{bmatrix}\end{aligned} \tag{8.28}$$

which shows the interrelationship between passenger flow within the MAS and the airline strategies about pricing and investment in the ground connection services. It can be seen from

Eq. (8.26) that the impact of parameters on the passenger flow distribution is consistent with the results presented in Section 3.2.3.3. The Eq. (8.28) can provide valuable information to airline operators on adjusting strategies to achieve the desired passenger flow. By substituting Eq. (8.28) into airline profit equations Eq. (3.12), the effect of pricing strategy adjustment on airline profits can be investigated. Besides, even with the linearity assumption and the closed-form solution of passenger flow distribution, airline profit formulations still complicated, therefore, airlines' pricing strategies under different games are analyzed in the numerical study.

8.2 Pseudo code of algorithms and flight schedules used in Chapter 4

8.2.1 Random allocation

The pseudo-code for the random allocation algorithm is shown as Algorithm 5.

Algorithm 5 Random allocation for a specific destination d

Step 1: Set $UB = 0$
Step 2: Pick a cargo (denoted by $\hat{m}$) randomly from $\mathcal{M}_d$; Construct available flight set for carrying the chosen cargo $\mathcal{K}'_{d,s} = \left\{k \in \mathcal{K}_s : w_{\hat{m}} \le y'_k, l_k < t_{m,s} < u_k, f_{\hat{m}k} < \sigma w_{\hat{m}}\right\}$.
if $\mathcal{K}'_s = \varnothing$ **then**
    Set $z_{\hat{m}} = 1$ and $x_{\hat{m},k} = 0$ for all $k \in \mathcal{K}_{d,s}$. Update $UB = UB + \sigma w_{\hat{m},s}$.
else
    Let $\hat{k} \in \arg\min_{k \in \mathcal{K}'} \left\{\beta_{\hat{m}k,s}\right\}$. Set $x_{\hat{m}\hat{k}} = 1$ and $x_{\hat{m}k} = 0$ for all $k \neq \hat{k}$. Update $UB = UB + f_{\hat{m}\hat{k}}$ and $y'_{k,s} = y'_{k,s} - w_{\hat{m},s}$.
end if
Step 3: Set $\mathcal{M}_{d,s} := \mathcal{M}_{d,s} \backslash \hat{m}$.
if $\mathcal{M}_{d,s} = \varnothing$ **then**
    STOP and report the solution with value UB.
else
    Go to Step 1.
end if

8.2.2 Lower bound replication (LBR) algorithm

The pseudo-code for the Lower bound replication (LBR) algorithm is shown as Algorithm 6.

Algorithm 6 Lower bound replication (LBR) for a specific destination d

Step 1: Set $\beta_{mk,s} := \beta_{mk,s}(\lambda_{k,s})$ for all (m,k) pairs under scenario s. Set $UB = 0$
Step 2: Pick a cargo (denoted by $\hat{m}$) randomly from $\mathcal{M}_{d,s}$. Let k' be the flight that cargo $\hat{m}$ is assigned in the lower bound solution, i.e., $x_{\hat{m}k'} = 1$.
if $w_{\hat{m},s} \le y'_{k',s}$ **then**
  Let $\hat{k} = k'$, $x_{\hat{m}\hat{k}} = 0$, $z_{\hat{m},s} = 0$, and $x_{\hat{m}k} = 0$ for all $k \neq \hat{k}, k \in \mathcal{K}_{d,s}$. Update $UB := UB + f_{\hat{m}\hat{k}}$, $y'_{k',s} := y'_{k',s} - w_{\hat{m},s}$.
else
  Construct available flight set for cargo m: $\mathcal{K}'_{d,s} = \left\{k \in K_s : w_{\hat{m}} \le y'_k, l_k < t_{m,s} < u_k, \left(f_{\hat{m}k} + \lambda_{k,s} w_{\hat{m},s}\right) < \sigma w_{\hat{m}}\right\}$.
  if $\mathcal{K}'_s = \varnothing$ **then**
    Set $z_{\hat{m}} = 1$ and $x_{\hat{m},k} = 0$ for all $k \in \mathcal{K}_{d,s}$.
    Update $UB = UB + \sigma w_{\hat{m},s}$.
  else
    Let $\hat{k} \in \arg\min_{k \in \mathcal{K}'_{d,s}} \left\{\beta_{\hat{m}k,s}\right\}$. Set $x_{\hat{m}\hat{k}} = 1$ and $x_{\hat{m},k} = 0$ for all $k \neq \hat{k}, k \in \mathcal{K}_{d,s}$.
    Update $UB := UB + f_{\hat{m}\hat{k}}$ and $y'_{k',s} := y'_{k',s} - w_{\hat{m},s}$.
  end if
end if
Step 3: Update $\mathcal{M}_{d,s} := \mathcal{M}_{d,s} \backslash \hat{m}$.
if $\mathcal{M}_{d,s} = \varnothing$ **then**
  STOP and report the solution with value UB.
else
  Go to Step 2.
end if

8.2.3 Greedy regret (RGT) algorithm for a specific destination d

The pseudo-code for the Greedy regret (RGT) algorithm is shown as Algorithm 7.

Algorithm 7 Greedy regret (RGT) algorithm

Step 1: Set $UB = 0$.
Step 2: Set $\mathcal{R}_s = \varnothing$.
for $m \in \mathcal{M}_{d,s}$ **do**
  Let $\mathcal{K}_{m,s} = \{k, w_{m,s} \leq y'_{k,s}, l_k < t_{m,s} < u_k, f_{mk} < \sigma w_m\}$.
  if $\mathcal{K}_{m,s} = \varnothing$ for some m **then**
    Let $\gamma_m = 0$ and $k_m = |K_s| + 1$.
  end if
  if $\left|\mathcal{K}_{m,s}\right| = 1$ **then**
    $\gamma_m := \max\left\{\sigma w_{\hat{m}} - f_{mk,s}, f_{mk,s} - \sigma w_{\hat{m}}\right\}$, and $k_m = k$ where $k \in \mathcal{K}_{m,s}$ and is the only one element in $\mathcal{K}_{m,s}$.
  end if
  if $\left|\mathcal{K}_{m,s}\right| \geq 2$ **then**
    Let $\|_m \in \arg\min\left\{f_{mk,s} : k \in \mathcal{K}_{m,s}\right\}$, for all $m \in \mathcal{M}_{d,s}$.
    Let $\gamma_m := \min_{k \in K_{m,s}, k \neq k_m}\left\{f_{mk,s} - f_{mk_m,s}\right\}$, for all $m \in \mathcal{M}_{d,s}$.
    Update $\mathcal{R}_s := \mathcal{R}_s \cup \{\gamma_m\}$.
  end if
end for
Step 3: Let $\hat{m} \in \arg\max_{m \in \mathcal{M}_{d,s}} \{\gamma_m : \gamma_m \in \mathcal{R}_s\}$. Let $\hat{k} := k_{\hat{m}}$.
Step 4: Allocate cargo $\hat{m}$ to flight $\hat{k}$ (or ad hoc services) and update the following parameters:
(a): Set $x_{\hat{m}\hat{k}} = 1$, $z_m = 0$ and $x_{\hat{m},k} = 0$ for all $k \neq \hat{k}, k \in \mathcal{K}_d$.
(b): Set $UB := UB + f_{\hat{m}\hat{k},s}$.
(c): Set $y'_{\hat{k},s} := y'_{\hat{k},s} - w_{\hat{m},s}$.
(d): Set $\mathcal{R}_s := \mathcal{R}_s \backslash \gamma_{\hat{m}}$
Step 5: $\mathcal{M}_{d,s} := \lceil, \mathcal{M}_s \backslash \hat{m}$.
if $\mathcal{M}_{d,s} = \varnothing$ **then**
  STOP and report the solution $\mathbf{x} = (..., x_{mk}, ...)$ with value UB.
else
  Go to Step 2.
end if

8.2.4 Combination of LBR and RGT

The pseudo-code for the algorithm combining the LBR algorithm and the RGT algorithm is shown as Algorithm 8.

Algorithm 8 Combination of LBR and RGT for a specific destination d

Step 1: Set $UB := 0$
Step 2:
for $m \in \mathcal{M}_{d,s}$ **do**
Let k' be the flight that cargo m is assigned to in the lower bound solution.
if $w_{m,s} \leq y'_{k',s}$ **then**
$\mathcal{M}_{d,s} := \mathcal{M}_{d,s} \backslash m$, Let $\hat{k} = k'$,$x_{m,\hat{k}} = 1$ and $x_{m,k} = 0$ for all $k \neq \hat{k}$. Update $UB := UB + f_{m\hat{k}}$, $y'_{k',s} := y'_{k',s} - w_{m,s}$.
end if
end for
if $\mathcal{M}_{d,s} = \emptyset$ **then**
STOP and report the solution $\mathbf{x} = (..., x, ...)$ with value UB.
end if
Step 3: Set $R_{,s} = \emptyset$.
for $m \in \mathcal{M}_s$ **do**
Let $\mathcal{K}_{m,s} = \{k, w_{m,s} \leq y'_{k,s}, l_k < t_{m,s} < u_k, f_{mk} < \sigma w_m\}$.
if $\mathcal{K}_{m,s} = \emptyset$ for some m **then**
Let $\gamma_m = 0$ and $k_m = |K| + 1$.
end if
if $\left|\mathcal{K}_{m,s}\right| = 1$ **then**
$\gamma_m := \max\left\{\sigma w_{\hat{m}} - f_{mk,s}, f_{mk,s} - \sigma w_{\hat{m}}\right\}$, and $k_m = k$ where $k \in \mathcal{K}_{m,s}$ and is the only one element in $\mathcal{K}_{m,s}$.
end if
if $\left|\mathcal{K}_{m,s}\right| \geq 2$ **then**
Let $k_m \in \arg\min\left\{f_{mk,s} : k \in \mathcal{K}_{m,s}\right\}$, for all $m \in \mathcal{M}_{d,s}$.
Let $\gamma_m := \min_{k \in K_{m,s}, k \neq k_m}\left\{f_{mk,s} - f_{mk_m,s}\right\}$, for all $m \in \mathcal{M}_{d,s}$.
Update $R_s := R_s \cup \{\gamma_m\}$.
end if
end for
Step 3: Let $\hat{m} \in \arg\max_{m \in \mathcal{M}_{d,s}} \{\gamma_m : \gamma_m \in \mathcal{R}_s\}$. Let $\hat{k} := k_{\hat{m}}$.
Step 4: Allocate cargo $\hat{m}$ to flight $\hat{k}$ (or ad hoc services) and update the following parameters:
(a): Set $x_{\hat{m}\hat{k}} = 1$, $z_m = 0$ and $x_{\hat{m},k} = 0$ for all $k \neq \hat{k}, k \in \mathcal{K}_d$.
(b): Set $UB := UB + f_{\hat{m}\hat{k},s}$.
(c): Set $y'_{\hat{k},s} := y'_{\hat{k},s} - w_{\hat{m},s}$.
(d): Set $\mathcal{R}_s := \mathcal{R}_s \backslash \gamma_{\hat{m}}$
Step 5: $\mathcal{M}_{d,s} := \mathcal{M}_{d,s} \backslash \hat{m}$.
if $\mathcal{M}_{d,s} = \emptyset$ **then**
STOP and report the solution $\mathbf{x} = (..., x_{mk}, ...)$ with value UB.
else
Go to Step 3.
end if

8.2.5 Simplified RGT algorithm

The pseudo-code for the simplified RGT algorithm is shown as Algorithm 9.

Algorithm 9 Simplified RGT algorithm for a specific destination d

---

Step 1: Set $UB = 0$.
Step 2: Set $\mathcal{R}_s = \emptyset$.
for $m \in \mathcal{M}_{d,s}$ **do**
  Let $\mathcal{K}_{m,s} = \{k, w_{m,s} \leq y'_{k,s}, l_k < t_{m,s} < u_k, f_{mk} < \sigma w_m\}$.
  if $\mathcal{K}_{m,s} = \emptyset$ for some m **then**
    Let $\gamma_m = 0$ and $k_m = \left|\mathcal{K}_{d,s}\right| + 1$.
  end if
  if $\left|\mathcal{K}_{m,s}\right| = 1$ **then**
    $\gamma_m := \max\left\{\sigma w_{\hat{m}} - f_{mk,s}, f_{mk,s} - \sigma w_{\hat{m}}\right\}$, and $k_m = k$, $k \in \mathcal{K}_{m,s}$.
  end if
  if $\left|K_{m,s}\right| \geq 2$ **then**
    Let $k_m \in \arg\min\left\{f_{mk,s} : k \in \mathcal{K}_{m,s}\right\}, \forall m \in \mathcal{M}_s$.
    Let $\gamma_m := \min_{k \in \mathcal{K}_{m,s}, k \neq k_m}\left\{f_{mk,s} - f_{mk_m,s}\right\}, \forall m \in \mathcal{M}_{d,s}$; Update $\mathcal{R}_s := \mathcal{R}_s \cup \{\gamma_m\}$.
  end if
end for
Step 3: Let $\hat{m} \in \arg\max_{m \in \mathcal{M}_{d,s}}\{\gamma_m : \gamma_m \in \mathcal{R}_s\}$. Let $\hat{k} := k_{\hat{m}}$.
Step 4: Allocate cargo $\hat{m}$ to flight $\hat{k}$ (or ad hoc services) and update the following parameters:
(a): Set $x_{\hat{m}\hat{k}} = 1$, $z_m = 0$ and $x_{\hat{m},k} = 0$ for all $k \neq \hat{k}$, $k \in \mathcal{K}_{d,s}$; $UB := UB + f_{\hat{m}\hat{k},s}$.
(b): Set $y'_{\hat{k},s} := y'_{\hat{k},s} - w_{\hat{m},s}$; $R_s := R_s \backslash \gamma_{\hat{m}}$.
Step 5: $\mathcal{M}_{d,s} := \mathcal{M}_{d,s} \backslash \hat{m}$.
if $\mathcal{M}_{d,s} = \emptyset$ **then**
  STOP and report the solution $\mathbf{x} = (\ldots, x_{mk}, \ldots)$ with value UB.
end if
Step 6: Set $n = 0$ and $N = |M_s|$
while $n \leq N$ **do**
  Let $n := n + 1$. Let $\hat{m} \in \arg\max_{m \in M_s}\{\gamma_m\}$. Let $\hat{k} := k_{\hat{m}}$.
  if $w_{\hat{m},s} \leq y'_{\hat{k},s}$ **then**
    Allocate cargo $\hat{m}$ to flight $\hat{k}$ and update the following parameters:
    (a) Set $x_{\hat{m}\hat{k}} = 1$ and $x_{\hat{m},k} = 0$ for all $k \neq \hat{k}$; $UB := UB + f_{\hat{m}\hat{k},s}$; $y'_{\hat{k},s} := y'_{\hat{k},s} - w_{\hat{m},s}$.
    (b) $\mathcal{M}_{d,s} := \mathcal{M}_{d,s} \backslash \hat{m}$; $\mathcal{R}_s := \mathcal{R}_s \backslash \gamma_m$.
  else
    Update $\mathcal{R}_s = \mathcal{R}_s \backslash \gamma_m$.
  end if
end while
Step 7:
if $M_s = \emptyset$ **then**
  STOP and report the solution $\mathbf{x}' = (\ldots, x', \ldots)$ with value UB.
else
  Go to Step 2.
end if

8.3 Flight schedules between HKIA and some chosen airports

Table 8.2: Cathay Pacific services from HKIA to selected destinations

	Flight	Schedule	Aircraft	Capacity	Flight	Schedule	Aircraft	Capacity
NRT	CX524	01:25–06:30	A330-300	44.8	CX526	08:15–10:50	B777	25.2
	CX548	09:05–14:15	B777	25.2	CX520	13:20–15:50	B777	25.2
	CX500	15:25–20:20	A350	17.0	–	–	–	–
TPE	CX488	08:00–09:45	A330-300	44.8	CX564	08:30–10:15	B777	25.2
	CX530	09:05–11:00	A330-300	44.8	CX450	10:20–12:05	B777	25.2
	CX494	10:25–12:05	A330-300	44.8	CX400	13:00–14:50	A321	11.5
	CX240	13:40–15:50	B777	25.2	CX420	15:20–17:25	A330-300	44.8
	CX464	19:40–21:25	A321	11.5	CX408	22:55–00:35+1	A330-300	44.8
PVG	CX316	08:50–11:35	A350	17.0	CX368	09:45–12:30	A350	17.0
	CX376	10:45–13:30	A330-300	44.8	CX360	13:35–16:15	A330-300	44.8
	CX380	15:05–17:45	A330-300	44.8	CX364	17:30–20:15	A330-300	44.8
	CX362	19:15–22:00	B777	25.2	CX302	21:15–23:55	B777	25.2
BKK	CX705	08:30–10:40	B777	25.2	CX615	12:20–14:05	B777	25.2
	CX653	12:50–15:35	A321	11.5	CX789	14:35–15:55	A330-300	44.8
	CX751	15:40–17:25	A330-300	44.8	CX707	16:30–18:50	B777	25.2
	CX709	18:15–20:40	A321	11.5	CX639	19:35–20:40	A350	17.0
KIX	CX566	01:45–06:10	A330-300	44.8	CX596	02:45–07:15	A350	17.0
	CX506	10:45–15:15	B777	25.2	CX598	13:20–17:50	A321	11.5
	CX502	16:40–21:05	A330-300	44.8	–	–	–	–
MNL	CX907	07:30–09:40	A321	11.5	CX901	09:00–11:20	B777	25.2
	CX919	14:30–15:45	B777	25.2	CX913	20:22–21:45	A330-300	44.8
	CX939	22:05–00:20+1	B777	25.2	–	–	–	–
SIN	CX659	01:40–05:40	A350	17.0	CX759	09:00–13:05	A321	11.5
	CX739	11:40–15:45	A350	17.0	CX791	12:50–16:50	A350	17.0
	CX685	15:45–19:50	B777	25.2	CX657	20:15–00:20+1	A330-300	44.8
	CX715	20:25–00:25+1	A330-300	44.8	–	–	–	–
LHR	CX257	08:10–15:00	A350	17.0	CX239	10:40–17:20	A350	17.0
	CX253	13:30–20:10	B777	25.2	CX251	23:00–05:25+1	B777	25.2
	CX255	23:55–06:30+1	B777	25.2	–	–	–	–

Notes: Only Cathay Pacific flights are shown. Aircraft abbreviations: A = Airbus, B = Boeing. Dashes indicate no additional flight. Flights' capacities are measured by tons; DA = Destination Airport

8.4 Appendix of Chapter 5

8.4.1 Proof of UE solution existence and uniqueness by proving the equivalent minimization program solution uniqueness

The equivalent minimization program to Eq. (5.10) for minimizing the total cost of all travelers can be written as

P 5.

$$min: TC\left(n_a, n_b\right) = \int_0^{F^{-1}(n_a)} c_a\left(x\right) f\left(x\right) dx + \int_{F^{-1}(D-n_h)}^{1} c_h\left(x\right) f\left(x\right) dx + c_o \cdot \left(D - n_a - n_h\right), \tag{8.29}$$

subject to

$$n_a \leq m_a, \tag{8.30a}$$

$$n_h \leq m_h, \tag{8.30b}$$

$$n_a + n_h \leq D, \tag{8.30c}$$

$$n_i \geq 0. \tag{8.30d}$$

The above problem is a travel mode choice problem with capacity constraints. The corresponding Lagrangian function with respect to Eq. (8.29) can be formulated as:

$$\begin{aligned} L\left(n_a, n_h, \eta, \lambda_a, \lambda_h\right) = & \int_0^{F^{-1}(n_a)} c_a\left(x\right) f\left(x\right) dx + \int_{F^{-1}(D-n_h)}^{1} c_h\left(x\right) f\left(x\right) dx + c_o \cdot \left(D - n_a - n_h\right) \\ & + \lambda_a \cdot \left(n_a - m_a\right) + \lambda_h \cdot \left(n_h - m_h\right) + \eta \cdot \left(n_a + n_h - D\right), \end{aligned} \tag{8.31}$$

where λ_a and λ_h are the multipliers associated with the transport capacity constrains in Eq. (8.30a) and Eq. (8.30b) and η is the multiplier with regard to the total demand constraint defined in Eq. (8.30c). The first-order optimality conditions can be derived as follows:

$$\frac{\partial L}{\partial n_a} \geq 0, n_a \geq 0, \frac{\partial L}{\partial n_a} \times n_a = 0, \tag{8.32a}$$

$$\frac{\partial L}{\partial n_h} \geq 0, n_h \geq 0, \frac{\partial L}{\partial n_h} \times n_h = 0, \tag{8.32b}$$

$$\frac{\partial L}{\partial \lambda_a} \leq 0, \lambda_a \geq 0, \frac{\partial L}{\partial \lambda_a} \times \lambda_a = 0, \tag{8.32c}$$

$$\frac{\partial L}{\partial \lambda_h} \leq 0, \lambda_h \geq 0, \frac{\partial L}{\partial \lambda_h} \times \lambda_h = 0, \tag{8.32d}$$

$$\frac{\partial L}{\partial \eta} \leq 0, \eta \geq 0, \frac{\partial L}{\partial \eta} \times \eta = 0. \tag{8.32e}$$

In details, the above conditions can be written as:

$$n_a \cdot \left[c_a\left(F^{-1}\left(n_a\right)\right) - c_o + \eta + \lambda_a\right] = 0, \tag{8.33a}$$

$$c_a\left(F^{-1}\left(n_a\right)\right) - c_o + \eta + \lambda_a \geq 0, \tag{8.33b}$$

$$n_a \geq 0, \tag{8.33c}$$

$$n_h \cdot \left[c_h\left(F^{-1}\left(n_h\right)\right) - c_o + \eta + \lambda_h\right] = 0, \tag{8.33d}$$

$$c_h\left(F^{-1}\left(n_h\right)\right) - c_o + \eta + \lambda_h \geq 0, \tag{8.33e}$$

$$\lambda_a\left(n_a - m_a\right) = 0, \tag{8.33f}$$

$$n_a - m_a \leq 0, \tag{8.33g}$$

$$\lambda_a \geq 0, \tag{8.33h}$$

$$\lambda_h\left(n_h - m_h\right) = 0, \tag{8.33i}$$

$$n_h - m_h \leq 0, \tag{8.33j}$$

$$\lambda_h \geq 0, \tag{8.33k}$$

$$\eta\left(n_a + n_h - D\right) = 0, \tag{8.33l}$$

$$n_a + n_h - D \leq 0, \tag{8.33m}$$

$$\eta \geq 0. \tag{8.33n}$$

Let $n_0 = D - n_a - n_b$, $c_i^* = c_o - \eta - \lambda_i$, $i = a, h$, then it is evident that the program modelled for minimization of total travel cost of all travelers is equivalent to the UE conditions.

Next, we check the rank of the Hessian matrix of the objective function in the equivalent minimization program, which can be calculated as:

$$|\mathbf{H}| = \begin{vmatrix} \frac{\partial^2 TC}{(\partial n_a)^2} & \frac{\partial^2 TC}{\partial n_a \partial n_h} \\ \frac{\partial^2 TC}{\partial n_h \partial n_a} & \frac{\partial^2 TC}{(\partial n_h)^2} \end{vmatrix} = \begin{vmatrix} c'_a \left(F^{-1}\right)' & 0 \\ 0 & -c'_h \left(F^{-1}\right)' \end{vmatrix} = -c'_a c'_h \left[\left(F^{-1}\right)'\right]^2 \tag{8.34}$$

As assumed, $F'(x) = f(x) > 0$, thus $(F^{-1})' > 0$. It is evident that $c'_a > 0$ and $c'_h < 0$, thus it can be easily proven that $|\mathbf{H}| > 0$, therefore, at the travel mode choice equilibrium, the numbers of air passengers and HSR passengers, i.e., n_a^* and n_h^*, are both unique.

References

Abdelghany, A., Abdelghany, K., & Azadian, F. (2017). Airline flight schedule planning under competition. *Computers & Operations Research*, *87*, 20–39.

Abenoza, R. F., Cats, O., & Susilo, Y. O. (2017). Travel satisfaction with public transport: Determinants, user classes, regional disparities and their evolution. *Transportation Research Part A: Policy and Practice*, *95*, 64–84.

van Ackooij, W., & Warin, X. (2020). On conditional cuts for stochastic dual dynamic programming. *EURO Journal on Computational Optimization*, *8*, 173–199.

Adisasmita, S. A., & Caroles, L. (2022). Multi-airport system development model: Case study of airports in Indonesia. *Civil Engineering Journal*, *7*, 182–193.

Adler, N., Pels, E., & Nash, C. (2010). High-speed rail and air transport competition: Game engineering as tool for cost-benefit analysis. *Transportation Research Part B: Methodological*, *44*, 812–833.

Amaruchkul, K. (2025). Capacity management of forwarder with multiple carriers under uncertain flight travel time and stochastic shipment demand. *International Transactions in Operational Research*, *32*, 3619–3666.

Amaruchkul, K., & Sae-Lim, P. (2011). Airline overbooking models with misspecification. *Journal of Air Transport Management*, *17*, 143–147.

An, Y., Zhang, Y., & Zeng, B. (2015). The reliable hub-and-spoke design problem: Models and algorithms. *Transportation Research Part B: Methodological*, *77*, 103–122.

Antonucci, L., Crocetta, C., d'Ovidio, F. D., & Toma, E. (2014). Passenger satisfaction: a multi-group analysis. *Quality & Quantity*, *48*, 337–345.

Araújo, T. C., & de Paula Hocayen, H. G. (2024). Navigating multi-airport systems: A case study of brazilian airport concessions and the multi-airport system of rio de janeiro. *Journal of Air Transport Management*, *114*, 102507.

Atakan, S., & Sen, S. (2018). A progressive hedging based branch-and-bound algorithm for mixed-integer stochastic programs. *Computational Management Science*, *15*, 501–540.

Aykin, T. (1995). The hub location and routing problem. *European Journal of Operational Research*, *83*, 200–219.

Azadian, F., Murat, A., & Chinnam, R. B. (2017). An unpaired pickup and delivery problem with time dependent assignment costs: Application in air cargo transportation. *European Journal of Operational Research*, *263*, 188–202.

Azadian, F., Murat, A. E., & Chinnam, R. B. (2012). Dynamic routing of time-sensitive air cargo using real-time information. *Transportation Research Part E: Logistics and Transportation Review*, *48*, 355–372.

Beaud, M., Blayac, T., & Stéphan, M. (2016). The impact of travel time variability and travelers' risk attitudes on the values of time and reliability. *Transportation Research Part B: Methodological*, *93*, 207–224.

Behiri, W., Belmokhtar-Berraf, S., & Chu, C. (2018). Urban freight transport using passenger rail network: Scientific issues and quantitative analysis. *Transportation Research Part E: Logistics and Transportation Review*, *115*, 227–245.

Behrens, C., & Pels, E. (2012). Intermodal competition in the London-Paris passenger market: High-speed rail and air transport. *Journal of Urban Economics*, *71*, 278–288.

Bergantino, A. S., & Madio, L. (2020). Intermodal competition and substitution. HSR versus air transport: Understanding the socio-economic determinants of modal choice. *Research in Transportation Economics*, *79*, 100823.

Bhat, C. R., & Srinivasan, S. (2005). A multidimensional mixed ordered-response model for analyzing weekend activity participation. *Transportation Research Part B: Methodological*, *39*, 255–278.

Billings, J. S., Diener, A. G., & Yuen, B. B. (2003). Cargo revenue optimisation. *Journal of Revenue and Pricing Management*, *2*, 69–79.

Birolini, S., Jacquillat, A., Cattaneo, M., & Antunes, A. P. (2021). Airline network planning: Mixed-integer non-convex optimization with demand–supply interactions. *Transportation Research Part B: Methodological*, *154*, 100–124.

Bodily, S., & Pfeifer, P. (1992). Overbooking decision rules. *Omega*, *20*, 129–133.

Bombelli, A., Santos, B. F., & Tavasszy, L. (2020). Analysis of the air cargo transport network using a complex network theory perspective. *Transportation Research Part E: Logistics and Transportation Review*, *138*, 101959.

Branda, M., & Matoušková, M. (2024). A Lagrangian relaxation algorithm for stochastic fixed interval scheduling problem with non-identical machines and job classes. *Computers & Operations Research*, *164*, 106542.

Brownstone, D., Bunch, D. S., & Train, K. (2000). Joint mixed logit models of stated and revealed preferences for alternative-fuel vehicles. *Transportation Research Part B: Methodological*, *34*, 315–338.

Büsing, C., Kadatz, D., & Cleophas, C. (2019). Capacity uncertainty in airline revenue management: Models, algorithms, and computations. *Transportation Science*, *53*, 383–400.

Butun, C., Petrovic, S., & Muyldermans, L. (2021). The capacitated directed cycle hub location and routing problem under congestion. *European Journal of Operational Research*, *292*, 714–734.

Campbell, J. F. (1994). Integer programming formulations of discrete hub location problems. *European journal of operational research*, *72*, 387–405.

Can, V. V. (2013). Estimation of travel mode choice for domestic tourists to Nha Trang using the multinomial probit model. *Transportation Research Part A: Policy and Practice*, *49*, 149–159.

Carmona, M. A. A., Nieto, F. S., & Gallego, C. E. V. (2020). A data-driven methodology for characterization of a terminal manoeuvring area in multi-airport systems. *Transportation Research Part C: Emerging Technologies*, *111*, 185–209.

Castillo-Manzano, J. I., Pozo-Barajas, R., & Trapero, J. R. (2015). Measuring the substitution effects between high speed rail and air transport in Spain. *Journal of Transport Geography*, *43*, 59–65.

Chang, L.-Y., & Sun, P.-Y. (2012). Stated-choice analysis of willingness to pay for low cost carrier services. *Journal of Air Transport Management*, *20*, 15–17.

Chen, S., Wu, L., Ng, K. K., Liu, W., & Wang, K. (2024). How airports enhance the environmental sustainability of operations: A critical review from the perspective of operations research. *Transportation Research Part E: Logistics and Transportation Review*, *183*, 103440.

Cheng, G., Guo, D., Shi, J., & Qin, Y. (2018). When packages ride a bus: Towards efficient city-wide package distribution. In *2018 IEEE 24th International Conference on Parallel and Distributed Systems (ICPADS)* (pp. 259–266).

Cheng, R., Jiang, Y., & Nielsen, O. A. (2023). Integrated people-and-goods transportation systems: from a literature review to a general framework for future research. *Transport Reviews*, *43*, 997–1020.

Cherukuri, A., & Cortés, J. (2019). Cooperative data-driven distributionally robust optimization. *IEEE Transactions on Automatic Control*, *65*, 4400–4407.

Cheung, T. K.-Y., Wong, W.-H., Zhang, A., & Wu, Y. (2020). Spatial panel model for examining airport relationships within multi-airport regions. *Transportation Research Part A: Policy and Practice*, *133*, 148–163.

De Neufville, R. (1995). Management of multi-airport systems: A development strategy. *Journal of Air Transport Management*, *2*, 99–110.

De Vos, J., Mokhtarian, P. L., Schwanen, T., Van Acker, V., & Witlox, F. (2016). Travel mode choice and travel satisfaction: bridging the gap between decision utility and experienced utility. *Transportation*, *43*, 771–796.

De Vos, J., & Witlox, F. (2017). Travel satisfaction revisited. on the pivotal role of travel satisfaction in conceptualising a travel behaviour process. *Transportation research part A: policy and practice*, *106*, 364–373.

Delgado, F., & Mora, J. (2021). A matheuristic approach to the air-cargo recovery problem under demand disruption. *Journal of Air Transport Management*, *90*, 101939.

Delgado, F., Sirhan, C., Katscher, M., & Larrain, H. (2020). Recovering from demand disruptions on an air cargo network. *Journal of Air Transport Management*, *85*, 101799.

Delgado, F., Trincado, R., & Pagnoncelli, B. K. (2019). A multistage stochastic programming model for the network air cargo allocation under capacity uncertainty. *Transportation Research Part E: Logistics and Transportation Review*, *131*, 292–307.

Derigs, U., Friederichs, S., & Schaefer, S. (2009). A new approach for air cargo network planning. *Transportation Science*, *43*, 370–380.

Devarasetty, P. C., Burris, M., & Shaw, W. D. (2012). The value of travel time and reliability-evidence from a stated preference survey and actual usage. *Transportation Research Part A: Policy and Practice*, *46*, 1227–1240.

Diana, M., & Mokhtarian, P. L. (2009). Grouping travelers on the basis of their different car and transit levels of use. *Transportation*, *36*, 455–467.

Dobruszkes, F. (2011). High-speed rail and air transport competition in Western Europe: A supply-oriented perspective. *Transport Policy*, *18*, 870–879.

Dobruszkes, F., Dehon, C., & Givoni, M. (2014). Does European high-speed rail affect the current level of air services? An EU-wide analysis. *Transportation Research Part A: Policy and Practice*, *69*, 461–475.

Dong, J.-X., Lee, C.-Y., & Song, D.-P. (2015). Joint service capacity planning and dynamic container routing in shipping network with uncertain demands. *Transportation Research Part B: Methodological*, *78*, 404–421.

D'Alfonso, T., Jiang, C., & Bracaglia, V. (2015). Would competition between air transport and high-speed rail benefit environment and social welfare? *Transportation Research Part B: Methodological*, *74*, 118–137.

Elhedhli, S., & Hu, F. X. (2005). Hub-and-spoke network design with congestion. *Computers & Operations Research*, *32*, 1615–1632.

Elhedhli, S., & Wu, H. (2010). A lagrangean heuristic for hub-and-spoke system design with capacity selection and congestion. *INFORMS Journal on Computing*, *22*, 282–296.

Ernst, A. T., & Krishnamoorthy, M. (1996). Efficient algorithms for the uncapacitated single allocation p-hub median problem. *Location science*, *4*, 139–154.

Fageda, X., & Fernandez-Villadangos, L. (2009). Triggering competition in the Spanish airline market: The role of airport capacity and low-cost carriers. *Journal of Air Transport Management*, *15*, 36–40.

Fan, Y., & Liu, C. (2010). Solving stochastic transportation network protection problems using the progressive hedging-based method. *Networks and Spatial Economics*, *10*, 193–208.

Fildes, R., & Goodwin, P. (2007). Against your better judgment? how organizations can improve their use of management judgment in forecasting. *Interfaces*, *37*, 570–576.

Gardiner, J., & Ison, S. (2008). The geography of non-integrated cargo airlines: an international study. *Journal of Transport Geography*, *16*, 55–62.

Gayle, P. G., & Yimga, J. O. (2018). How much do consumers really value air travel on-time performance, and to what extent are airlines motivated to improve their on-time performance? *Economics of Transportation*, *14*, 31–41.

Gong, Z., Zhang, F., Liu, W., & Graham, D. J. (2023). On the effects of airport capacity expansion under responsive airlines and elastic passenger demand. *Transportation Research Part B: Methodological*, *170*, 48–76.

Grauberger, W., & Kimms, A. (2016). Revenue management under horizontal and vertical competition within airline alliances. *Omega-International Journal of Management Science*, *59*, 228–237.

Greene, W., & Hensher, D. (2003). A latent class model for discrete choice analysis: contrasts with mixed logit. *Transportation Research Part B: Methodological*, *37*, 681–698.

Greene, W. H., & Hensher, D. A. (2013). Revealing additional dimensions of preference heterogeneity in a latent class mixed multinomial logit model. *Applied Economics*, *45*, 1897–1902.

Gui, Y., Gong, B., & Cheng, Y. (2008). Research on air cargo overbooking model. In *2008 4th International Conference on Wireless Communications, Networking and Mobile Computing* (pp. 1–4). IEEE.

Haddadi, S. (1999). Lagrangian decomposition based heuristic for the generalized assignment problem. *INFOR: Information Systems and Operational Research*, *37*, 392–402.

Han, D. L., Tang, L. C., & Huang, H. C. (2010). A Markov model for single-leg air cargo revenue management under a bid-price policy. *European Journal of Operational Research*, *200*, 800–811.

Hasan, F., & Kargarian, A. (2024). Accelerating L-shaped two-stage stochastic SCUC with learning integrated benders decomposition. *IEEE Transactions on Industrial Informatics*, *20*, 14144–14153.

He, Y., Wu, T., Zhang, C., & Liang, Z. (2015). An improved mip heuristic for the intermodal hub location problem. *Omega-International Journal of Management Science*, *57*, 203–211.

Hensher, D. A., & Greene, W. H. (2003). The mixed logit model: the state of practice. *Transportation*, *30*, 133–176.

Hensher, D. A., & Rose, J. M. (2007). Development of commuter and non-commuter mode choice models for the assessment of new public transport infrastructure projects: A case study. *Transportation Research Part A: Policy and Practice*, *41*, 428–443.

Hess, S., Adler, T., & Polak, J. W. (2007). Modelling airport and airline choice behaviour with the use of stated preference survey data. *Transportation Research Part E: Logistics and Transportation Review*, *43*, 221–233.

Hou, M., Wang, K., Yang, H., & Zhang, A. (2022). Airport-airline relationship, competition and welfare in a multi-airport system the case of new Beijing Daxing Airport. *Journal of Transport Economics and Policy*, *56*, 156–189.

Hou, S., Zhang, Z., Peng, J., & Chen, X. (2025). Multi-airport system management strategies considering air-rail intermodality and social welfare. *Transportation Research Part E: Logistics and Transportation Review*, *194*, 103882.

Hu, R., Huang, M., Zhang, J., & Witlox, F. (2023). On the matthew effect in a multi-airport system: Evidence from the viewpoint of airport green efficiency. *Journal of Air Transport Management*, *106*, 102304.

Huang, K., & Chang, K.-c. (2010). An approximate algorithm for the two-dimensional air cargo revenue management problem. *Transportation Research Part E: Logistics and Transportation Review*, *46*, 426–435.

Huang, W., Ding, Y., & Jian, S. (2024). Strategic coopetition among transportation service providers considering supply–demand congestion effects and asymmetric bargaining power. *Transportation Research Part B: Methodological*, *188*, 103043.

Ivaldi, M., & Vibes, C. (2008). Price competition in the intercity passenger transport market: A simulation model. *Journal of Transport Economics and Policy*, *42*, 225–254.

Jaillet, P., Song, G., & Yu, G. (1996). Airline network design and hub location problems. *Location Science*, *4*, 195–212.

Jeet, V., & Kutanoglu, E. (2007). Lagrangian relaxation guided problem space search heuristics for generalized assignment problems. *European Journal of Operational Research*, *182*, 1039–1056.

Jiang, C., & Zhang, A. (2016). Airline network choice and market coverage under high-speed rail competition. *Transportation Research Part A: Policy and Practice*, *92*, 248–260.

Jiang, X., Zhang, X., Lu, W., Zhang, L., & Chen, X. (2017). Competition between high-speed rail and airline based on game theory. *Mathematical Problems in Engineering*, *2017*, 1748691.

Jung, S.-Y., & Yoo, K.-E. (2014). Passenger airline choice behavior for domestic short-haul travel in South Korea. *Journal of Air Transport Management*, *38*, 43–47.

Justin, C. Y., Payan, A. P., & Mavris, D. N. (2022). Integrated fleet assignment and scheduling for environmentally friendly electrified regional air mobility. *Transportation Research Part C: Emerging Technologies*, *138*, 103567.

Kashifi, M. T., Jamal, A., Kashefi, M. S., Almoshaogeh, M., & Rahman, S. M. (2022). Predicting the travel mode choice with interpretable machine learning techniques: A comparative study. *Travel Behaviour and Society*, *29*, 279–296.

Kasilingam, R. G. (1997). An economic model for air cargo overbooking under stochastic capacity. *Computers & Industrial Engineering*, *32*, 221–226.

Kenan, N., Jebali, A., & Diabat, A. (2018). An integrated flight scheduling and fleet assignment problem under uncertainty. *Computers & Operations Research*, *100*, 333–342.

Khassiba, A., Bastin, F., Cafieri, S., Gendron, B., & Mongeau, M. (2020). Two-stage stochastic mixed-integer programming with chance constraints for extended aircraft arrival management. *Transportation Science*, *54*, 897–919.

Kian, R., & Kargar, K. (2016). Comparison of the formulations for a hub-and-spoke network design problem under congestion. *Computers & Industrial Engineering*, *101*, 504–512.

Kiraci, K. (2025). The nexus between air cargo and international trade: Empirical evidence from country groups. *Journal of Air Transport Management*, *125*.

Klindokmai, S., Neech, P., Wu, Y., Ojiako, U., Chipulu, M., & Marshall, A. (2014). Evaluation of forecasting models for air cargo. *International Journal of Logistics Management*, *25*, 635–655.

Kupfer, F., Kessels, R., Goos, P., Van de Voorde, E., & Verhetsel, A. (2016). The origin-destination airport choice for all-cargo aircraft operations in Europe. *Transportation Research Part E: Logistics and Transportation Review*, *87*, 53–74.

Lakew, P. A., & Tok, Y. C. A. (2015). Determinants of air cargo traffic in California. *Transportation Research Part A: Policy and Practice*, *80*, 134–150.

Lall, A. (2018). Delays in the New York City metroplex. *Transportation Research Part A: Policy and Practice*, *114*, 139–153.

Lange, A. (2019). Does cargo matter? the impact of air cargo operations on departure on-time performance for combination carriers. *Transportation Research Part A: Policy and Practice*, *119*, 214–223.

Levin, Y., Nediak, M., & Topaloglu, H. (2012). Cargo capacity management with allotments and spot market demand. *Operations Research*, *60*, 351–365.

Li, X., Ma, R., Guo, Y., Wang, W., Yan, B., & Chen, J. (2021). Investigation of factors and their dynamic effects on intercity travel modes competition. *Travel Behaviou and Society*, *23*, 166–176.

Li, Z.-C., Tu, N., Fu, X., & Sheng, D. (2022). Modeling the effects of airline and high-speed rail cooperation on multi-airport systems: The implications on congestion, competition and social welfare. *Transportation Research Part B: Methodological*, *155*, 448–478.

Lijesen, M., & Behrens, C. (2017). The spatial scope of airline competition. *Transportation Research Part E: Logistics and Transportation Review*, *99*, 1–13.

Listes, O., & Dekker, R. (2005). A scenario aggregation-based approach for determining a robust airline fleet composition for dynamic capacity allocation. *Transportation Science*, *39*, 367–382.

Liu, M., Sun, Z., Zhang, X., & Chu, F. (2017). A two-stage no-wait hybrid flow-shop model for the flight departure scheduling in a multi-airport system. In *Proceedings of The 2017 IEEE 14th International Conference on Networking, Sensing and Control (ICNSC 2017)* (pp. 495–500).

Liu, P., Liao, F., Tian, Q., Huang, H.-J., & Timmermans, H. (2020). Day-to-day needs-based activity-travel dynamics and equilibria in multi-state supernetworks. *Transportation Research Part B: Methodological*, *132*, 208–227.

Liu, S., Wan, Y., Ha, H.-K., Yoshida, Y., & Zhang, A. (2019). Impact of high-speed rail network development on airport traffic and traffic distribution: Evidence from China and Japan. *Transportation Research Part A: Policy and Practice*, *127*, 115–135.

Lohatepanont, M., & Barnhart, C. (2004). Airline schedule planning: Integrated models and algorithms for schedule design and fleet assignment. *Transportation Science*, *38*, 19–32.

Löhndorf, N., & Shapiro, A. (2019). Modeling time-dependent randomness in stochastic dual dynamic programming. *European Journal of Operational Research*, *273*, 650–661.

Loo, B. P. (2008). Passengers' airport choice within multi-airport regions (MARs): some insights from a stated preference survey at Hong Kong International Airport. *Journal of Transport Geography*, *16*, 117–125.

Lu, Y., Lang, M., Sun, Y., & Li, S. (2020). A fuzzy intercontinental road-rail multi-modal routing model with time and train capacity uncertainty and fuzzy programming approaches. *IEEE Access*, *8*, 27532–27548.

Ma, H.-L., Sun, Y., Mo, D. Y., & Wang, Y. (2025). Impact of passenger unused baggage capacity on air cargo delivery. *Annals of Operations Research*, *348*, 1069–1085.

Ma, M., Chen, Y., Liu, W., & Waller, S. T. (2023a). An economic analysis of a multi-modal transportation system with ride-sourcing services and multi-class users. *Transport Policy*, *140*, 1–17.

Ma, M., Zhang, F., Liu, W., & Dixit, V. (2023b). On urban co-modality: Non-cooperative and cooperative games among freight forwarder, carrier and transit operator. *Transportation Research Part C: Emerging Technologies*, *153*, 104234.

Ma, W., Wang, Q., Yang, H., Zhang, A., & Zhang, Y. (2019). Effects of Beijing-Shanghai high-speed rail on air travel: Passenger types, airline groups and tacit collusion. *Research in Transportation Economics*, *74*, 64–76.

Magana, U., Mansouri, S. A., & Spiegler, V. L. M. (2017). Improving demand forecasting in the air cargo handling industry: a case study. *International Journal of Logistics - Research and Applications*, *20*, 359–380.

Malokin, A., Circella, G., & Mokhtarian, P. L. (2019). How do activities conducted while commuting influence mode choice? Using revealed preference models to inform public transportation advantage and autonomous vehicle scenarios. *Transportation Research Part A: Policy and Practice*, *124*, 82–114.

Martín, J. C., & Voltes-Dorta, A. (2011). The dilemma between capacity expansions and multi-airport systems: Empirical evidence from the industry's cost function. *Transportation Research Part E: Logistics and Transportation Review*, *47*, 382–389.

Martín, J. C., & Román, C. (2003). Hub location in the South-Atlantic airline market -

a spatial competition game. *Transportation Research Part A: Policy and Practice*, *37*, 865–888.

Masson, R., Trentini, A., Lehuédé, F., Malhéné, N., Péton, O., & Tlahig, H. (2017). Optimization of a city logistics transportation system with mixed passengers and goods. *EURO Journal on Transportation and Logistics*, *6*, 81–109.

McDonnell, S., & Zellner, M. (2011). Exploring the effectiveness of bus rapid transit a prototype agent-based model of commuting behavior. *Transport Policy*, *18*, 825–835.

McFadden, D., & Train, K. (2000). Mixed MNL models for discrete response. *Journal of Applied Econometrics*, *15*, 447–470.

Mo, P., Yao, Y., D'Ariano, A., & Liu, Z. (2023). The vehicle routing problem with underground logistics: Formulation and algorithm. *Transportation Research Part E: Logistics and Transportation Review*, *179*, 103286.

Moussawi-Haidar, L. (2014). Optimal solution for a cargo revenue management problem with allotment and spot arrivals. *Transportation Research Part E: Logistics and Transportation Review*, *72*, 173–191.

Murça, M. C. R., & Hansman, R. J. (2019). Identification, characterization, and prediction of traffic flow patterns in multi-airport systems. *IEEE Transactions on Intelligent Transportation Systems*, *20*, 1683–1696.

Negm, H., De Vos, J., & El-Geneidy, A. (2024). Does it matter if you like it? Exploring the relationship between travel mode choice, preference, and satisfaction. *Transportation Research Part D: Transport and Environment*, *127*, 104053.

Noruzoliaee, M., Zou, B., & Zhang, A. (2015). Airport partial and full privatization in a multi-airport region: Focus on pricing and capacity. *Transportation Research Part E: Logistics and Transportation Review*, *77*, 45–60.

Oktal, H., & Ozger, A. (2013). Hub location in air cargo transportation: A case study. *Journal of Air Transport Management*, *27*, 1–4.

Park, Y., & Ha, H.-K. (2006). Analysis of the impact of high-speed railroad service on air transport demand. *Transportation Research Part E: Logistics and Transportation Review*, *42*, 95–104.

Pels, E., Nijkamp, P., & Rietveld, P. (2000). Airport and airline competition for passengers departing from a large metropolitan area. *Journal of Urban Economics*, *48*, 29–45.

Pels, E., Njegovan, N., & Behrens, C. (2009). Low-cost airlines and airport competition. *Transportation Research Part E: Logistics and Transportation Review*, *45*, 335–344.

Pilar Socorro, M., Betancor, O., & de Rus, G. (2018). Feasibility and desirability of airport competition: The role of product substitutability and airlines' nationality. *Journal of Air Transport Management*, *67*, 224–231.

Pimentel, C., & Alvelos, F. (2018). Integrated urban freight logistics combining passenger and freight flows – mathematical model proposal. *Transportation Research Procedia*, *30*, 80–89.

Prato, C. G., Halldórsdóttir, K., & Nielsen, O. A. (2017). Latent lifestyle and mode choice decisions when travelling short distances. *Transportation*, *44*, 1343–1363.

Rajan, S., Sundar, K., & Gautam, N. (2022). Routing problem for unmanned aerial vehicle patrolling missions-a progressive hedging algorithm. *Computers & Operations Research*, *142*, 105702.

Ramanujam, V., & Balakrishnan, H. (2009). Estimation of arrival-departure capacity trade-offs in multi-airport systems. In *Proceedings of The 48th IEEE Conference on Decision and Control, 2009 held jointly with The 2009 28th Chinese Control Conference (CDC/CCC 2009)* (pp. 2534–2540).

Ramirez-Pico, C., Ljubic, I., & Moreno, E. (2023). Benders adaptive-cuts method for two-stage stochastic programs. *Transportation Science*, *57*, 1252–1275.

Raturi, V., & Verma, A. (2020). A game-theoretic approach to analyse inter-modal competition between high-speed rail and airlines in the Indian context. *Transportation Planning and Technology*, *43*, 20–47.

Reis, V., & Silva, J. (2016). Assessing the air cargo business models of combination airlines. *Journal of Air Transport Management*, *57*, 250–259.

Rockafellar, R. T., & Wets, R. J.-B. (1991). Scenarios and policy aggregation in optimization under uncertainty. *Mathematics of Operations Research*, *16*, 119–147.

Rodbundith, T. S., Sirisawat, P., & Hasachoo, N. (2021). E-commerce: Challenges that lies ahead of the future air cargo operation. In *2021 IEEE International Conference on Industrial Engineering and Engineering Management (IEEE IEEM21)* (pp. 134–137).

Rodrigue, J.-P. (2012). The geography of global supply chains: Evidence from third-party logistics. *Journal of Supply Chain Management*, *48*, 15–23.

Rodriguez-Martin, I., Salazar-Gonzalez, J.-J., & Yaman, H. (2014). A branch-and-cut algorithm for the hub location and routing problem. *Computers & Operations Research*, *50*, 161–174.

Roman, C., Espino, R., & Martin, J. C. (2007). Competition of high-speed train with air transport: The case of Madrid-Barcelona. *Journal of Air Transport Management*, *13*, 277–284.

Ruan, L., Gardi, A., & Sabatini, R. (2021). Operational efficiency analysis of Beijing multi-airport terminal airspace. *Journal of Air Transport Management*, *92*, 102013.

Ryley, T. (2006). Use of non-motorised modes and life stage in Edinburgh. *Journal of Transport Geography*, *14*, 367–375.

Sahoo, R., Pasayat, A. K., Bhowmick, B., Fernandes, K., & Tiwari, M. K. (2022). A hybrid ensemble learning-based prediction model to minimise delay in air cargo transport using bagging and stacking. *International Journal of Production Research*, *60*, 644–660.

Saxena, N., Rashidi, T. H., & Auld, J. (2019). Studying the tastes effecting mode choice behavior of travelers under transit service disruptions. *Travel behaviour and society*, *17*, 86–95.

Schwanen, T., & Mokhtarian, P. L. (2005). What affects commute mode choice: Neighborhood physical structure or preferences toward neighborhoods? *Journal of transport geography*, *13*, 83–99.

Shaban, I. A., Wang, Z. X., Chan, F. T. S., Chung, S. H., Eltoukhy, A. E. E., & Qu, T. (2019). Price setting for extra-baggage service for a combination carrier using the newsvendor setup. *Journal of Air Transport Management*, *78*, 1–14.

Shang, X., Jia, B., Yang, K., Yuan, Y., & Ji, H. (2021). A credibility-based fuzzy programming model for the hierarchical multimodal hub location problem with time uncertainty in cargo delivery systems. *International Journal of Machine Learning and Cybernetics*, *12*, 1413–1426.

Shen, C.-C., Yeh, C.-C., & Lin, C.-N. (2022). Using the perspective of business information technology technicians to explore how information technology affects business competitive advantage. *Technological Forecasting and Social Change*, *184*, 121973.

Sherali, H., Bish, E., & Zhu, X. (2006). Airline fleet assignment concepts, models, and algorithms. *European Journal of Operational Research*, *172*, 1–30.

Sherali, H. D., Bae, K.-H., & Haouari, M. (2013). A benders decomposition approach for an integrated airline schedule design and fleet assignment problem with flight retiming, schedule balance, and demand recapture. *Annals of Operations Research*, *210*, 213–244.

Sidiropoulos, S., Majumdar, A., & Han, K. (2018). A framework for the optimization of terminal airspace operations in multi-airport systems. *Transportation Research Part B: Methodological*, *110*, 160–187.

Sourek, D., & Seidlova, A. (2018). Approach to location of air cargo terminals. In *Transport Means 2018, PTS I-III* (pp. 1376–1378).

Suryani, E., Chou, S.-Y., & Chen, C.-H. (2012). Dynamic simulation model of air cargo demand forecast and terminal capacity planning. *Simulation Modelling Practice and Theory*, *28*, 27–41.

Susilo, Y. O., & Cats, O. (2014). Exploring key determinants of travel satisfaction for multi-modal trips by different traveler groups. *Transportation Research Part A: Policy and Practice*, *67*, 366–380.

Tang, C.-H., Yan, S., & Chen, Y.-H. (2008). An integrated model and solution algorithms for passenger, cargo, and combi flight scheduling. *Transportation Research Part E: Logistics and Transportation Review*, *44*, 1004–1024.

Tian, Z., Feng, T., Timmermans, H. J., & Yao, B. (2021). Using autonomous vehicles or shared cars? Results of a stated choice experiment. *Transportation Research Part C: Emerging Technologies*, *128*, 103117.

Totamane, R., Dasgupta, A., & Rao, S. (2014). Air cargo demand modeling and prediction. *IEEE Systems Journal*, *8*, 52–62.

Tsunoda, Y. (2018). Transportation policy for high-speed rail competing with airlines. *Transportation Research Part A: Policy and Practice*, *116*, 350–360.

Van Hui, Y., Gao, J., Leung, L., & Wallace, S. (2014). Airfreight forwarder's shipment planning under uncertainty: A two-stage stochastic programming approach. *Transportation Research Part E: Logistics and Transportation Review*, *66*, 83–102.

Vancroonenburg, W., Verstichel, J., Tavernier, K., & Berghe, G. V. (2014). Automatic air cargo selection and weight balancing: A mixed integer programming approach. *Transportation Research Part E: Logistics and Transportation Review*, *65*, 70–83.

Vaze, V., & Barnhart, C. (2012). Modeling airline frequency competition for airport congestion mitigation. *Transportation Science*, *46*, 512–535.

Verweij, B., Ahmed, S., Kleywegt, A., Nemhauser, G., & Shapiro, A. (2003). The sample average approximation method applied to stochastic routing problems: A computational study. *Computational Optimization and Applications*, *24*, 289–333.

Vythoulkas, P. C., & Koutsopoulos, H. N. (2003). Modeling discrete choice behavior using concepts from fuzzy set theory, approximate reasoning and neural networks. *Transportation Research Part C: Emerging Technologies*, *11*, 51–73.

Wada, M., Delgado, F., & Pagnoncelli, B. K. (2017). A risk averse approach to the capacity allocation problem in the airline cargo industry. *Journal of the Operational Research Society*, *68*, 643–651.

Wan, Y., Ha, H.-K., Yoshida, Y., & Zhang, A. (2016). Airlines' reaction to high-speed rail entries: Empirical study of the Northeast Asian market. *Transportation Research Part A: Policy and Practice*, *94*, 532–557.

Wang, C., Jiang, C., & Zhang, A. (2021). Effects of airline entry on high-speed rail. *Transportation Research Part B: Methodological*, *154*, 242–265.

Wang, C.-H., Zhang, W., Dai, Y., & Lee, Y.-C. (2022a). Frequency competition among airlines on coordinated airports network. *European Journal of Operational Research*, *297*, 484–495.

Wang, D., Liao, F., Gao, Z., & Timmermans, H. (2022b). A generalized mean-variance metric of route choice model under travel time uncertainty. *Transportmetrica A: Transport Science*, *18*, 299–323.

Wang, J., Bonilla, D., & Banister, D. (2016). Air deregulation in China and its impact on airline competition 1994-2012. *Journal of Transport Geography*, *50*, 12–23.

Wang, K., Xia, W., Zhang, A., & Zhang, Q. (2018). Effects of train speed on airline demand and price: Theory and empirical evidence from a natural experiment. *Transportation Research Part B: Methodological*, *114*, 99–130.

Wang, L., Mao, J., Li, L., Li, X., & Tu, Y. (2023). Prediction of estimated time of arrival for multi-airport systems via "Bubble" mechanism. *Transportation Research Part C: Emerging Technologies*, *149*, 104065.

Wang, W., Sun, H., & Wu, J. (2020a). How does the decision of high-speed rail operator affect social welfare? Considering competition between high-speed rail and air transport. *Transport Policy*, *88*, 1–15.

Wang, Y., Sun, L., Teunter, R. H., Wu, J., & Hua, G. (2020b). Effects of introducing low-cost high-speed rail on air-rail competition: Modelling and numerical analysis for Paris-Marseille. *Transport Policy*, *99*, 145–162.

Wang, Y., & Zhang, Y. (2021). Prediction of runway configurations and airport acceptance rates for multi-airport system using gridded weather forecast. *Transportation Research Part C: Emerging Technologies*, *125*, 103049.

Wang, Y.-J., & Kao, C.-S. (2008). An application of a fuzzy knowledge system for air cargo overbooking under uncertain capacity. *Computers & Mathematics with Applications*, *56*, 2666–2675.

Wannakrairot, A., & Phumchusri, N. (2016). Two-dimensional air cargo overbooking models under stochastic booking request level, show-up rate and booking request density. *Computers & Industrial Engineering*, *100*, 1–12.

Watson, J.-P., & Woodruff, D. L. (2011). Progressive hedging innovations for a class of stochastic mixed-integer resource allocation problems. *Computational Management Science*, *8*, 355–370.

Wei, W., & Hansen, M. (2007). Airlines' competition in aircraft size and service frequency in duopoly markets. *Transportation Research Part E: Logistics and Transportation Review*, *43*, 409–424.

Wiesemann, W., Kuhn, D., & Sim, M. (2014). Distributionally robust convex optimization. *Operations Research*, *62*, 1358–1376.

Xia, W., Jiang, C., Wang, K., & Zhang, A. (2019). Air-rail revenue sharing in a multi-airport system: Effects on traffic and social welfare. *Transportation Research Part B: Methodological*, *121*, 304–319.

Xia, W., & Zhang, A. (2016). High-speed rail and air transport competition and cooperation: A vertical differentiation approach. *Transportation Research Part B: Methodological*, *94*, 456–481.

Xiao, F., Guo, S., Huang, L., Huang, L., & Liang, Z. (2022). Integrated aircraft tail assignment and cargo routing problem with through cargo consideration. *Transportation Research Part B: Methodological*, *162*, 328–351.

Xiao, Y., Fu, X., & Zhang, A. (2016). Airport capacity choice under airport-airline vertical arrangements. *Transportation Research Part A: Policy and Practice*, *92*, 298–309.

Xiong, C., Yang, D., & Zhang, L. (2018). A high-order hidden Markov model and its applications for dynamic car ownership analysis. *Transportation Science*, *52*, 1365–1375.

Xu, Y., Wandelt, S., & Sun, X. (2021). Airline integrate d robust sche duling with a variable neighborhood search based heuristic. *Transportation Research Part B: Methodological*, *149*, 181–203.

Yan, S., Chen, S.-C., & Chen, C.-H. (2006). Air cargo fleet routing and timetable setting with multiple on-time demands. *Transportation Research Part E: Logistics and Transportation Review*, *42*, 409–430.

Yang, H., & Zhang, A. (2012). Effects of high-speed rail and air transport competition on prices, profits and welfare. *Transportation Research Part B: Methodological*, *46*, 1322–1333.

Yang, X., Kong, X. T. R., & Huang, G. Q. (2024). Synchronizing crowdsourced co-modality between passenger and freight transportation services. *Transportation Research Part E: Logistics and Transportation Review*, *184*, 103490.

Yang, X., Wu, W., & Huang, G. Q. (2023). A crowdsourced co-modality transportation system integrating passenger and freight. *Advanced Engineering Informatics*, *58*, 102142.

Zhang, A. (2003). Analysis of an international air-cargo hub: the case of Hong Kong. *Journal of Air Transport Management*, *9*, 123–138.

Zhang, A., Fu, X., & Yang, H. G. (2010). Revenue sharing with multiple airlines and airports. *Transportation Research Part B: Methodological*, *44*, 944–959.

Zhang, A., Wan, Y., & Yang, H. (2019). Impacts of high-speed rail on airlines, airports and regional economies: A survey of recent research. *Transport Policy*, *81*, A1–A19.

Zhang, A., & Zhang, Y. (2006). Airport capacity and congestion when carriers have market power. *Journal of Urban Economics*, *60*, 229–247.

Zhang, A., & Zhang, Y. (2010). Airport capacity and congestion pricing with both aeronautical and commercial operations. *Transportation Research Part B: Methodological*, *44*, 404–413.

Zhang, C., Xie, F., Huang, K., Wu, T., & Liang, Z. (2017). MIP models and a hybrid method for the capacitated air-cargo network planning and scheduling problems. *Transportation Research Part E: Logistics and Transportation Review*, *103*, 158–173.

Zhang, D., Yu, C., & Lau, H. (2016). An integrated flight scheduling and fleet assignment method based on a discrete choice model. *Computers & Industrial Engineering*, *98*, 195–210.

Zhang, Y., Negenborn, R. R., & Atasoy, B. (2023). Synchromodal freight transport replanning under service time uncertainty: An online model-assisted reinforcement learning. *Transportation Research Part C: Emerging Technologies*, *156*, 104355.

Zhao, L., Li, H., Li, M., Sun, Y., Hu, Q., Mao, S., Li, J., & Xue, J. (2018). Location selection of intra-city distribution hubs in the metro-integrated logistics system. *Tunnelling and Underground Space Technology*, *80*, 246–256.

Zhao, X., Wang, Y., Li, L., & Delahaye, D. (2022). A queuing network model of a multi-airport system based on point-wise stationary approximation. *Aerospace*, *9*, 390.

Zheng, H., Sun, H., Zhu, S., Kang, L., & Wu, J. (2023). Air cargo network planning and scheduling problem with minimum time: A matrix-based ALNS heuristic. *Transportation Research Part C: Emerging Technologies*, *156*, 104307.

Zhou, H., Norman, R., Xia, J., Hughes, B., Kelobonye, K., Nikolova, G., & Falkmer, T. (2020). Analysing travel mode and airline choice using latent class modelling: A case study in Western Australia. *Transportation Research Part A: Policy and Practice*, *137*, 187–205.

Zhou, H., Xia, J., Norman, R., Hughes, B., Nikolova, G., Kelobonye, K., Du, K., & Falkmer, T. (2019). Do air passengers behave differently to other regional travellers?: A travel mode choice model investigation. *Journal of Air Transport Management*, *79*, 101682.

Zhu, S., Bell, M. G., Schulz, V., & Stokoe, M. (2023). Co-modality in city logistics: Sounds good, but how? *Transportation Research Part A: Policy and Practice*, *168*, 103578.

Zietsman, D., & Vanderschuren, M. (2014). Analytic Hierarchy Process assessment for potential multi-airport systems - The case of Cape Town. *Journal of Air Transport Management*, *36*, 41–49.

Zou, M., Li, M., Lin, X., Xiong, C., Mao, C., Wan, C., Zhang, K., & Yu, J. (2016). An agent-based choice model for travel mode and departure time and its case study in Beijing. *Transportation Research Part C: Emerging Technologies*, *64*, 133–147.

Zuo, Y., Liu, T.-L., & Liu, W. (2025). On the competition and collaboration in a multi-airport system considering ground connection between airports. *Transportation Research Part A: Policy and Practice*, *192*, 104387.